2018-06-01

Parametric Study on Multi-Story, Partially Grouted, Perforated, Masonry Shear Walls by Finite Element Analysis

Kyle Henry Chavez
Brigham Young University

Parametric Study on Multi-Story, Partially Grouted, Perforated, Masonry Shear Walls by Finite Element Analysis

Kyle Henry Chavez

A thesis submitted to the faculty of
Brigham Young University
in partial fulfillment of the requirements for the degree of

Master of Science

Fernando S. Fonseca, Chair
David W. Jensen
Paul William Richards

Department of Civil and Environmental Engineering

Brigham Young University

ABSTRACT

Parametric Study on Multi-Story, Partially Grouted, Perforated,
Masonry Shear Walls by Finite Element Analysis

Kyle Henry Chavez
Department of Civil and Environmental Engineering, BYU
Master of Science

In this study, parameters related to material properties, geometry, and external stimuli were examined individually to determine their influence on multi-story, partially grouted, perforated (openings), masonry shear walls using a finite element software FormWorks. The parameters studied were: the strength of grouted masonry prisms $f'_{m,grouted}$; the strength of un-grouted (hollow) masonry prisms $f'_{m,ungrouted}$; the ratio of mortar shear strength to masonry compressive strength; vertical and horizontal reinforcement ratios in terms of size and spacing of reinforcement; axial load; aspect ratio; and openings that were vertically and horizontally altered. To perform this study, finite element models were validated against the response of three experimental walls of two unique types that were built ½ scale and tested in a lab. The validated finite element models were designated as "base models" which accurately predicted the maximum strength of each wall within a tolerance of 5.9%, 3.3%, and 1.8%. Following validation, each parameter in question was varied individually to identify and quantify the sensitivity of the parameter and to observe the changes in shear capacity and deflection for this unique configuration of masonry shear walls. To capture the impact of these parameters, 38 different shear wall models were built and tested. The results were compared against the Masonry Standards Joint Committee (MSJC) (2013) code predictions using the applicable shear strength equations.

Results of this study are specific to cantilever type masonry shear walls with large aspect ratios and openings in every story. Shear wall capacity was considered sensitive to the following parameters: compressive strength of grouted masonry; compressive strength of un-grouted masonry; joint strength ratio; vertical reinforcement ratio; axial stress; aspect ratio; and opening width. Shear wall capacity was considered not sensitive to the following parameters: horizontal reinforcement ratio; vertical reinforcement spacing; and horizontal reinforcement spacing. The sensitivity of shear wall capacity to opening height was determined inconclusive. The sensitivities were determined by fitting trend lines to the results of shear capacity vs. each parameter individually. Each MSJC (2013) code prediction un-conservatively over-predicted the shear wall capacity except one wall configuration that had a joint strength ratio of 0.045.

Keywords: multi-story, partially grouted, openings, masonry, shear wall, parameters, finite element analysis

ACKNOWLEDGEMENTS

It is a great privilege to perform research at such an amazing institution where students and faculty alike desire further light and knowledge in their respective fields. I am extremely grateful for the resources allocated to me in order to accomplish this work. Specifically, I thank those whose funding turned this research from a possibility into a reality. I am especially thankful for my advisor Dr. Fernando S. Fonseca for sharing his knowledge, time, expertise, resources, and labor in helping me complete this research. I express my gratitude to the Civil Engineering Department for the scholarships available and awarded to me. I would like to specifically mention by name those who transformed our thoughts and ideas into tangible specimens: David Anderson (Lab Manager), Rodney Mayo (Assistant Lab Manager), Ernesto Fortes, Jeffrey Buxton, David Ochoa, Rawley Selk, Clay Hanson, Aaron Roper, Theodore Moffett, and Ryan Beaumont. I thank Dr. Joseph Eixenberger for his advice and guidance related to the finite element analyses performed. I also thank Craig Shaw and his support staff for providing an optimized data collection process and aiding to solve technical issues. Additionally, I thank Kim Glade for her extra efforts that went above and beyond her required role.

There are many others who's behind the scenes support allowed for the completion of this research. First and foremost, I express my love and gratitude for my wife Davita Jewel Chavez and daughter Jodi Anne Chavez. In more ways than can be written my wife has stepped up, stepped in, reached out, lifted, sustained, and supported me. Similarly, in more ways than she knows, my daughter has expressed unconditional love. Lastly I would like to thank all family and friends who have extended love and support throughout this process. I could not have completed this work without the much needed and timely retreats.

TABLE OF CONTENTS

LIST OF TABLES

LIST OF FIGURES

1 INTRODUCTION

1.1 Background

Masonry is one of the oldest and most durable methods of construction which is evidenced by the ancient structures that still stand today. From pyramids to castles, bridges to lighthouses, masonry can be seen as withstanding the test of time. Masonry is anything constructed out of materials that are stacked individually to create a non-homogenous structure capable of acting together as a system. Over millennia, masonry has evolved to its modern form that we know today.

Today, the majority of masonry structures are constructed by stacking standard sized clay or concrete blocks on a bed of mortar while also separating each block vertically with mortar on each side to secure the blocks together. The horizontal mortar joints are known as bed joints and the vertical mortar joints are known as head joints. Blocks may be solid or hollow depending on their usage. Where blocks are hollow, additional materials are often added to fill voids in the system. Grout is used to fill the hollow cells of masonry structures to increase the strength and stiffness of a wall. If all the cells of a masonry wall are grouted, the wall is said to be fully grouted. If some of the cells left un-grouted, the wall is said to be partially grouted or un-grouted respectively. Reinforcement may also be included in the system to resist tensile forces and increase the ductility of a wall. It is common to space reinforcement out such that not every cell

contains reinforcement. Wherever reinforcement is placed, whether vertically or horizontally, grout is also placed to bond the reinforcement to the masonry blocks.

The main lateral force resisting system in masonry structures is called a masonry shear wall. Shear walls are structural elements that use in-plane strength to resist lateral forces caused by wind or seismic events. The load that a masonry shear wall is capable of resisting is a function of many parameters. These parameters include: wall height to width ratio (aspect ratio); whether the wall is fully grouted or partially grouted; size and spacing of reinforcement; the presence of window or door openings; the strength of each individual masonry constituent; external conditions such as boundary conditions or axial load.

1.1.1 Area of focus

Masonry shear wall response has been studied extensively. The majority of the research has been performed on single-story, fully-grouted walls with no openings (non-perforated). The current code equations for shear design are based upon such tests and empirical solutions performed and reported by Shing et al. (1990) (MSJC 2013). Additional research has delved into the effects of partial grouting and openings, however their effects are less understood. Ghanem et al. (1992) studied the effects of partial grouting and concluded that partially reinforced masonry walls were strongly dependent upon the distribution of reinforcement. Yanez et al. (2004) conducted a study on the various opening sizes in single story, single aspect ratio walls with reinforcement placed only around the perimeter of the openings. The authors determined that the current methodology for analysis which considers the shear capacity as proportional to the net shear area is appropriate and conservative.

The purpose of this research is to combine elements from many previous studies to determine the effects of parameters associated with material properties, wall geometry, and external stimuli for multi-story, partially grouted, perforated (containing openings) masonry shear walls. To perform this study, testing experimental wall specimens was coupled with finite element analysis. Once the experimental walls were tested and analyzed, a finite element representation of the walls was built and validated against the data. After the model was validated, individual parameters were varied in a controlled manner to determine their influence on the response of masonry shear walls. These results were compared against the MSJC (2013) code predictions for shear wall capacity.

1.1.2 Research

To accomplish the objectives of this research, three experimental specimens displaying two configurations of wall were first constructed and tested. The layout of the walls includes the following details: ½ scale CMU blocks constructed in the running bond layout; three-stories with reinforced concrete floor beams separating each story; window openings located in the center of each story; vertically grouted cells at the ends of the wall and adjacent to the openings; and an axial load uniformly distributed and applied across the top of the wall. The difference between the two wall types is in the grouted horizontal coarse running underneath the opening in each story. One wall had the grouted horizontal coarse run the entire length of the wall and the other two walls had the grouted horizontal coarse only underneath the opening in each story (see Figure 1-1). Note that the experimental walls were intended to gather real responses for calibration and not to perform the parametric analysis. Therefore, providing two similar yet different wall configurations increased model robustness. The results of the tests were compared against a finite element model of the same walls. After validating the model, a numerical

parametric study using the model allowed for predetermined parameters to be changed and investigated. The parametric study performed in this finite element analysis includes 2 validated base models and 38 unique parametric modifications to obtain trends and results. Lastly, current code predictions for this wall configuration were calculated and compared against the experimental and numerical results (Appendix A).

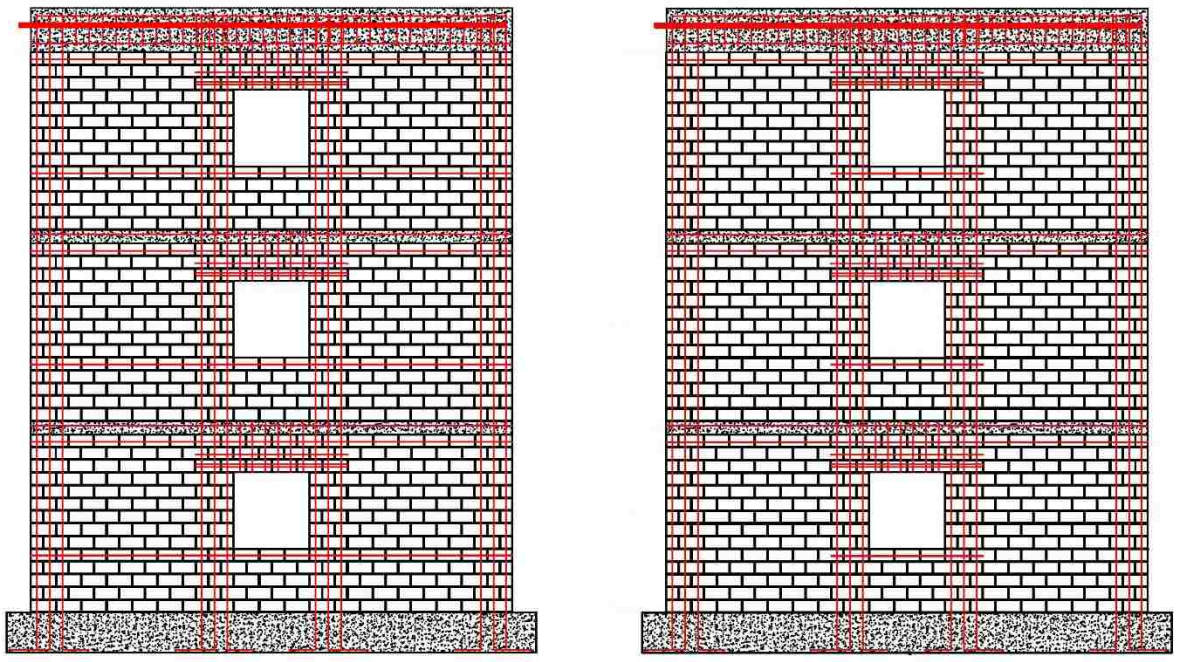

Figure 1-1:Difference in experimental specimens – wall 1 (left) and walls 2&3 (right)

This research was unique in that it tested representations of masonry shear walls that are multi-story (large aspect ratios), partially grouted, and perforated. In other words, there has been little research performed on multi-story walls that includes all of the design parameters described. It was expected that testing such walls would confirm current knowledge of the relationship of parameters such as aspect ratio, axial load, and masonry compressive strength and

shed light on less understood parametric relationships such as reinforcement ratios, mortar shear strength, and opening height and width, for this unique wall type. It was hoped that additional awareness would provide a need for involving new parameters for analysis and offer limitations of current parameters with respect to the response of the masonry shear walls in question.

2 LITERATURE REVIEW

Mastsumura (1987) studied the in-plane behavior of 57 concrete masonry and 23 clay masonry (brick) walls with the intent of presenting a formula to predict the shear strength of reinforced masonry walls. The wall specimen dimensions were within a range of 160 – 180 cm (5'3" – 5'11") tall, 80 – 200 cm (2'6" – 6'7") wide, and 15 – 19 cm (6" – 7.5") thick. The research considered the response of shear walls with respect to reinforcement ratios, shear-span ratios (aspect ratios), axial stresses, strengths of materials, and partial versus fully grouted walls.

Matsumura reported that the shear strength was directly related to the masonry compressive strength, f'_m. In other words, an increase in the masonry compressive strength resulted in an increase in the shear strength. This relationship was found to be proportional to $\sqrt{f'_m}$. Other relationships were also evaluated. The relationship between shear strength and axial load was determined as $\tau_u = \tau_{ua} + 0.2\sigma_o$, where τ_{ua} is the shear strength of the wall without axial stress and σ_o is the axial stress. The relationship between horizontal shear reinforcement and shear strength was determined to be $\tau_u = 0.18\gamma\delta\sqrt{\rho_h \, {}_h\sigma_y \, f'_m}$, where γ = 1.0 for fully grouted concrete masonry, γ = 0.6 for partially grouted concrete masonry; δ = 1.0 for loading creating an inflection point in the mid-height of wall (fixed end loading), δ = 0.6 for loading a cantilever wall (wall type loading); ρ_h = horizontal reinforcement ratio; ${}_h\sigma_y$ = yield stress of the shear reinforcement. The relationship between aspect ratio and shear strength was found to be

inversely proportional. In order to only consider the effects of aspect ratio, Matsumura normalized the shear strength values by removing the contributions of axial stress and horizontal shear reinforcement. Thus the influence of the aspect ratio (h/d) was expressed in equation 2-1.

$$\left(\frac{1}{kp}\right)\left(\frac{\tau_u}{\sqrt{f'_m}} - 0.18\gamma\delta\sqrt{\rho_{h\ h}\sigma_y\ f'_m} - \frac{0.2\sigma_o}{\sqrt{f'_m}}\right) = \frac{0.76}{\frac{h}{d}+0.7} + 0.012 \qquad \text{Equation 2-1}$$

where $k_p = 1.16P_t^{0.3}$ and P_t = flexural (vertical) reinforcement ratio. From this equation the aspect ratio may be solved for by substituting the appropriate values into the left side of the formula and computing h/d. Ultimately the equation produced by Matsumura to predict the total shear strength of masonry walls was determined by incorporating each contributing components into the following equation:

$$V_u = \left(k_u k_p\left(\frac{0.76}{\frac{h}{d}+0.7} + 0.012\right)\sqrt{f'_m} + 0.18\gamma\delta\sqrt{\rho_{h\ h}\sigma_y\ f'_m} + 0.2\sigma_o\right)10^3 tj \qquad \text{Equation 2-2}$$

where $k_u = 1.0$ for fully grouted masonry, $k_u = 0.8$ for partially grouted concrete masonry (beam type loading), $k_u = 0.64$ partially grouted concrete masonry (wall type loading); t = thickness of the wall; j = (7/8)*d; d = effective length of wall (the distance from the extreme compression fiber to the centroid of flexural tension reinforcement).

Shing et al. (1988) similarly conducted a study on sixteen reinforced masonry wall panels to examine the influence of the amount of reinforcement and applied axial stress on the in-plane resistance of masonry shear walls. The test specimens were constructed of full-scale, hollow, 6 in. x 8 in. x 16 in. blocks in a running bond pattern to form 6 ft. x 6 ft. walls. The walls were fully grouted with uniformly distributed vertical and horizontal reinforcement. The vertical reinforcement ratios were taken as 0.38%, 0.54%, and 0.74% whereas the horizontal reinforcement ratios were taken as 0.14% and 0.24%. From the experimental results it was concluded that using an adequate amount of horizontal reinforcement might avoid a brittle shear

failure. For example, wall specimen 9 had a horizontal reinforcement ratio of 0.14%. During testing a diagonal crack occurred at roughly 0.3 in. of displacement. The wall failed shortly thereafter at approximately 0.5 in. of displacement. On the other hand, specimen 13 had a horizontal reinforcement ratio of 0.24% (a 71% increase). During testing a diagonal crack occurred at roughly 0.35 in. of displacement yet the wall continued to resist load until failing at a displacement of roughly 1 in. (For a visual comparison of the hysteresis curves for specimens 9 and 13 see Figure 2-1.) Although specimen 13 also had additional vertical reinforcement in relation to specimen 9, the study determined a clear correlation with increased horizontal reinforcement and increased strength and ductility. Additional findings concluded that the shear and flexure failure modes are highly sensitive to applied axial stress. Further testing using finite element models were developed and compared against the experimental results to determine if such modeling could produce adequate results. The numerical model results were within 10% of the experimental results for shear controlled specimens and within 6% of the experimental results for flexure. The analytical results were considered reasonable, however, the model could not accurately represent diagonal crack opening. It was concluded that using discrete crack modeling would provide a more sophisticated and accurate approach to predicting the shear strength of masonry walls.

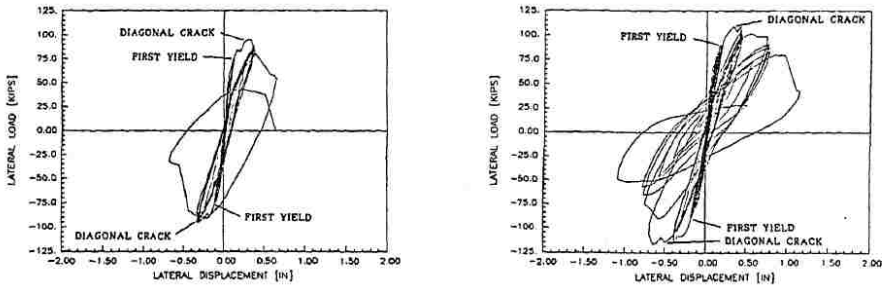

(c) Specimen 9 (d) Specimen 13

Figure 2-1: Horizontal reinforcement ratios of 0.0014 (left) and 0.0024 (right)

In a related study, Shing et al. (1990) examined the data from the same 6ft x 6ft reinforced masonry shear wall study completed in 1988 to evaluate the validity of the then current design formulas. At the time, the Uniform Building Code (UBC) formula for nominal shear strength of masonry walls was $V_n = V_m + V_s$, where $V_m = 1.2A\sqrt{f'_m}$ and $V_s = A\rho_n f_y$ (UBC 1988). The authors concluded that the behavior of the walls was extremely complicated after diagonal cracking occurs. Once diagonal cracking occurs, the residual strength of the masonry is left to the shear resistance in the compression toe, aggregate-interlock forces, horizontal reinforcement, and the dowel forces of the flexural reinforcement. In addition, the aggregate interlock forces depend on the axial load, which in turn limits crack opening. The code specifications were viewed as overly simplistic to deal with these complexities and consequently Shing (1990) developed new relationships and equations.

While total horizontal reinforcement had long been considered to be an important contributor to the shear resistance of masonry, it was observed that the top and bottom reinforcing bars do not have adequate development lengths when diagonal cracking occurs to develop tensile resistance. In essence, only the interior reinforcement was activated by diagonal cracking. With this consideration, the following modified formula was presented for the shear strength of horizontal reinforcement: $V_s = (\frac{l-2d'}{s} - 1)A_h f_y$, where l = horizontal length of the wall, d' = the distance of the extreme vertical steel from the edge of wall, s = the vertical spacing of horizontal reinforcement, and A_h = the area of one horizontal reinforcing bar. Using the new equation to determine the contribution of steel in masonry shear walls and subtracting those values from the observed total shear strength, the shear contribution of masonry, V_m, was calculated and compared against the code specifications for masonry shear strength. Shing (1990) determined that the code was overly conservative by a factor of three. In other words, the

observed masonry shear wall strength was determined to be three times higher than what the current code equations predicted. Based on this data Shing (1990) developed an equation for the contribution of the masonry shear strength as: $V_m = (0.0018(\rho_v f_y + \sigma_c) + 2)A\sqrt{f'_m}$, where ρ_v = vertical reinforcement ratio, and A = cross sectional area. The total shear strength of masonry walls, similar to the UBC (1988) equation, was determined as the sum of the reinforcement contribution, V_s, and the masonry contribution V_m. The research completed and presented by Shing (1990) is the basis for the current Masonry Standards Joint Committee (MSJC) 2013 design equations. Subsequent research has since validated these equations (Davis 2010).

As noted by Shing (1990), because these walls were fully grouted, the diagonal tensile cracks propagated through the masonry units rather than along the mortar joints. The conclusion was drawn that mortar joints had little influence on the shear strength of the fully grouted specimens tested. Later research on partially grouted masonry shear walls would confirm that mortar joints are indeed the inherent planes of weakness and therefore critical with respect to partially grouted masonry shear wall strength (Shing and Coa 1997, Drysdale et al. 1999).

Currently, nominal masonry shear strength is determined as the sum of the contributions of nominal masonry shear strength and nominal shear strength provided by reinforcement. Nominal masonry shear strength is a function of aspect ratio, net shear area, masonry compressive strength, axial load, and a factor that applies a 25% reduction for any configuration of partial grouting. Nominal shear strength provided by reinforcing steel is a function of the area of shear reinforcing steel, reinforcement spacing, yield strength of the steel, and length of shear wall. Additionally, limits are imposed by the code based on aspect ratio (MSJC 2013). Tests related to almost all of these parameters was performed in this research.

Fattal (1993) proposed a modified version of the equations presented by Matsumura (1988) for estimating the strength of partially grouted masonry shear walls. For simplicity of comparison, the equations by Matsumura were rearranged by Fattal from their form previously described above to a decomposed version that separates the main shear strength contributors. The equation was rearranged into the following: $v_p = v_m + v_s + v_q$ where v_m represents the shear strength contribution of masonry, v_s represents the shear strength contribution of steel, and v_q represents the shear strength contribution of axial stress.

$$v_m = \left[\left(\frac{0.76}{r_d+0.7} + 0.012\right)(4.04)(\rho_{va})^{0.3}(k_u)(f_m)^{0.5}\right]\left(\frac{d}{L}\right) \quad \text{Equation 2-3}$$

$$v_s = \left[0.157\left(\rho_h f_{yh}\right)^{0.5}(\gamma)(\delta)(f_m)^{0.5}\right]\left(\frac{d}{L}\right) \quad \text{Equation 2-4}$$

$$v_q = [0.175(q)]\left(\frac{d}{L}\right) \quad \text{Equation 2-5}$$

Results of 72 specimens from 3 experimental programs were compared against the predicted strengths of the original equation. These comparisons illuminated deficiencies in the correlation of individual parameters to shear strength including axial load, aspect ratio, and the amount of horizontal and vertical reinforcement. The new proposed equation altered the original form to improve the empirical correlation of these parameters based on post-cracking mechanisms. The modification of v_m was considered because of the effect of dowel action. Dowel action implies that longitudinal reinforcement contributes to the shear capacity. In other words, for the masonry to fail in shear, the longitudinal reinforcement would likewise have to yield or shear and is therefore capable of transferring forces perpendicular to their axis (Kotsovos 1999). The modifications of v_s were considered because of the decreasing influence of increasing horizontal shear reinforcement. The modifications of v_q were related to the effect of aggregate

interlock. Numerical constants were imposed to provide empirical accuracy. The final equations proposed by Fattal were $v_p = v_m + v_s + v_q$ where,

$$v_m = k_o k_u \left(\frac{0.5}{r+0.8} + 0.8\right)(f_m)^{0.5}(f_{yv})^{0.5}(\rho_v)^{0.7} \quad \text{Equation 2-6}$$

$$v_s = k_o 0.011(\gamma)(\delta)(f_{yh})(\rho_h)^{0.31} \quad \text{Equation 2-7}$$

$$v_q = (k_o)0.012(f_m) + 0.2(q) \quad \text{Equation 2-8}$$

The modified equations by Fattal were observed to show substantially better correlations with the test results than the original equation by Matsumura. Predicted strengths varied from 41% to 146% of measured strength of which 68% of the predicted strengths were within 20% of the measured strengths. Fattal concluded that additional refinement of the equations was necessary to produce a predictive shear strength equation with more accurate results.

Shing and Cao (1997) performed experimental research to study the seismic resistance of partially grouted reinforced masonry shear walls. The authors performed finite element modeling to predict the behavior of partially grouted masonry shear walls. The study used two types of elements to model the behavior of partially grouted masonry shear walls. The first used a plasticity-based element to represent the shear and tensile behavior of a mortar joint. The second used smeared crack elements to represent the behavior of masonry units. Masonry compressive strength, masonry tensile strength, elastic modulus, strain, and other parameters were input into the model as determined by test results and derivations. With these parameters the model was calibrated to match the experimental results.

One of the challenges in this study resulted from the lack of information available on the tensile and shear behavior of masonry bed and head joints. This was due to the complexity of the joint itself. Mortar joints at the grouted sections of masonry walls influenced the wall less as the

majority of the load was resisted by the stiff grout. However, joints at the un-grouted sections of masonry walls relied upon on the interface between the mortar and masonry units to transfer shear. Therefore, the mortar joints where there was grouted masonry were assumed to have the same strength as the grouted masonry units and the mortar joints where un-grouted masonry was located were assumed to have a strength of $0.05f'_m$.

The numerical results showed that the horizontal reinforcement had little influence on the load-displacement curves. Experimental results, however, indicated the opposite – that there was a direct relationship between the amount of horizontal reinforcement and shear strength. The model was therefore an inaccurate representation of actual specimens. The discrepancy was explained through the failure mechanisms of the walls in the model. Failures in the model were dominated by shear sliding of the bed joints adjacent to the bond beam. Since sliding in the model occurred above the bond beam where the horizontal shear reinforcement was located, the horizontal reinforcement was never engaged and therefore could not contribute to the shear strength. The failure mechanisms of the experimental results showed little to no sliding. In addition, crack patterns from the finite element model showed cracking on only half the wall height whereas cracking in the experimental model showed cracking along the full height of the wall. It was noted that these discrepancies may be due to the finite element model having loaded the wall monotonically where the experimental wall was loaded cyclically. Another possible contributor to the differences in failure mechanisms may be a result of a contradiction between actual bond strength and modeled bond strength. The discrepancies described above show the complexity of masonry shear wall systems and the difficulty to accurately capture these relationships in a numerical model.

More recently, Voon and Ingham (2006) performed a study on 10 single-story reinforced concrete masonry shear walls. Of these walls, 8 were fully grouted and 2 were partially grouted. Parameters that were varied in the study included horizontal shear reinforcement, applied axial load, and aspect ratio. The results indicated that by increasing the horizontal shear reinforcement ratio from 0.01 to 0.05, the shear strength capacity increased 10% and the ductility of the wall would improve. The ductility also increased if the same shear reinforcement ratio was spread over the height of the wall via more bars with smaller diameters. The axial stress was also determined to directly influence shear strength. An increase from 0 – 0.25 MPa and 0.25 – 0.50 MPa resulted in increased maximum shear strengths capacities from 215 kN to 244 kN to 263 kN, respectively. These changes correspond to a 13% and additional 8% increase in strength. Conversely, the ductility decreased with increasing axial load. The grout spacing was also determined to play a major role in shear wall strength. By decreasing from 5 grouted vertical cores down to 3 vertical cores (out of 9 total vertical cores), the wall strength was reduced by 50%. Lastly, the aspect ratio was determined to be inversely related to shear strength – that is as aspect ratio increased, shear capacity decreased.

Additional research by Voon and Ingham (2008) was conducted on 8 partially grouted, single-story, perforated concrete masonry shear walls. The varied parameters were the height of the openings, amount of trimming reinforcement (horizontal reinforcement located underneath the window openings), and the length of the walls. The authors observed that as the height of the opening increased from 1,200 mm (specimen 2) to 2,000 mm (full height) (specimen 3), the shear strength of the walls decreased from 41.2 kN to 34.4 kN. In other words, a 67% increase in the size of the opening resulted in a 20% decrease in strength. Figure 2-2 depicts this increase in opening size. The increase in trimming reinforcement led to both an increase in strength and an

increase in ductility. As the length of the trimming reinforcement was extended from only underneath the opening (specimen 2) to running the entire length of the wall (specimen 4), the shear strength increased from 41.2 kN to 52.4 kN – a 27% increase in strength. Figure 2-3 illustrates this change in trimming reinforcement. The length of the shear wall directly affects the force per length of wall or, in other words, the effective shear area available in the piers (vertical spanning portion of the wall on the sides of the opening that resist shear loads). The authors determined that a 50% increase in the length of the piers for a 4200 mm wall resulted in a 100% increase in strength.

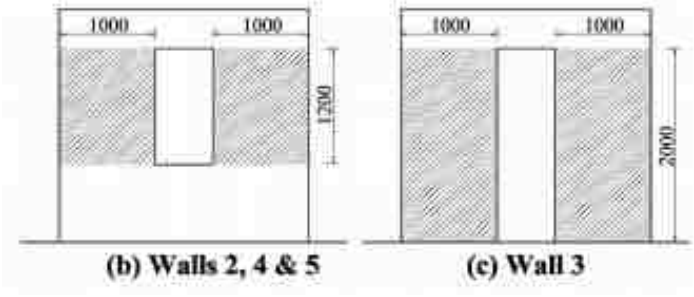

Figure 2-2: Increased vertical opening

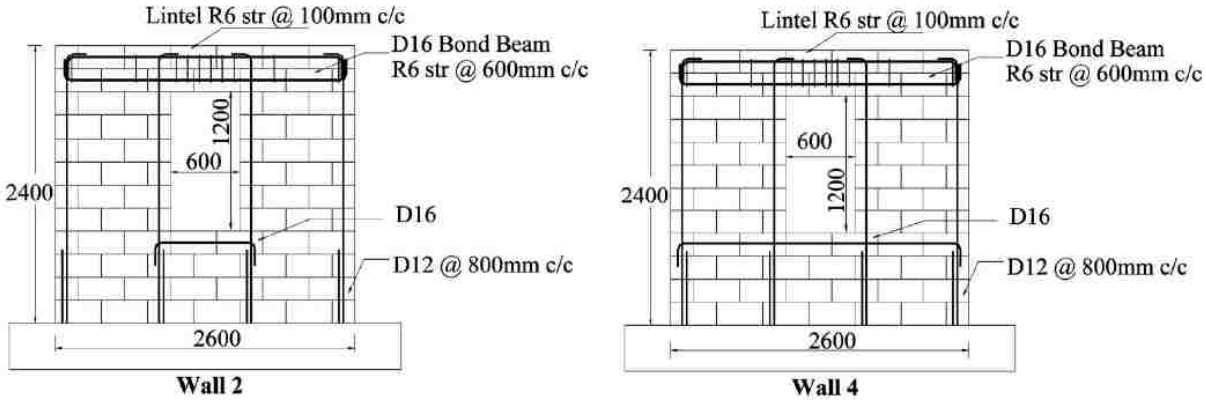

Figure 2-3: Increased trimming reinforcement

Minaie (2009) also studied the parameters affecting partially grouted shear walls. The author concluded that the current Masonry Standards Joint Committee (MSJC) design equations for masonry drastically overestimated the strength of partially grouted walls. The inaccuracies were shown to amplify with increasing shear wall area, increasing vertical and horizontal grout spacing, increasing reinforcement spacing, and wall aspect ratios below 1.0. Additionally, the mortar properties were determined to be unclear in their effect on partially grouted shear walls. Elmapruk (2010) also concluded that the MSJC shear design equations for partially grouted masonry shear walls were highly un-conservative and overestimate the shear strength. In his study of 6 partially grouted squat masonry shear walls, it was determined that there exists a reinforcement ratio beyond which any increase in reinforcement does not result in an increase of shear strength. Nolph (2010) presented research that supported this claim. The author concluded that the maximum shear reinforcement ratio after which no additional shear capacity is obtained appears to be in the range of 0.085% - 0.100% based on a 48 in. grout spacing.

Haach, Vasconcelos, and Lourenco (2011) studied the parameters of aspect ratio, boundary conditions, and vertical and horizontal reinforcement ratios using finite element modeling. A finite element model was developed using the software DIANA®, which was validated against previously tested experimental wall data. The experimental data came from small walls with dimensions of 1206 mm x 800 mm x 100 mm (4’ x 2’7” x 4”), an axial load of 0.56 MPa and 1.30 MPa, vertical reinforcement ratio of 0.098%, and horizontal reinforcement ratios of 0.053%, 0.094%, and 0.126%. Using a micro-modeling approach, the experimental and analytical data sets were calibrated with strength differences within 10%. The authors concluded that lower aspect ratios predominantly develop shear failure modes, whereas higher aspect ratios predominantly develop flexure failure modes. In addition, boundary conditions were determined

to influence the failure mode. Cantilever walls were observed to fail more in flexure whereas fixed end walls were observed to fail more in shear. The effect of vertical reinforcement on lateral strength depended on the failure mode. Lateral strength increased from vertical reinforcement when flexure was the failure mode whereas minimal effects were observed when shear was the failure mode. Horizontal reinforcement was determined to engage after diagonal cracking as it provides a re-distribution of stresses from the masonry to the reinforcement. Thus, horizontal reinforcement was observed to increase lateral strength regardless of the failure mode.

Long, Hamid, and Drysdale (2005) studied the feasibility of using half-scale modelling for in-plane behavior of masonry shear walls. The study observed strength, stress-strain relationships, and failure modes for axial compression and diagonal tension tests. The results of the axial compression tests report the observed masonry compressive strengths (f'_m) of both hollow and grouted, full and half scale units. For hollow units, an average (f'_m) of 23.0 MPa for full scale units and 24.2 MPa for half scale units was determined. For grouted units, an average (f'_m) of 17.1 MPa for full scale units and 17.4 for half scale units was determined. The diagonal tension tests produced significantly more scatter with reasonable results. The results indicated that half-scale units are capable of accurately modelling full-scale masonry as a direct model. In other words, the use of scale factors is not necessary when direct modelling is feasible (Harris 1999).

The review of literature has brought to light important methods and conclusions to be used and compared against in this research. As described, the key parameters influencing shear wall strength include horizontal reinforcement, axial stress, partial or full grouting, aspect ratio, and the strengths of individual constituents. Results of this study will likely confirm previous conclusions while also shedding light on less understood effects such as mortar joint strength.

3 PROCEDURES

3.1 Introduction

In order to effectively perform a parametric analysis using numerical modeling, a numerical model was first calibrated against results based on physical experimental data. Experimental test walls were constructed to obtain data for shear wall response to cyclic loading of two configurations of multi-story, partially grouted, perforated shear walls. The walls were constructed by a mason with the aid of graduate students and research assistants. A custom testing frame was also designed and constructed. Data collection was obtained by means of string potentiometers, strain gauges, LVDT's, actuators, and their respective software. A comprehensive overview of the experimental work is described in detail in Fortes (2017). After completing the physical testing in the laboratory, a finite element model was built using a software program titled FormWorks in VecTor 2. The software used for this experiment is specific to 2 dimensional analyses and effective for masonry and reinforced concrete materials. Once the finite element model was complete, it was validated against the experimental data. Following validation, the model was used to perform a parametric study and the results were compared to the MSJC (2013) code predictions for shear capacity.

3.2 Walls

The foundation of each test wall specimen was constructed of reinforced concrete. Each foundation had dimensions of 13 ft. x 4 ft. x 1 ft. The reinforcement cage had slightly smaller dimensions of 12'8" x 3'8" x 9" and was built using #5 rebar as the top and bottom longitudinal bars and #3 rebar as the transverse bars. Vertical dowels extended up out of the cage to connect the wall to the foundation. The locations of these dowels were as follows: one reinforcement bar in each of the first three vertical cores on the ends of the wall and one reinforcement bar in each of the first three vertical cores adjacent to the openings. Additionally, four #5 U-shaped rebar were tied to the reinforcement cage such that the U would protrude up and out of the foundation to serve as pick points for transporting the wall to the testing location. Pencil rods were secured to the forms at intervals of roughly 2.5 ft. to prevent bowing. Polyvinl chloride (PVC) pipe sections were also tied in specified locations throughout the foundation in order to allow the passing of dywidag rods through the concrete and effectively fix the base to the 3 ft. thick structural floor. Figure 3-1 shows the foundation prior to pouring. Concrete from a ready mix plant was used in the pour and cylinders were cast to determine the concrete properties.

Figure 3-1: Foundation prior to pour

Once the concrete had set, a mason began constructing the walls. The blocks used in each wall were ½-scale concrete masonry units (CMU's) with nominal dimensions of 8" x 4" x 4". The average dimensions of each block actually measured 7.3" x 3.5" x 3.5" and these dimensions were used for subsequent calculations and modeling. The construction itself made use of the running bond pattern. The vertical reinforcement extending out of the foundation continued upward in their respective cores until reaching the top of the wall. Splicing the vertical reinforcement was necessary roughly every story; however, each bar was spliced such that the location of the splice occurred in the middle of the story and not at the reinforced concrete floors. Horizontal reinforcement spanned the entire length of the 5th and top courses of each story in wall 1 and along the length of the opening plus three additional cores on each side of the opening of each story in walls 2 and 3. Local horizontal reinforcement spanned the length of the openings plus three additional cores on either side of the openings in the two courses immediately above the opening in every story as well. Small vertical ties (0.165 in. diameter) were placed one in each vertical core along the length of the horizontal reinforcement directly above the openings and extended up into the reinforced concrete beam representing floor levels. Grout was solely placed in cells containing reinforcement. At the first and second floor levels, a 4 in. thick reinforced concrete beam with #3 longitudinal and transverse rebar was poured to simulate typical floors. The third floor was a 13 in. deep reinforced concrete beam, which was used to transfer load from the actuator to the wall. Total wall dimensions were 14'9" tall, 12'8" wide, and 3.5" thick. The window openings in each story had dimensions of 23 in. tall by 22 in. wide. Each window was centered horizontally and removed courses 6 through 11 of each 14 course story. Wall specimens were cured for 28 days prior to testing. Figure 3-2 depicts a completed

wall prior to testing. Note that the contrasting black and white painted dots were not used in this research.

Figure 3-2: Completed wall prior to testing

3.3 Test Procedures

A customized reaction frame was constructed to allow the actuator to apply a quasistatic, displacement controlled, cyclic load to the top of the wall. Figure 3-3 shows the reaction frame and supports. The main vertical reaction column was a customized W-shape with stiffeners and was secured to the structural floor with tensioned dywidag rods. Three additional diagonal supports were bolted to the main column to provide the necessary in-plane strength and reduce

any bending or deflection of the main column. These diagonal supports were also secured to the structural floor with tensioned dywidag rods. In addition to in-plane supports, one out-of-plane diagonal support was secured to the reaction frame to resist any unexpected out-of-plane force. The actuator was bolted to the main vertical reaction column and was supported underneath using steel columns. On the back side of the wall, out-of-plane supports were installed to prevent any unwanted out-of-plane movement and are shown in Figure 3-4. To accomplish this, three special channels were bolted to the reinforced concrete floors of each story of the wall. A sturdy aluminum shape was placed through each row of channels on each floor. Each aluminum shape was capable of attaching to corresponding arms which were themselves bolted to vertical columns. Thus out-of-plane movement was prevented in either direction with the out-of-plane supports located on only one side.

Figure 3-3: Reaction frame for testing

Figure 3-4: Out-of-plane supports

Once each wall was in place, string potentiometers and LVDT's were attached at selected locations for data measurement. Strain gages were electrically connected that were already attached to the reinforcement prior to pouring concrete or grout. The load protocol used for testing was determined as follows: The load protocol was displacement controlled with 2 complete repetitions of pushing and pulling within each cycle. For the first set of 7 cycles, each cycle would increase in displacement by 0.8 mm (0.0315 in. ≈ 1/32 in.). The next set of 11

cycles increased in displacement by 2.0 mm (0.0787 in. ≈ 5/64 in.). The following set of 13 cycles increased in displacement by 3.2 mm (0.126 in. ≈ 1/8 in.). The last set of 6 cycles increased in displacement by 4.8 mm (0.189 in. ≈ 3/16 in.). The load protocol is shown in Figure 3-5.

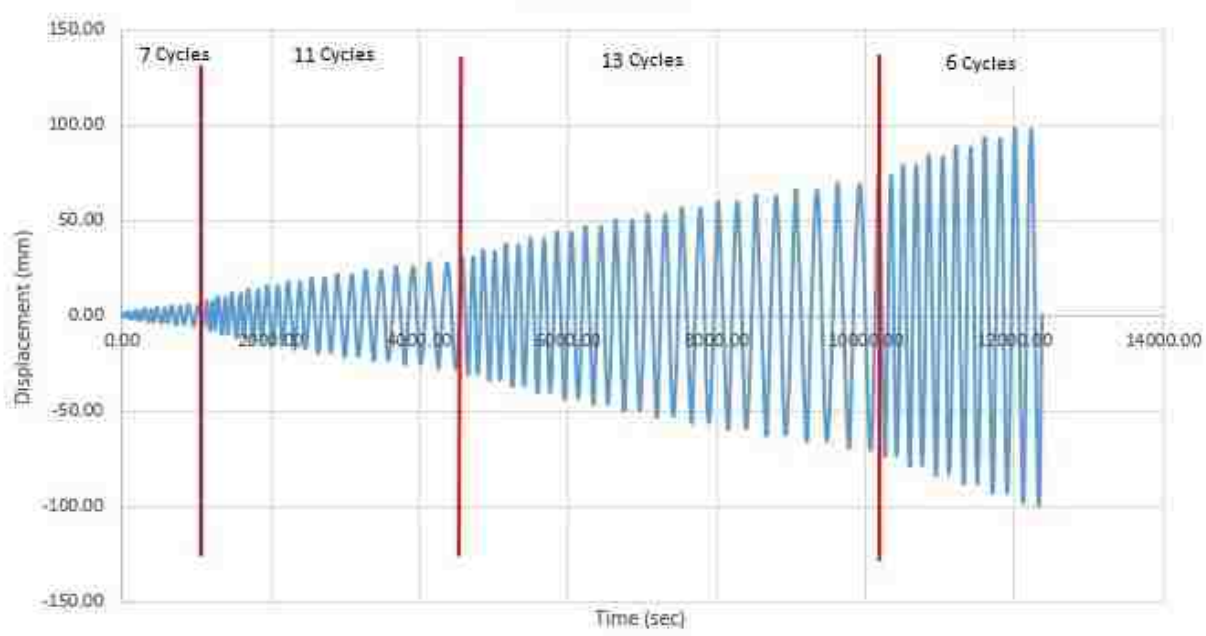

Figure 3-5: Actuator load protocol

An axial load of 11.43 kips corresponding to an axial stress of 21.48 psi was placed on top of each wall using a 10-ton crane. The load was applied by placing a heavy built up steel shape. Underneath the steel was a neoprene mat roughly ¾ in. thick in order to reduce the possibility of stress concentrations. Figure 3-6 shows the axial load in place.

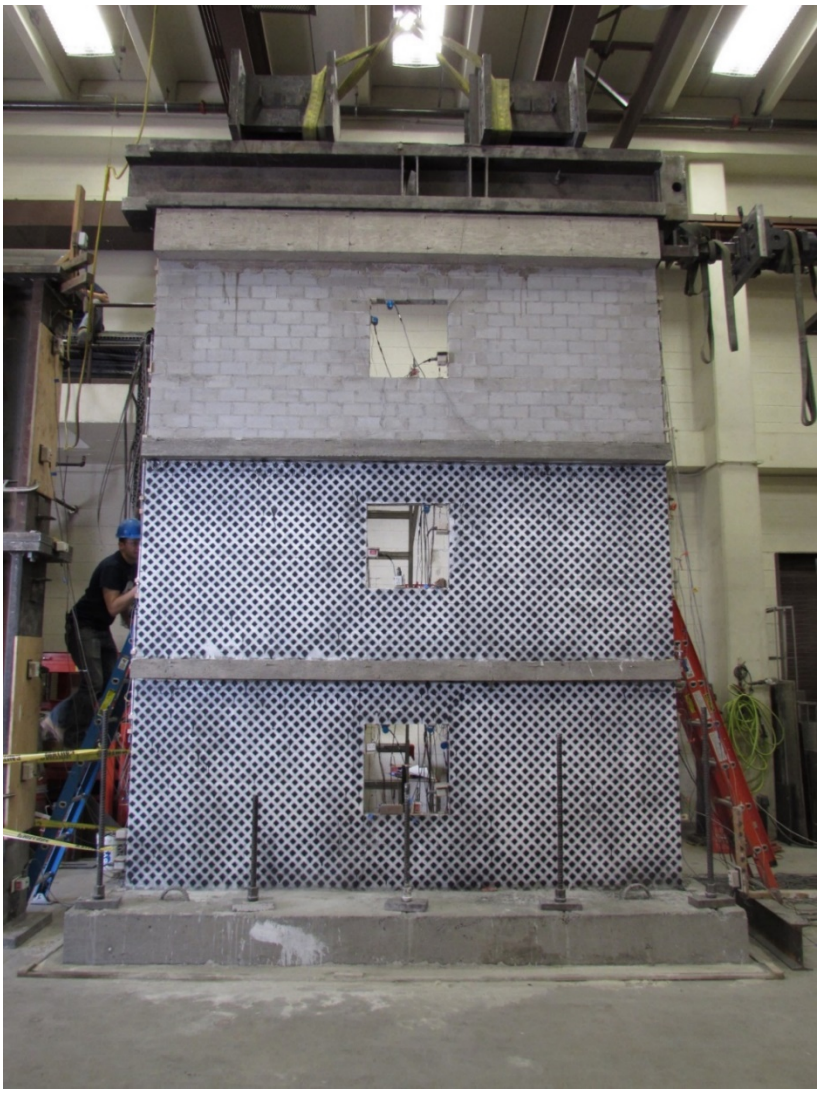

Figure 3-6: Axial load placed on wall

3.4 Finite Element Modeling

The two modeling approaches commonly implemented when using finite element analysis are macro and micro modeling (Chaimoon and Attard 2006). Macro modeling takes a broad approach in applying material properties to the computer model. In other words, there is no distinction between the mortar joints and the masonry unit, rather their properties are smeared into an average that is applied to the entire system. The advantages of such modeling techniques

are speed in both building and running models. Good models of simple configurations are capable of obtaining accurate results. Micro modeling follows a more detailed approach in building a model that distinguishes between constituents. Thus, material properties are distinguished for un-grouted masonry units, grouted masonry units, mortar, and reinforcement. The advantages of using micro modeling techniques are a better understanding of load path, crack propagation, failure modes, and (appropriate for this study) the effects of parameters on masonry shear walls. In order to accurately and effectively model the complex system that was physically tested, a micro modeling approach was used to model the shear walls in this research.

The software VecTor 2 was chosen as the program to model the masonry walls. This software is currently a free program that was developed at the University of Toronto over the course of two decades. The software itself is a suite of programs that may be used for nonlinear finite element analysis. The preprocessor, FormWorks, was used to build the model and run the analysis whereas the postprocessors, Janus and Augustus, were used to obtain, sift, and analyze the necessary data. The theoretical bases of VecTor 2 are the Modified Compression Field Theory and the Disturbed Stress Field Model which are capable analytical tools for predicting the response of reinforced concrete elements to in-plane normal and shear stresses (VecTor 2 Manual). While VecTor 2 was originally developed for the use of reinforced concrete, it has been expanded to effectively model other materials including masonry, steel, and orthotropic wood.

As mentioned, the model was constructed in the preprocessor program FormWorks. To appropriately accommodate for the placement of discrete reinforcement and to obtain more accurate results from the finite element method, the nodes and elements were modeled as square instead of rectangular like the CMU's. Thus the model contains elements with nominal

dimensions of 4” x 4” x 4” whereas the nominal dimensions of the actual CMU’s were 8” x 4” x 4”. Consequently, the model encompasses 39 nodes with 38 elements per complete course whereas the physical walls contained 19 CMU’s in a complete course. The finite element model is shown in Figure 3-7 and the color scheme described in Table 3-1.

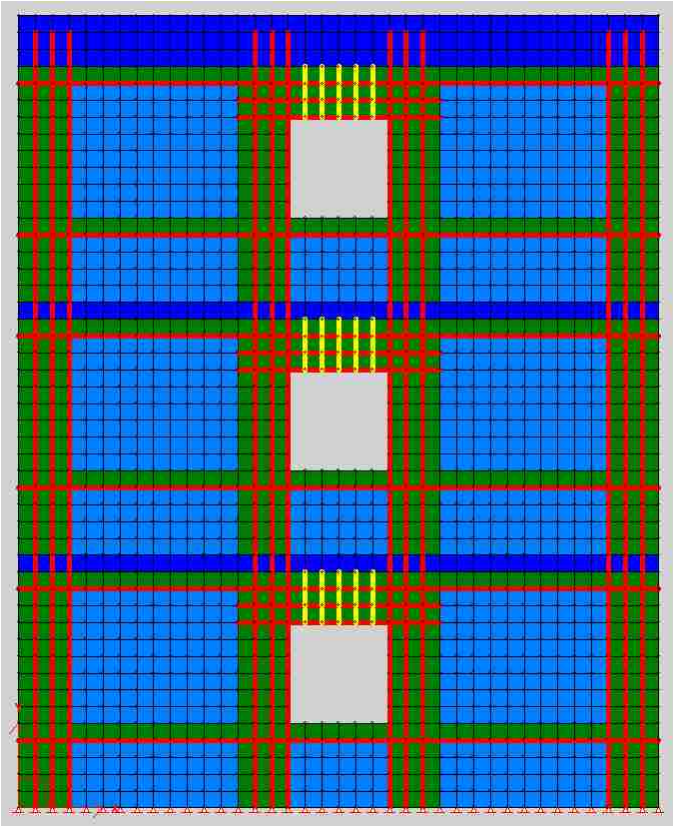

Figure 3-7: Finite element model of experimental wall

Table 3-1: Finite element model color scheme

Color	Description
Aqua Blue	Un-grouted Portion of the Wall
Royal Blue	Reinforced Concrete
Green	Grouted Portion of the Wall
Red	#3 Reinforcement
Yellow	0.165 in. (4.2 mm) Diameter Reinforcement

The model required various inputs for which both material testing and engineering judgement were necessary prior to being changed. A brief explanation will be given regarding which inputs were used for certain materials and why they were changed or left unchanged.

Figure 3-8 shows the Define Material Properties box. This figure in particular shows the properties for Material 1 which corresponds to the un-grouted (aqua blue) elements. Materials 1 – 5 all had similar inputs, however, only a description of Materials 1 and 3 was given in order to fully explain all categories of the Define Material Properties box. Furthermore, the descriptions of each material listed was presented in Table 3-2 for reference. Under the Material Properties section of the box, the Reference Type refers to the corresponding type of material which in the case of Material 1 was masonry. The Thickness T was calculated from the thickness of the two outer flanges of the CMU's. The thickness of the two flanges added together was approximately 1.5 in. (38.1 mm). The Compressive Strength f_{my} was determined from a hallow prism test on multiple blocks which resulted in an average strength of 1803.2 psi (12.43 MPa). The Tensile Strength f_{ty} was neglected and therefore taken as 0 MPa. The Initial Elastic Modulus E_{my} was determined to be 18,605.1 MPa and was calculated from equation 3-1, which is the default value within the VecTor 2 program. The Joint Spacing corresponded to the actual joint spacing of the physical walls which for bed joints was 8 in. (203.2 mm) in the "perpendicular to y direction" and for head joints was 4 in. (101.6 mm) in the "perpendicular to x direction". Note that the bed joint dimension for each element was input as 8 in. (203.2 mm), however the width of the element was only 4 in. (101.6 mm). Joint properties are smeared across a single finite element (VecTor2 Manual). Therefore, a possible consequence of creating a model with 2 elements per CMU is indirectly adding a joint in the middle of each CMU where there was no joint present in the experimental walls. No description of applying elements in this manner was provided in the

VecTor2 Manual. The section entitled Smeared Reinforcement Properties was not used in Material 1, which can be verified by noting the Reinforcement Components section is empty.

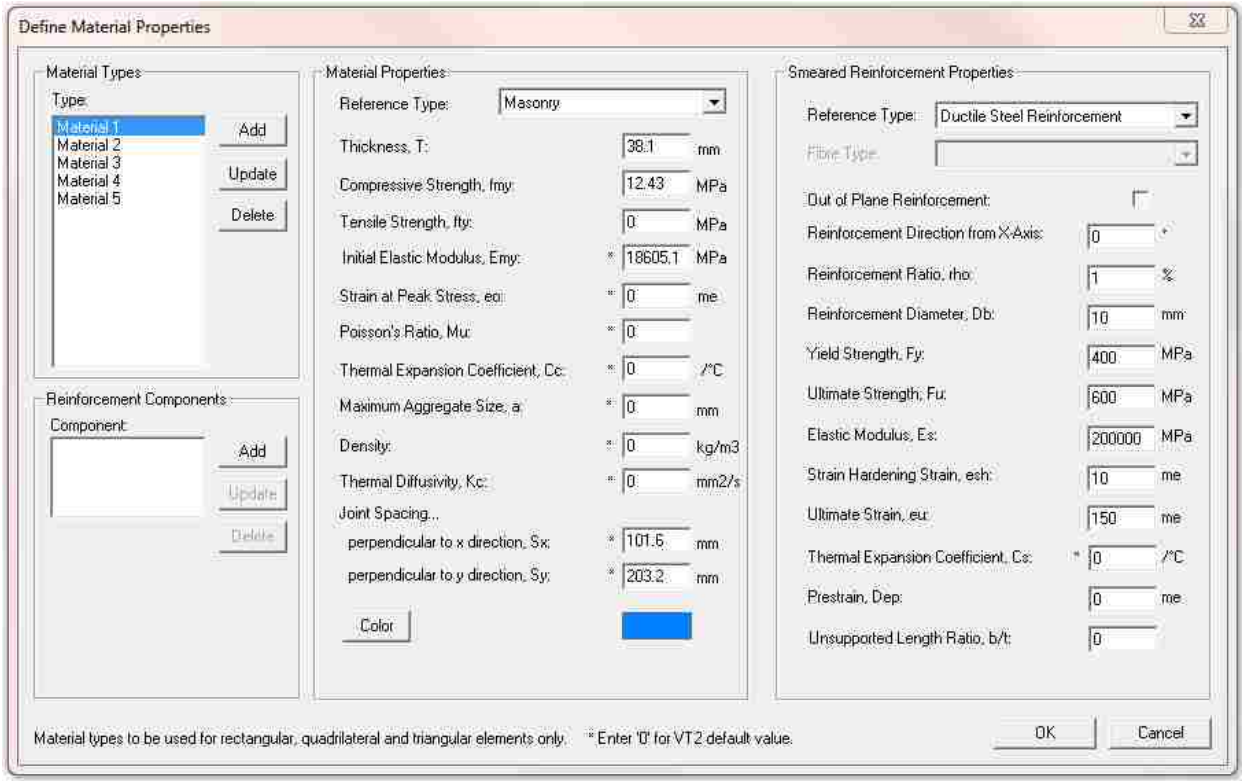

Figure 3-8: Inputs under define material properties box for Material 1

Table 3-2: Material description for finite element model

Name	Description
Material 1	Un-grouted Portion of the Wall
Material 2	Grouted Portion of the Wall
Material 3	Floor 1
Material 4	Floor 2
Material 5	Floor 3

$$E = 3320\sqrt{f'm} + 6900\ MPa \qquad \text{Equation 3-1}$$

Figure 3-9 again displays the Define Material Properties Box, however, this time presented for Material 3. This material corresponds to the Royal Blue elements representing the first reinforced concrete floor. The Material Properties section contains similar information to that of Material 1 described in the previous paragraph, however, the values were unique to Material 3. The Smeared Reinforcement Properties section now contains valuable information regarding the reinforcement located inside the reinforced concrete floor. The Reference Type refers to the type of reinforcement used, which in this case was Ductile Steel Reinforcement. Reinforcement 1, under the Reinforcement Components section, represents the out-of-plane reinforcement which is confirmed by the checked box for Out-of-Plane Reinforcement under the Smeared Reinforcement Properties section. The Reinforcement Direction from the X-Axis is an input value between 0º and 360º used for in-plane reinforcement, therefore, when referring to out-of-plane reinforcement a value automatically outside this range is applied. The Reinforcement Ratio refers to the ratio of cross-sectional area of the reinforcement to the area of concrete over which it is smeared, as a percentage (VecTor 2 Manual). The calculation of 34 #3 bars divided by the out-of-plane area resulted in a percentage of 0.65%. The diameter of #3 rebar is 3/8 in. (9.5 mm). The Yield Strength, Ultimate Strength, and Elastic Modulus inputs were the results of an average of 3 test specimens shown in Table 3-3. The remaining inputs were left unchanged at their default values. Reinforcement 2 under the Reinforcement Components section represents the in-plane reinforcement which is confirmed in Figure 3-10 by the un-checked box

for Out-of-Plane Reinforcement under the smeared Reinforcement Properties section. The remaining inputs for Reinforcement 2 are similar to the inputs previously described.

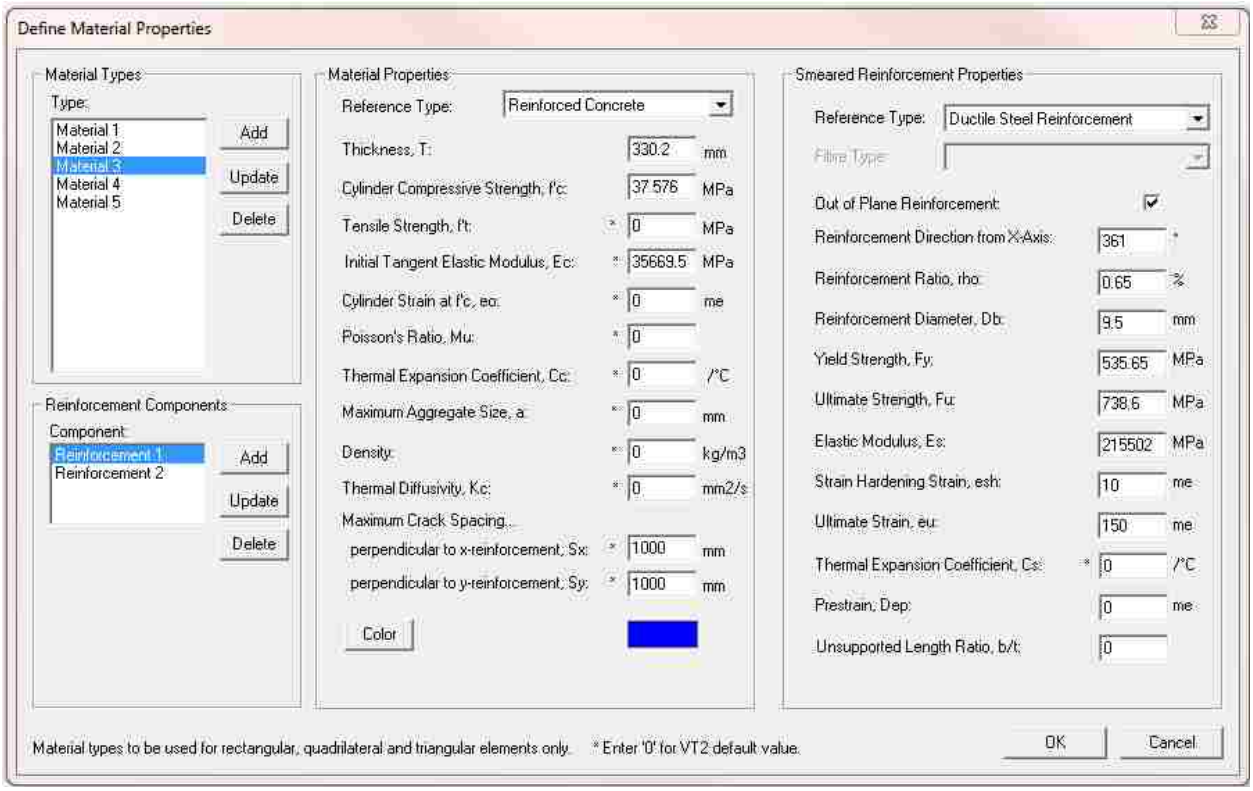

Figure 3-9: Inputs under define material properties box for Material 3

Table 3-3: Reinforcement properties for #3 rebar

Sample	Yield Strength (ksi)	Ultimate Strength (ksi)	Elastic Modulus (ksi)
1	81.70	106.72	37,885
2	73.96	106.29	28,093
3	77.41	108.37	27,791
Average	**77.69**	**107.13**	**31,256**

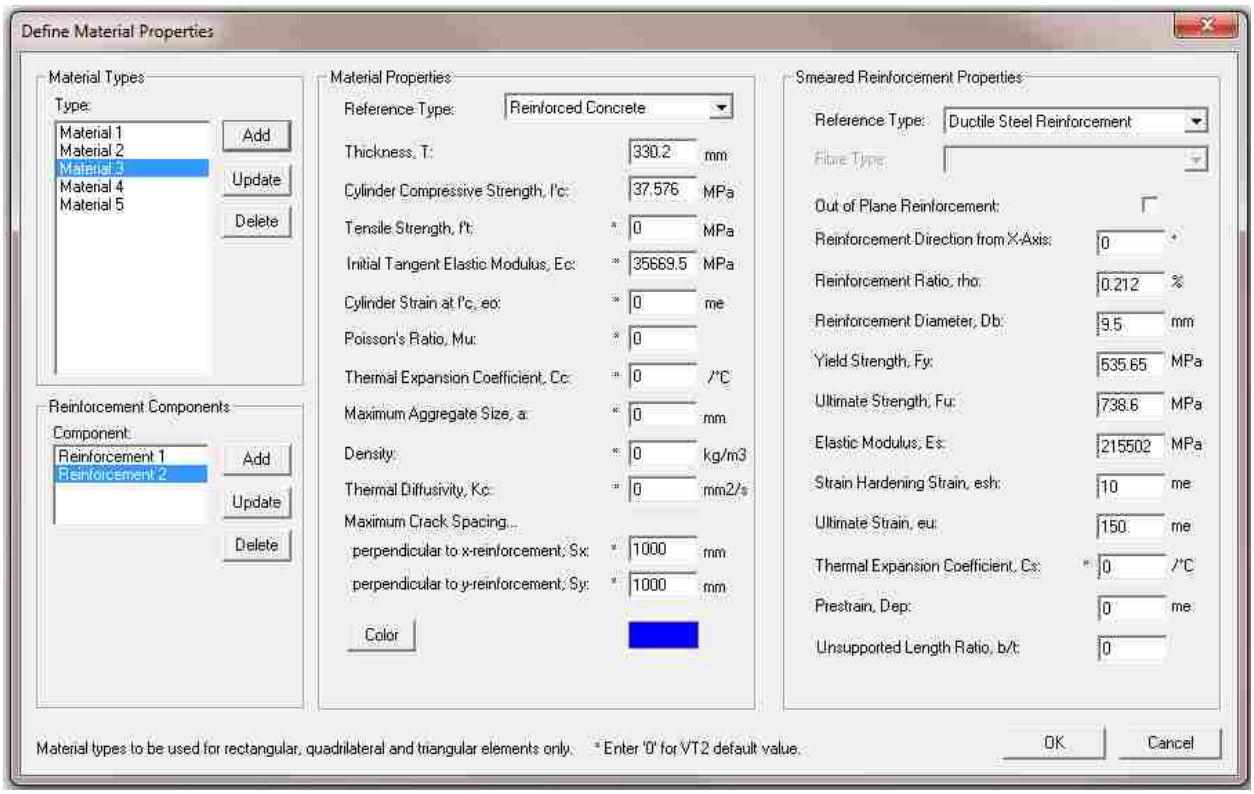

Figure 3-10: Out of Plane Reinforcement is left unchecked

Discrete reinforcement properties were entered separately from the smeared reinforcement properties. The discrete reinforcement represents the horizontal and vertical bars inside the grouted cells, whereas the smeared reinforcement represents the steel cages located inside the reinforced concrete beams. To input the properties of discrete reinforcement, the Define Reinforcement Properties box was used and is shown in Figure 3-11 and Figure 3-12. For discrete reinforcement, Reinforcement 1 represents the #3 bar (red elements in Figure 3-7) used for both horizontal and vertical steel. Reinforcement 2 represents the 0.165 in. diameter bar (yellow elements in Figure 3-7) used as the vertical reinforcement just above the openings. The

Reference Type refers to the type of reinforcement used which in this case was Ductile Steel Reinforcement. The Cross-Sectional Area and Reinforcement Diameter were calculated and measured properties. The Yield Strength, Ultimate Strength, and Elastic Modulus inputs were the results of an average of 3 test specimens and input accordingly.

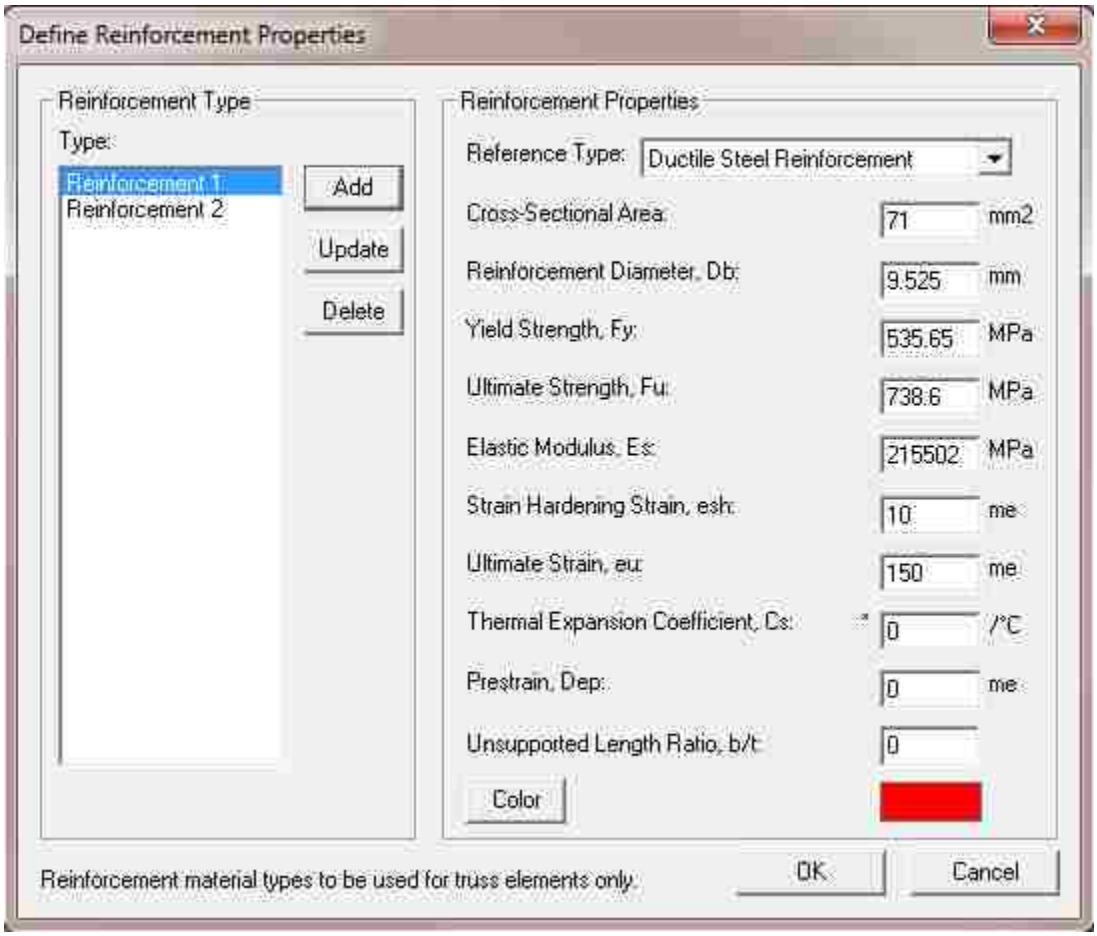

Figure 3-11: Input properties for #3 reinforcement bar

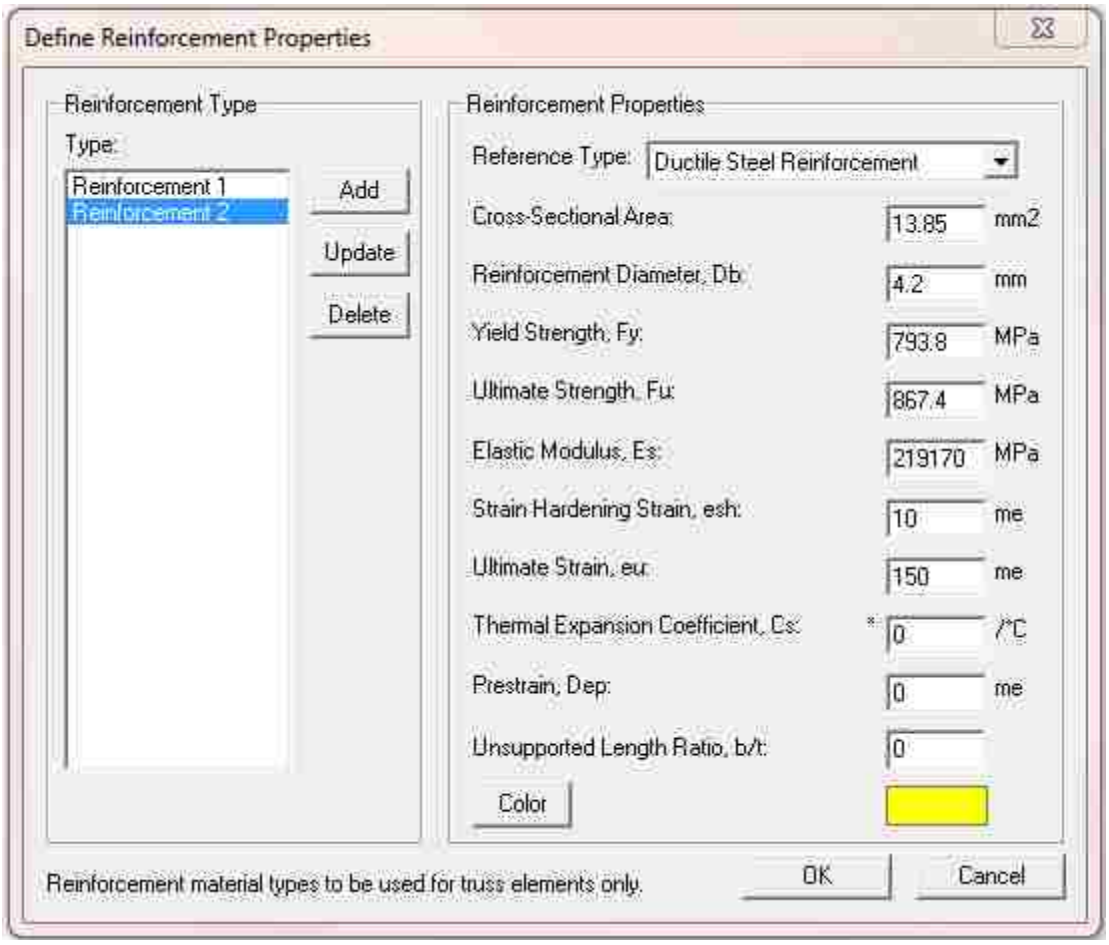

Figure 3-12: Input properties of 4.2 mm reinforcement bar

Additional model inputs were located within the Define Job box, which is shown in Figure 3-13. An explanation of the pertinent inputs is given for the Job Control tab. As only one input was changed under each of the Models and Auxiliary tabs, only brief explanations of these tabs is mentioned. Within the Job Control tab, the Structure Type under the Structure Data section was changed to Plane Membrane (2-D) which by definition was the type of model that was analyzed. The Starting load stage no. under the Loading Data section was set at 1 as each

analysis was a distinct test and not the continuation of a previously initiated analysis. The No. of load stages was calculated as 18,834 using a specific formula unique to VecTor 2 shown in equation 3.2. Variables contained in this formula are further defined below the equation. Activated load cases are those whose boxes were checked, which in this model were Case 1 and Case 2. Load Case 1 represented the axial and self-weight loads. Since these loads were constant, the Initial and Final Factor inputs are defined as the same value of 1. The Incremental Factor was entered as 0 because no increase in axial and self-weight loads were desired between load stages. The load type for these loads was considered monotonic. The initial load stage was input as 1 so as to have these loads applied throughout the duration of the test. Load Case 2 represented the reverse cyclic displacement of the actuator. In this case, the Initial Factor was entered as 0 and the Final Factor was entered as 0.8 which signifies the displacement at the first load stage was 0 and the maximum displacement of the first set of repetitions was 0.8. The Incremental Factor was set at 0.2 thus requiring 16 load stages to complete one cycle – 4 load stages from start (0) to maximum displacement (0.8), 4 load stages from maximum displacement (0.8) back to initial value (0), 4 load stages from initial value (0) to maximum negative displacement (-0.8), and 4 load stages from maximum negative displacement (-0.8) back to initial value (0). There were 2 repetitions at each displacement in the experimental load protocol, thus the same was desired in the theoretical model. The Cyclic Incremental Factor of 2.65 is described in the following paragraph. It was desired to start the Reverse Cyclic loading procedure immediately, thus the Initial Load Stage was entered as 1.

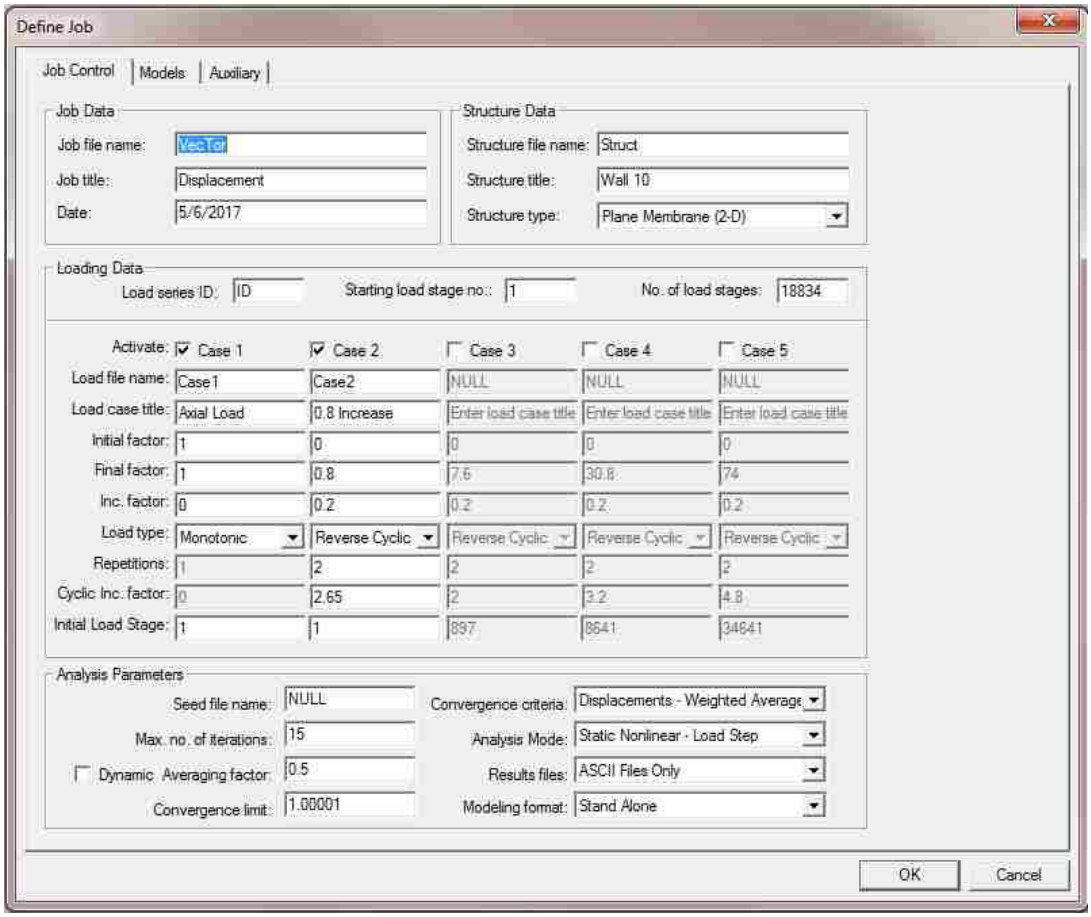

Figure 3-13: Inputs for the Job Control tab of the Define Job box

$$No.Stages = 4(R * S)\left(\frac{LF_f - LF_i}{LS_{inc}}\right) + \left(\frac{2*R*C_{inc}}{LS_{inc}}\right)(S(S-1)) + 1 \qquad \text{Equation 3-2}$$

R = number of repetitions

S = number of sets of full repetitions

LF_f = final load factor

LF_i = initial load factor

LS_{inc} = load factor increment for each load stage

C_{inc} = cyclic load factor increment

The Cyclic Incremental Factor is the change in the final load factor from one set of repetitions to the next. The value of 2.65 was calculated using a weighted average of the number

of cycles and displacements at each cycle. This calculation is shown in equation 3-3. The loading protocol for the actuator (Figure 3-5) was predetermined to be 7 cycles of 0.8 mm increases, followed by 11 cycles of 2 mm increases, followed by 13 cycles of 3.2 mm increases, and concluded with 6 cycles of 4.8 mm increases. To perform the finite element analysis by running the model in a single event, only a single Cyclic Incremental Factor may be input. Thus the weighted average of 2.65 was used. A graphical representation in Figure 3-14 shows how the finite element load protocol initially had slightly higher displacements than the actuator load protocol, however, with increasing load stages the experimental displacements soon became equal to and then slightly greater than the finite element displacements. Therefore, the weighted average was determined to be a reasonable representation of the experimental testing.

$$Cyclic\ Incremental\ Factor = \frac{7(0.8)+11(2)+13(3.2)+6(4.8)}{37} = 2.65 \qquad \text{Equation 3-3}$$

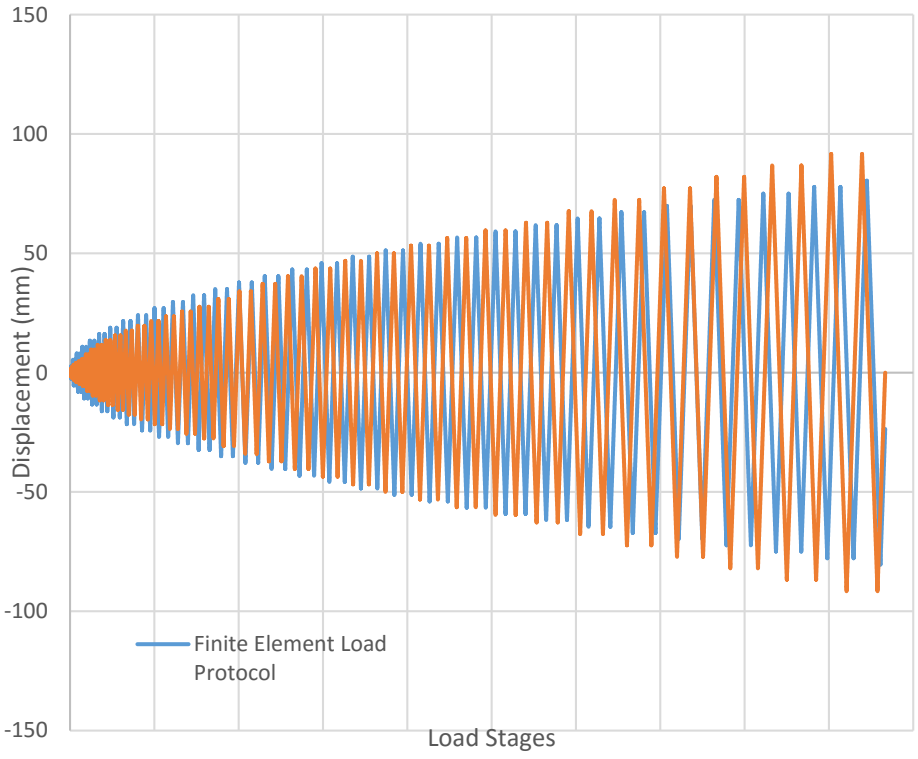

Figure 3-14: Comparison of actuator load protocol and finite element load protocol

The Analysis Parameters section of the Job Control tab also contained pertinent inputs. The Max. no. of iterations refers to the maximum number of attempts that the computer performed calculations in order to reach a convergence of the solution. This value was input such that no matter the convergence quality, VecTor2 proceeds to the next load stage once the specified number of iterations has been performed. A value of 15 was determined to produce an adequate convergence of the solution. This was confirmed and displayed in Figure 3-15. After 15 iterations, the convergence value was very close to the convergence limit. The convergence limit is the ratio of the current convergence value to the previous convergence value. As this value approaches 1, the more stringent the convergence criterion becomes. During this research, the Convergence limit was decided to be 1.00001. With these definitions of maximum iterations and convergence limit the solution would either be very accurate or after 15 iterations would be considered close enough for the program to continue to run. Lastly the Convergence criteria input was a weighted average of the displacements and the analysis mode for this type of quasistatic testing was Static Nonlinear – Load Step.

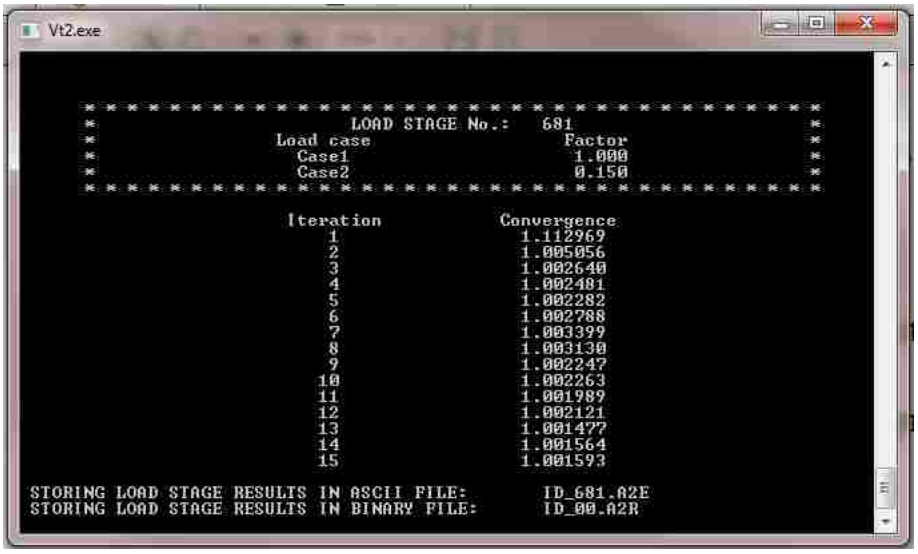

Figure 3-15: Convergence after 15 iterations

The Models tab of the Define Job box is displayed in Figure 3-16. The inputs represent distinct mathematical constitutive models. At each load step the structure stiffness is determined from stresses and strains calculated using these models (VecTor2 Manual). Thus it is essential to use a model that accurately captures wall behavior. The Compression Pre-Peak input under the Concrete Models section used the Hognestad (Parabola) model. This model is a simple response curve suitable for normal concrete strengths < 40 MPa. None of the masonry walls in question had masonry compressive strengths greater than 40 MPa, therefore this model was an appropriate choice. The Compression Post-Peak input was decided as the Base Curve. This model is a valid selection if the Hognestad (Parabola) model is used as the Compression Pre-Peak response (VecTor2 Manual). For the remaining models, it is recommended the default models be used (VecTor2 Manual) which proved appropriate for this study.

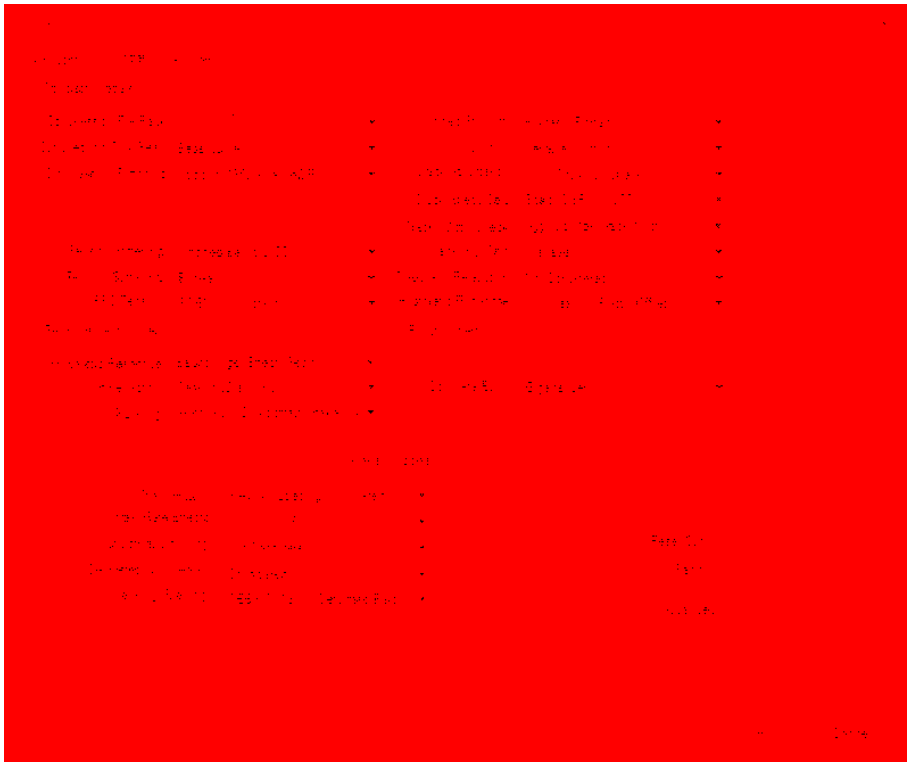

Figure 3-16: Inputs for the Models tab of the Define Job box

The Auxiliary Tab of the Define Job box is displayed in Figure 3-17. In this tab, only the Joint Shear Strength Ratio was changed. The joint shear strength ratio is the ratio between the shear strength of the joints and the maximum compressive strength (VecTor2 Manual). The shear strength of the mortar was not a parameter previously determined in the lab; therefore, this value was approximated as the Nominal Masonry Shear Strength specified by MSJC (2013) (equation 3-4). The maximum compressive strength of masonry was calculated using equation 3-5. The Joint Shear Strength ratio was calculated as 0.0189 (see Appendix A for calculations). The calculated value was reasonable as it was close to the default value of 0.01.

$$V_{nm} = \left[4.0 - 1.75\left(\frac{M_u}{V_u d_v}\right)\right] A_{nv}\sqrt{f'_m} \qquad \text{Equation 3-4}$$

$$C = A_n f'_m \qquad \text{Equation 3-5}$$

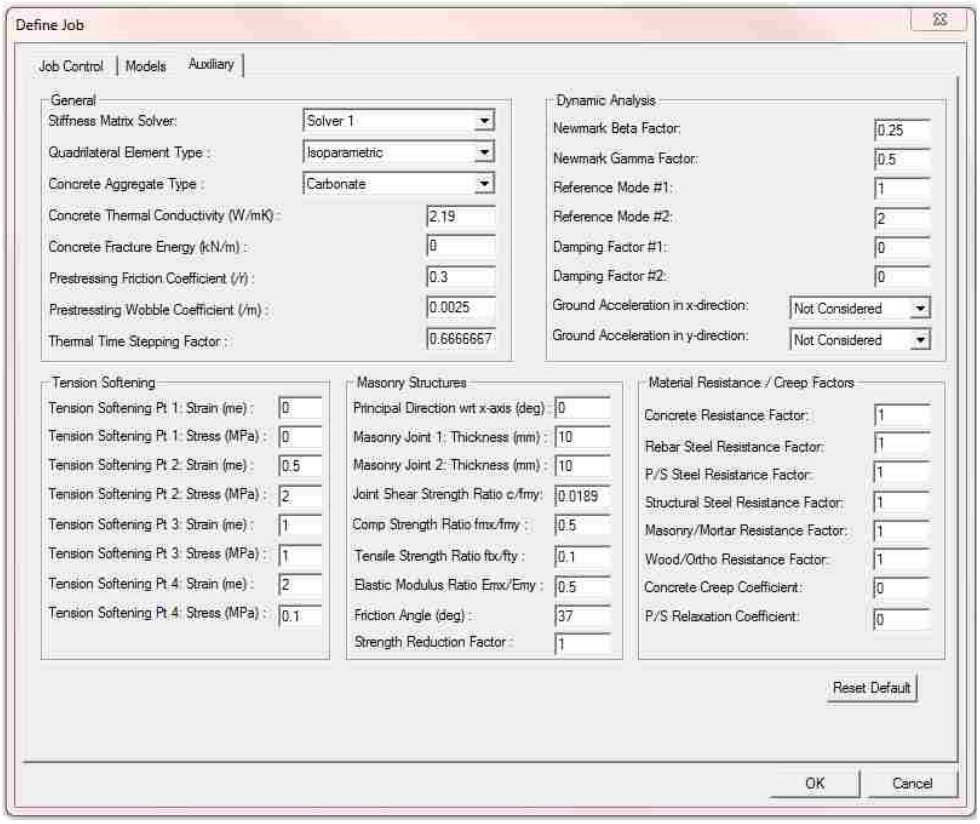

Figure 3-17: Inputs for the Auxiliary tab of the Define Job box

Once the characteristic properties of the masonry wall were set, the boundary conditions, applied axial load, and self-weight of the masonry was added to the model. Each node along the bottom row was restrained in both the x and y (in-plane and out-of-plane) directions. An axial load of 11.43 kips representing the applied axial load of the experimental wall was added to the model as vertical downward nodal loads along the top of the wall (see Figure 3-18). As FormWorks is a software that uses SI units, 11.43 kips was converted to kilo-newtons (kN) and distributed along the elements to obtain a uniform load of 1.34 kN/node. The self-weight of the masonry was input into the model as a mass density and the software calculates the gravity load based on element volume. As displayed in Figure 3-18, the mass densities used for the reinforced concrete (royal blue), grouted masonry (green), and un-grouted masonry (light blue) were 2400 kg/m^3 (150 pcf), 2250 kg/m^3 (140.5 pcf), and 1018 kg/m^3 (63.6 pcf) respectively. For calculations of the determined mass density, refer to Appendix A.

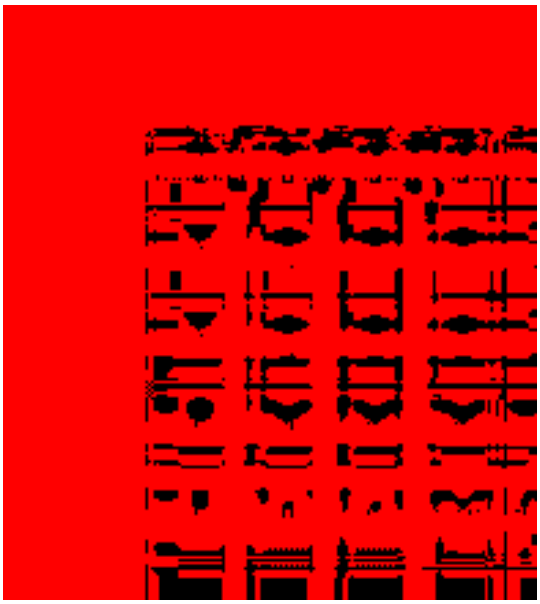

Figure 3-18: Axial load applied to nodes on top of wall and element mass densities

After the representative model was completed with the corresponding material properties and section geometries entered, the model was analyzed and compared with the experimental results and MSJC (2013) code calculations. The experimental results of the load-displacement curve indicated that wall 1 was capable of resisting a maximum of 24.8 kips. while displacing a total of 0.552 in. at maximum capacity. The theoretical results of the load-displacement curve indicated that the representative model was capable of resisting a maximum of 23.4 kips. while displacing 0.666 in. at maximum capacity. The MSJC (2013) code prediction for shear strength of wall 1 was calculated as 30.2 kips (see Appendix A for calculations). The model strength was conservatively within 6% of the experimental measured strength and the model displacement was within 20% of the experimental displacement corresponding to the maximum strength for wall 1. The code un-conservatively over-predicted the observed shear wall capacity by 29.1%. The experimental results for walls 2 and 3 indicated maximum shear strengths of 22.8 kips with corresponding displacement of 0.451 in. and 22.5 kips. with corresponding displacement of 0.477 in. The finite element model for these walls a reached peak strength of 23.2 kips and corresponding displacement of 0.558 in. The MSJC (2013) code prediction for shear strength of walls 2 and 3 was calculated as 30.2 kips (see Appendix A for calculations). The model was within 1.8% and 3.2% of maximum shear capacity and within 23.7% and 17.0% of corresponding displacement for walls 2 and 3 respectively. The code un-conservatively over-predicted the observed shear wall capacity by 32.5% and 34.2% for walls 2 and 3 respectively. According to the results, the models were considered validated. Graphical representations of the backbone curves for the experimental and finite element models are shown in Figure 3-19 and Figure 3-20. For full hysteresis curves of the experimental and finite element models, see Appendix B Figures B-1 to B-5.

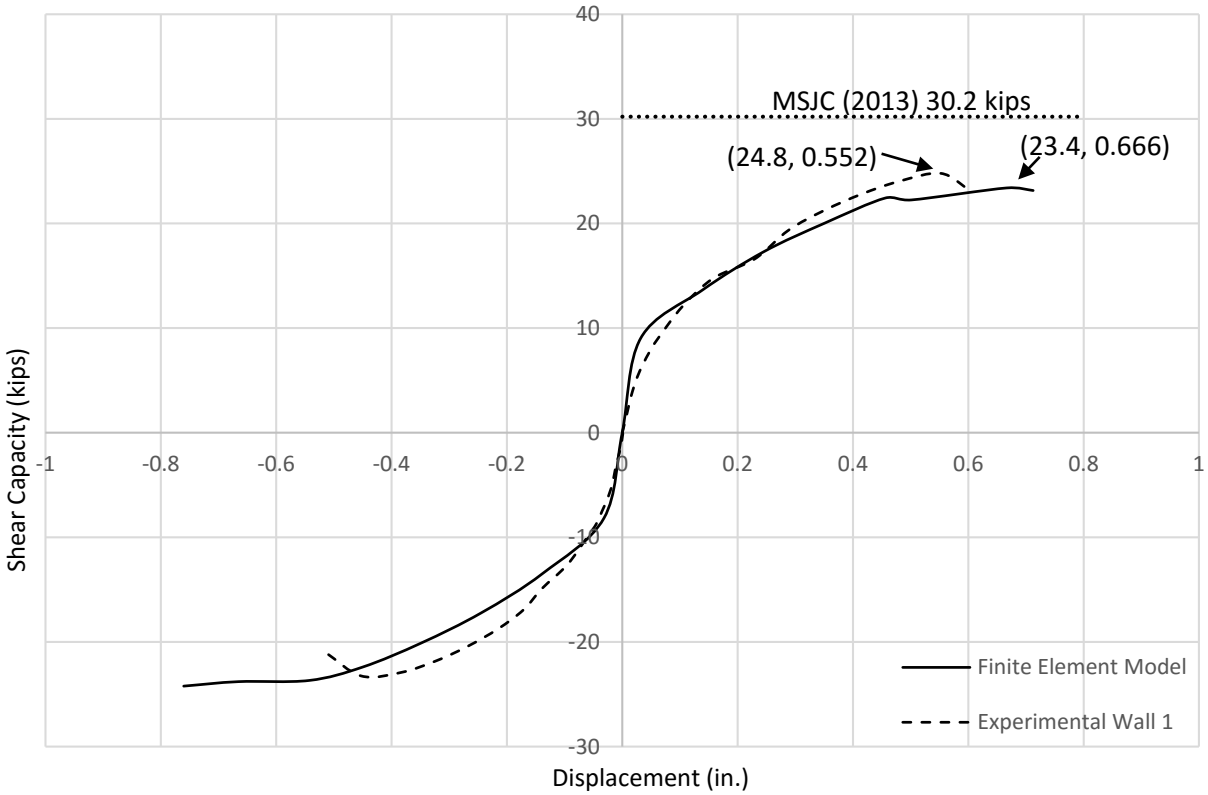

Figure 3-19: Backbone curves of wall 1 vs. finite element model

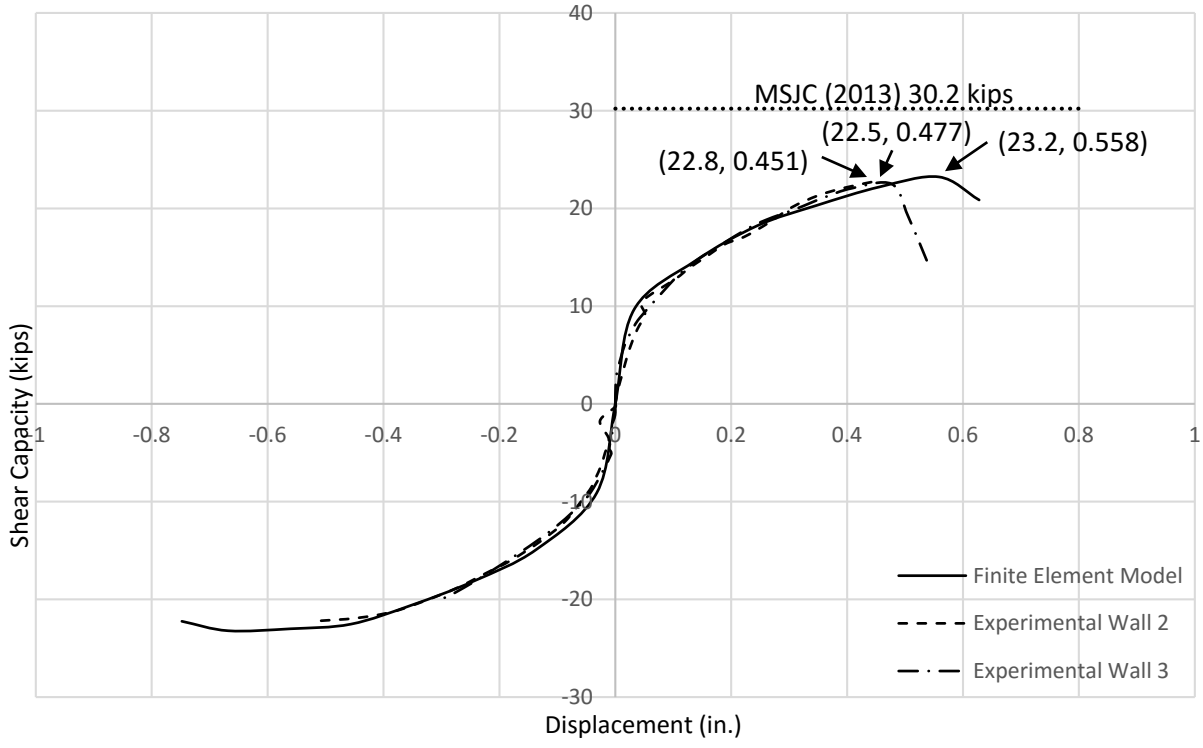

Figure 3-20: Backbone curves of walls 2 and 3 vs. finite element model

To further validate the finite element models, crack propagations observed in the experimental walls were compared with the crack patterns of the model. In Figure 3-21 and Figure 3-22, the red lines of the finite element model show the crack directions. The fewer but thicker red lines represent cracks > 2 mm. The outer images are photographs taken from wall 1 which show step cracking through the mortar in approximately the same locations. Such similarities further validate the models in question. For enlarged crack pattern images of the experimental walls see Appendix C Figures C-1 to C-5.

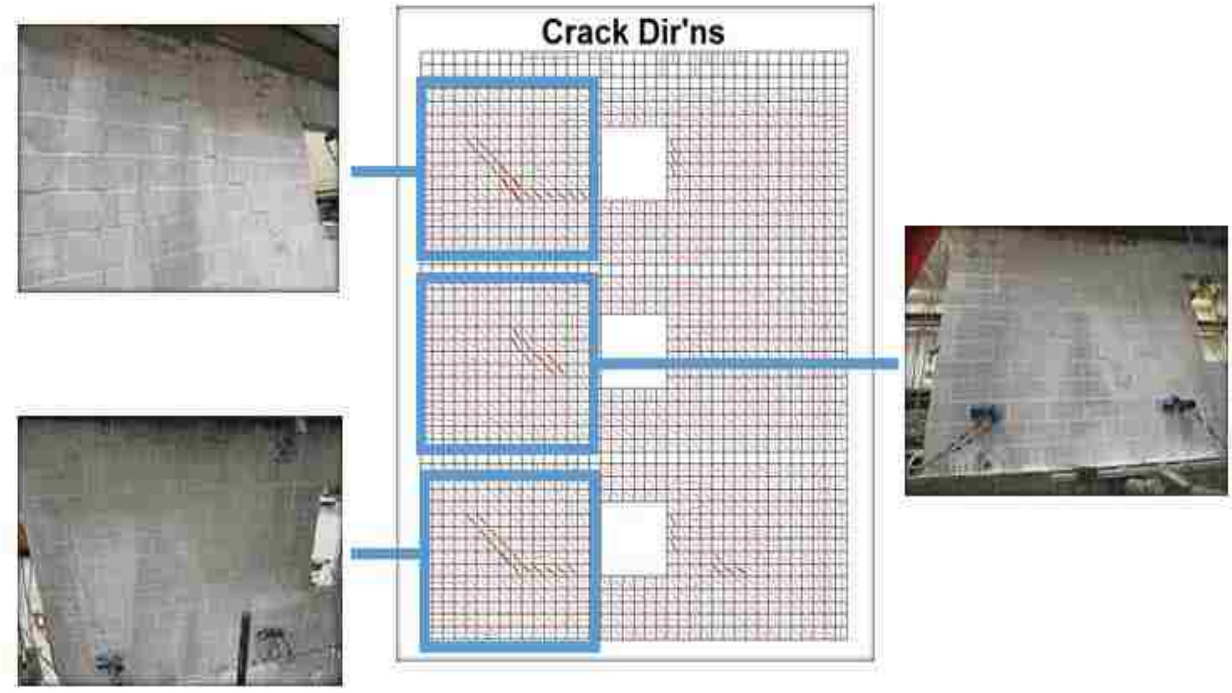

Figure 3-21: Cracks noted in push regime of experimental wall and finite element model

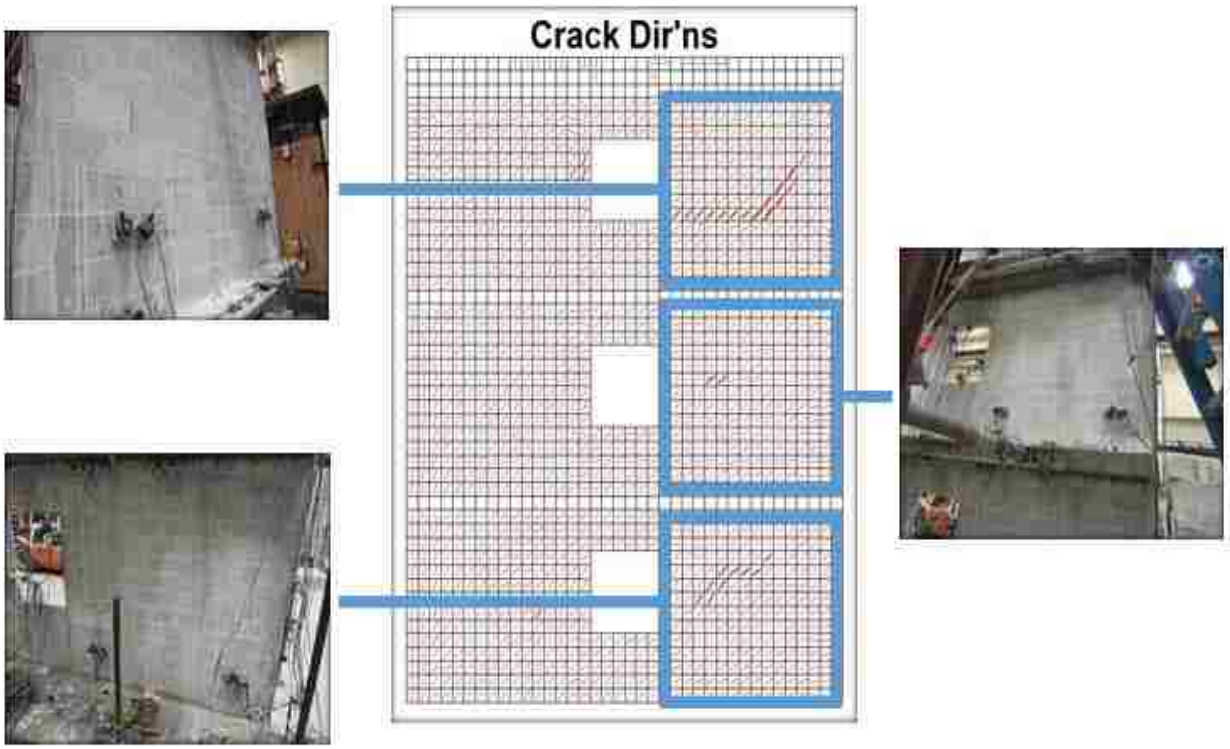

Figure 3-22: Cracks noted in pull regime of experimental wall and finite element model

The limit after which no additional load could be carried by the experimental walls resulted from a combination of shear failure and de-bonding between the reinforcement and grout (Fortes 2017). The shear failure was characterized by diagonal cracking and sliding as shown in Figure 3-23 and Figure 3-24. De-bonding of the reinforcement was internal and therefore not visible; however, it was deemed implied and necessary for such large cracks to open.

Figure 3-23: Diagonal Cracking

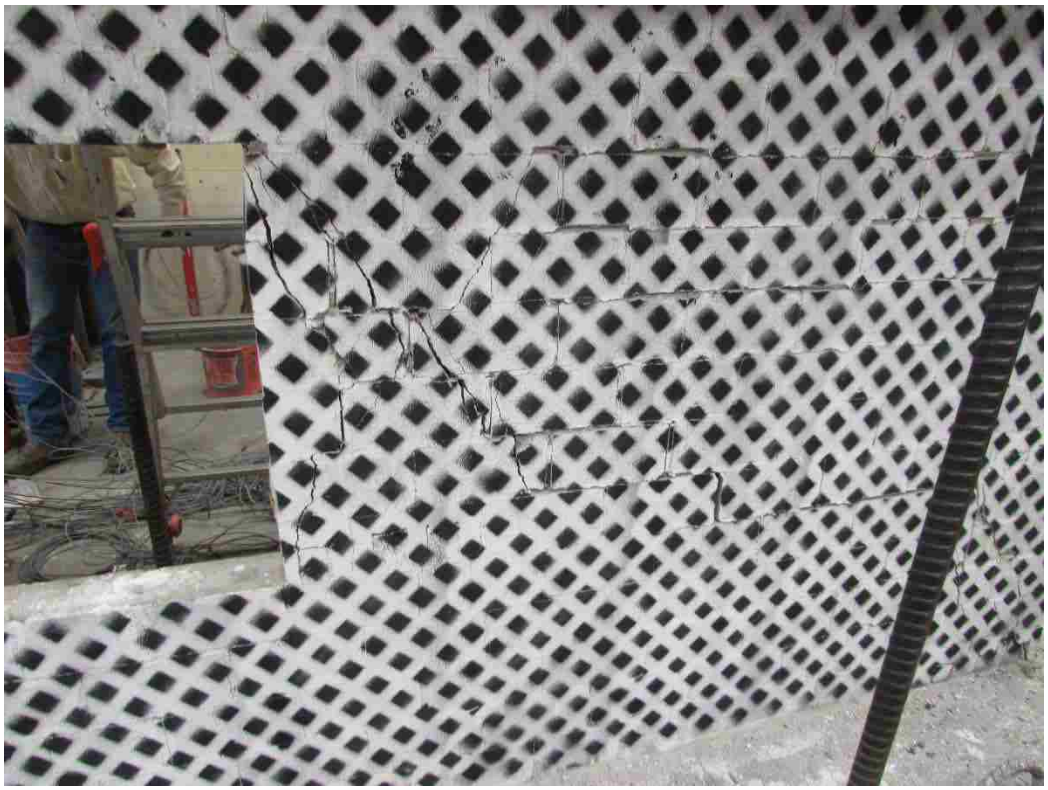

Figure 3-24: Diagonal cracking and sliding

3.5 Parameters

As demonstrated in previous research, parameters that influence the shear strength of a masonry wall include: the strength of individual components (mortar, grouted masonry units, un-grouted masonry units, and reinforcement), applied axial load, aspect ratio (height-to-width ratio), reinforcement size and spacing, and the presence of openings within the wall. In order to determine the effect of each of these parameters, one variable was varied from the validated "base models" and a finite element analysis was run after each modification. This section describes the variables that were modified and why the values determined were appropriate for each variable.

3.5.1 Strength of Grouted Masonry Units

Grout is an important constituent of masonry that provides additional strength in walls by filling voids and creating a bond between the masonry units and the reinforcement. The grouted masonry units are an integral part of a partially grouted masonry shear wall system. Therefore, the compressive strength of grouted masonry units affects the performance of the wall. Discrete grout elements and properties were unable to be added to the finite element model, however, the strength of grouted masonry units ($f'_{m,grouted}$) was varied by changing the input for grouted masonry compressive strengths. This input refers to the value of f_{my} in Figure 3-8 for Material 2. The base model value of f_{my} equal to 2139.3 psi (14.75 MPa) was determined from compression testing of the experimental grouted prisms. ASTM C90 *Standard Specification for Loadbearing Concrete Masonry Units* states that the minimum compressive strength for normal weight CMU's is 1800 psi (12.41 MPa) for an individual unit and 2000 psi (13.79 MPa) for an average group of three units. The base model was close to these minimum masonry compressive strengths, consequently only values larger than the base model were chosen to vary this

parameter. It is not unreasonable to consider grouted masonry strengths as high as 3500 psi, therefore three values of 2500 psi, 3000 psi, and 3500 psi were considered sufficient to observe the effects on shear capacity. These values along with their corresponding equivalent in MPa (necessary for input into FormWorks) are listed in Table 3-4.

Table 3-4: Models modifying $f'_{m,grouted}$

	Grouted Masonry Strength (psi)	Grouted Masonry Strength (MPa)
Base Model	2139.3	14.75
Model 1	2500	17.24
Model 2	3000	20.68
Model 3	3500	24.13

3.5.2 Strength of Un-grouted Masonry Units

The un-grouted masonry units make up the majority of masonry units used in the tested multi-story masonry shear walls. It is predicted that varying the compressive strength of the un-grouted masonry units ($f'_{m,ungrouted}$) will directly affect the strength of the masonry shear wall. This input refers to the value of f_{my} in Figure 3-8 for Material 1. The base model f_{my} value equal to 1805.7 psi (12.45 MPa) was determined from compression testing of the experimental un-grouted masonry prisms. ASTM C90 *Standard Specification for Loadbearing Concrete Masonry Units* states that the required minimum compressive strength of concrete masonry units is 1800 psi (12.41 MPa) for an individual unit and 2000 psi (13.79 MPa) for an average group of three units. As the base model was close to the required minimum values only larger values were chosen to vary this parameter. It is not uncommon to specify masonry strengths up to 3500 psi, therefore three values of 2,500 psi, 3000 psi, and 3500 psi were determined to be used in testing.

To compare with the influence of the compressive strength of grouted masonry, the same values are used. These values and their corresponding equivalent in MPa are listed in Table 3-5.

Table 3-5: Models modifying $f'_{m,ungrouted}$

	CMU Strength (psi)	CMU Strength (MPa)
Base Model	1805.7	12.45
Model 1	2500	17.24
Model 2	3000	20.68
Model 3	3500	24.13

3.5.3 Mortar

Mortar is the constituent of a masonry wall that bonds one masonry unit to another. Mortar is placed horizontally as bed joints and vertically as head joints between each unit to help the nonhomogeneous masonry wall act uniformly. The shear strength of the mortar will likely have an effect on the performance of the wall. Discrete mortar elements are unable to be added to the finite element model, however, the Joint Strength Ratio input in the model includes the mortar strength within it. The Joint Strength Ratio (J.S.R.) as defined by VecTor 2 is the ratio between the mortar shear strength to the masonry compressive strength. Thus to vary the mortar shear strength, the masonry compressive strength must be considered as constant. As the masonry wall consisted of both grouted and un-grouted portions, a weighted average of the masonry compressive strengths was used to determine the J.S.R. The un-grouted masonry units

had compressive strengths of 1805.7 psi (12.45 MPa) whereas the grouted masonry units had compressive strengths of 2139.3 psi (14.75 MPa) and the resulting weighted average was determined to be 2033.4 psi (14.02 MPa). By varying the Joint Strength Ratio and solving for Mortar Shear Strength using equation 3-6, the corresponding values were determined. Although the Joint Strength Ratio is a parameter unique to VecTor 2, previous research has tested samples with ratios of mortar shear strength to masonry compressive strength ranging from 0.025 to 0.045 (Sarangapani 2005, Reddy 2008, Alecci 2013). Additionally, Shing and Cao (1997) reported that determining mortar properties for their study was difficult, however, it is essential to the understanding of partially grouted masonry shear walls. Minaie (2009) reported that the mortar properties were determined to be unclear in their effect on partially grouted shear walls. Thus to gain a better understanding of how the joint strength ratio affects the performance of a masonry wall, a large variety of values were considered and tested. Joint Strength Ratio values along with the corresponding Mortar Shear Strength tested are listed in Table 3-6. Although the values determined were based on a constant masonry compressive strength, the data produced may also conclude how the effects of a constant mortar shear strength and varying average masonry compressive strength may affect the performance of a masonry wall. If the base model mortar shear strength value of 0.265 MPa is considered constant and the same varied Joint Strength Ratio's are applied to equation 3-7, then it was as if the average Masonry Compressive Strength was varied using the values listed in Table 3-7.

$$J.S.R = \frac{Mortar\ Shear\ Strength}{Masonry\ Compressive\ Strength} = \frac{X}{14.02\ MPa} \qquad \text{Equation 3-6}$$

Table 3-6: Models modifying J.S.R. by varying mortar shear strength

	Mortar Shear Strength (MPa)	Joint Strength Ratio
Base Model	0.2650	0.0189
Model 1	0.1402	0.0100
Model 2	0.2103	0.0150
Model 3	0.2804	0.0200
Model 4	0.3505	0.0250
Model 5	0.4206	0.0300
Model 6	0.4907	0.0350
Model 7	0.5608	0.0400
Model 8	0.6309	0.0450

$$J.S.R = \frac{Mortar\ Shear\ Strength}{Masonry\ Compressive\ Strength} = \frac{0.265}{X} \qquad \text{Equation 3-7}$$

Table 3-7: Models modifying J.S.R. by varying masonry compressive strength

	Masonry Compressive Strength (MPa)	Joint Strength Ratio
Base Model	14.02	0.0189
Model 1	26.5	0.01
Model 2	17.67	0.015
Model 3	13.25	0.02
Model 4	10.6	0.025
Model 5	8.83	0.03
Model 6	7.57	0.035
Model 7	6.63	0.04
Model 8	5.89	0.045

3.5.4 Reinforcement

Reinforcement is used in masonry to provide additional flexure and shear strength to the wall. Masonry is a brittle material that has low tensile strength, therefore, reinforcement is added in increase ductility and further resist tensile stresses after cracking. To accurately determine the influence of reinforcement on the strength of masonry shear walls, flexural and shear reinforcement ratios were considered. The reinforcement in flexure refers to the vertical bars,

whereas the horizontal reinforcement refers to the shear reinforcement. The effects of reinforcement ratios on shear capacity may vary as a result of changing either the size or the spacing of bars. First the size of each type of reinforcement was varied. The base model, which was representative of the experimental walls, was built with #3 reinforcement (0.11 in2) as both the flexural and shear reinforcement. To gather a better understanding of how the size of the reinforcement and corresponding reinforcement ratios affects masonry shear strength, unique combinations of flexural and shear reinforcement sizes were tested. A description of the reinforcement color scheme is given in Table 3-8. The reinforcement size combinations are summarized in Table 3-9 and visual representations are found in Figure 3-26 to Figure 3-31. Additional tests were run considering various spacings while maintain constant reinforcement ratios. The tests varied both horizontal reinforcement spacing and vertical reinforcement spacing and are noted in Table 3-10 and Table 3-11, respectively. Visual representations of these modifications are shown in Figure 3-33 to Figure 3-37.

Fattal (1993) adjusted the original shear equations proposed by Matsumura (1988) because of the decreasing influence of increasing horizontal shear reinforcement. It is expected that a similar trend be observed in these tests. Elmapruk (2010), in a study of short partially grouted masonry shear walls, determined that there exists a reinforcement ratio beyond which any increase in reinforcement does not result in an increase of shear strength. Nolph (2010) supported this claim and concluded that the maximum shear reinforcement ratio after which no additional shear capacity is obtained appears to be in the range of 0.085% - 0.100% based on the net area. The proposed tests should be able to verify the validity of these claims for these wall types.

Table 3-8: Reinforcement color scheme

Reinforcement Size	Color
0.165 in. φ	Yellow
#2	Orange
#3	Red
#4	Purple

Table 3-9: Models modifying reinforcement ratios relative to size

	Vertical Bars	Vertical Reinforcement Ratio ρ_v	Horizontal Bars	Horizontal Reinforcement Ratio ρ_h	
Base Model	#3	0.0025	#3	0.00105	Figure 3-25
Model 1	#2	0.0011	#3	0.00105	Figure 3-26
Model 2	#4	0.0045	#3	0.00105	Figure 3-27
Model 3	#3	0.0025	#2	0.00048	Figure 3-28
Model 4	#3	0.0025	#4	0.00191	Figure 3-29
Model 5	#2	0.0011	#2	0.00048	Figure 3-30
Model 6	#4	0.0045	#4	0.00191	Figure 3-31

Table 3-10: Models modifying horizontal spacing of vertical reinforcement

	Vertical Reinforcement Ratio ρ_v	Horizontal Reinforcement Ratio ρ_h	Horizontal Spacing	
Base Model	0.0025	0.00105	44 in.	Figure 3-25: Base Model
Model 1	0.0025	0.00105	24 in.*	Figure 3-33
Model 2	0.0025	0.00105	16 in.	Figure 3-34

*2 bars at center of piers with spacing of 24 in. from pier edge reinforcement. Refer to figure.

Table 3-11: Models modifying vertical spacing of horizontal reinforcement

	Vertical Reinforcement Ratio, ρ_v	Horizontal Reinforcement Ratio, ρ_h	Vertical Spacing	
Base Model	0.0025	0.00105	36 in.	Figure 3-25
Model 1	0.0025	0.00105	24 in.*	Figure 3-35
Model 2	0.0025	0.00105	20 in.	Figure 3-36
Model 3	0.0025	0.00105	44 in.	Figure 3-37

*2 bars at center of piers with spacing of 24 in. from top/bottom of piers. Refer to figure.

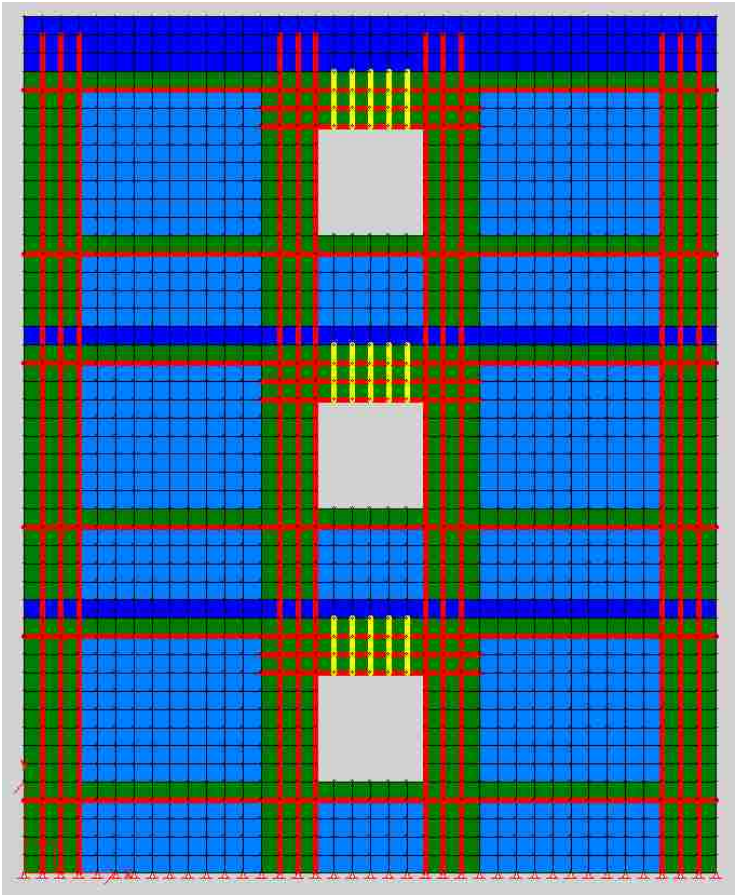

Figure 3-25: Base Model

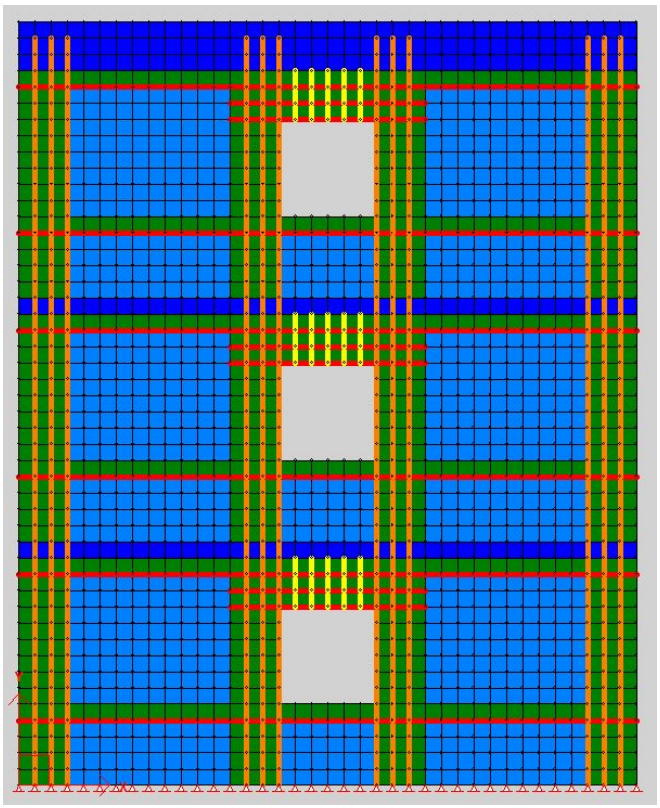

Figure 3-26: #2 vertical bars and #3 horizontal bars

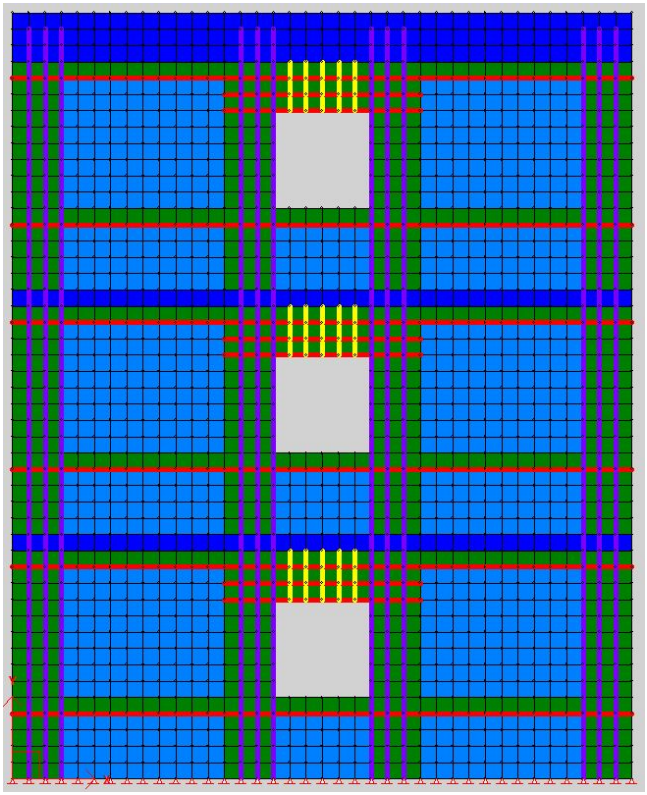

Figure 3-27: #4 vertical bars and #3 horizontal bars

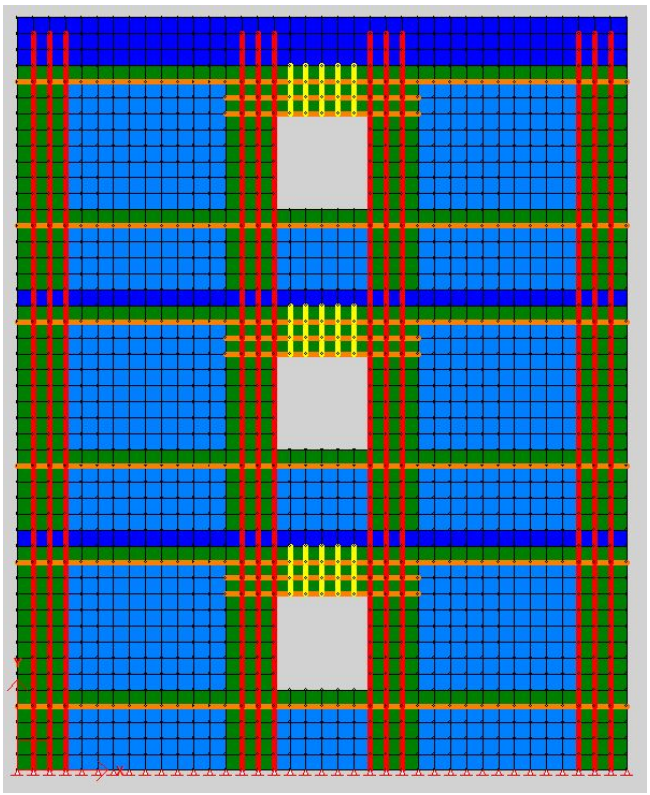

Figure 3-28: #3 vertical bars and #2 horizontal bars

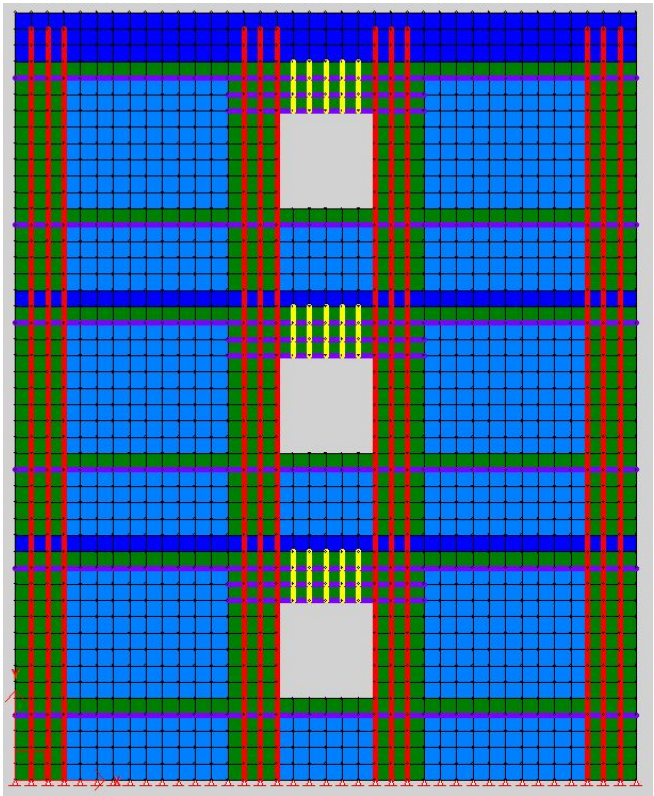

Figure 3-29: #3 vertical bars and #4 horizontal bars

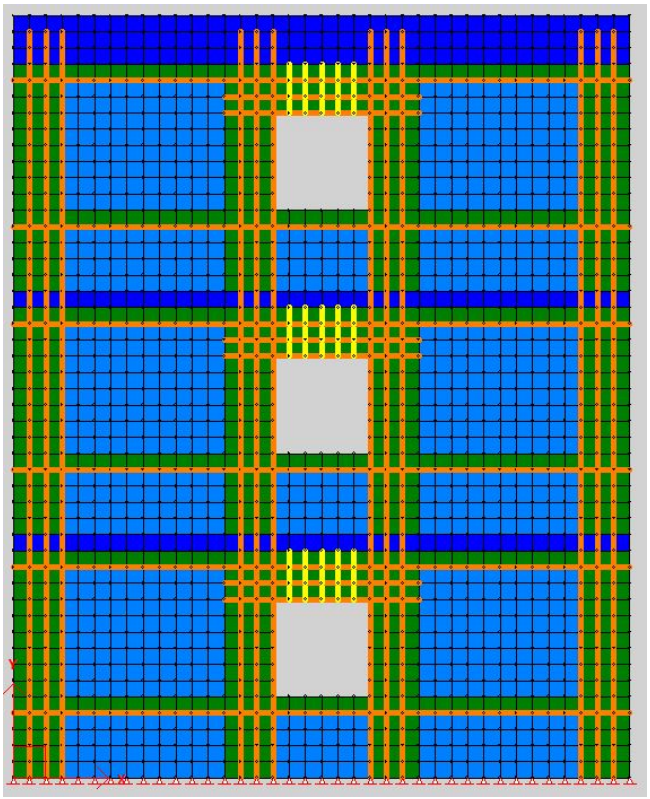

Figure 3-30: #2 vertical and horizontal bars

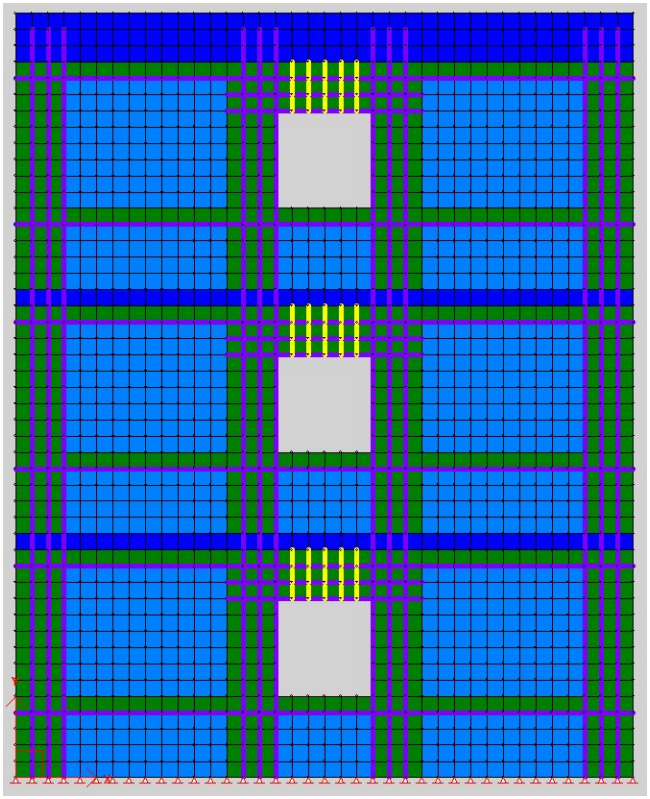

Figure 3-31: #4 vertical and horizontal bars

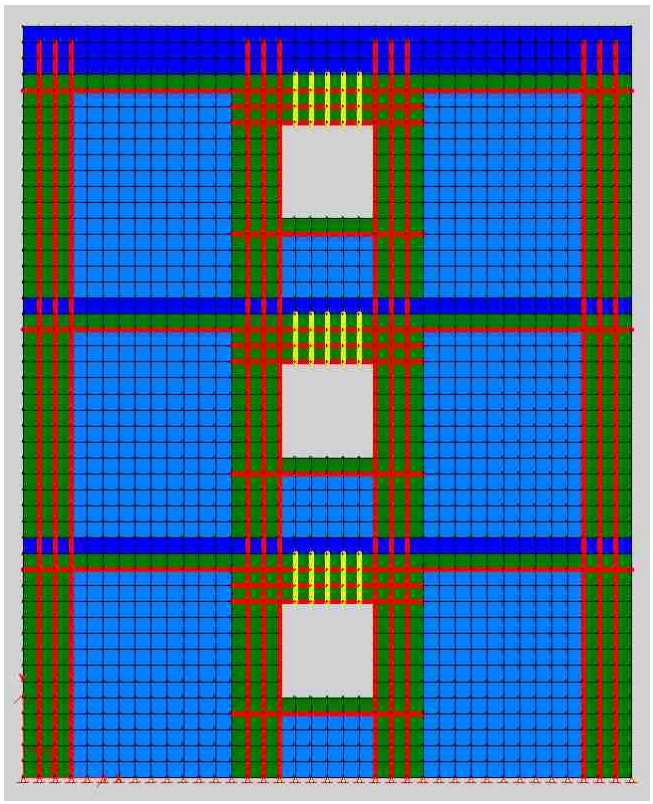

Figure 3-32: Base Model

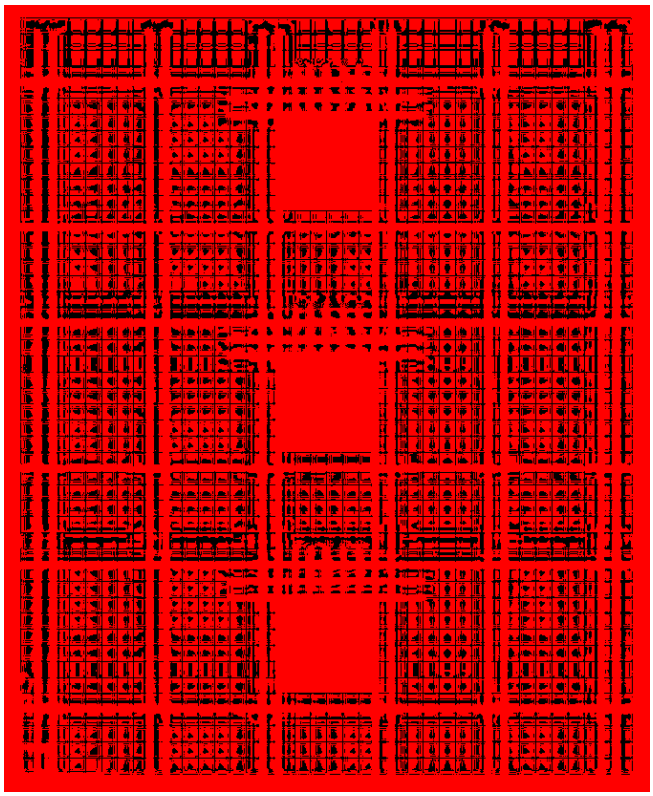

Figure 3-33: 24 in. horizontal spacing of vertical reinforcement

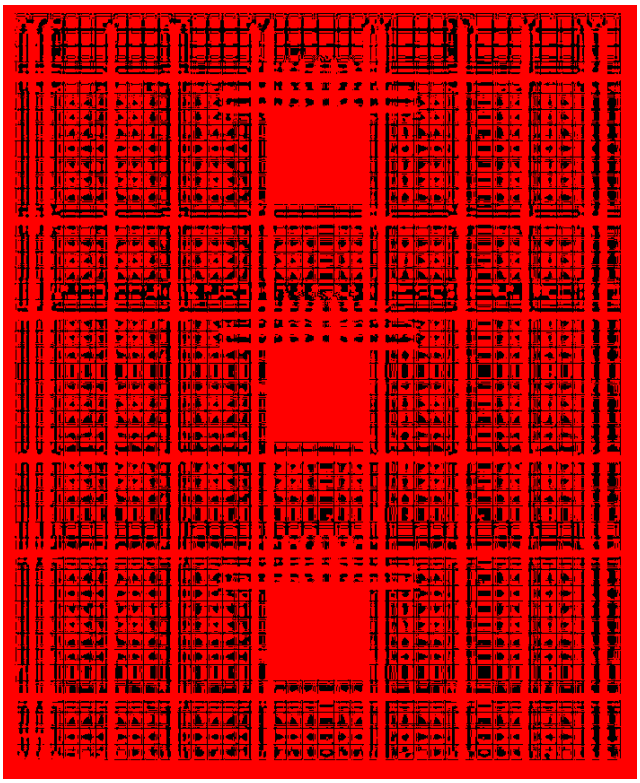

Figure 3-34: 16 in. horizontal spacing of vertical reinforcement

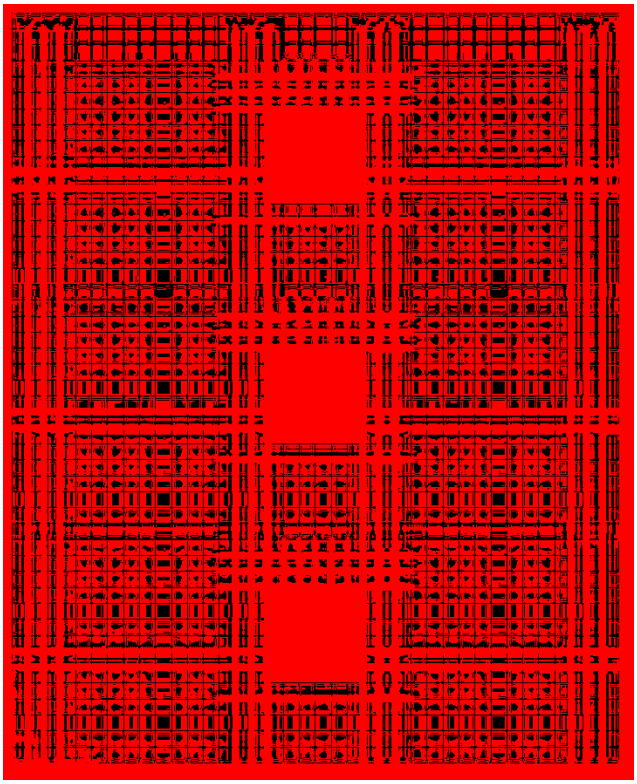

Figure 3-35: 24 in. vertical spacing of horizontal reinforcement

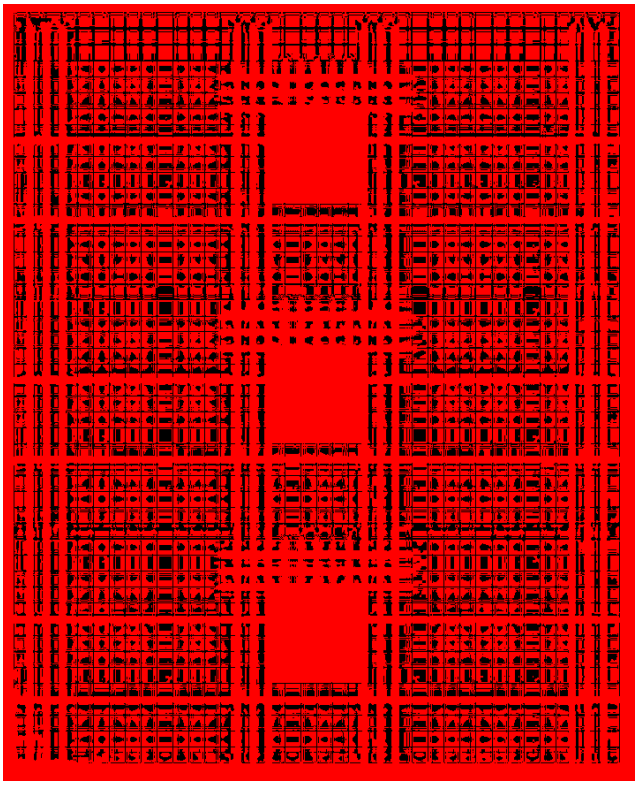

Figure 3-36: 20 in. vertical spacing of horizontal reinforcement

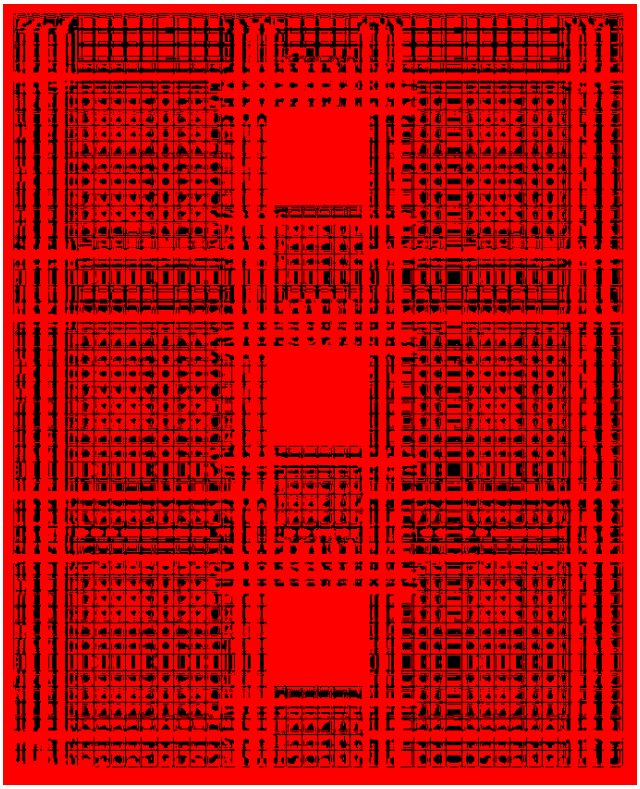

Figure 3-37: 44 in. vertical spacing of horizontal reinforcement

3.5.5 Axial Stress

Increasing axial load has been shown to increase the shear capacity and decrease the ductility of masonry shear walls. One of the mechanisms to produce increased shear capacity is due to aggregate interlock. Shing (1988) concluded that the shear and flexure failure mechanisms are highly sensitive to applied axial stress. Additionally, Voon and Ingham (2006) determined the increase in axial stress from 0 – 0.25 MPa and 0.25 – 0.50 MPa resulted in 13% and additional 8% increases in strength. Therefore, varying this parameter is expected to affect the response of these walls. The base model was loaded with 11.43 kips corresponding to an axial stress of 21.48 psi. To determine the influence of this parameter, values of 0 kips, 5 kips, and 15 kips were tested. These tests with their corresponding axial stresses are summarized in Table 3-12.

Table 3-12: Models modifying axial stress

	Axial Load (kips)	Axial Stress (psi)	Axial Load (kN)	Axial Stress (MPa)
Base Model	11.43	21.48	50.84	0.1481
Model 1	0.00	0.00	0.00	0.0000
Model 2	5.00	9.40	22.24	0.0648
Model 3	15.00	28.19	66.72	0.1943
Model 4	20.00	37.59	88.96	0.2592
Model 5	25.00	46.98	111.2	0.3239

3.5.6 Aspect Ratio

The aspect ratio by definition is the ratio of the height/width of each wall. The physical specimens and the base model were scaled representatives of a three-story masonry structure with an aspect ratio of 1.24. Much of the research performed on masonry walls in the past has been on walls with aspect ratios of 1.0. This includes the research performed by Shing (1990)

from which the current code equations for nominal masonry shear strength are derived (MSJC 2013). Past research has concluded that masonry shear strength is inversely proportional to the aspect ratio of masonry shear walls. Additionally, Haach, Vasconcelos, and Lourenco (2011) concluded that lower aspect ratios predominantly develop shear failure modes, whereas higher aspect ratios predominantly develop flexure failure modes. To better understand the effects of aspect ratio on the response of partially grouted masonry shear walls with openings, models with an aspect ratio both above and below 1.0 were considered and are summarized in Table 3-13. Figure 3-38 to Figure 3-40 illustrate these tests.

Table 3-13: Models modifying aspect ratio

	Aspect Ratio	No. of Stories
Base Model	1.24	3
Model 1	0.45	1
Model 2	0.84	2
Model 3	1.63	4

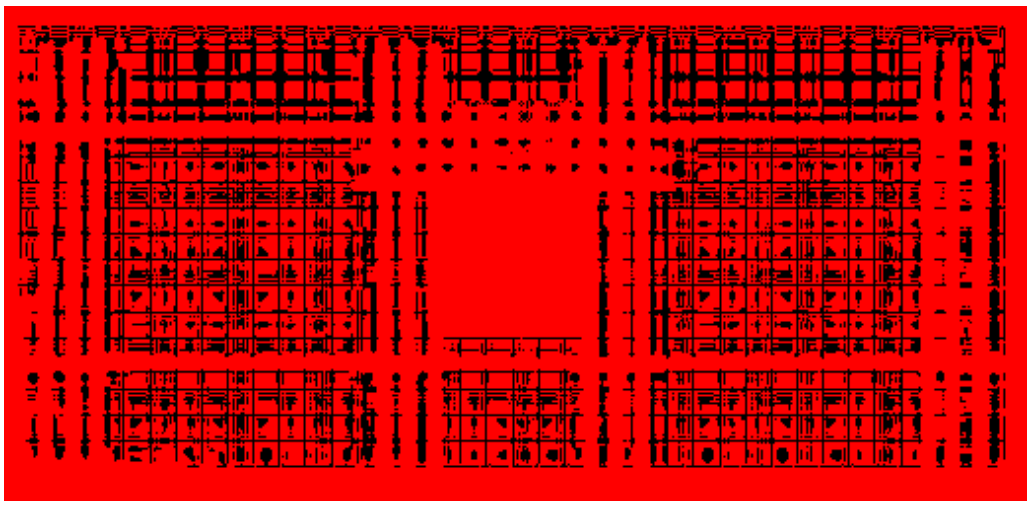

Figure 3-38: Aspect ratio 0.45 (single story)

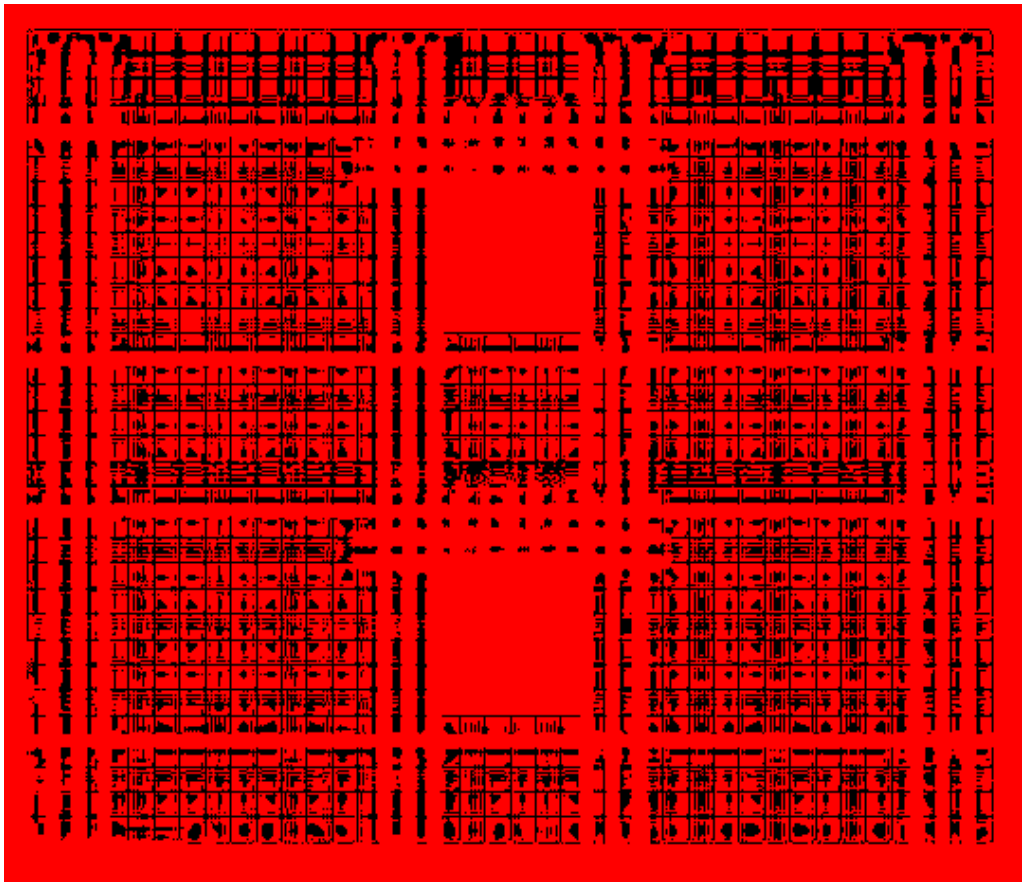

Figure 3-39: Aspect Ratio 0.84 (two story)

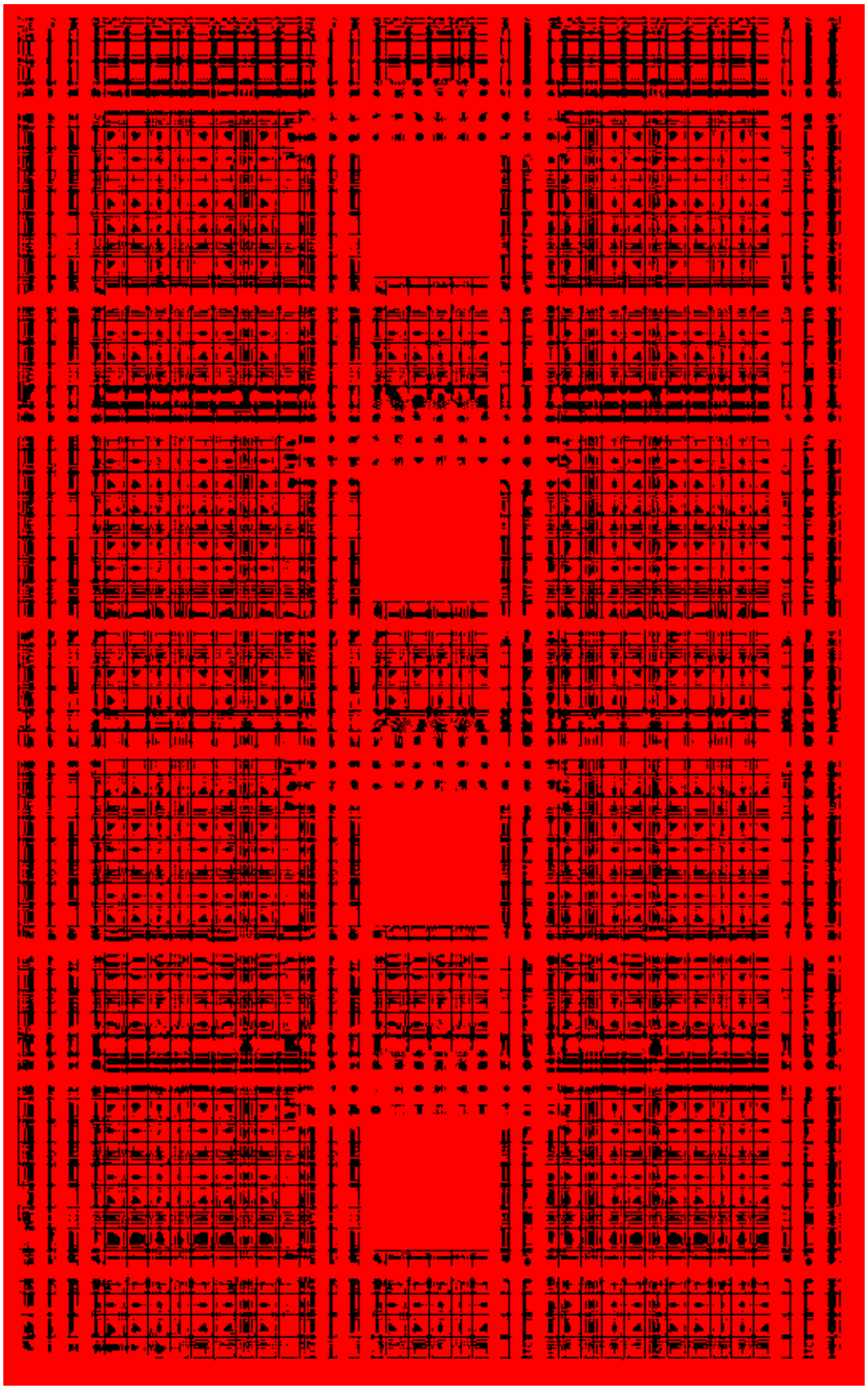

Figure 3-40: Aspect ratio 1.63 (4 story)

3.5.7 Openings

Openings, such as windows and doors, in masonry shear walls constitute a reduction in the amount of material present to resist shear loads as well as a redirection of load path. In other words, openings are capable of significantly altering the response of masonry shear walls. Voon and Ingham (2008) observed that as the height of the opening increased from 1,200 mm (specimen 2) to 2,000 mm (full height) (specimen 3), the shear strength of their single-story walls decreased from 38.4 kN to 30.8 kN. The authors further described that as the height of openings increased the reduction of strength could be attributed to a more steeply inclined diagonal strut in the piers of the wall. Ultimately this reduces the horizontal shear component that is capable of being resisted as shown in Figure 3-41. The openings in the multi-story masonry shear walls for this study were located at every level. Table 3-14 summarizes the opening dimensions for both the base model and the tests performed. Visual representations of these tests are shown in Figure 3-42 to Figure 3-46. Models 1, 2, and 3 retained a constant width while varying the height of the opening whereas models 3 and 4 retained a constant height while modifying the width of the opening.

Figure 3-41: Diagonal struts become steeper with smaller horizontal component

Table 3-14: Models modifying opening height and opening width

	Height	Opening Height/ Story Height	Width	Opening Width/ Story Width
Model 1	19 in.	0.3166	22 in.	0.1447
Base Model	23 in.	0.3833	22 in.	0.1447
Model 2	27 in.	0.4500	22 in.	0.1447
Model 3	31 in.	0.5166	22 in.	0.1447
Model 4	23 in.	0.3833	30 in.	0.1974
Model 5	23 in.	0.3833	38 in.	0.2500

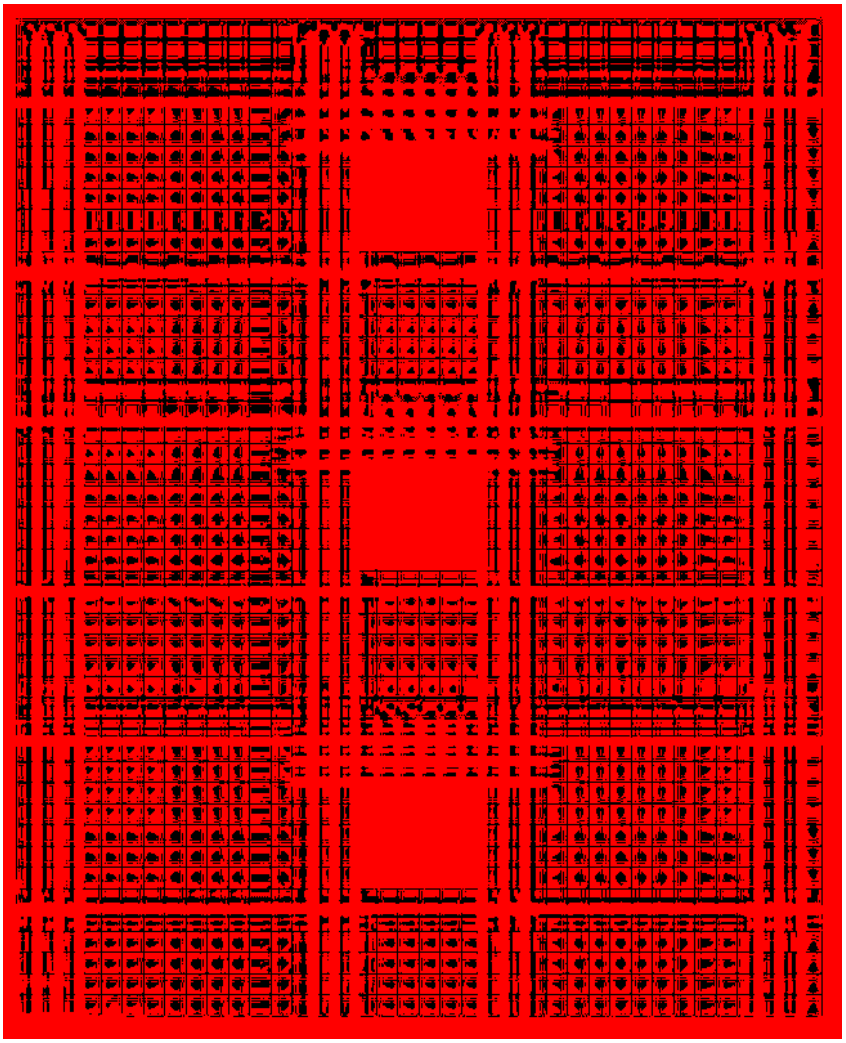

Figure 3-42: Opening height reduced 1 course from base model

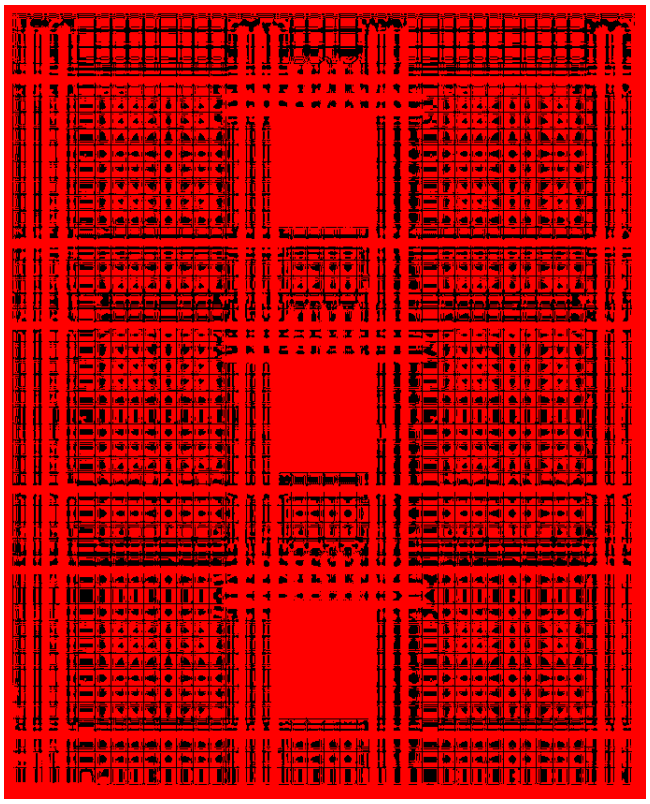

Figure 3-43: Opening height increased 1 course from base model

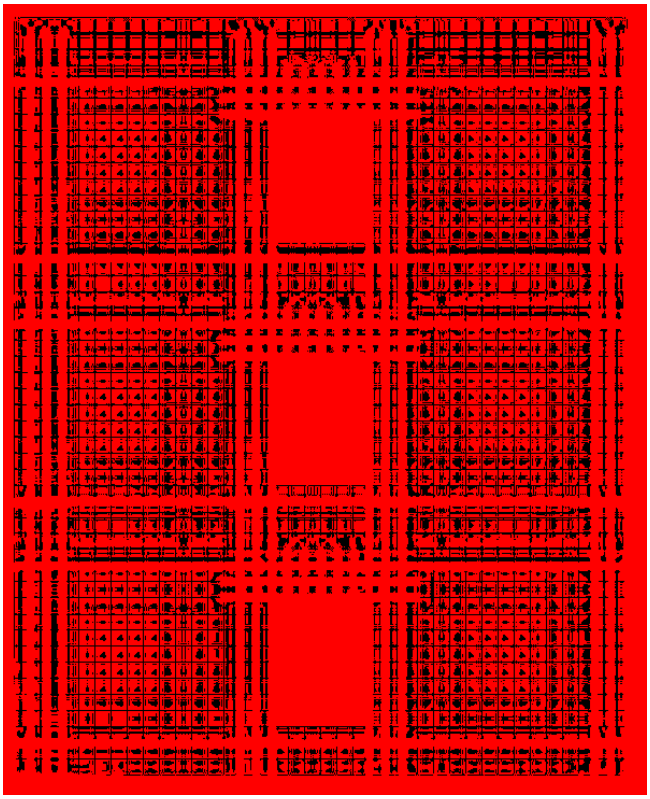

Figure 3-44: Opening height increased 2 courses from base model

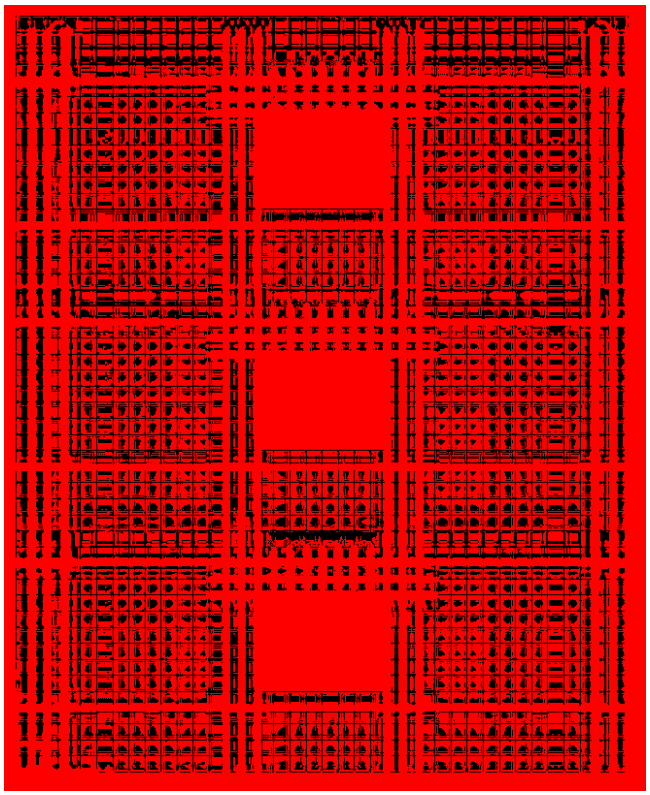

Figure 3-45: Opening width increased 1 element per side from base model

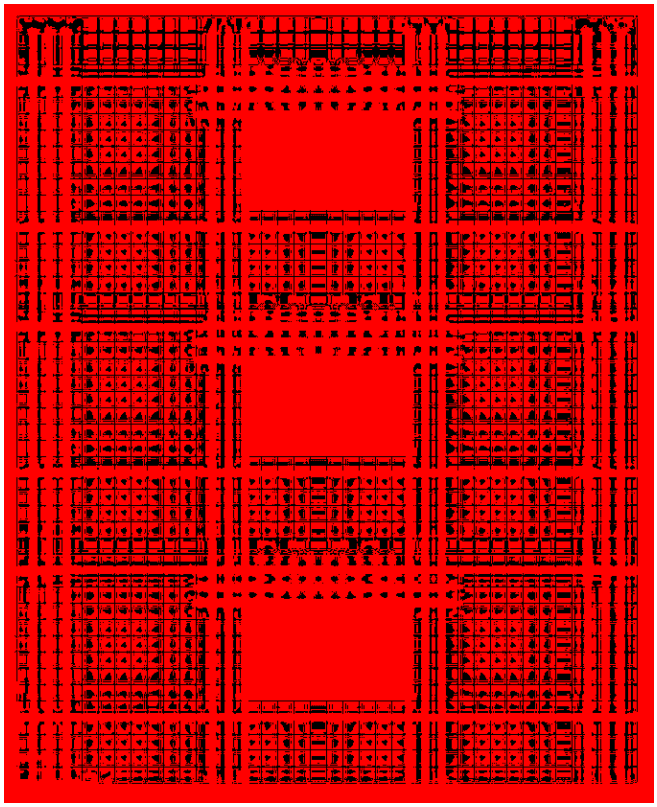

Figure 3-46: Opening width increased 2 elements per side from base model

4 RESULTS AND DISCUSSION

4.1 Introduction

This chapter presents a discussion of the results for each of the analytical parametric analyses previously described. Each section corresponds to one of the studied parameters. The results are compared with the predicted capacity from the MSJC (2013) code equations. As part of the results, the sensitivity of each parameter is described. The sensitivity quantifies the expected change in capacity based on the varied parameter. The sensitivity is reported mathematically via trend lines and returns a percentage value of the strength of the validated base model. These sensitivities are bounded by the data points for the walls tested in this research. In other words, interpolation beyond the boundaries of the walls tested may not be representative of actual wall response and is not recommended.

It is important to note that these results are specific to cantilever type masonry shear walls with large aspect ratios and an opening in each story. The material strengths, geometry, and location of reinforcement used in this study include certain implications with the results. For example, cantilever type masonry shear walls with large aspect ratios typically fail in a flexural failure mode. Such failure modes are often characterized by flexural cracking, yielding of longitudinal reinforcement, and crushing of masonry. The walls tested in this research exhibited a mixed flexural – shear failure mode as they displayed signs of flexural cracking, crushing of the masonry, and diagonal shear cracking that follows a stepping pattern along the masonry

joints (Buxton 2017). The results gathered from this study are therefore directly applicable to walls of similar nature.

Additionally, post-peak response of the finite element models do not accurately capture the strength degradation of the experimental walls as noted in comparing hysteresis curves in Figures B-1 to B-5 of Appendix B. Experimental wall 1 experienced rapid strength degradation after 0.65 in. of displacement whereas the model maintained strength carrying capacity until approximately 1.0 in. of displacement. Although the post-peak response of the model is less accurate, the pre-peak and peak responses are considered accurate and representative of similar masonry shear walls.

4.2 Strength of Grouted Masonry Units

The compressive strength of grouted masonry, $f'_{m,grouted}$, was varied using values of 2500 psi, 3000 psi, and 3500 psi in the finite element model. The load-displacement curves for the various grouted masonry strengths are shown in Figure 4-1 and numerical results are tabulated in Table 4-1. A direct relationship between grouted masonry strength and ultimate shear capacity V_{max}. The initial increase in model shear capacity from 23.4 kips to 26.4 kips (+12.8%). However, further increases in $f'_{m,grouted}$ reveal only small increases, i.e., when $f'_{m,grouted}$ increased from 2500 psi to 3000 psi a 1.6% increase in strength was observed. Furthermore, as $f'_{m,grouted}$ increased from 3000 psi to 3500 psi a 1.9% increase in strength was observed. Therefore, the shear capacity is only sensitive to the strength of grouted masonry when $f'_{m,grouted}$ is within approximately 40% of $f'_{m,ungrouted}$. The MSJC (2013) code equations un-conservatively over-predicted the capacity of the numerically modeled shear walls by 18% - 29% for this parameter (see Appendix A for calculations).

Table 4-1: Results of model tests for f'$_{m,grouted}$

	Ultimate Shear Capacity, V_{max} (kips)	Corresponding Deflection (in.)	Stiffness (kips/in.)	MSJC Code Strength (kips)	MSJC/ V_{max}	V_{max}/ Base Model
f'm,grouted 2139 psi Base Model	23.4	0.667	35.1	30.2	1.290	1.000
f'm,grouted 2500 psi	26.4	0.751	35.1	31.3	1.186	1.128
f'm,grouted 3000 psi	26.8	0.666	40.2	32.6	1.218	1.144
f'm,grouted 3500 psi	27.2	0.877	31.1	34.0	1.249	1.163

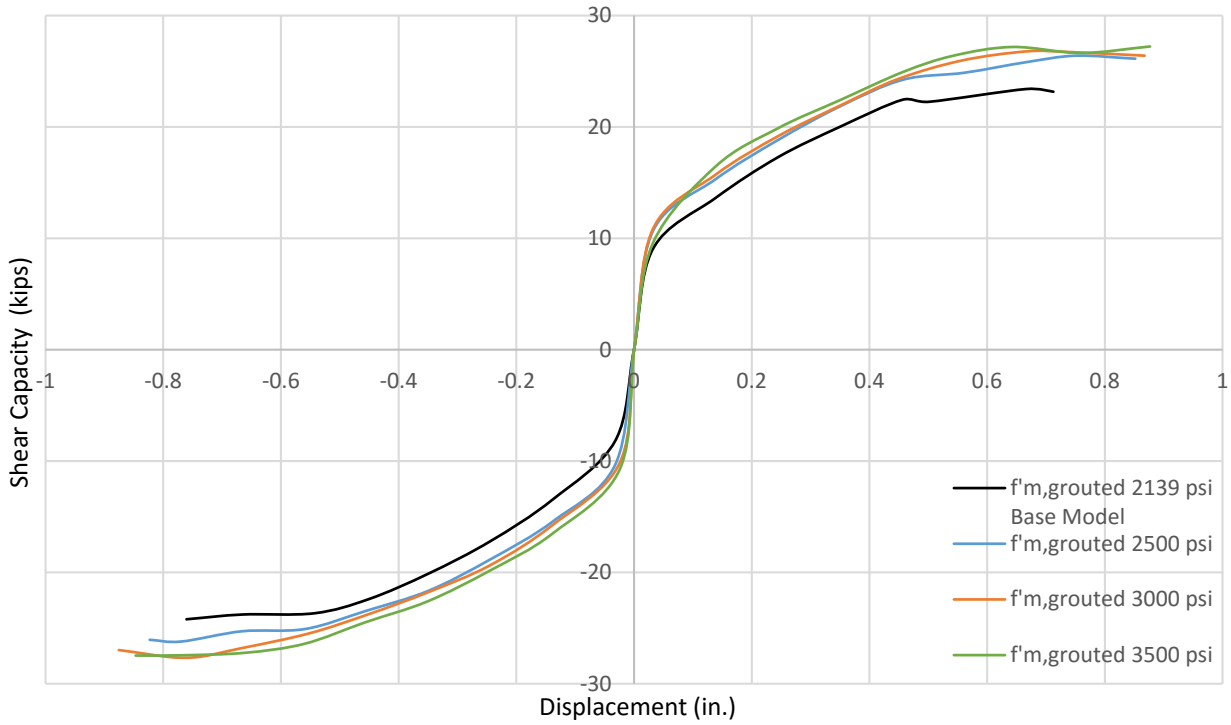

Figure 4-1: Backbone curves for modified f'$_{m,grouted}$ values

Figure 4-2 describes the sensitivity of shear capacity to the compressive strength of grouted masonry. For values of f'$_{m,grouted}$ between 2139 psi and 2500 psi (when the compressive strength of grouted masonry was less than approximately 40% larger than the compressive

strength of un-grouted masonry) the shear capacity increases approximately 0.035% for every increase in 1 psi. However, for values of $f'_{m,grouted}$ between 2500 psi and 3500 psi (when the compressive strength of grouted masonry was greater than approximately 40% larger than the compressive strength of un-grouted masonry) the shear capacity only increases approximately 0.007% for every increase in 1 psi. Thus, increases in shear capacity are considered negligible after the ratio $f'_{m,grouted}/f'_{m,ungrouted}$ is larger than 1.40.

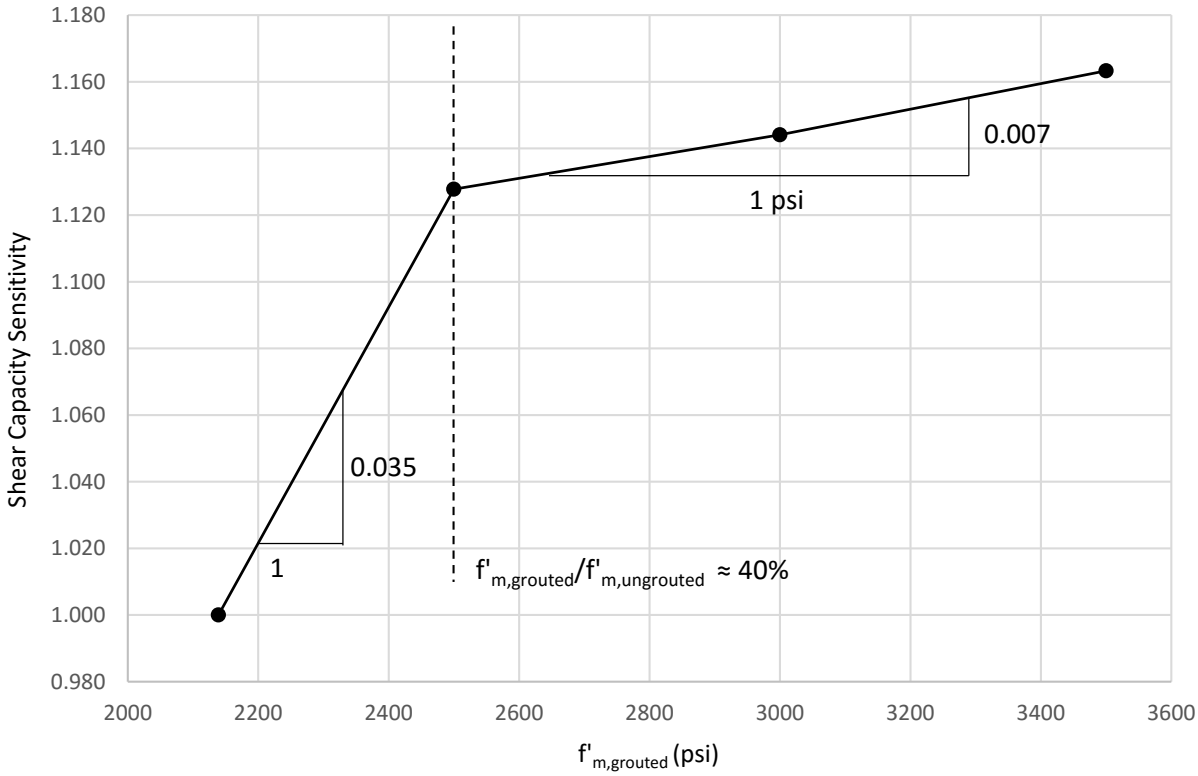

Figure 4-2: Sensitivity to the compressive strength of grouted masonry ($f'_{m,grouted}$)

The corresponding deflection at which maximum capacity occurred appears to increase with increasing $f'_{m,grouted}$. As $f'_{m,grouted}$ increased from 2139 psi to 2500 psi to 3500 psi, the

corresponding deflection at maximum load increased from 0.667 in. to 0.751 in. to 0.877 in respectively. However, there is an anomaly to the trend with 3000 psi which reached maximum strength at 0.666 in. Therefore, the results are considered inconclusive with respect to $f'_{m,grouted}$ and the stiffness of these types of wall configurations.

The number of grouted masonry elements within the model constitute roughly 41% of the total number of elements. A significant number of these grouted masonry elements were located at the extreme edges of the walls. In the partially grouted flexural failure type system which were observed for these walls, the extreme grouted and reinforced cells on the ends of the wall experience the largest compression and tension forces due to flexure. However, the hollow unreinforced and un-grouted masonry cells are a weak link as the shear stresses must pass through these areas causing failure in the wall. Thus as strength was increased in the grouted areas of the model, only slightly more load was resisted. For large aspect ratio masonry shear walls that experience flexural failure it is believed that the added strength to the grouted masonry (especially the grouted masonry located at the extreme edges of the wall) will strengthen the wall against toe crushing and flexural cracking, but not from diagonal shear cracking. This is observed in Figure 4-3 which shows how the lateral load travels diagonally and vertically to the extreme wall edge during a push or pull cycle. The red and blue indicate large and even larger vertical stresses respectively. The large forces are able to collected in the grouted edges of the wall, however, damage to the un-grouted masonry occurs as the shear stresses transfer through these areas.

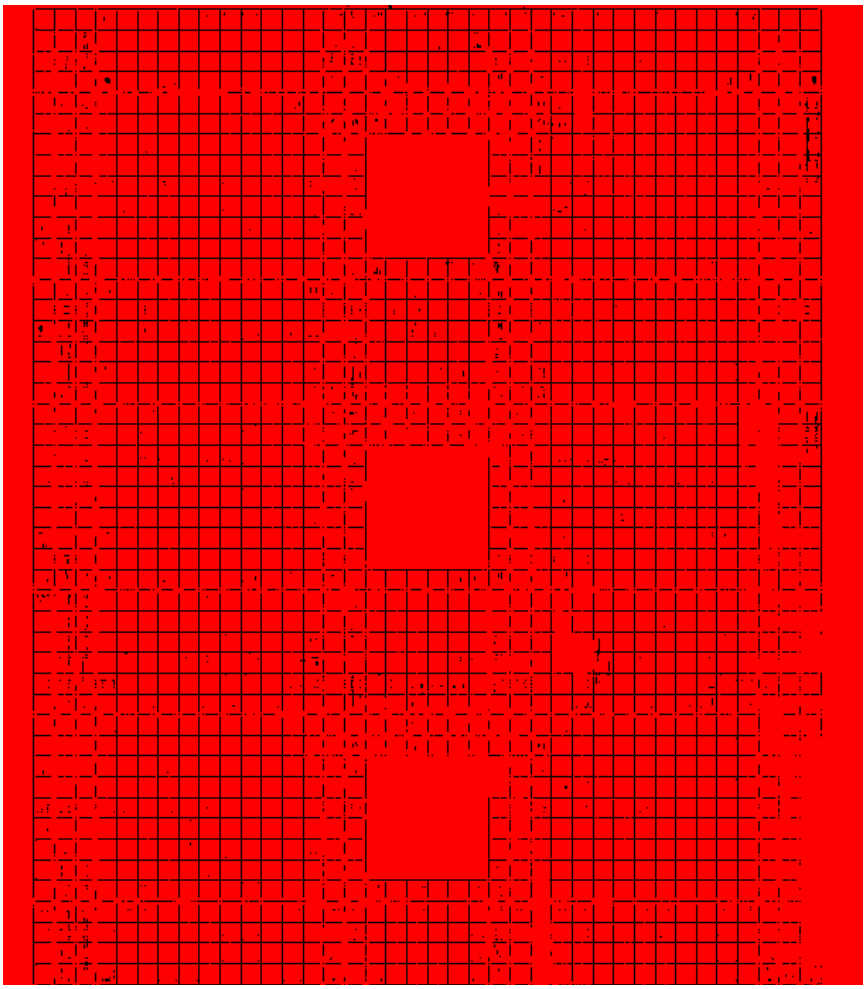

Figure 4-3: Vertical stresses passing diagonally through the wall and collected at the toe

4.3 Strength of Un-grouted Masonry Units

The load-displacement curves for un-grouted masonry strength ($f'_{m,ungrouted}$) are displayed in Figure 4-4 and numerical results are tabulated in Table 4-2. The trend indicates that increasing un-grouted masonry strength directly increased the ultimate shear capacity of the wall. Large strength increases occurred (+12.0%) and (+17.0%) when increasing from 1805.7 psi to 2500 psi and 2500 psi to 3000 psi respectively. A smaller increase, however, of 5.1% was noted when increasing $f'_{mungrouted}$ from 3000 psi to 3500 psi. The MSJC (2013) code equations un-

conservatively over-predicted the capacity of the numerically modeled shear walls by approximately 17% - 29% for this parameter (see Appendix A for calculations).

Table 4-2: Results of model tests for f'$_{m,ungrouted}$

	Ultimate Shear Capacity, V_{max} (kip)	Corresponding Deflection (in.)	Stiffness (kips/in.)	MSJC Code Strength (kips)	MSJC/ V_{max}	V_{max}/ Base Model
f'm,ungrouted 1805.7 psi Base Model	23.4	0.667	35.1	30.2	1.290	1.000
f'm,ungrouted 2500 psi	26.2	0.561	46.7	33.4	1.274	1.120
f'm,ungrouted 3000 psi	30.2	0.729	41.4	35.6	1.179	1.290
f'm,ungrouted 3500 psi	31.4	0.729	43.1	37.6	1.198	1.341

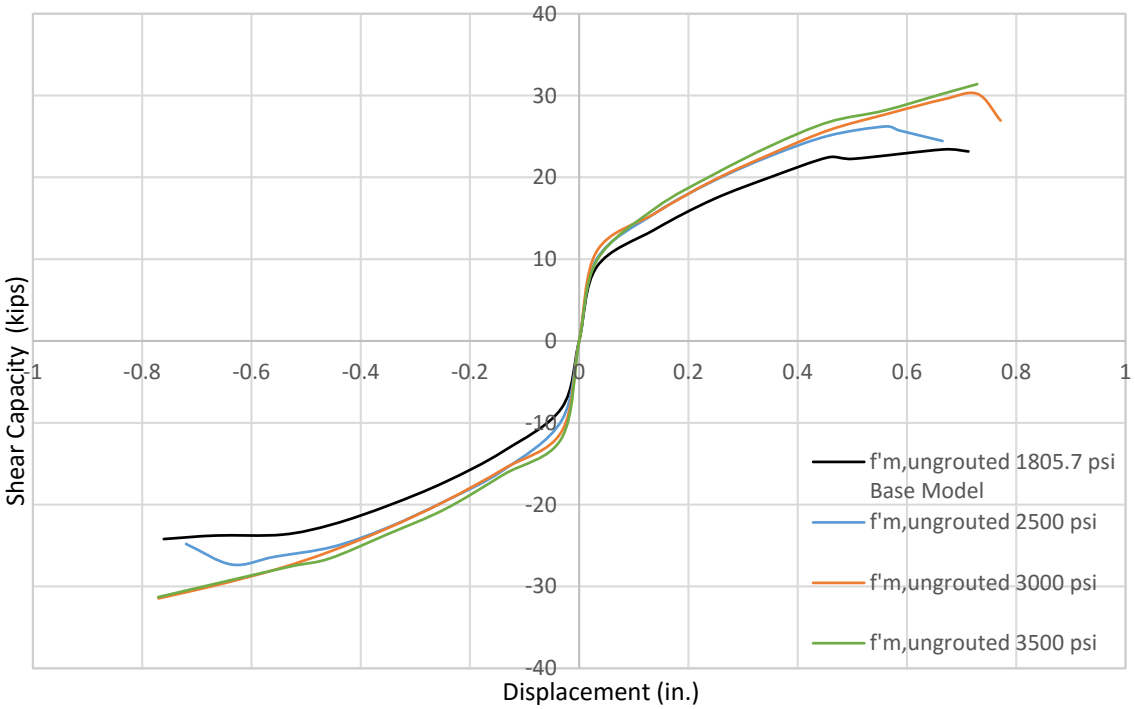

Figure 4-4: Backbone curves for modified f'$_{m,ungrouted}$ values

The sensitivity of shear strength with respect to the compressive strength of un-grouted masonry is described in Figure 4-5. A linear trend line with an R^2 value of 0.9674 was applied to the plot. The trend line describes the response of shear capacity as increasing 0.02% per increase in 1 psi bounded between a range of 1806 psi to 3500 psi. Although the slope appears to be tapering from 3000 psi to 3500 psi, additional models are necessary to determine relationships outside of the bounded range.

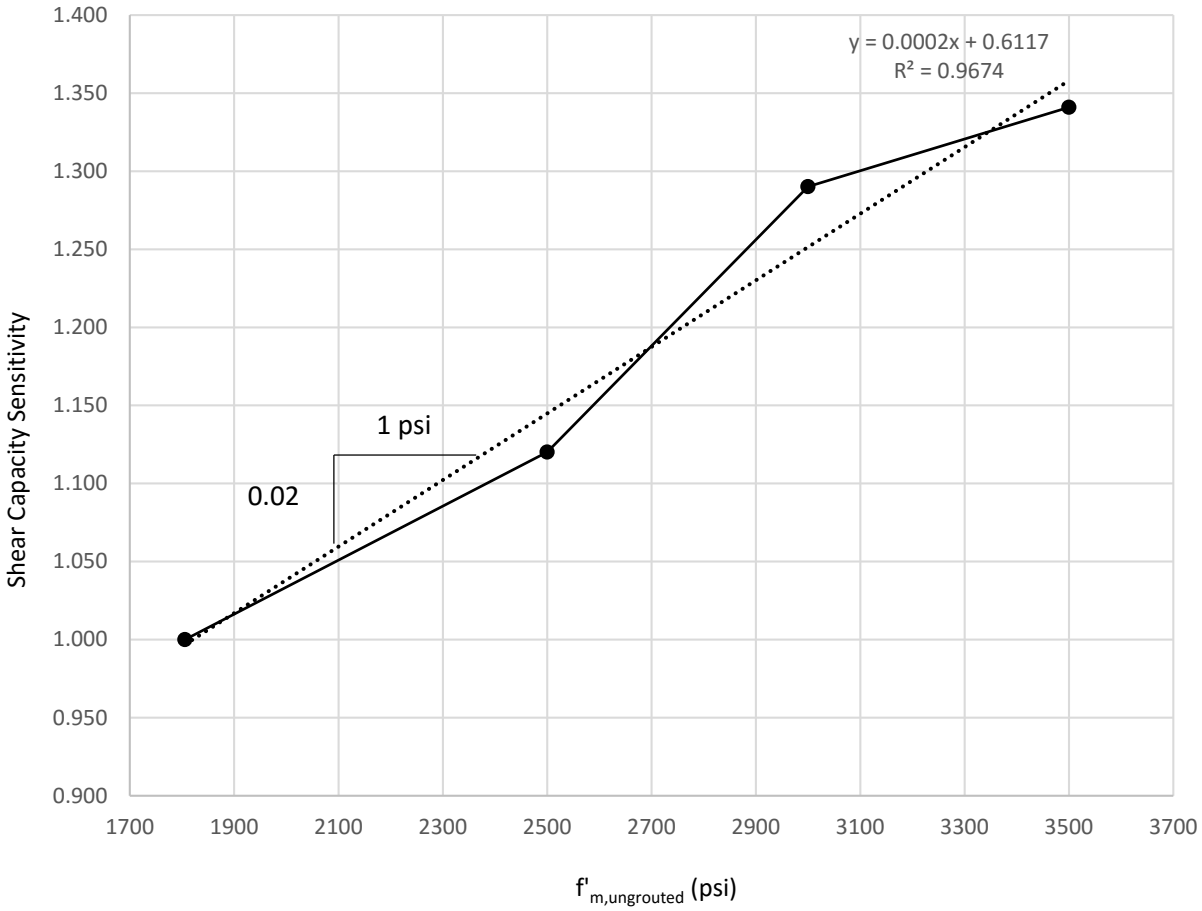

Figure 4-5: Sensitivity to the compressive strength of un-grouted masonry ($f'_{m,ungrouted}$)

The un-grouted masonry units constitute the majority of the CMU's within the partially grouted walls tested in this research. During experimental testing in the lab, failure occurred in a diagonal stepping crack pattern through the mortar joints of the un-grouted concrete masonry units as seen in Figure 4-6. Similar cracking was observed in the finite element model as shown in Figure 4-7. Note that exact diagonal stepping through mortar joints is unable to be discretely modeled by the finite elements, however, the crack directions are similar. Such cracking designates the location of large tensile stresses. The joints have the lowest capacity to resist the stresses in the system. Because masonry compressive testing considers both CMU and joint strength, increasing $f'_{m,ungrouted}$ will strengthen these areas where cracking occurred. It is therefore reasonable and expected that increasing the strength of the location of failure will increase the shear capacity of the wall.

Figure 4-6: Diagonal cracks stepping through mortar joints

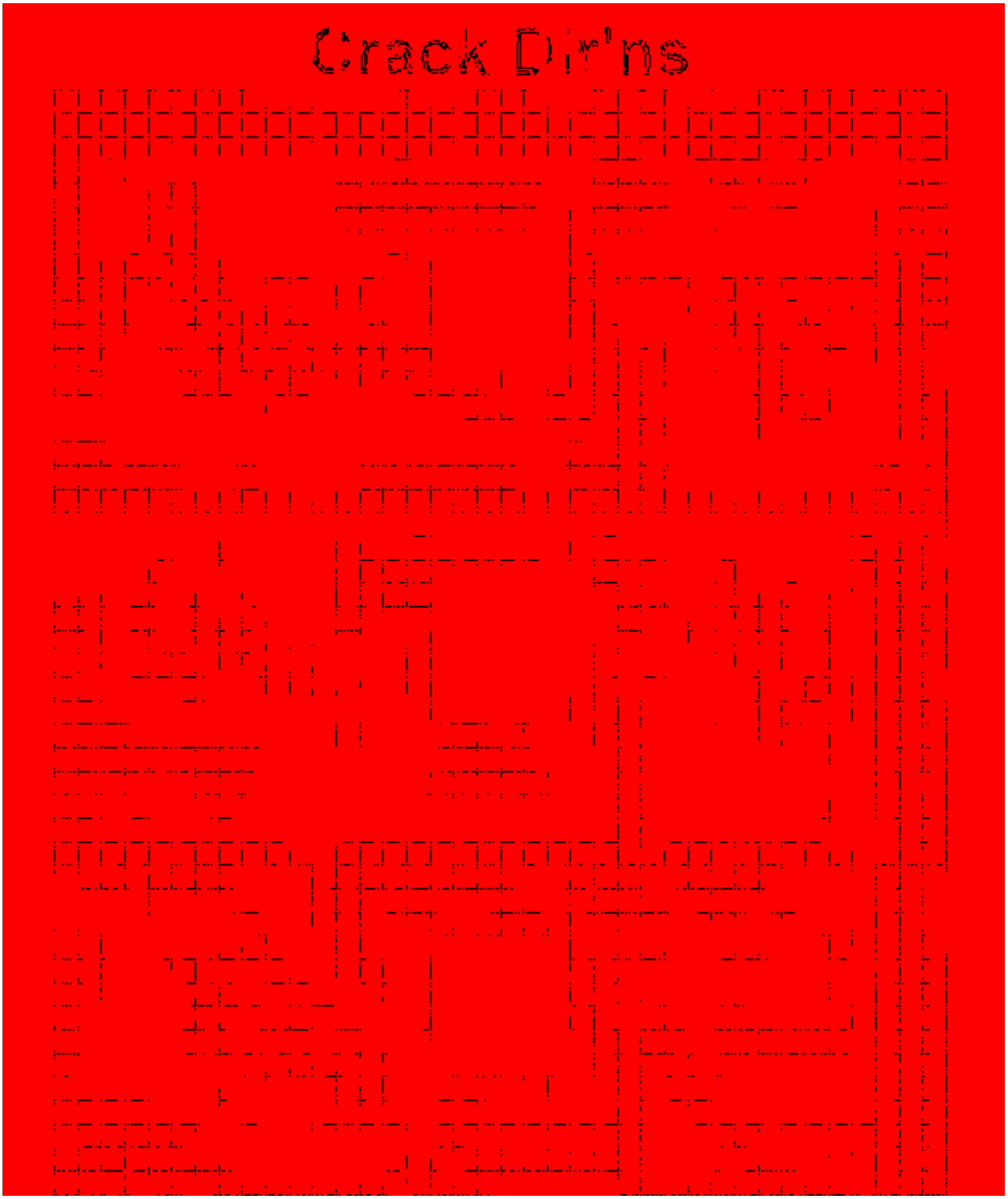

Figure 4-7: Diagonal cracks observed in tests with finite element model

The corresponding deflection at which maximum capacity occurred was observed to first decrease and then increase with increasing $f'_{m,ungrouted}$. As $f'_{m,ungrouted}$ increased from 1806 psi to 2500 psi, the deflection at maximum capacity decreased from 0.667 in to 0.561 in. However, when increasing from 2500 psi to 3000 psi to 3500 psi, the corresponding deflection at maximum load increased from 0.561 in. to 0.729 in. to 0.729 in respectively. Therefore, the effects of $f'_{m,ungrouted}$ on stiffness and deflection of these types of wall configurations is considered inconclusive.

4.4 Mortar

The strength of mortar was varied by modifying the input value for joint strength ratio (J.S.R.). The J.S.R. is the ratio between the mortar shear strength to the masonry compressive strength (VecTor 2). The masonry compressive strength was taken as constant, therefore, the mortar shear strength is considered directly proportional to increasing J.S.R, i.e., increasing mortar shear strength directly increases the shear wall capacity. Figure 4-8 depicts the backbone curves for the tested models. Table 4-3 illustrates that increasing the J.S.R. from 0.010 to 0.015 yielded a 9.6% increase in shear capacity. Further increases from 0.020 to 0.025 returned a 7.9% increase in shear capacity. This is notable and reasonable as partially grouted masonry shear walls typically develop cracks along the mortar planes of the hollow masonry units. Such diagonal stepping cracks were likewise present for the experimental walls tested in this research. By strengthening these planes of weakness it seems conclusive that ultimate shear capacity would therefore increase. Conversely, it appears that as J.S.R. increases, the displacement at which failure occurs decreases, however, this trend did not hold for every test as shown in Table 4-3.

The MSJC (2013) code equations predicted the capacity of the shear wall as 30.2 kips for each of the modifications to joint strength ratio. The MSJC (2013) equations only contain an input for the compressive strength of masonry. The compressive strength of masonry was considered constant for these models; therefore, while increasing J.S.R. resulted in increased capacity observed in the model, it had no effect on the MSJC (2013) predicted shear capacity. Thus the MSJC (2013) equations predicted the shear wall capacity of the numerical models by an un-conservative 57% to a conservative 95%. The accuracy of the MSJC (2013) equations depends heavily upon the J.S.R. of the model. As J.S.R. increases from 0.01 to 0.04, the accuracy of the MSJC (2013) equations consistently improves. At a J.S.R value of 0.045, the MSJC (2013) equations accurately and conservatively predicted the shear capacity of the wall. Based on this research, the MSJC (2013) equations are capable of accurately predicting shear capacity for multi-story, partially grouted, perforated masonry shear walls with a joint strength ratio of 0.40 and 0.45. Further research is necessary to validate or refute this hypothesis.

Table 4-3: Results of model tests for J.S.R.

	Ultimate Shear Capacity, V_{max} (kip)	**Corresponding Deflection (in.)**	**Stiffness (kips/in)**	**MSJC Code Strength (kips)**	**MSJC/ V_{max}**	**V_{max}/ Base Model**
J.S.R. 0.01	19.3	0.857	22.6	30.2	1.562	0.826
J.S.R. 0.015	21.6	0.548	39.4	30.2	1.399	0.922
Base Model 0.0189	23.4	0.667	35.1	30.2	1.290	1.000
J.S.R. 0.02	23.7	0.768	30.9	30.2	1.275	1.012
J.S.R. 0.025	25.5	0.668	38.2	30.2	1.183	1.091
J.S.R. 0.03	26.6	0.770	34.5	30.2	1.137	1.135
J.S.R. 0.035	28.3	0.561	50.4	30.2	1.069	1.207
J.S.R. 0.04	29.5	0.565	52.2	30.2	1.024	1.260
J.S.R. 0.045	31.7	0.546	58.1	30.2	0.952	1.355

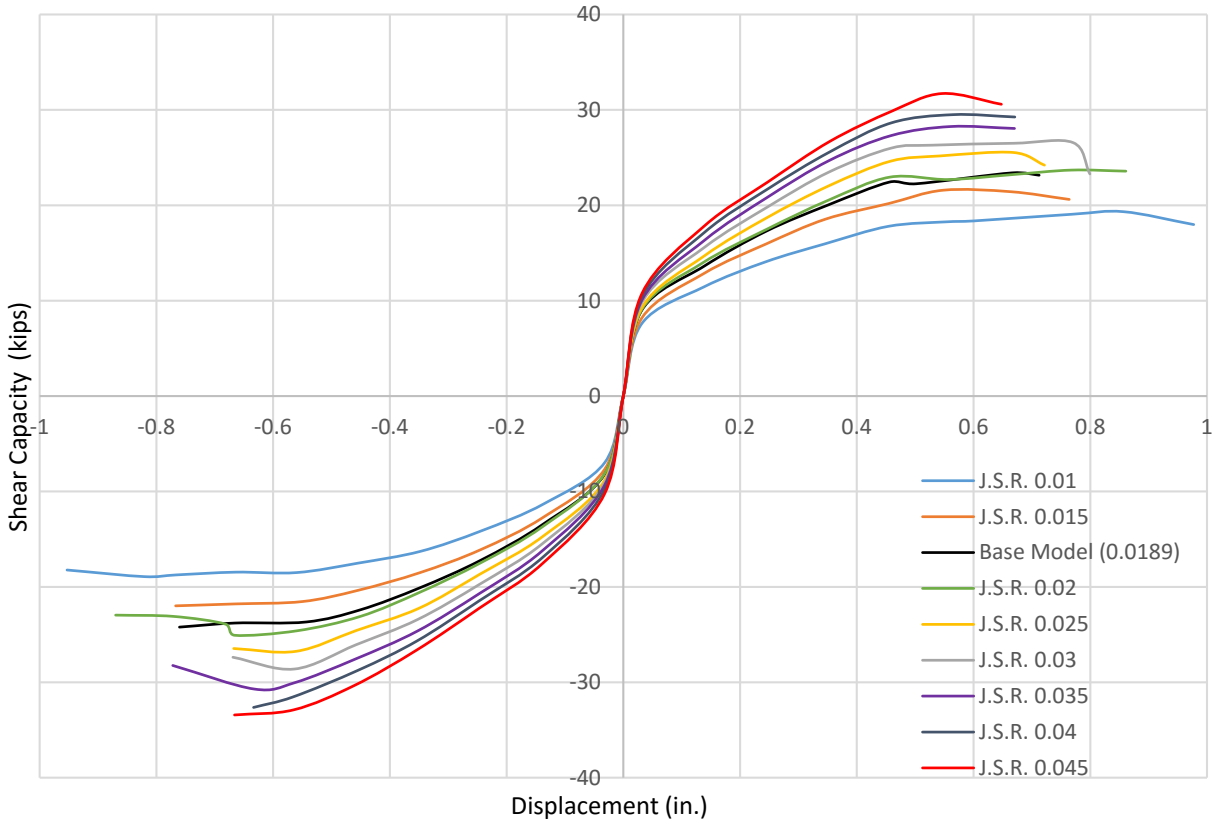

Figure 4-8: Backbone curves for modified Joint Strength Ratio values

Results indicate that shear wall capacity is sensitive to the mortar shear strength. The sensitivity of shear strength with respect to the joint strength ratio is described in Figure 4-9. A linear trend line with an R^2 value of 0.9893 was applied to the plot. The trend line describes the response of shear capacity as increasing 14.2% per increase in joint strength ratio of 0.01 bounded between a range of 0.01 psi to 0.045 psi. These results shed light on the importance of the relationship between mortar properties and partially grouted masonry shear wall response. Shing and Cao (1997) reported that determining mortar properties for their study was difficult, however, it is essential to the understanding of partially grouted masonry shear walls. Minaie (2009) reported that the mortar properties were determined to be unclear in their effect on

partially grouted shear walls. This study concludes that increasing the masonry shear strength has a direct influence on the ultimate shear capacity and stiffness of the wall response.

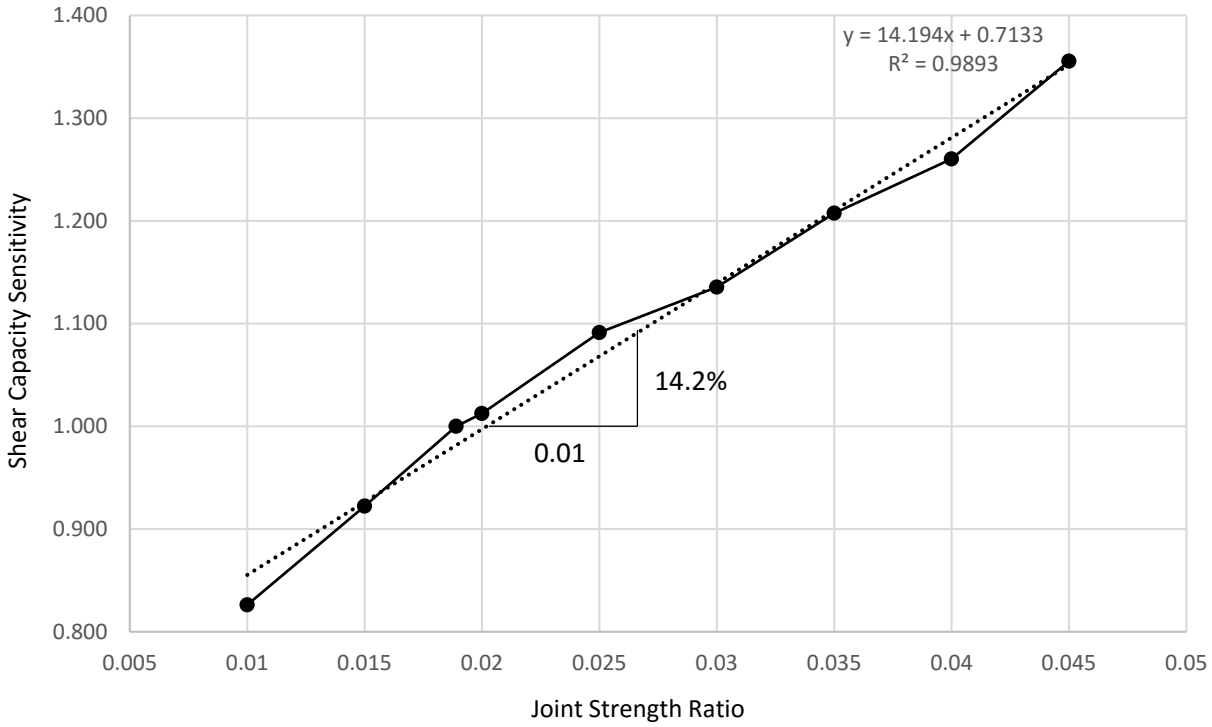

Figure 4-9: Sensitivity to the joint strength ratio

To appropriately accommodate for the placement of discrete reinforcement and to obtain more accurate results from the finite element method, the nodes and elements were modeled as square instead of rectangular like the CMU's. Thus the model contains elements with nominal dimensions of 4" x 4" x 4" whereas the nominal dimensions of the actual CMU's were 8" x 4" x 4". Consequently, the model encompasses 39 nodes with 38 elements per complete course whereas the physical walls contained 19 CMU's in a complete course. Note that the bed joint dimension for each element was input as 8 in. (203.2 mm), however the width of the element was

only 4 in. (101.6 mm). Joint properties are smeared across a single finite element (VecTor2 Manual). Therefore, a possible consequence of creating a model with 2 elements per CMU is indirectly adding a joint in the middle of each CMU where there was no joint present in the experimental walls. No description of applying elements in this manner was provided in the VecTor2 Manual. Further research regarding the size of elements used for modeling would provide additional insight on the effect of using elements smaller than the size of the CMU.

4.5 Reinforcement

Reinforcement was studied by modifying two distinct variables: reinforcement size and spacing. It should be noted that the size and spacing variables will have more or less influence on the wall depending on the wall dimensions. Therefore, the modification of the reinforcement size and spacing variables are in reality determining the effects of vertical and horizontal reinforcement ratios and the spacing of these ratios throughout the wall.

This parametric study did not determine the yielding of vertical or horizontal reinforcement for each parametric model. However, the yielding of vertical and horizontal reinforcement was determined for the base model. Figure 4-10 and Figure 4-11 show the stress strain curves for select vertical and horizontal reinforcement elements. Figure 4-10 indicates that the vertical reinforcement was close to yielding, i.e., the vertical reinforcement resisted 75.1 ksi of stress and the specified yield stress was 77.7 ksi as determined from laboratory tests. Figure 4-11 indicates that the horizontal reinforcement resisted only 5.47 ksi of stress. Thus, the importance of vertical (flexural) reinforcement for this configuration of masonry shear wall cannot be understated. Further research is necessary to observe the sensitivity of shear wall response to reinforcement yielding and varying yield stresses of vertical and horizontal reinforcement.

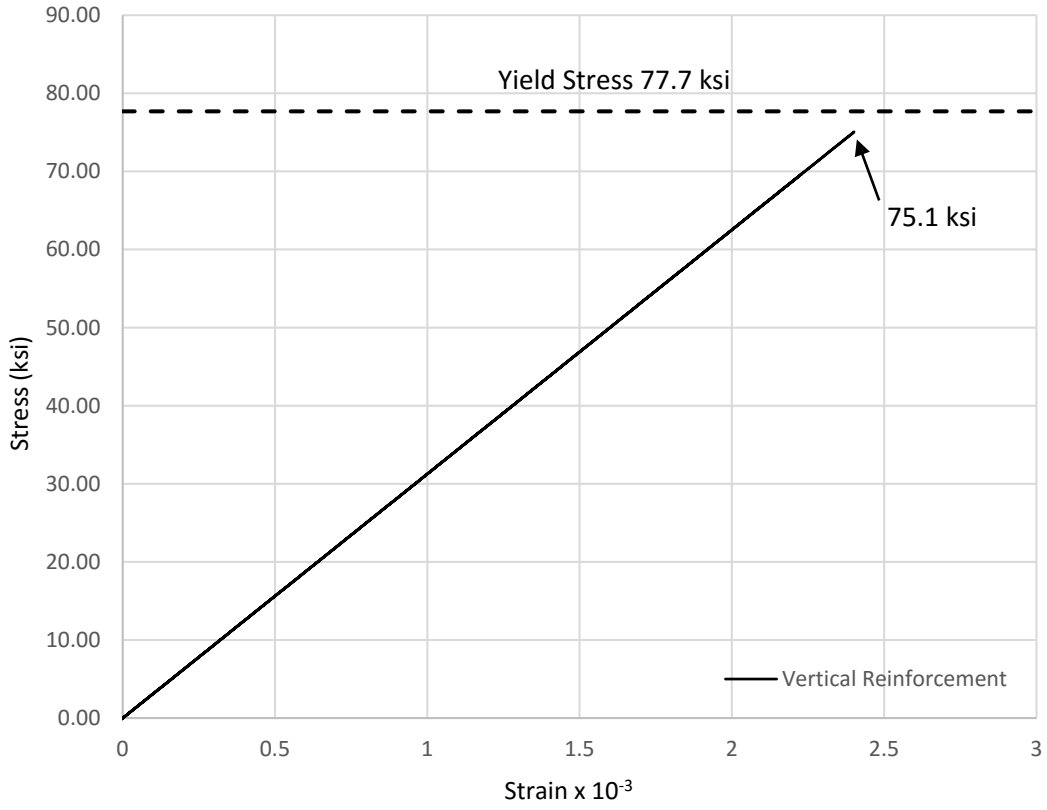

Figure 4-10: Stress strain curve for vertical reinforcement at bottom wall edge

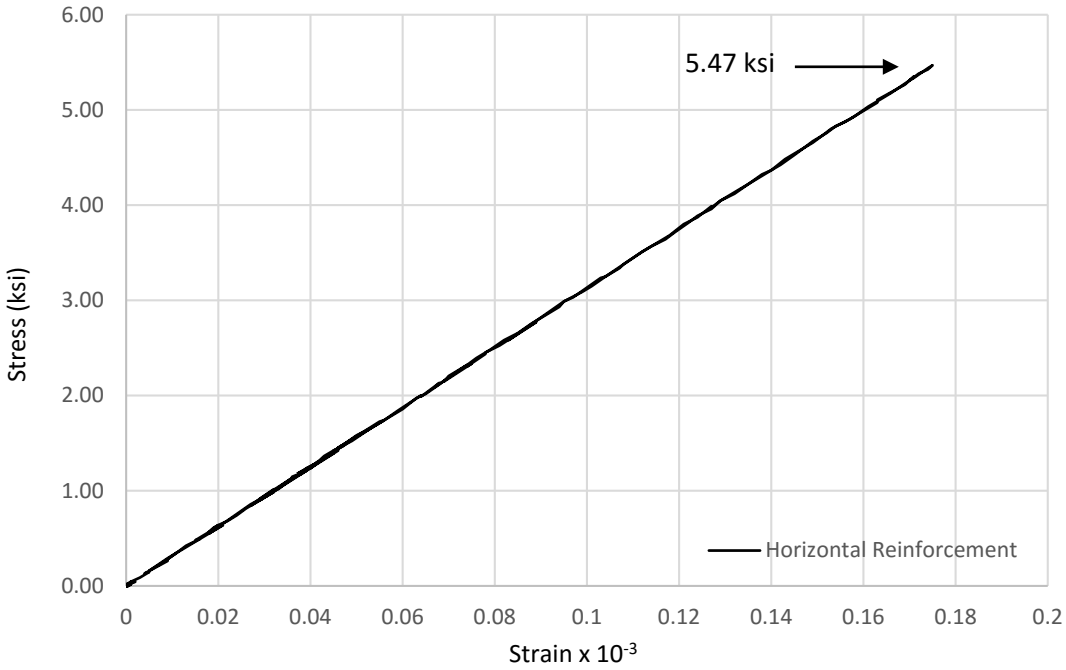

Figure 4-11: Stress strain curve for horizontal reinforcement at top of wall

4.5.1 Size

The size of the reinforcement was varied between #2 (0.05 in.^{2}), #3 (0.11 in.^{2}), and #4 (0.20 in.^{2}) rebar both in the horizontal and vertical directions. Corresponding reinforcement ratios for each test are tabulated in Table 4-4. For visual representations of each test refer to Figure 3-26 through Figure 3-31. Figure 4-12 depicts the resulting load-displacement curves of the various combinations of reinforcement sizes. The curves reveal distinct groupings which are associated with the size of vertical reinforcement present in the wall. The group with the lowest common ultimate capacities corresponds to walls with #2 vertical reinforcement; the group with the highest common ultimate capacities corresponds to walls with #4 vertical reinforcement; the group in the middle corresponds to the walls with #3 vertical reinforcement. An increase in lateral strength of roughly 20% was observed when increasing the vertical reinforcement ratio (ρ_v) from 0.0011 (#2 bar) to 0.0025 (#3 bars). Likewise, a 10% increase in lateral strength was observed when increasing ρ_v from 0.0025 (#3 bar) to 0.0045 (#4 bar).

The MSJC (2013) code equations predicted a value of 30.2 kips for each of the models that modified both vertical and horizontal reinforcement ratios (see Appendix A for calculations). Thus the equations un-conservatively over-predicted the capacity of the numerically modeled shear walls by approximately 17% - 67% for this parameter. The discrepancy between the MSJC (2013) equations and the model shear capacity increased with decreasing vertical reinforcement ratio as the MSJC (2013) equations consider only horizontal shear reinforcement to predict capacity. The model results, however, indicated an increase in capacity due to increasing vertical flexure reinforcement. The need to incorporate this parameter into the predictive code equations for shear capacity is apparent for this configuration of masonry shear walls.

Table 4-4: Results of model tests for reinforcement ratios varied by size

	Vertical Reinf. Ratio, ρ_v	Horizontal Reinf. Ratio, ρ_h	Ultimate Shear Capacity, V_{max} (kip)	Corr. Def. (in.)	MSJC Code Strength (kips)	MSJC/ V_{max}	V_{max}/ Base Model
#2 Vertical	0.0011	0.00105	18.7	0.765	30.2	1.619	0.797
#2	0.0011	0.00048	19.0	0.883	30.2	1.592	0.811
#2 Horizontal	0.0025	0.00048	23.3	0.768	30.2	1.294	0.997
#3 Base Model	0.0025	0.00105	23.4	0.667	30.2	1.290	1.000
#4 Horizontal	0.0025	0.00191	23.6	0.760	30.2	1.277	1.011
#4	0.0045	0.00191	26.2	0.655	30.2	1.154	1.118
#4 Vertical	0.0045	0.00105	25.7	0.422	30.2	1.173	1.100

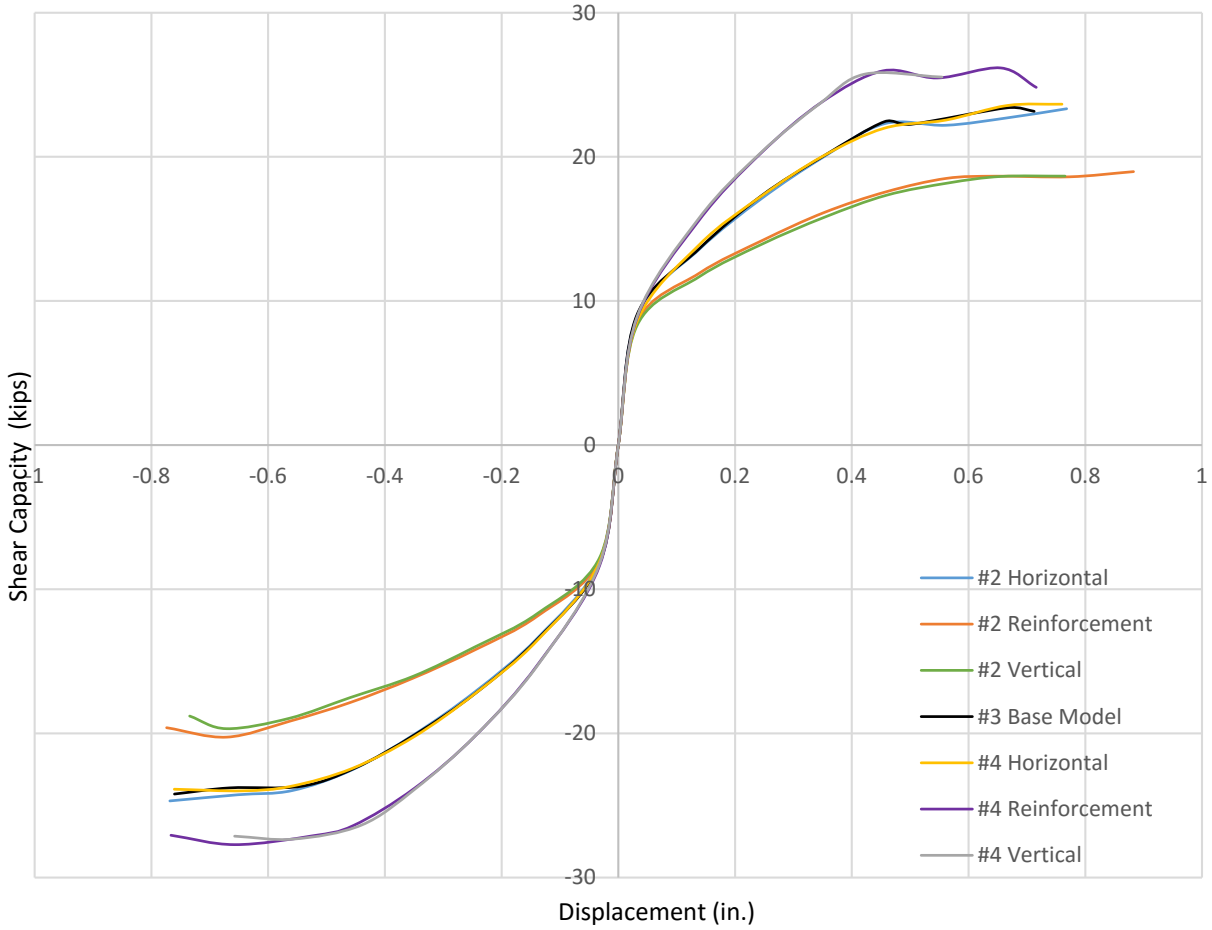

Figure 4-12: Backbone curves for modified reinforcement ratios (sizes)

The sensitivity of shear strength with respect to the vertical reinforcement ratio is described in Figure 4-13. A logarithmic trend line with an R^2 value of 0.9904 was applied to the plot. The trend line describes the shear capacity mathematically as $\{y = 0.2169 \ln x + 2.2818\}$ bounded between ratios of 0.0011 to 0.0045. The results found in this study are consistent with research performed by Haach, Vasconcelos, and Lourenco (2011). Their study concluded that the effect of vertical reinforcement on lateral strength was found to depend on the failure mode. Lateral strength increased from vertical reinforcement when flexure was the failure mode whereas minimal effects were observed when shear was the failure mode. The same observation was made in this study.

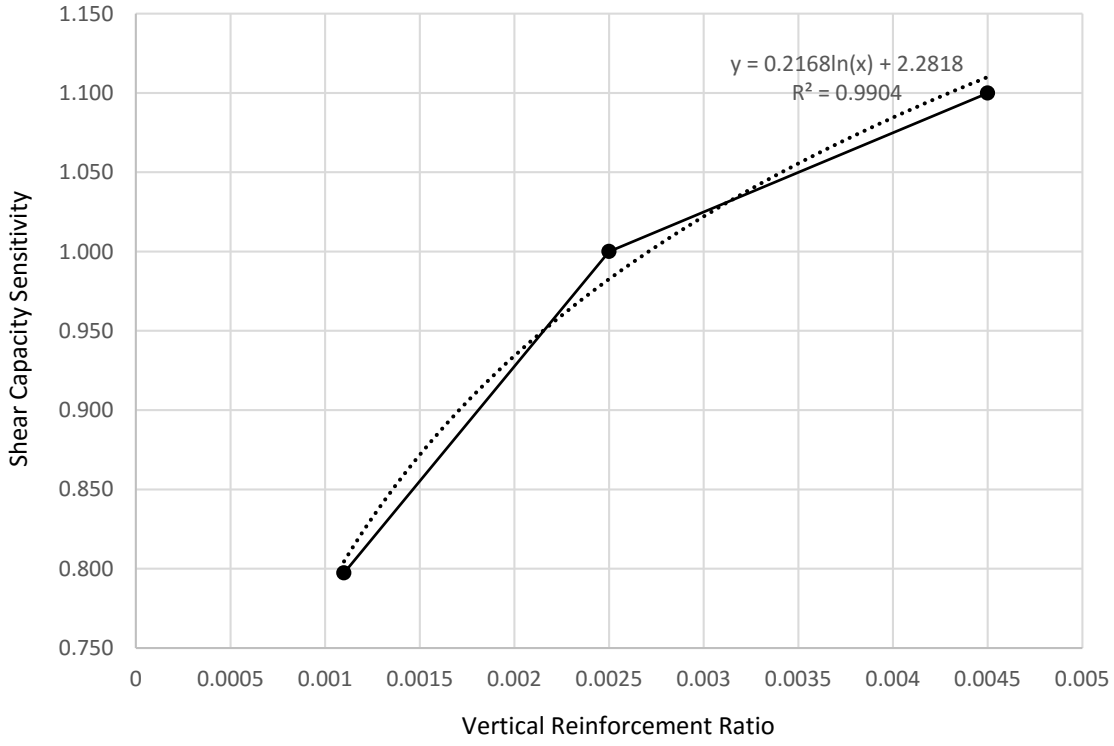

Figure 4-13: Sensitivity to the vertical reinforcement ratio

The aspect ratio of the walls considered in this research was 1.24. Based on aspect ratio alone, it would be presumed that the failure mode of these walls would be flexural. The observed failure of the walls was a mixed flexural – shear failure mode. In other words, the walls exhibited behavior of flexural failure by toe crushing (Figure 4-3 and Figure 4-14) and shear failure by diagonal stepping cracks (Figure 4-6 and Figure 4-7). The relationship between shear wall capacity and vertical reinforcement ratio has been shown to depend on failure mode and therefore partially on aspect ratio (Haach.2011). Although the wall characterized both types of failure modes, the shear wall response was much more sensitive to varying vertical reinforcement ratios than the response to varying horizontal reinforcement ratios. This indicates that when flexure is the failure mode, vertical reinforcement provides significant contributions to lateral strength.

Figure 4-14: Toe crushing of experimental masonry wall

The influence of varying horizontal reinforcement size within each grouping appears to be minimal. Walls with the same vertical reinforcement and differing horizontal reinforcement resulted in only 2% differences in strength with the larger reinforcement ratio reaching a larger capacity. The sensitivity of shear strength with respect to the horizontal reinforcement ratio is described in Figure 4-15. A trend line was not imposed as the response of shear capacity was considered negligible with respect to this parameter. Elampruk (2010), in a study of short partially grouted shear walls, stated that there appears to be a horizontal reinforcement ratio after which no further increase in reinforcement will result in increased capacity. Nolph (2010) reported that the maximum shear reinforcement ratio after which no additional shear capacity is obtained appears to be in the range of 0.00085 - 0.001 based on a 48 in. grout spacing. The walls that Nolph tested were also of smaller aspect ratio and no openings, however, a similar maximum reinforcement ratio might exist for these types of walls. Therefore, it is possible that the capacity could not be increased with changes to this parameter.

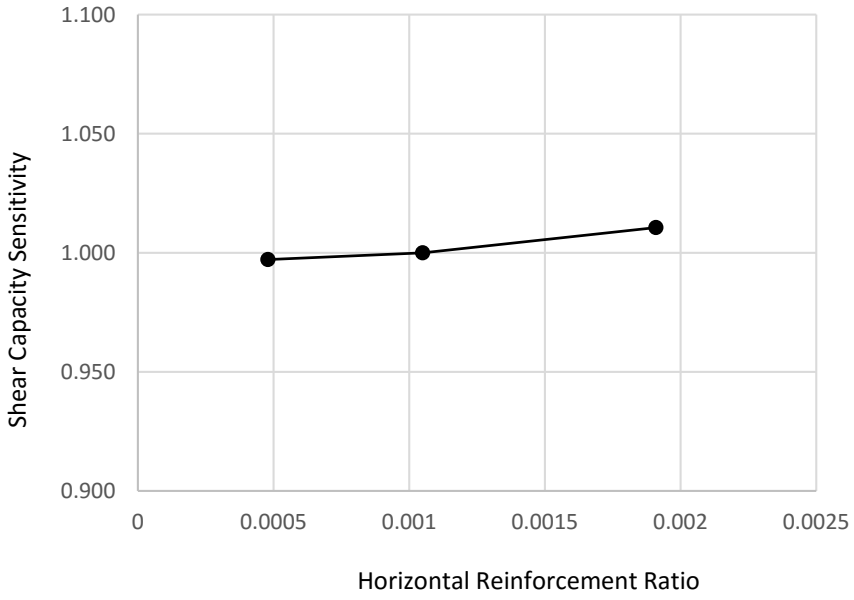

Figure 4-15: Sensitivity to the horizontal reinforcement ratio

4.5.2 Spacing

The reinforcement spacing parameter varied the reinforcement layout for both vertical and horizontal reinforcement while maintaining constant reinforcement ratios. For visual representations of the reinforcement configurations refer to Figure 3-33 to Figure 3-37. Note that all dimensions refer to the spacing between reinforcement bars, except for those dimensions with an asterisk (*). The asterisk denotes dimensions of the inner reinforcement to the top and bottom of the pier. Refer to Figure 3-33 and Figure 3-35 for clarification.

The results indicate that spacing of reinforcement ratios does not significantly impact shear capacity. Table 4-5 shows that shear capacity of the varied models is within 2% of the shear capacity of the base model. The MSJC (2013) code equations predicted a value of 30.2 kips for each of the models that modified the horizontal spacing of vertical reinforcement. The MSJC (2013) code equations un-conservatively over-predicted the capacity of the numerically modeled shear walls by approximately 27% - 30% for this parameter. The ductility, however, appears to improve significantly when the vertical reinforcement is spread evenly over the wall. The wall with a 16 in. horizontal spacing of vertical reinforcement reached ultimate capacity at approximately 0.87 in. whereas walls with a horizontal spacing of 24 in. and larger reached ultimate capacities at approximately 0.65 in. Figure 4-16 shows the corresponding backbone curves for the various tests for horizontal spacing of reinforcement. Figure 4-17 indicates that the sensitivity of shear capacity to varying horizontal spacing of vertical reinforcement is negligible.

Table 4-5: Results of model tests for varied horizontal spacing of vertical reinforcement

	Vertical Reinf. Ratio, ρ_v	Horizontal Reinf. Ratio, ρ_h	Ultimate Shear Capacity, V_{max} (kip)	Corr. Def. (in.)	MSJC Code Strength (kips)	MSJC/ V_{max}	V_{max}/ Base Model
16 in. Horizontal Spacing	0.0025	0.00105	23.7	0.874	30.2	1.276	1.012
24 in. Horizontal Spacing	0.0025	0.00105	23.2	0.634	30.2	1.300	0.992
44 in. Horizontal Spacing Base Model	0.0025	0.00105	23.4	0.667	30.2	1.290	1.000

*2 bars at center of piers with spacing of 24 in. from pier edge. Refer to figure.

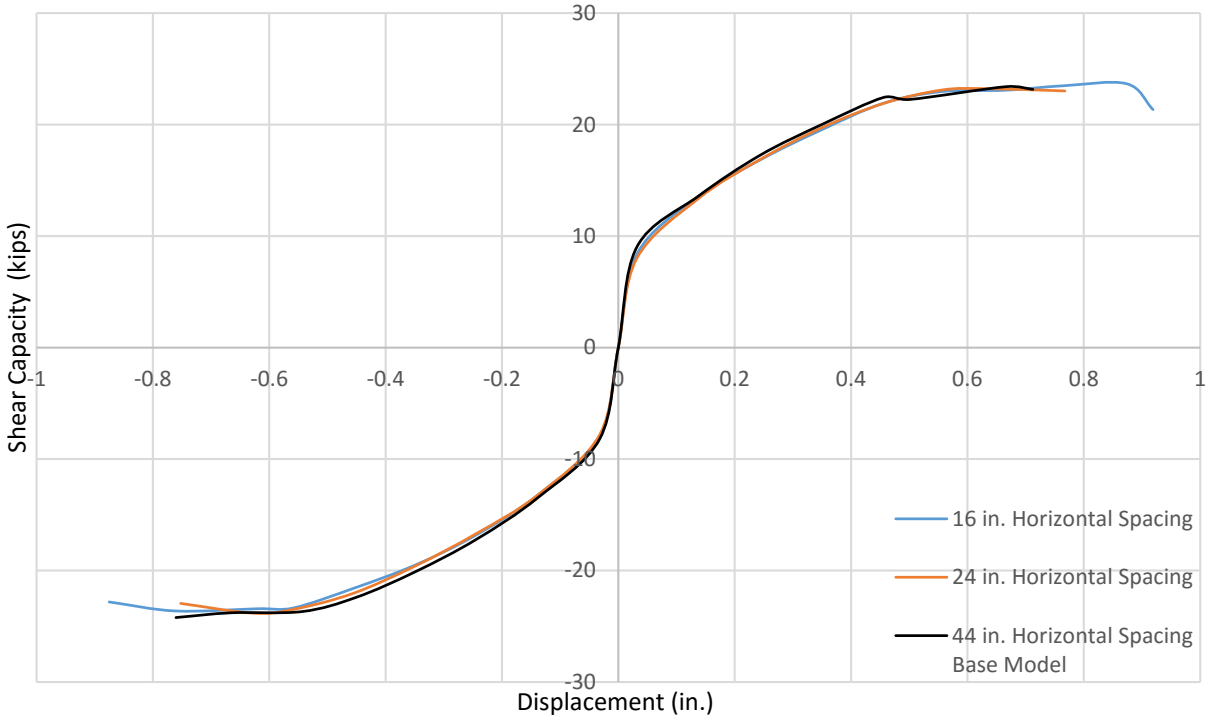

Figure 4-16: Backbone curves for horizontal reinforcement spacing

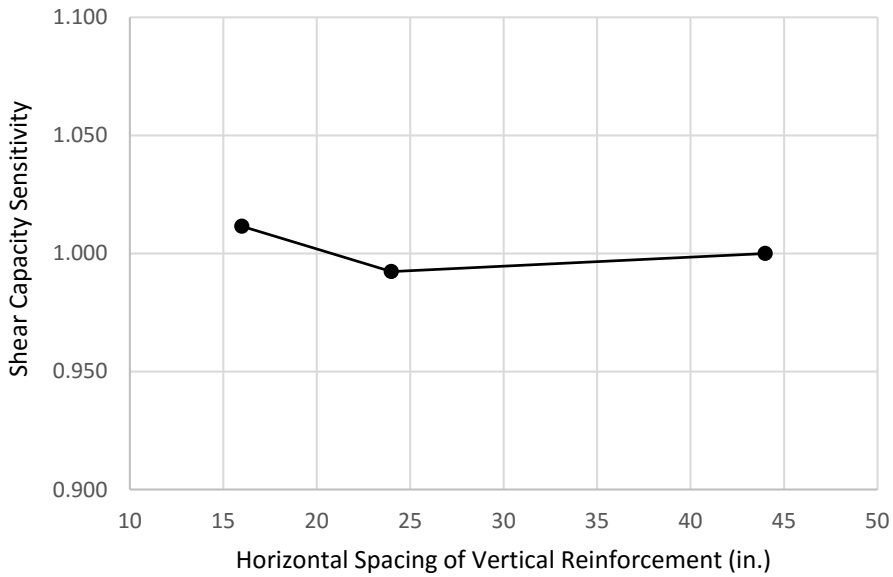

Figure 4-17: Sensitivity to the horizontal spacing of vertical reinforcement

The results also indicate that shear capacity is not sensitive to varying vertical spacing of horizontal reinforcement as all tests reached maximum capacity within 6% of the base model. Additionally, an inconsistent trend occurred when varying this parameter, i.e., as spacing increased, capacity slightly increased and as spacing decreased capacity increased. Nevertheless, the wall with the most uniformly spaced reinforcement reached both the greatest shear capacity and ductility. Table 4-6 shows that shear capacity of the model with 20 in. vertical spacing reached a maximum capacity of 24.9 kips, whereas all other models resulted in lower strengths regardless of the trend. Additionally, the wall with a 20 in. vertical spacing of horizontal reinforcement reached ultimate capacity at approximately 0.86 in. whereas walls with a horizontal spacing of 24 in. and larger reached ultimate capacities less than approximately 0.65 in. The MSJC (2013) code equations un-conservatively over-predicted the capacity of the

numerically modeled shear walls by 21% - 29% for this parameter. Figure 4-18 shows the corresponding backbone curves for the various tests for horizontal spacing of reinforcement.

Table 4-6: Results of model tests for varied vertical spacing of horizontal reinforcement

	Vertical Reinf. Ratio, ρ_v	Horizontal Reinf. Ratio, ρ_h	Ultimate Shear Capacity, V_{max} (kip)	Corr. Def. (in.)	MSJC Code Strength (kips)	MSJC/ V_{max}	V_{max}/ Base Model
20 in. Vertical Spacing	0.0025	0.00105	24.9	0.861	30.2	1.215	1.062
24 in. Vertical Spacing	0.0025	0.00105	24.2	0.534	30.2	1.247	1.035
36 in. Vertical Spacing Base Model	0.0025	0.00105	23.4	0.667	30.2	1.290	1.000
44 in. Vertical Spacing	0.0025	0.00105	24.3	0.644	30.2	1.244	1.037

*2 bars at center of piers with spacing of 24 in. from top/bottom of piers. Refer to figure.

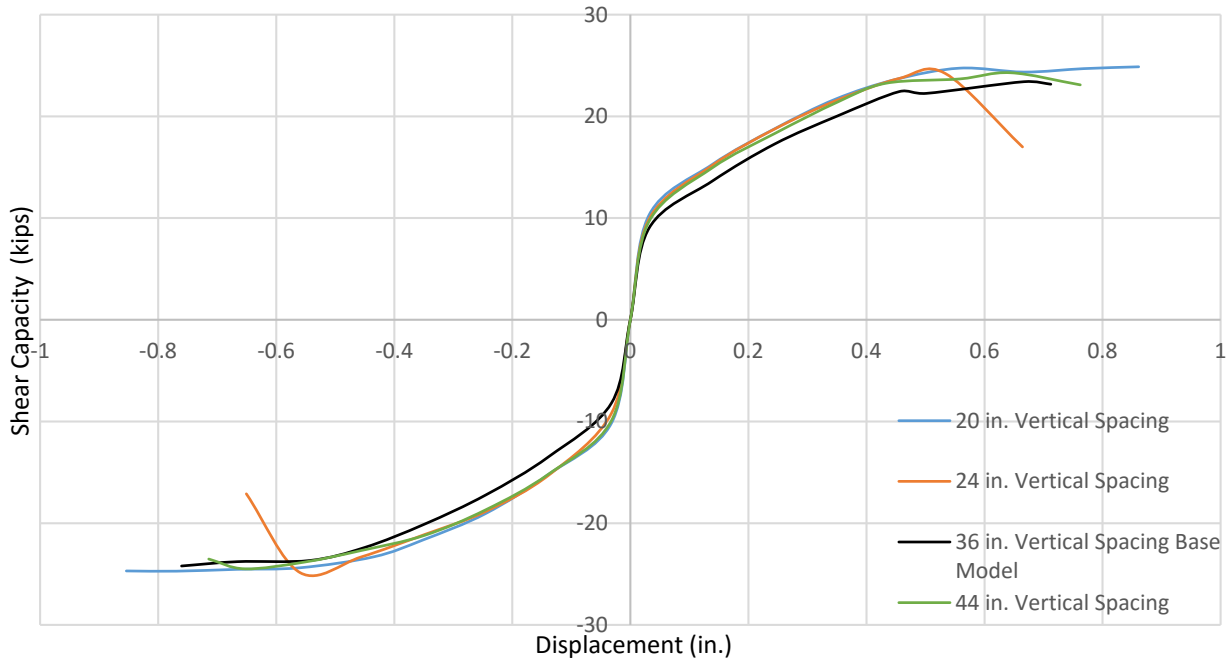

Figure 4-18: Backbone curves for vertical reinforcement spacing

Although shear capacity was affected by less than 6% from the models varying horizontal spacing of vertical reinforcement, the sensitivity was described by a quadratic trend line with an R^2 value of 0.9933 as shown in Figure 4-17. The trend line is represented mathematically by the function $y = 0.0003x^2 - 0.0233x + 1.391$ and bounded by the spacing of 20 in. to 44 in.

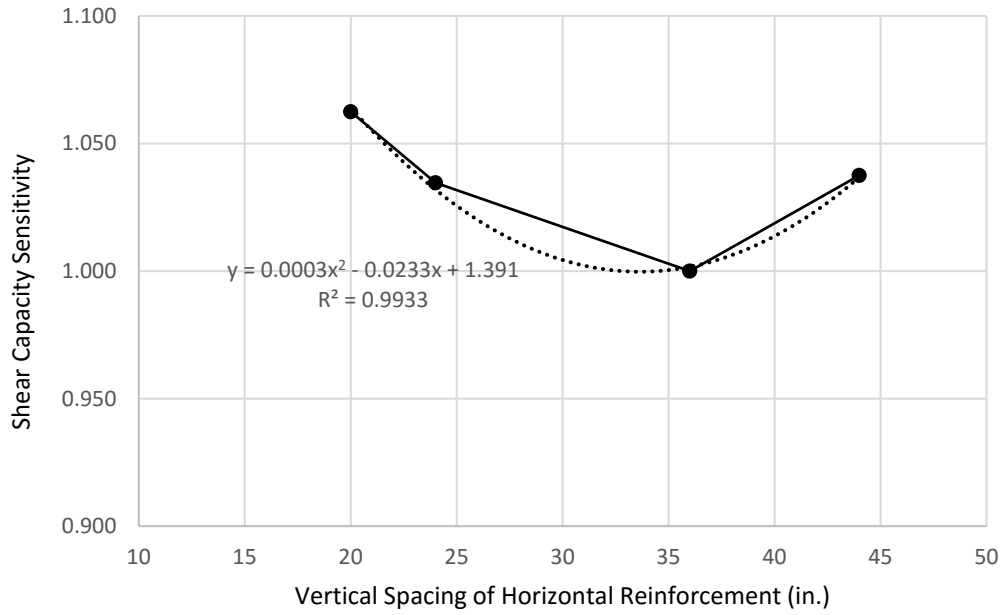

Figure 4-19: Sensitivity to the vertical spacing of horizontal reinforcement

4.6 Axial Stress

Axial load was varied by applying loads of 0 kips, 5 kips, 11.43 kips (base model), 15 kips, 20 kips, and 25 kips to the top of the masonry wall. Axial load has more or less influence on the wall depending on wall dimensions. Therefore, the modification of axial load is actually determining the effects of axial stress. The MSJC (2013) code equations predicted a value of 30.2 kips for each of the models that axial stress (see Appendix A for calculations). Although the

MSJC (2013) equations consider shear capacity as a function of axial load, the maximum limiting shear capacity formula does not consider axial load. Thus, the shear capacity was calculated as 30.2 kips for each model. The MSJC (2013) code equations un-conservatively over-predicted the capacity of the numerically modeled shear walls by 16% - 37% for this parameter. The results show that ultimate shear capacity and ductility are a function axial stress (Table 4-7) (Figure 4-20). These adjustments in shear wall response represent changes from a less flexural type failure mode to a more shear type failure mode with increasing axial stress. With little or no axial load present the structure reached ultimate shear capacities at deformations near 0.87 in. However, when 25.0 kips (46.98 psi) of axial load was introduced, the structure reached ultimate shear capacity at a deformation of 0.56 in.

Table 4-7: Results of model tests for axial load

	Ultimate Shear Capacity, V_{max} (kip)	**Corr. Def. (in.)**	**Stiffness (kip/in)**	**Stiffness/ Base Model**	**MSJC Code Strength (kips)**	**MSJC/ V_{max}**	**V_{max}/ Base Model**
Axial Load 0 kip (0.00 psi)	22.0	0.750	29.3	0.834	30.2	1.375	0.939
Axial Load 5.0 kip (9.40 psi)	23.1	0.873	26.5	0.754	30.2	1.307	0.988
Axial Load 11.43 kip (21.48 psi)	23.4	0.667	35.1	1.000	30.2	1.290	1.000
Axial Load 15.0 kip (28.19 psi)	23.9	0.561	42.7	1.217	30.2	1.261	1.023
Axial Load 20.0 kip (37.59 psi)	25.1	0.767	32.7	0.932	30.2	1.203	1.073
Axial Load 25.0 kip (46.98 psi)	26.0	0.556	46.7	1.331	30.2	1.161	1.111

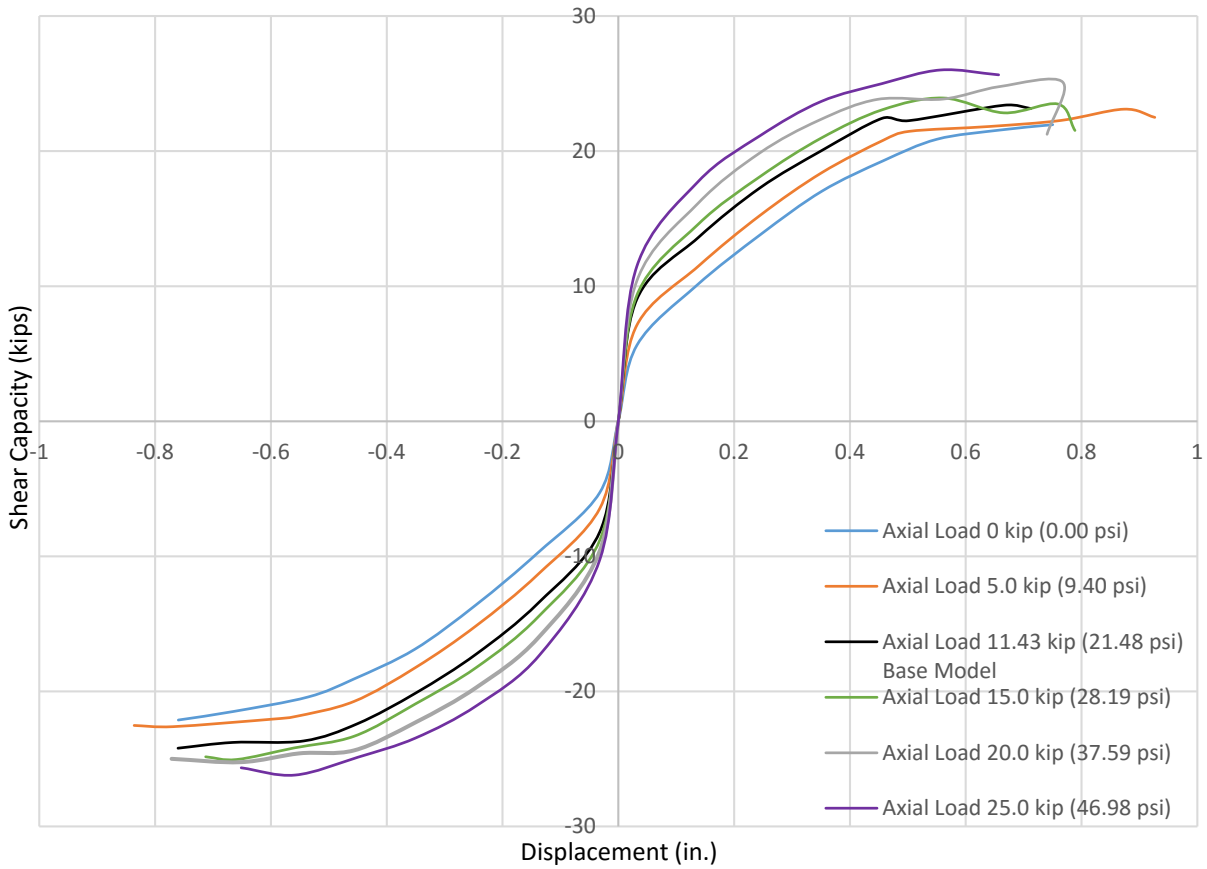

Figure 4-20: Backbone curves for modified axial stress values

The shear capacity of the wall was considered sensitive to axial stress. Figure 4-21 describes the sensitivity of shear capacity to axial stress. A linear trend line with an R^2 value of 0.9623 was applied to the plot. The trend line describes the response of shear capacity as increasing 0.35% per increase in 1 psi bounded between a range of 0 psi to 47 psi.

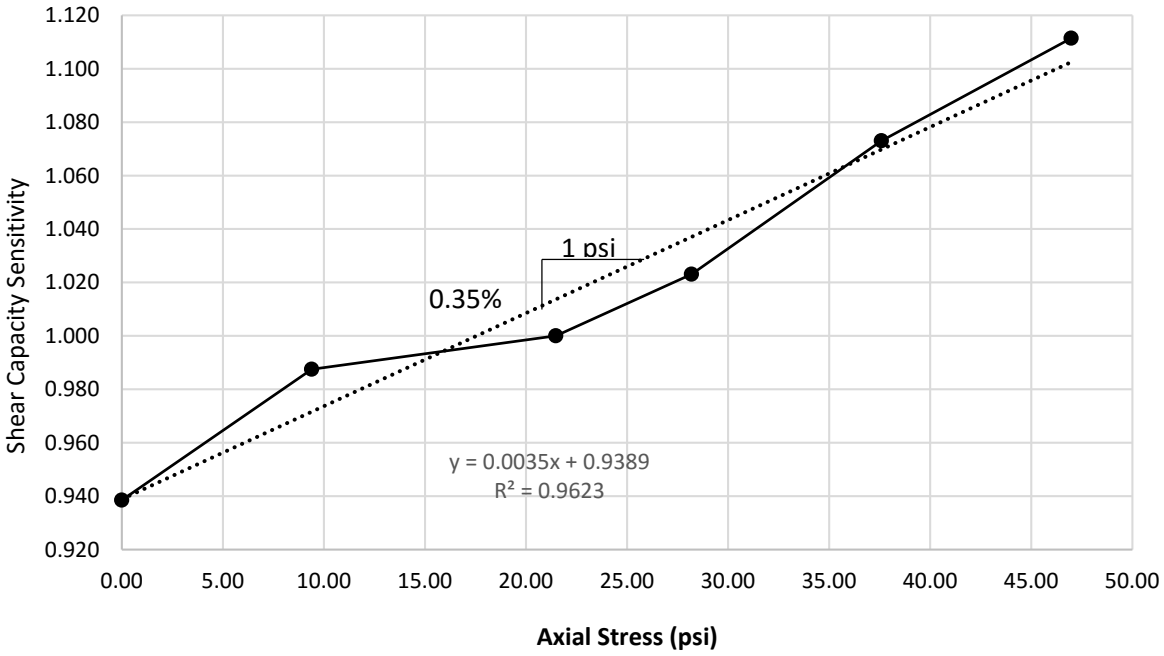

Figure 4-21: Sensitivity to axial stress

4.7 Aspect Ratio

The aspect ratios (height/width ratios) were modified by adding and removing entire stories from the model. The various aspect ratios considered were 0.45 (1 story), 0.84 (2 story), 1.24 (3 story), and 1.63 (4 story). For a visual representation of the models tested, see Figure 3-38 to Figure 3-40. Table 4-8 displays the numerical results of maximum shear capacities and corresponding displacements; Figure 4-22 shows the load-displacement curves. The results indicate that aspect ratio is inversely related to shear capacity and stiffness. In other words, as aspect ratio increase shear capacity and stiffness decrease. The 1-story model resisted a maximum of 27.7 kips of shear load whereas the 2-story model resisted 25.1 kips of shear load, a decrease of approximately 10%. The drop in capacity from the 2-story to 3-story model was 25.1 kips to 23.4 kips, approximately 7%. The drop in shear capacity from the 3-story to 4-story model was 23.4 kips to 22.4 kips, approximately 4%. The MSJC (2013) code equations un-

conservatively over-predicted the capacity of the numerically modeled shear walls by approximately 29% - 71% for this parameter (see Appendix A for calculations).

Table 4-8: Results of model tests for aspect ratio

	Ultimate Shear Capacity, V_{max} (kip)	Corr. Def. (in.)	Stiffness (kip/in)	Stiffness/ Base Model	MSJC Code Strength (kips)	MSJC/ V_{max}	V_{max}/ Base Model
Aspect Ratio 0.45 (1 Story)	27.7	0.241	114.9	3.273	47.3	1.709	1.183
Aspect Ratio 0.84 (2 Story)	25.1	0.444	56.4	1.606	39.4	1.572	1.071
Aspect Ratio 1.24 (3 Story) Base Model	23.4	0.667	35.1	1.000	30.2	1.290	1.000
Aspect Ratio 1.63 (4 Story)	22.4	0.981	22.8	0.650	30.2	1.350	0.956

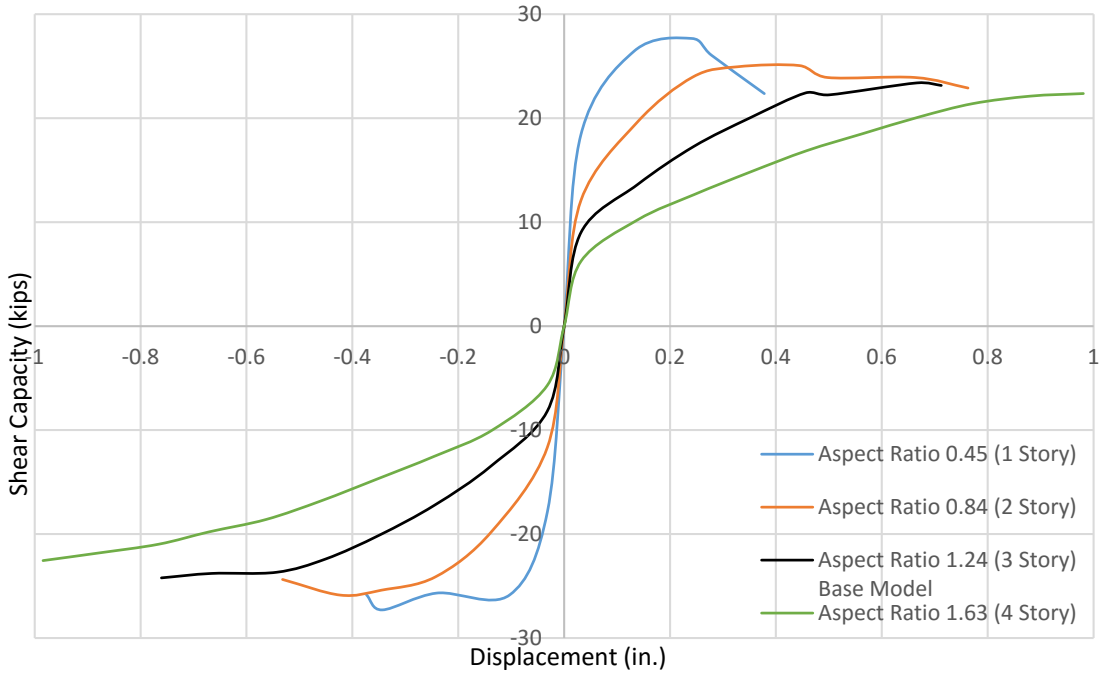

Figure 4-22: Backbone curves for modified aspect ratio values

The adjustments in the load-displacement curves with aspect ratio represent changes from a less flexural type failure mode to a more shear type failure mode The wall with an aspect ratio of 0.45 reached its maximum shear capacity at a displacement of 0.241 in. whereas the wall with an aspect ratio of 0.84 reached its maximum shear capacity at a displacement of 0.444 in. The change in stiffness was a decrease from 114.9 kips/in. to 56.4 kips/in, approximately 100%. The load-displacement curves indicate that shear wall stiffness is extremely sensitive to the aspect ratio. The sensitivity of shear capacity to aspect ratio is described in Figure 4-23. A quadratic trend line with an R^2 value of 0.9995 was applied to the plot. The trend line describes the shear capacity mathematically as $\{y = 0.1091x^2 - 0.4176x + 1.3475\}$ bounded between aspect ratios of 0.45 to 1.63.

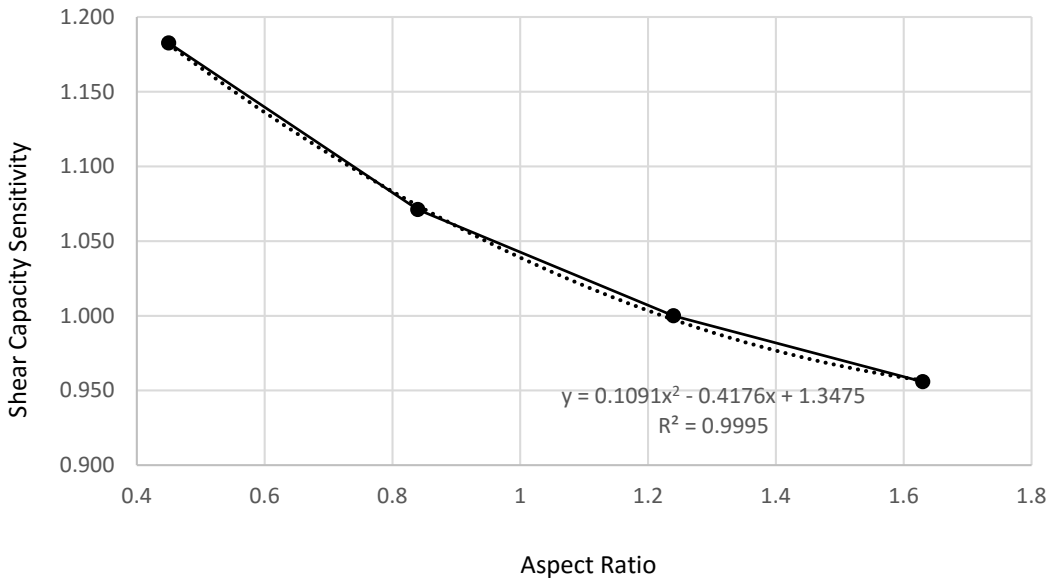

Figure 4-23: Sensitivity to aspect ratio

4.8 Openings

To study the effects of openings, modifications were made to the opening size both in the vertical and horizontal directions. In the vertical direction, tests were run by increasing or decreasing the height of the openings one course at a time. The results indicate the difficulty of capturing the effects of this parameter. As the opening height was decreased by a single course from 23 in. to 19 in., the capacity slightly increased from 23.4 kips to 23.5 kips as shown in Table 4-9 and Figure 4-24. This trend would seem reasonable, i.e., as the opening became smaller, the capacity would increase. However, as the opening height increased by a single course from 23 in. to 27 in., the capacity also increased from 23.4 kips to 23.8 kips. Interestingly, all of the vertical changes in opening height resulted in small capacity variations within 2% of the base model. The MSJC (2013) code equations un-conservatively over-predicted the capacity of the numerically modeled shear walls by approximately 28% - 31% for this parameter.

Table 4-9: Results of model tests for opening height

	Ultimate Shear Capacity, V_{max} (kip)	**Corresponding Deflection (in.)**	**MSJC Code Strength (kips)**	**MSJC/ V_{max}**	**V_{max}/ Base Model**
Opening Height 19 in.	23.5	0.769	30.2	1.283	1.006
23 in. (H) x 22 in. (W) Base Model	23.4	0.667	30.2	1.290	1.000
Opening Height 27 in.	23.8	0.666	30.2	1.271	1.015
Opening Height 31 in.	23.0	0.667	30.2	1.311	0.985

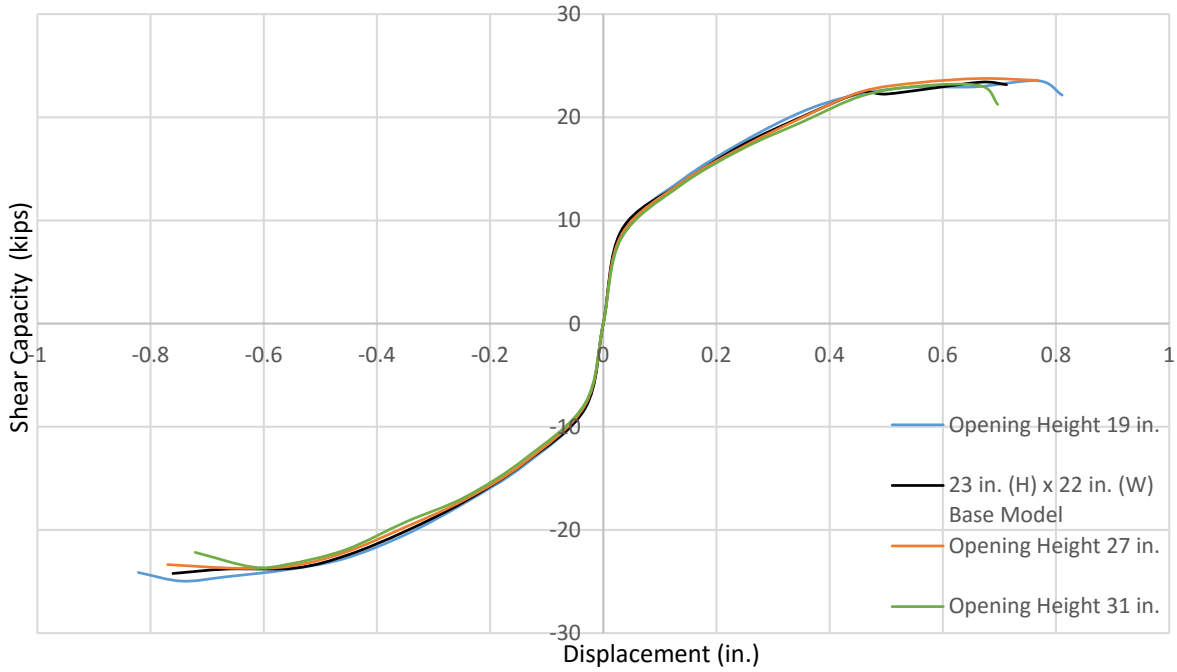

Figure 4-24: Backbone curves for modified heights of openings

Due to the inconclusive results obtained with respect to vertical changes in opening size from the previous tests, additional models were built and tested using the validated model for walls 2 and 3 (Appendix C Figures C-7 to C-9). The difference in the models is that walls 2 and 3 have trimming reinforcement located only underneath the opening (Figure 1-1). In these additional tests, the same opening heights were varied. As noted in Table 4-10, shear capacity decreased from 23.2 kips to 22.7 kips as the opening height decreases from 23 in. to 19 in.; however, shear capacity also decreased from 23.2 kips to 22.6 kips to 22.4 kips as the opening height increases from 23 in. to 27 in. to 31 in. All tests resulted in less than 4% changes in capacity. Likewise, the discrepancy between the MSJC (2013) code equations and observed model shear capacity increased to approximately 30% - 35% for this parameter (see Appendix A for calculations). The additional results were also inconclusive.

Table 4-10: Additional results of model tests for opening heights

	Ultimate Shear Capacity, V_{max} (kip)	Corresponding Deflection (in.)	MSJC Code Strength (kips)	MSJC/ V_{max}	V_{max}/ Base Model
Opening Height 19 in.	22.7	0.652	30.2	1.329	0.979
23 in. (H) x 22 in. (W) Base Model	23.2	0.558	30.2	1.300	1.000
Opening Height 27 in.	22.6	0.557	30.2	1.335	0.974
Opening Height 31 in.	22.4	0.526	30.2	1.347	0.965

Three multi-story, partially grouted, perforated masonry shear wall specimens with door openings were experimentally tested in research performed by Buxton (2017). These walls were identical to the walls tested in this research, varying only in opening size from a 23 in. window configuration to a 44 in. door configuration, see Figure 4-25. Table 4-11 shows that two of the walls with door openings resulted in higher capacities than the wall with window openings; however, one of the walls with door openings resulted in lower capacities than the wall with window openings. Figure 4-26 shows the backbone curves of these various experimental walls. Similarly, the MSJC (2013) code equations un-conservatively over-predicted the capacity of these experimental shear walls by approximately 14% - 40%. The experimental results are therefore also inconclusive and further investigation is needed to relate vertical opening size to shear wall capacity if there indeed exists a relationship. Figure 4-25 shows that shear strength is not sensitive to the height of an opening. The conclusions drawn in this research suggest that it is possible that shear capacity is not influenced by the vertical opening dimension.

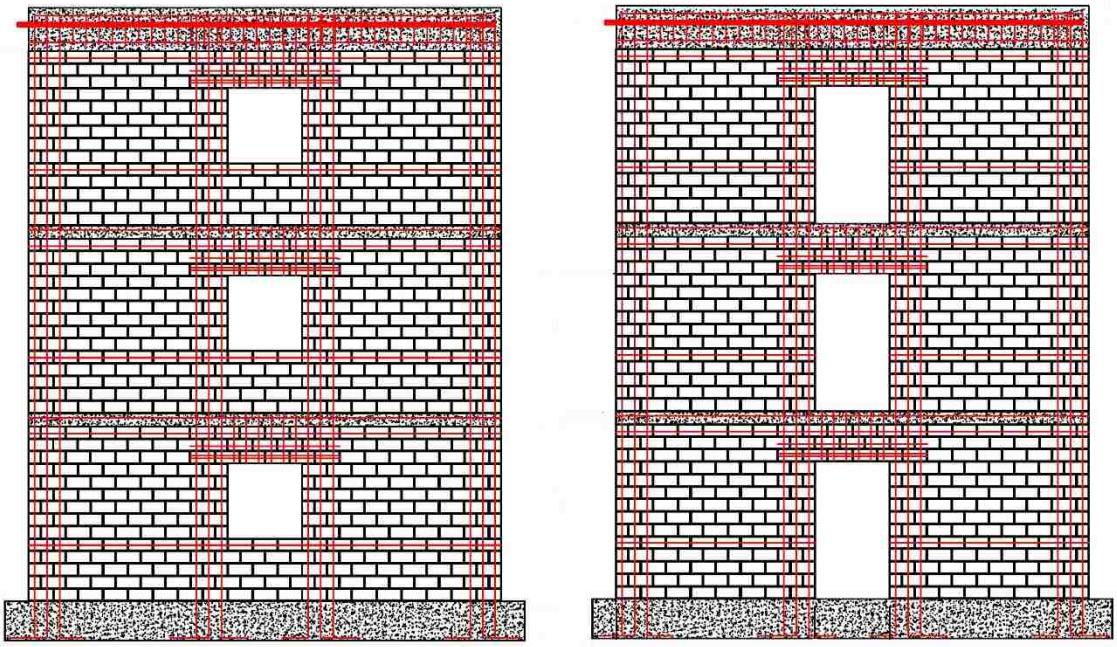

Figure 4-25: Walls tested in this research (left) vs. walls tested in Buxton (2017)(right)

Table 4-11: Experimental results of walls with window and door openings

	Ultimate Shear Capacity, V_{max} (kip)	**Corresponding Deflection (in.)**	**MSJC Code Strength (kips)**	**MSJC/ V_{max}**
Experimental Wall 1 (Window)	24.8	0.552	30.2	1.218
Experimental Wall 4 (Door)	26.5	0.566	30.2	1.138
Experimental Wall 5 (Door)	21.6	0.510	30.2	1.395
Experimental Wall 6 (Door)	25.1	0.727	30.2	1.204

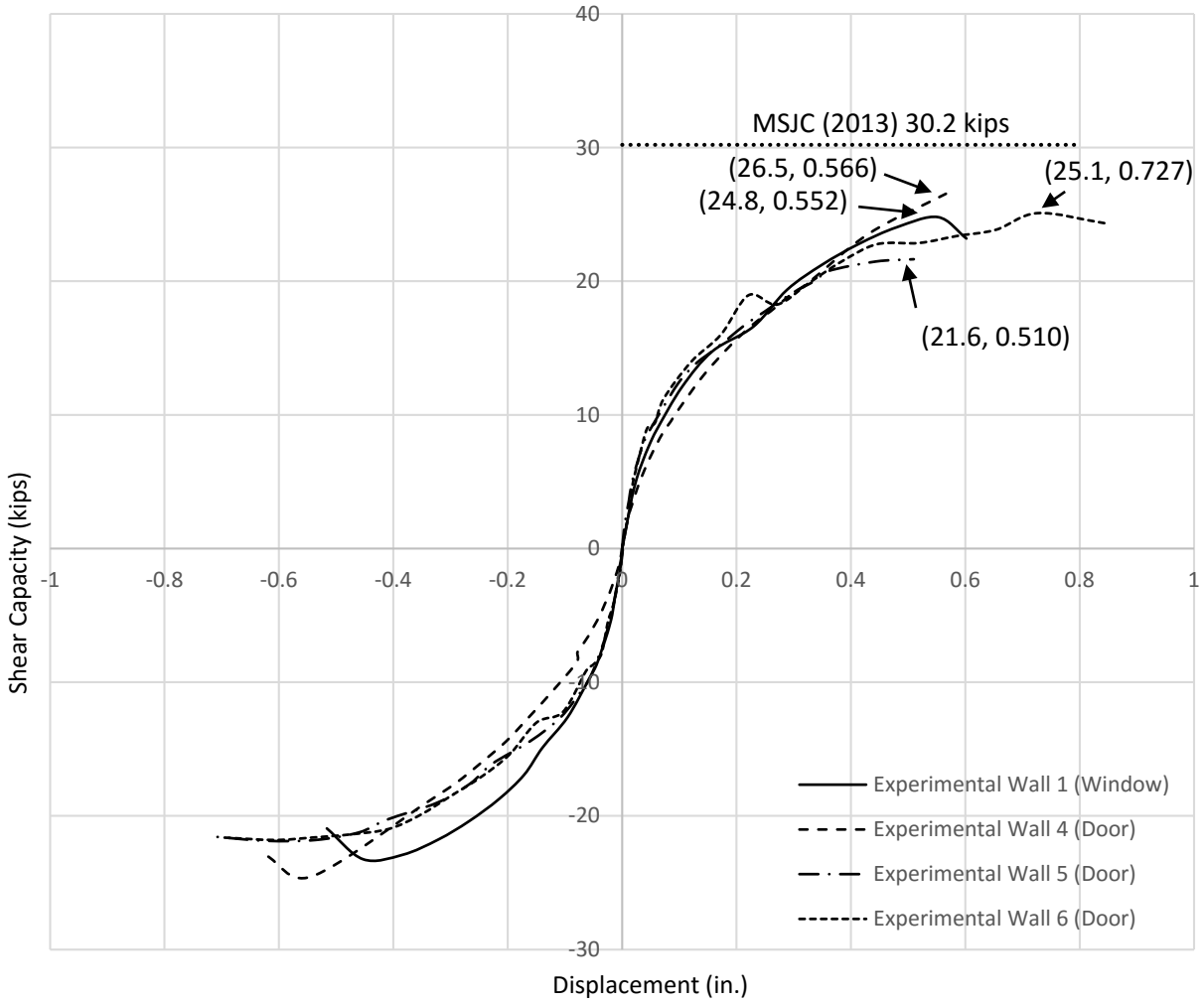

Figure 4-26: Backbone curves for experimental walls with window and door openings

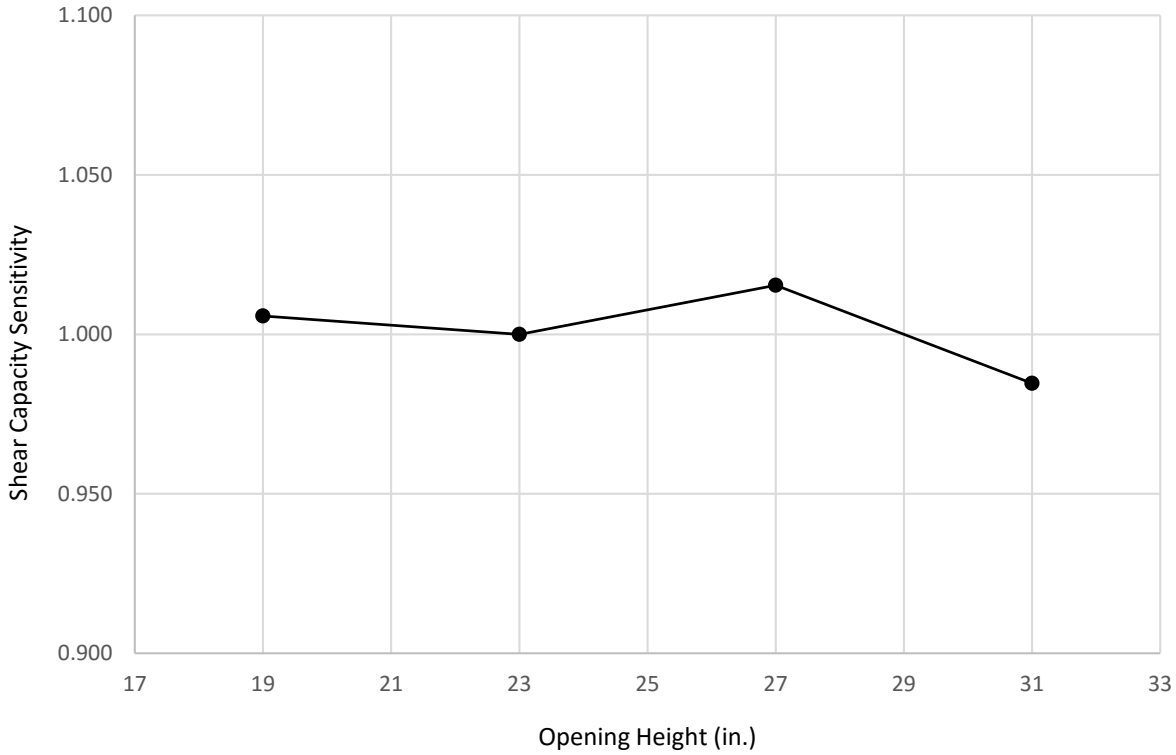

Figure 4-27: Sensitivity to vertical opening height

One possible explanation for the increase in shear capacity is as the window opening becomes taller is that there is a change in the load path and stress distribution associated with the change in wall geometry. In other words, as the opening becomes taller the system changes from acting like a single shear wall to acting like two piers that are rigidly connected with a concrete beam at every story. When lateral load is applied to the system of two piers connected rigidly at the floor levels, the load path is "attracted" to these rigid elements which induces less stress on the unreinforced masonry and mortar joints where failure had occurred previously. Further research is needed to validate or refute this hypothesis.

In the horizontal direction, the opening widths were enlarged by one element (½ of a CMU) per side for each model test. A clear trend is established; i.e., Table 4-12 shows that as the

width of the opening increases from 22 in. to 30 in. to 38 in., the shear capacity decreases from 23.4 kips to 22.9 kips to 22.1 kips, respectively. The backbone curves for the tested models are shown in Figure 4-28. Although the initial decrease in capacity is only approximately 2%, the following decrease in capacity is approximately 6% and is therefore nonlinear. In other words, shear capacity decreases at an increasing rate with respect to opening width. This suggests that shear capacity is sensitive to opening width as shown in Figure 4-27. A quadratic trend line with an R^2 value of 1.0 was applied to the plot. The trend line describes the shear capacity mathematically as $y = -0.0001x^2 + 0.0033x + 0.9812$ bounded between opening widths of 22 in. to 38 in (corresponding to opening width/story width ratios of 0.145 to 0.250 as noted in Table 3-14). The MSJC (2013) code equations un-conservatively over-predicted the capacity of the numerically modeled shear walls by approximately 25% - 29% for this parameter (see Appendix A for calculations). No major changes in ductility are noted with respect to the changes in opening width tested in this research.

Table 4-12: Results of model tests for opening width

	Ultimate Shear Capacity, V_{max} (kip)	**Corresponding Deflection (in.)**	**MSJC Code Strength (kips)**	**MSJC/ V_{max}**	**V_{max}/ Base Model**
23 in. (H) x 22 in. (W) Base Model	23.4	0.667	30.2	1.290	1.000
Opening Width 30 in.	22.9	0.664	28.9	1.260	0.980
Opening Width 38 in.	22.1	0.538	27.6	1.248	0.945

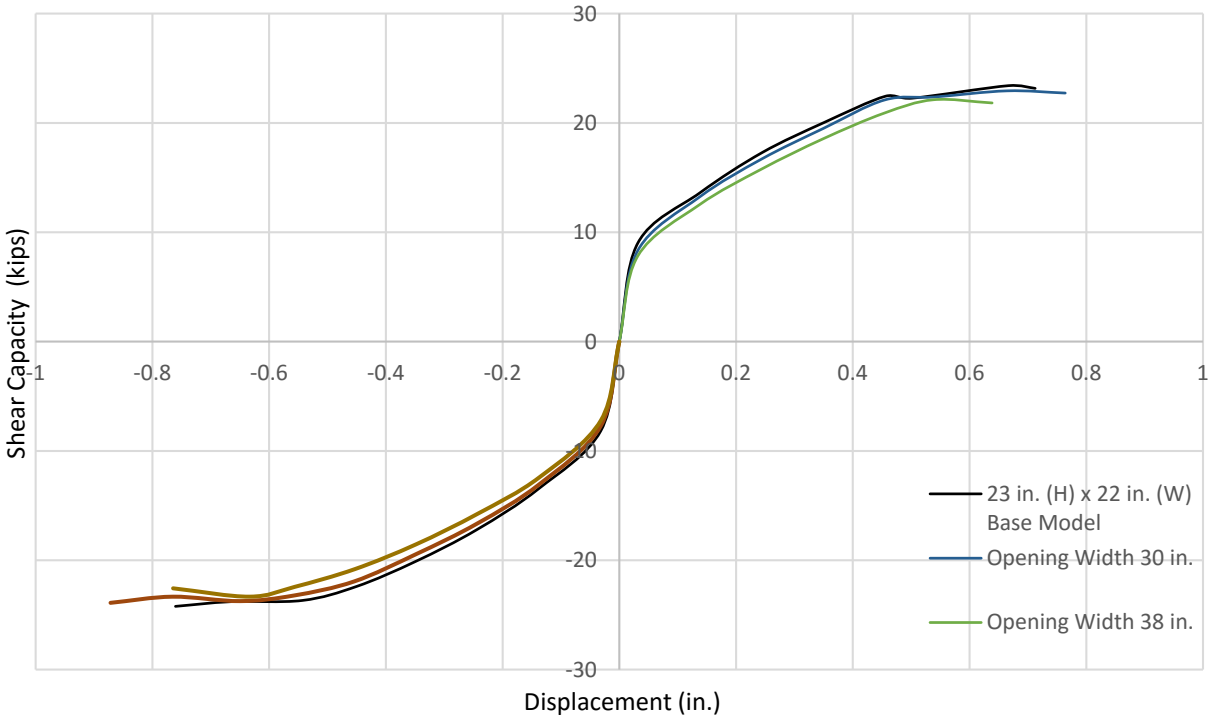

Figure 4-28: Backbone curves for modified widths of openings

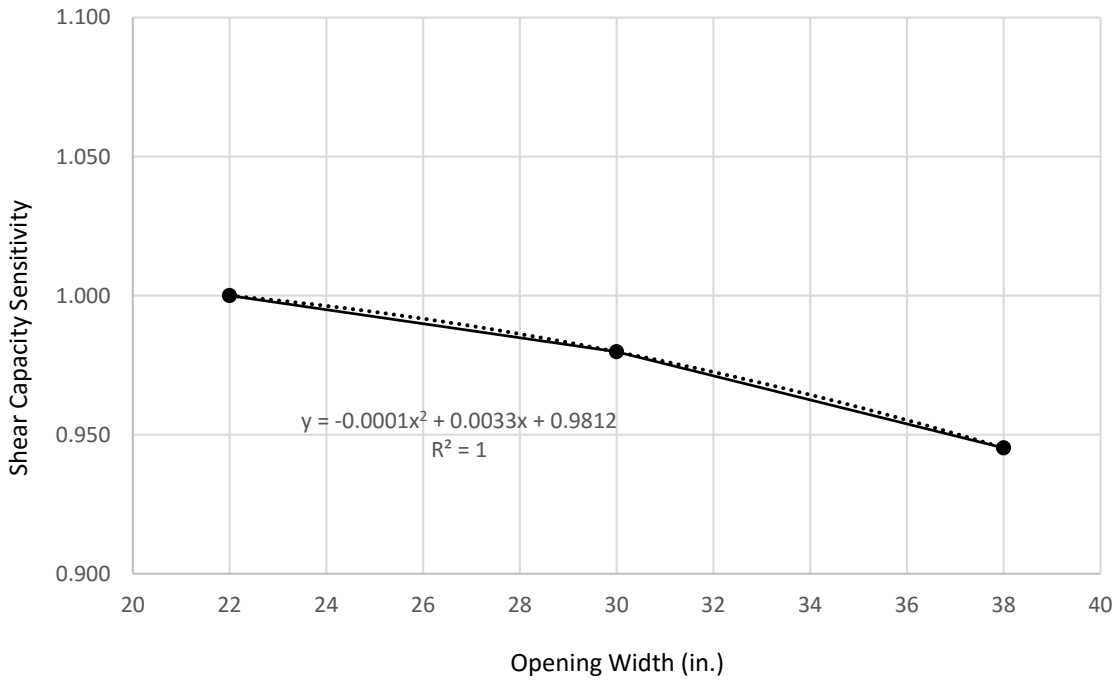

Figure 4-29: Sensitivity to horizontal opening width

5 CONCLUSIONS

5.1 Introduction

The purpose of this study was to determine the significance and sensitivity of various parameters that influence the response of multi-story, partially grouted, perforated masonry shear walls. The shear capacity of these type of walls is considered sensitive to the following parameters: compressive strength of grouted masonry; compressive strength of un-grouted masonry; joint strength ratio; vertical reinforcement ratio; axial stress; aspect ratio; and opening width. The shear capacity of these type of walls is considered not sensitive to the following parameters: horizontal reinforcement ratio; vertical reinforcement spacing; and horizontal reinforcement spacing. Opening height was determined inconclusive in its effect on these type of walls.

5.2 Summary

The findings of this research are summarized below. As part of the results, the sensitivity of each parameter is described. The sensitivity quantifies the expected change in capacity based on the varied parameter. The sensitivity is reported mathematically via trend lines and returns a percentage value of the strength of the validated base model. These findings represent the response of multi-story (large aspect ratio), partially grouted, perforated (openings), cantilever type, masonry shear walls.

- The response of the masonry shear walls in question is sensitive to the grouted masonry prism strength up to approximately 40% larger than un-grouted masonry prism strength. When $f'_{m,grouted}$ is within this range, shear capacity increases approximately 0.035% per increase in 1 psi (Figure 4-2). When $f'_{m,grouted}$ is larger than $f'_{m,ungrouted}$ by more than 40%, negligible strength gain occurs. The MSJC (2013) code equations un-conservatively over-predicted the capacity of the numerically modeled shear walls by 18% - 29% for this parameter. The effects of grouted masonry prism strength on ductility is inconclusive. When flexure is the failure mode, grouted masonry on the extremities plays an important role in resisting the flexural induced forces. Shear capacity increases are limited as the shear load must still pass through the weaker un-grouted portions of the masonry.
- The shear strength of the masonry walls in question is sensitive to the un-grouted masonry prism strength. The sensitivity is described by a linear trend line such that shear capacity increases 0.02% per increase in 1 psi (Figure 4-5). The MSJC (2013) code equations un-conservatively over-predicted the capacity of the numerically modeled shear walls by approximately 17% - 29% for this parameter. The effects of un-grouted masonry prism strength on ductility is inconclusive.
- The shear strength of the masonry walls in question is sensitive and directly proportional to the ratio of mortar shear strength to masonry compressive strength, i.e., the joint strength ratio (J.S.R.). The sensitivity is described by a linear trend line such that shear capacity increases 14.2% per increase of 0.01 in J.S.R. (Figure 4-9). The MSJC (2013) equations predicted the shear wall capacity of the numerical models from an un-conservative 57% to a conservative 95%. The

accuracy of the MSJC (2013) equations depends heavily upon the J.S.R. of the model. At a J.S.R value of 0.045, the MSJC (2013) equations accurately and conservatively predicted the shear capacity of the wall. Ductility decreases as the J.S.R. increases.

- The in-plane response of the masonry walls in question is sensitive to vertical reinforcement ratios; however, it is not sensitive to horizontal reinforcement ratios. In other words, when flexure is the failure mode, flexural reinforcement ratios significantly affects the lateral strength. Strength differences of 20% and 10% were noted as vertical reinforcement ratios increased from #2 to #3 to #4 vertical bars, respectively. The sensitivity of this parameter is described mathematically by the logarithmic trend line $y = 0.2304 \ln x + 2.3579$, where y = shear capacity sensitivity and x = vertical reinforcement ratio (Figure 4-13). The MSJC (2013) equations un-conservatively over-predicted the capacity of the numerically modeled shear walls by approximately 17% - 67% for vertical and horizontal reinforcement ratios. No significant changes were observed with changes in horizontal reinforcement ratios (Figure 4-15). Ductility was not sensitive to this parameter.
- The shear capacity is not sensitive to the spacing of vertical and horizontal reinforcement with constant vertical and horizontal reinforcement ratios (Figure 4-17 and Figure 4-19). The MSJC (2013) code equations un-conservatively over-predicted the capacity of the numerically modeled shear walls by approximately 27% - 30% for horizontal spacing of vertical reinforcement and by 21% - 29% for vertical spacing of horizontal reinforcement. The ductility noticeably increased when the spacing of both vertical and horizontal reinforcement decreased.

Maximum capacity was reached at approximately 0.86 in. of displacement vs. 0.65 in. of displacement with a horizontal spacing of vertical reinforcement of 16 in. vs. 24 in. Similarly, maximum capacity was reached at approximately 0.86 in. of displacement vs. 0.65 in. of displacement with a vertical spacing of horizontal reinforcement of 20 in. vs. 36 in.

- The response of the masonry walls in question is sensitive to axial stress. The sensitivity is described by a linear trend line such that shear capacity increases 0.35% per increase in 1 psi (Figure 4-21). The MSJC (2013) code equations un-conservatively over-predicted the capacity of the numerically modeled shear walls by 16% - 37% for this parameter. Stiffness also consistently increased with each increase in axial stress. As axial stress increases, the wall response becomes more brittle.
- The in-plane response of the masonry walls in question is sensitive to the aspect ratio. As aspect ratios increase from 0.45 to 0.84 to 1.24, strength losses of approximately 10%, 7%, and 4% occurred, respectively. The sensitivity is described mathematically by the quadratic trend line $y = 0.1091x^2 - 0.4176x + 1.3475$, where y = shear capacity sensitivity and x = aspect ratio (Figure 4-23). Stiffness drastically changed with aspect ratio. The MSJC (2013) code equations un-conservatively over-predicted the capacity of the numerically modeled shear walls by approximately 29% - 71% for this parameter. As aspect ratios increase from 0.45 to 0.84 to 1.24 to 1.63, stiffness losses of approximately 165%, 60%, and 35% occurred, respectively.

- The effect of opening height for capacity of the masonry shear walls in question is determined inconclusive, however, results indicate that this parameter is not sensitive to shear wall capacity (Figure 4-27). As opening heights vary vertically, the load path changed such that maximum load capacity slightly increased as opening heights were increased or decreased. Further research is needed to validate or refute these hypotheses. Shear capacity is sensitive to increases in opening width. The sensitivity is described mathematically by the quadratic trend line $y = -0.0001x^2 + 0.0033x + 0.9812$, where y = shear capacity sensitivity and x = opening width (Figure 4-29). As opening width increases, the masonry piers decrease and reduce shear capacity. The MSJC (2013) code equations un-conservatively over-predicted the capacity of the numerically modeled shear walls by approximately 28% - 31% for opening height and approximately 30% - 35% for opening width.

5.3 Additional Areas of Research

The accuracy of the results produced from the numerical parametric analysis performed in this research study depends entirely upon the ability of the model to truly represent the experimental model. Though the models were validated, further confirmation of their accuracy would improve the reliability of the conclusions drawn in this research. One method to further validate the models is to predict masonry shear wall responses using the models and verify the numerical results with a larger variety of wall configurations for experimental study. A collaborative work could be studied and compared against data from other experimental tests previously performed on multi-story, partially grouted, perforated masonry shear walls.

The response of the masonry shear walls relative to vertical opening sizes was considered inconclusive. Voon and Ingham (2008) however, observed a decrease in shear capacity with increasing vertical opening height in their study of single story, perforated masonry shear walls. These inconsistencies need to be verified. As for this research, it is thought that as vertical opening size increases in every story, the load path is directed more towards the rigid concrete floor which can increase capacity to a certain degree. Further study of the change in load path and failure mechanisms of these wall configurations could represent a significant contribution.

The boundary conditions of the model highly influence the shear wall response (Haach 2011). Additional insight relative to the parameters that affect fixed-end masonry shear wall response would make an important contribution to the field. Performing a fixed end wall study in the laboratory and building a model that could be validated and used for parametric analysis would illuminate differences between cantilever type walls and fixed end type walls.

Post-peak degradation was inaccurately captured in the models used for this research. The experimental walls had very little ductility after reaching capacity, whereas the models maintained capacity significantly longer than observed in the lab. More accurate post-peak models that are applicable to masonry shear walls studied in this research would prove beneficial to accurately capturing the entire response of the wall.

The shear strength of mortar relative to the compressive strength of masonry significantly influenced the shear capacity of the masonry walls. Likewise, the compressive strength of un-grouted masonry ($f'_{m,ungrouted}$) was found to impact the shear capacity of the walls significantly more than the compressive strength of grouted masonry ($f'_{m,grouted}$). Implementing these parameters into the nominal shear equations for masonry shear walls should be considered versus the parameter f'_m which currently encompasses all of these parameters.

To appropriately accommodate for the placement of discrete reinforcement and to obtain more accurate results from the finite element method, the nodes and elements were modeled as square instead of rectangular like the CMU's. Thus the model contains elements with nominal dimensions of 4" x 4" x 4" whereas the nominal dimensions of the actual CMU's were 8" x 4" x 4". Consequently, the model encompasses 39 nodes with 38 elements per complete course whereas the physical walls contained 19 CMU's in a complete course. Note that the bed joint dimension for each element was input as 8 in. (203.2 mm), however the width of the element was only 4 in. (101.6 mm). Joint properties are smeared across a single finite element (VecTor2 Manual). Therefore, a possible consequence of creating a model with 2 elements per CMU is indirectly adding a joint in the middle of each CMU where there was no joint present in the experimental walls. No description of applying elements in this manner was provided in the VecTor2 Manual. Further research regarding the size of elements used for modeling would provide additional insight on the effect of using elements smaller than the size of the CMU.

REFERENCES

Alecci, V., Fagone, M., Rotunno, T., De Stefano, M. (2013). "Shear strength of brick masonry walls assembled with different types of mortar.", *Elsevier,* Construction and Building Materials, 40(2013) 1038-1045, https://www.sciencedirect.com/science/article/pii/S0950061812009439

ASTM Standard C90. "Standard Specification for Loadbearing Concrete Masonry Units." American Society for Testing and Materials, ASTM International, West Conshohocken, Pennsylvania, www.astm.org

Buxton, J. R. (2017). "Strut-and-Tie Modeling of Multistory, Partially-Grouted, Concrete Masonry Shear Walls with Openings." Master of Science, Brigham Young University, Provo, Utah.

Chaimoon, K., and Attard, M. M. (2007). "Modeling of Unreiforced Masonry Walls Under Shear and Compression." *Elsevier*, Engineering Structures, 29(2007) 2056-2068. https://www.sciencedirect.com/science/article/pii/S0141029606004305

Davis, C. L., McLean, D. I., and Ingham, J. M. (2010). "Evaluation of Design Provisions for In-Plane Shear in Masonry Walls.", *TMS Journal December 2010*.

Drysdale, R. G., Hamid, A., and Baker, L. R. (1999). Masonry structures: behavior and design, 2nd ed., The Masonry Society, Boulder, Colo

Elampruk, J. H. (2010). "Shear Strength of Partially Grouted Squat Masonry Shear Walls." Master of Science in Civil Engineering, Washington State University, Pullman, Washington.

Fattal, S. G. (1993). "Strength of Partially-Grouted Masonry Shear Walls Under Lateral Loads.", *National Institute of Standards and Technology*, NISTIR 5147, https://www.nist.gov/publications/analysis-partially-grouted-masonry-shear-walls

Fortes, E.S. (2017). "Caracterizacão da Alvenaria Estrutural de Alta Resistência.", Ph. D. Dissertation (In Portuguese), Universidade Federal De São Carlos, São Paulo, Brazil.

Ghanem, G. M., Essawy, A. S., and Hamid, A. A. (1992). "Effect of Steel Distribution on the Behavior of Partially Reinforced Masonry Shear Walls." *Proc., 6th Canadian Masonry Symp., University of Saskatchewan, Saskatoon, Sask., Canada.*

Haach, V. G., Vasconcelos, G., and Lourenco, P.B. (2011). "Parametrical Study of Masonry Walls Subjected to In-Plane Loading Through Numerical Modeling." *Elsevier*, Engineering Structures, 33(2011) 1377-1389. https://www.sciencedirect.com/science/article/pii/S0141029611000423

Harris, H. G., Sabnis, G. (1999). *Structural Modeling and Experimental Techniques 2nd edition*. CRC Press, Boca Raton, Florida.

International Conference of Building Officials (1988). "Uniform Building Code 1988." Whittier, California. Pg. 218.

Long, L., Hamid, A. A., Drysdale, R. G. (2005). "Small-Scale Modelling of Concrete Masonry Using ½-Scale Units: A Preliminary Study." *10th Canadian Masonry Symposium, Banff, Alberta, June 8-12 2005*.

Kotsovos, M. D., Pavlovic, M. N., Jelic, I. (1999). "A study of dowel action in reinforced concrete beams." *Magazine of Concrete Research*, 51, No. 2, April, 131-141. https://www.icevirtuallibrary.com/doi/abs/10.1680/macr.1999.51.2.131

Mapefill (2014). "High-flow non-shrink cementitious anchoring grout." Mapei. http://www.mapei.com/public/COM/products/305_mapefill_gb.pdf

Matsumura, A. (1987). "Shear Strength of Reinforced Hollow Unit Masonry Walls.", *2nd Meeting of the Joint Technical Coordinating Committee on Masonry Research, U.S.-Japan Coordinated Program for Masonry Building Research, Keystone Colorado, U.S.A., September 8-10 1986.*

Matsumura, A. (1988). "Shear Strength of Reinforced Masonry Walls.", *Proceedings of Ninth World Conference on Earthquake Engineering August 2-9, 1988, Tokyo-Kyoto, Japan.*

Masonry Standards Joint Committee (MSJC) (2013). Building Code Requirements for Masonry Structures (TMS 402-13, ACI 530-13, and ASCE 5-13). The Masonry Society, American Concrete Institute, and ASCE, Boulder, Colorado; Farmington Hills, Michigan; and Reston, Virginia.

Minaie, E. (2009). "Behavior and Vulnerability of Reinforced Masonry Shear Walls." Doctor of Philosophy, Drexel University, Philadelphia, Pennsylvania.

Nolph, S. M. (2010). "In-Plane Shear Performance of Partially Grouted Masonry Shear Walls." Master of Science in Civil Engineering, Washington State University, Pullman, Washington.

Reddy, B. V. V., and Vyas, C. V. U. (2008). "Influence of shear bond strength on compressive strength and stress-strain characteristics of masonry.", *Materials and Structures*, 41:1697–1712, https://link.springer.com/article/10.1617/s11527-008-9358-x

Sarangapani, G., Reddy, B. V. V., and Jagadish, K. S. (2005). "Brick-Mortar Bond and Masonry Compressive Strength.", *Journal of Materials in Civil Engineering*, 17(2): 229-237, https://ascelibrary.org/doi/abs/10.1061/(ASCE)0899-1561(2005)17:2(229)

Shing, P. B., Klamerus, E., Spaeh, H., and Noland, J. L. (1988). "Seismic Performance of Reinforced Masonry Shear Walls.", *Proceedings of Ninth World Conference on Earthquake Engineering August 2-9, 1988, Tokyo-Kyoto, Japan.*

Shing, P. B., Schuller, M., and Hoskere, V. S. (1990). "In-Plane Resistance of Reinforced Masonry Shear Walls.", *Journal of Structural Engineering*, 116(3): 619-640, https://ascelibrary.org/doi/abs/10.1061/(ASCE)0733-9445(1990)116:3(619).

Shing, P. B., and Cao, L. (1997). "Analysis of Partially Grouted Masonry Shear Walls.", *National Institute of Standards and Technology*, NIST GCR 97-710, https://www.nist.gov/publications/analysis-partially-grouted-masonry-shear-walls.

Voon, K. C., and Ingham, J. M. (2006). "Experimental In-Plane Shear Strength Investigation of Reinforced Concrete Masonry Walls.", *Journal of Structural Engineering*, 132(3): 400-408, https://ascelibrary.org/doi/abs/10.1061/(ASCE)0733-9445(2006)132:3(400).

Voon, K. C., and Ingham, J. M. (2007). "Design Expression for the In-Plane Shear Strength of Reinforced Concrete Masonry Walls.", *Journal of Structural Engineering*, 133(5): 706-713, https://ascelibrary.org/doi/abs/10.1061/(ASCE)0733-9445(2007)133:5(706).

Voon, K. C., and Ingham, J. M. (2008). "Experimental In-Plane Shear Investigation of Reinforced Concrete Masonry Walls with Openings.", *Journal of Structural Engineering*, 134(5): 758-768, https://ascelibrary.org/doi/abs/10.1061/(ASCE)0733-9445(2008)134:5(758).

Watterson, S. M., and Fonseca, F. S. (2012). "Strength of Masonry Prisms with High Amounts of Supplemental Cementitious Materials", *15th International Brick and Block Masonry Conference.*

Wong, P. S., Vecchio, F. J., and Trommels, H. (2002). "VecTor2 & FormWorks User's Manual." University of Toronto, Toronto, Ontario, Canada.

Yanez, F., Maximiliano, A., Homberg, A., and Ogaz, O. (2004). "Behavior of Confined Masonry Shear Walls with Large Openings.", *13th World Conference on Earthquake Engineering Vancouver, B.C., Canada, August 1-6, 2004*, Paper No. 3438.

APPENDIX A. CALCULATIONS

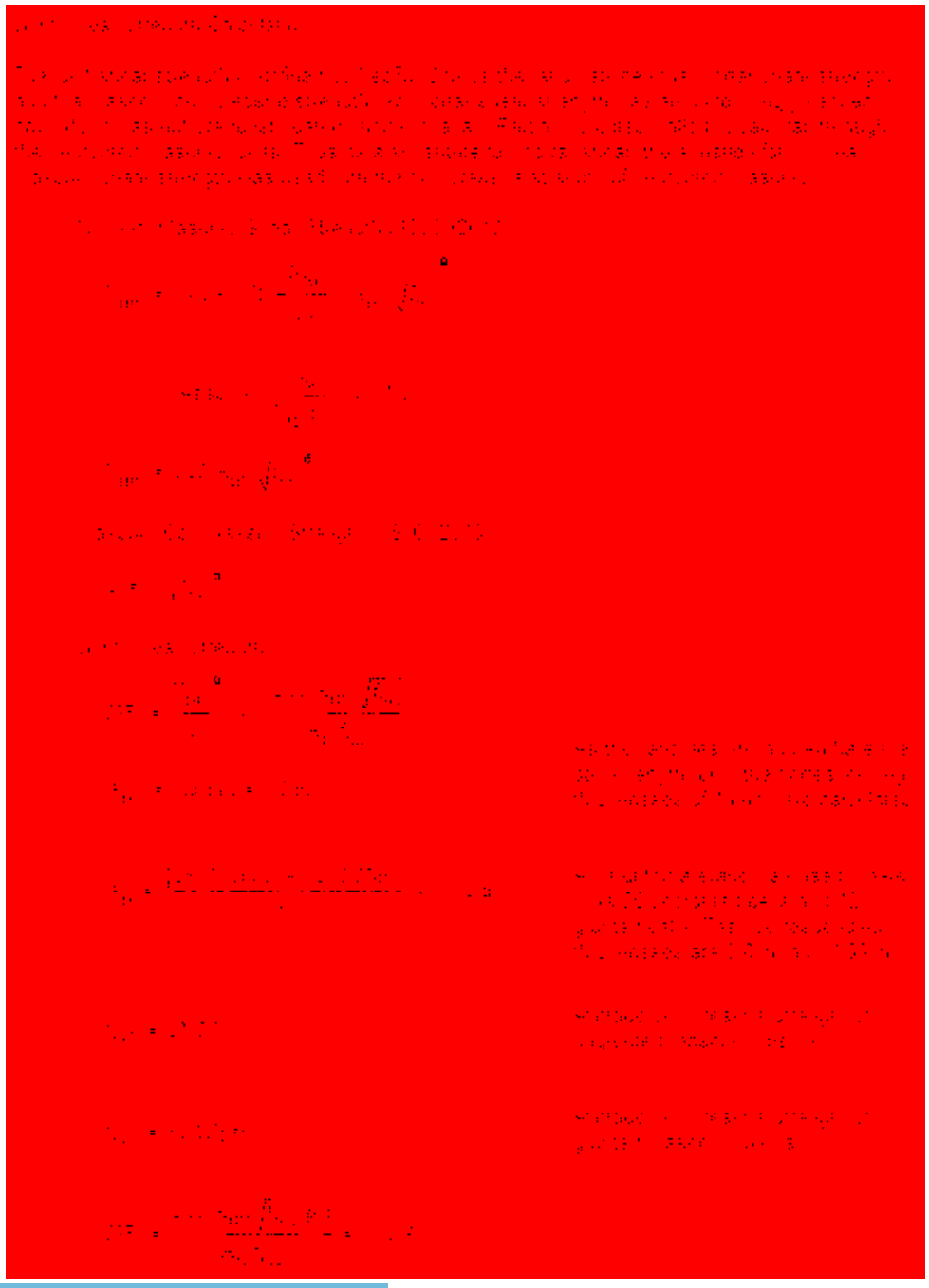

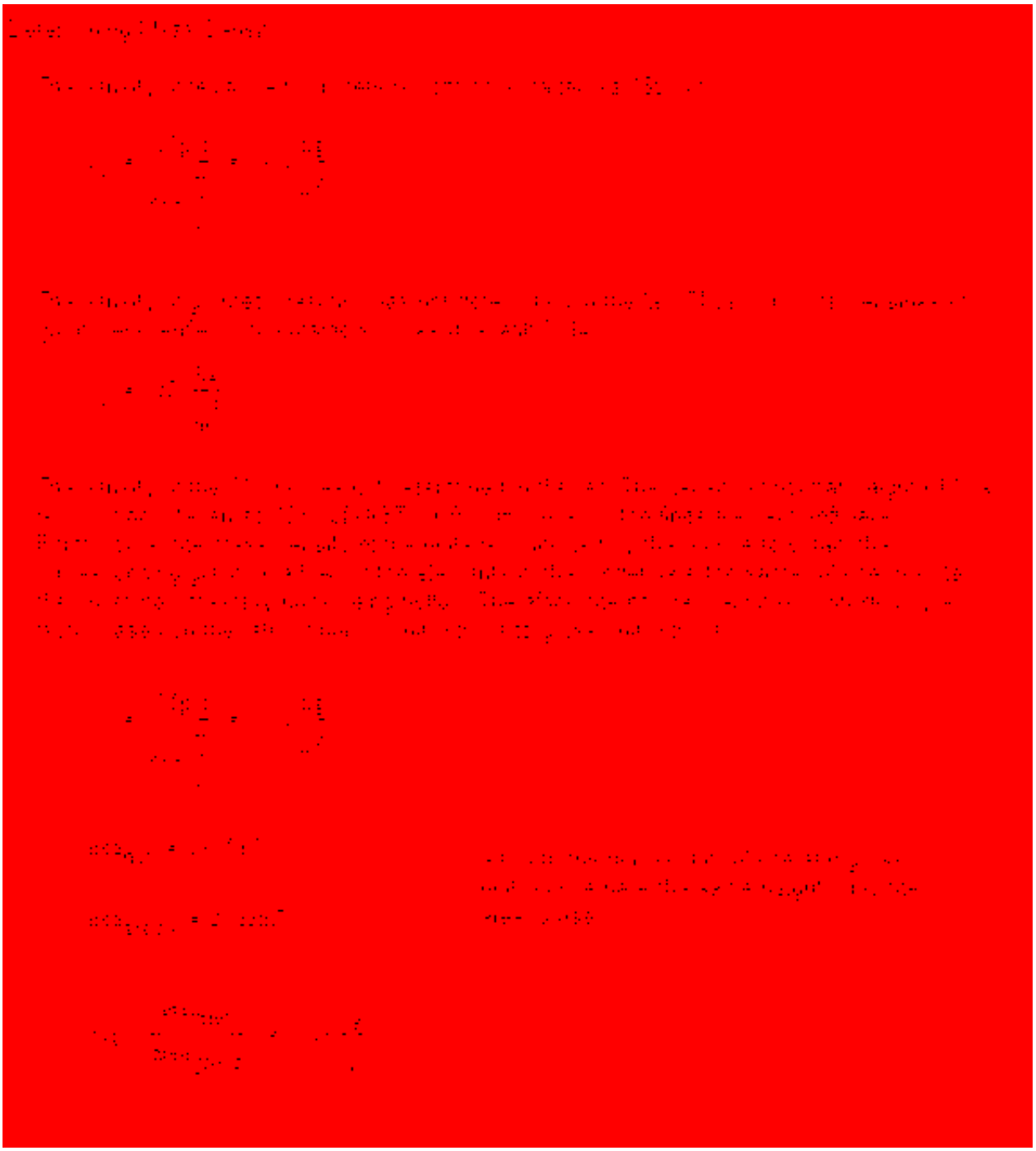

Wall 1 Code Calculation of Nominal Shear Strength (MSJC 2013)

Given & Assumptions

The ratio Mu/(Vu*dv) can be simplified for a cantilever wall to hw/dv, where hw is the height of the wall and dv is the width of the wall. Additionally, the code states this value "need not be taken greater than 1.0".

The net shear area Anv was determined as a cross section through the opening and summing the net area for 10 hollow masonry units and the net area for 6 solid (grouted) masonry units.

The compressive strength of masonry used in these calculations is the weighted average of the ungrouted compressive strength and the grouted compressive strength.

The load factor used for axial load is taken as 1.2.

The yield strength fy was determined from tensile tests. See Table 3-3.

As the spacing of horizontal shear reinforcement wasn't uniform for the experimental wall, thus an average spacing was calculated as the height divided by the number of bars (6).

The strength reduction factor "shall be taken as 0.80 for masonry subject to shear".

$A_{hollow} := 13.15\,in^2$

$A_{solid} := 25.83\,in^2$

$A_{nv} = (10 \cdot A_{hollow}) + (6 \cdot A_{solid}) = 286.48\,in^2$

$f_{mungrouted} := 1805.7$

$f_{mgrouted} := 2139.3$

$f_m := \frac{10 \cdot f_{mungrouted} + 6 f_{mgrouted}}{16} = 1930.8$

$h_w := 14.75\,ft$

$d_v := 12.66\,ft$

$P_u := 1.2 \cdot 11.43\,kip$

$A_{bars} := 0.1\,in^2$

$A_v := 6 \cdot A_{bars} = 0.6\,in^2$

$f_y := 77.69\,ksi$

$s := \frac{h_w}{6} = 29.5\,in$

$\gamma_g := 0.75$

$\phi := 0.80$

Nominal Masonry Shear Strength

$$V_{nm} := \left(4.0 - 1.75 \min\left(\frac{h_w}{d_v}, 1.0\right)\right) \cdot A_{nv} \cdot \sqrt{f_m}\,psi + 0.25 P_u = 31.752\,kip$$

Nominal Shear Strength Provided by Reinforcement

$$V_{ns} := 0.5 \left(\frac{A_v}{s}\right) \cdot f_y \cdot d_v = 132.03\,kip$$

Nominal Shear Strength - The sum of the nominal masonry shear strength and the shear strength provided by reinforcement.

$$\phi V_n = \phi \cdot (V_{nm} + V_{ns}) \cdot \gamma_g = 98.269\,kip$$

Maximum Limited Nominal Shear Strength (hw/dv $\geq$ 1.0)

$$\phi V_{nmax} := \phi \cdot \left(4 \cdot A_{nv} \cdot \sqrt{f_m}\,psi\right) \cdot \gamma_g = 30.212\,kip$$

Walls 2 and 3 Code Calculation of Nominal Shear Strength (MSJC 2013)

Given & Assumptions

The ratio Mu/(Vu*dv) can be simplified for a cantilever wall to hw/dv, where hw is the height of the wall and dv is the width of the wall. Additionally, the code states this value "need not be taken greater than 1.0".

The net shear area Anv was determined as a cross section through the opening and summing the net area for 10 hollow masonry units and the net area for 6 solid (grouted) masonry units.

The compressive strength of masonry used in these calculations is the weighted average of the ungrouted compressive strength and the grouted compressive strength.

The load factor used for axial load is taken as 1.2.

The yield strength fy was determined from tensile tests. See Table 3-3.

As the spacing of horizontal shear reinforcement wasn't uniform for the experimental wall, thus an average spacing was calculated as the height divided by the number of bars (3).

The strength reduction factor "shall be taken as 0.80 for masonry subject to shear".

$A_{hollow} := 13.15in^2$

$A_{solid} := 25.83in^2$

$A_{nv} := (10 \cdot A_{hollow}) + (6 \cdot A_{solid}) = 286.48in^2$

$f_{mungrouted} := 1805.7$

$f_{mgrouted} := 2139.3$

$f_m := \frac{10 \cdot f_{mungrouted} + 6 f_{mgrouted}}{16} = 1930.8$

$h_w := 14.75ft$

$d_v := 12.66ft$

$P_u := 1.2 \cdot 11.43kip$

$A_{bars} := 0.11in^2$

$A_v := 3 \cdot A_{bars} = 0.33in^2$

$f_y := 77.69ksi$

$s := \frac{h_w}{3} = 59in$

$\gamma_g := 0.75$

$\phi := 0.80$

Nominal Masonry Shear Strength

$$V_{nm} := \left(4.0 - 1.75 \min\left(\frac{h_w}{d_v}, 1.0\right)\right) \cdot A_{nv} \cdot \sqrt{f'_m psi} + 0.25 P_u = 31.752kip$$

Nominal Shear Strength Provided by Reinforcement

$$V_{ns} := 0.5\left(\frac{A_v}{s}\right) \cdot f_y \cdot d_v = 33.007kip$$

Nominal Shear Strength - The sum of the nominal masonry shear strength and the shear strength provided by reinforcement.

$$\phi V_n := \phi \cdot (V_{nm} + V_{ns}) \cdot \gamma_g = 38.856kip$$

Maximum Limited Nominal Shear Strength (hw/dv $\geq$ 1.0)

$$\phi V_{nmax} := \phi \cdot \left(4 \cdot A_{nv} \cdot \sqrt{f'_m psi}\right) \cdot \gamma_g = 30.212kip$$

Grouted Masonry Strength 2500 psi - Nominal Shear Strength (MSJC 2013)

Given & Assumptions

The ratio Mu/(Vu*dv) can be simplified for a cantilever wall to hw/dv, where hw is the height of the wall and dv is the width of the wall. Additionally, the code states this value "need not be taken greater than 1.0".

The net shear area Anv was determined as a cross section through the opening and summing the net area for 10 hollow masonry units and the net area for 6 solid (grouted) masonry units.

The compressive strength of masonry used in these calculations is the weighted average of the ungrouted compressive strength and the grouted compressive strength.

The load factor used for axial load is taken as 1.2.

The yield strength fy was determined from tensile tests. See Table 3-3.

As the spacing of horizontal shear reinforcement wasn't uniform for the experimental wall, thus an average spacing was calculated as the height divided by the number of bars (6).

The strength reduction factor "shall be taken as 0.80 for masonry subject to shear".

$A_{hollow} := 13.15in^2$

$A_{solid} := 25.8in^2$

$A_{nv} = (10 \cdot A_{hollow}) + (6 \cdot A_{solid}) = 286.48in^2$

$f_{mungrouted} := 1805.7$

$f_{mgrouted} := 2500$

$f_m = \frac{10 \cdot f_{mungrouted} + 6 f_{mgrouted}}{16} = 2066.1$

$h_w := 14.75ft$

$d_v := 12.66ft$

$P_u = 1.2 \cdot 11.43kip$

$A_{bars} := 0.11in^2$

$A_v := 6 \cdot A_{bars} = 0.66in^2$

$f_y := 77.69ksi$

$s := \frac{h_w}{6} = 29.5in$

$\gamma_g := 0.75$

$\phi := 0.80$

Nominal Masonry Shear Strength

$$V_{nm} = \left(4.0 - 1.75 \min\left(\frac{h_w}{d_v}, 1.0\right)\right) \cdot A_{nv} \cdot \sqrt{f_m psi} + 0.25 P_u = 32.728kip$$

Nominal Shear Strength Provided by Reinforcement

$$V_{ns} := 0.5 \left(\frac{A_v}{s}\right) f_y \cdot d_v = 132.03kip$$

Nominal Shear Strength - The sum of the nominal masonry shear strength and the shear strength provided by reinforcement.

$$\phi V_n = \phi \cdot (V_{nm} + V_{ns}) \cdot \gamma_g = 98.855kip$$

Maximum Limited Nominal Shear Strength

$$\phi V_{nmax} := \phi \cdot \left(4 \cdot A_{nv} \cdot \sqrt{f_m psi}\right) \gamma_g = 31.252kip$$

Grouted Masonry Strength 3000 psi - Nominal Shear Strength (MSJC 2013)

Given & Assumptions

The ratio Mu/(Vu*dv) can be simplified for a cantilever wall to hw/dv, where hw is the height of the wall and dv is the width of the wall. Additionally, the code states this value "need not be taken greater than 1.0".

The net shear area Anv was determined as a cross section through the opening and summing the net area for 10 hollow masonry units and the net area for 6 solid (grouted) masonry units.

The compressive strength of masonry used in these calculations is the weighted average of the ungrouted compressive strength and the grouted compressive strength.

The load factor used for axial load is taken as 1.2.

The yield strength fy was determined from tensile tests. See Table 3-3.

As the spacing of horizontal shear reinforcement wasn't uniform for the experimental wall, thus an average spacing was calculated as the height divided by the number of bars (6).

The strength reduction factor "shall be taken as 0.80 for masonry subject to shear".

$A_{hollow} := 13.15in^2$

$A_{solid} := 25.83in^2$

$A_{nv} = (10 \cdot A_{hollow}) + (6 \cdot A_{solid}) = 286.48in^2$

$f_{mungrouted} := 1805.7$

$f_{mgrouted} := 3000$

$f_m = \frac{10 \cdot f_{mungrouted} + 6 f_{mgrouted}}{16} = 2253.6$

$h_w := 14.75ft$

$d_v := 12.66ft$

$P_u := 1.2 \cdot 11.43kip$

$A_{bars} := 0.11in^2$

$A_v := 6 \cdot A_{bars} = 0.66in^2$

$f_y := 77.69ksi$

$s := \frac{h_w}{6} = 29.5in$

$\gamma_g := 0.75$

$\phi := 0.80$

Nominal Masonry Shear Strength

$$V_{nm} = \left(4.0 - 1.75 \min\left(\frac{h_w}{d_v}, 1.0\right)\right) \cdot A_{nv} \cdot \sqrt{f_m}psi + 0.25 P_u = 34.028kip$$

Nominal Shear Strength Provided by Reinforcement

$$V_{ns} := 0.5\left(\frac{A_v}{s}\right) f_y \, d_v = 132.03kip$$

Nominal Shear Strength - The sum of the nominal masonry shear strength and the shear strength provided by reinforcement.

$$\phi V_n = \phi \cdot (V_{nm} + V_{ns}) \cdot \gamma_g = 99.635kip$$

Maximum Limited Nominal Shear Strength

$$\phi V_{nmax} := \phi \cdot \left(4 \cdot A_{nv} \cdot \sqrt{f_m}psi\right) \gamma_g = 32.639kip$$

Grouted Masonry Strength 3500 psi - Nominal Shear Strength (MSJC 2013)

Given & Assumptions

The ratio Mu/(Vu*dv) can be simplified for a cantilever wall to hw/dv, where hw is the height of the wall and dv is the width of the wall. Additionally, the code states this value "need not be taken greater than 1.0".

The net shear area Anv was determined as a cross section through the opening and summing the net area for 10 hollow masonry units and the net area for 6 solid (grouted) masonry units.

The compressive strength of masonry used in these calculations is the weighted average of the ungrouted compressive strength and the grouted compressive strength.

The load factor used for axial load is taken as 1.2.

The yield strength fy was determined from tensile tests. See Table 3-3.

As the spacing of horizontal shear reinforcement wasn't uniform for the experimental wall, thus an average spacing was calculated as the height divided by the number of bars (6).

The strength reduction factor "shall be taken as 0.80 for masonry subject to shear".

$A_{hollow} := 13.15in^2$

$A_{solid} := 25.83in^2$

$A_{nv} := (10 \cdot A_{hollow}) + (6 \cdot A_{solid}) = 286.48in^2$

$f_{mungrouted} := 1805.7$

$f_{mgrouted} := 3500$

$f_m := \frac{10 \cdot f_{mungrouted} + 6 f_{mgrouted}}{16} = 2441.1$

$h_w := 14.75ft$

$d_v := 12.66ft$

$P_u := 1.2 \cdot 11.43kip$

$A_{bars} := 0.11in^2$

$A_v := 6 \cdot A_{bars} = 0.66in^2$

$f_y := 77.69ksi$

$s := \frac{h_w}{6} = 29.5in$

$\gamma_g := 0.75$

$\phi := 0.80$

Nominal Masonry Shear Strength

$$V_{nm} := \left(4.0 - 1.75 \cdot \min\left(\frac{h_w}{d_v}, 1.0\right)\right) \cdot A_{nv} \cdot \sqrt{f'_m psi} + 0.25 P_u = 35.276kip$$

Nominal Shear Strength Provided by Reinforcement

$$V_{ns} := 0.5 \left(\frac{A_v}{s}\right) \cdot f_y \cdot d_v = 132.03kip$$

Nominal Shear Strength - The sum of the nominal masonry shear strength and the shear strength provided by reinforcement.

$$\phi V_n := \phi \cdot (V_{nm} + V_{ns}) \cdot \gamma_g = 100.383kip$$

Maximum Limited Nominal Shear Strength

$$\phi V_{nmax} := \phi \left(4 \cdot A_{nv} \cdot \sqrt{f'_m psi}\right) \gamma_g = 33.97kip$$

Ungrouted Masonry Strength 2500 psi - Nominal Shear Strength (MSJC 2013)

Given & Assumptions

The ratio Mu/(Vu*dv) can be simplified for a cantilever wall to hw/dv, where hw is the height of the wall and dv is the width of the wall. Additionally, the code states this value "need not be taken greater than 1.0".

The net shear area Anv was determined as a cross section through the opening and summing the net area for 10 hollow masonry units and the net area for 6 solid (grouted) masonry units.

The compressive strength of masonry used in these calculations is the weighted average of the ungrouted compressive strength and the grouted compressive strength.

The load factor used for axial load is taken as 1.2.

The yield strength fy was determined from tensile tests. See Table 3-3.

As the spacing of horizontal shear reinforcement wasn't uniform for the experimental wall, thus an average spacing was calculated as the height divided by the number of bars (6).

The strength reduction factor "shall be taken as 0.80 for masonry subject to shear".

$A_{hollow} := 13.15in^2$

$A_{solid} := 25.83in^2$

$A_{nv} := (10 A_{hollow}) + (6 A_{solid}) = 286.48in^2$

$f_{mungrouted} := 2500$

$f_{mgrouted} := 2139$

$f_m := \frac{10 f_{mungrouted} + 6 f_{mgrouted}}{16} = 2364.6$

$h_w := 14.75ft$

$d_v := 12.66ft$

$P_u := 1.2 \cdot 11.43kip$

$A_{bars} := 0.1in^2$

$A_v := 6 A_{bars} = 0.66in^2$

$f_y := 77.69ksi$

$s := \frac{h_w}{6} = 29.5in$

$\gamma_g := 0.75$

$\phi := 0.80$

Nominal Masonry Shear Strength

$$V_{nm} := \left(4.0 - 1.75 \min\left(\frac{h_w}{d_v}, 1.0\right)\right) A_{nv} \sqrt{f_m psi} + 0.25 P_u = 34.773kip$$

Nominal Shear Strength Provided by Reinforcement

$$V_{ns} := 0.5 \left(\frac{A_v}{s}\right) f_y d_v = 132.03kip$$

Nominal Shear Strength - The sum of the nominal masonry shear strength and the shear strength provided by reinforcement.

$$\phi V_n := \phi (V_{nm} + V_{ns}) \gamma_g = 100.082kip$$

Maximum Limited Nominal Shear Strength

$$\phi V_{nmax} := \phi \left(4 A_{nv} \sqrt{f_m psi}\right) \gamma_g = 33.434kip$$

Ungrouted Masonry Strength 3000 psi - Nominal Shear Strength (MSJC 2013)

Given & Assumptions

The ratio Mu/(Vu*dv) can be simplified for a cantilever wall to hw/dv, where hw is the height of the wall and dv is the width of the wall. Additionally, the code states this value "need not be taken greater than 1.0".

The net shear area Anv was determined as a cross section through the opening and summing the net area for 10 hollow masonry units and the net area for 6 solid (grouted) masonry units.

The compressive strength of masonry used in these calculations is the weighted average of the ungrouted compressive strength and the grouted compressive strength.

The load factor used for axial load is taken as 1.2.

The yield strength fy was determined from tensile tests. See Table 3-3.

As the spacing of horizontal shear reinforcement wasn't uniform for the experimental wall, thus an average spacing was calculated as the height divided by the number of bars (6).

The strength reduction factor "shall be taken as 0.80 for masonry subject to shear".

$A_{hollow} := 13.15in^2$

$A_{solid} := 25.83in^2$

$A_{nv} := (10 \cdot A_{hollow}) + (6 \cdot A_{solid}) = 286.48in^2$

$f_{mungrouted} := 3000$

$f_{mgrouted} := 2139$

$f_m := \frac{10 \cdot f_{mungrouted} + 6 f_{mgrouted}}{16} = 2677.1$

$h_w := 14.75ft$

$d_v := 12.66ft$

$P_u := 1.2 \cdot 11.43kip$

$A_{bars} := 0.1in^2$

$A_v := 6 \cdot A_{bars} = 0.66in^2$

$f_y := 77.69ksi$

$s := \frac{h_w}{6} = 29.5in$

$\gamma_g := 0.75$

$\phi := 0.80$

Nominal Masonry Shear Strength

$$V_{nm} := \left(4.0 - 1.75 \min\left(\frac{h_w}{d_v}, 1.0\right)\right) \cdot A_{nv} \sqrt{f_m psi} + 0.25 P_u = 36.78kip$$

Nominal Shear Strength Provided by Reinforcement

$$V_{ns} := 0.5 \left(\frac{A_v}{s}\right) f_y \, d_v = 132.03kip$$

Nominal Shear Strength - The sum of the nominal masonry shear strength and the shear strength provided by reinforcement.

$$\phi V_n := \phi \cdot (V_{nm} + V_{ns}) \cdot \gamma_g = 101.286kip$$

Maximum Limited Nominal Shear Strength

$$\phi V_{nmax} := \phi \cdot \left(4 \cdot A_{nv} \sqrt{f_m psi}\right) \gamma_g = 35.575kip$$

Ungrouted Masonry Strength 3500 psi - Nominal Shear Strength (MSJC 2013)

Given & Assumptions

The ratio Mu/(Vu*dv) can be simplified for a cantilever wall to hw/dv, where hw is the height of the wall and dv is the width of the wall. Additionally, the code states this value "need not be taken greater than 1.0".

The net shear area Anv was determined as a cross section through the opening and summing the net area for 10 hollow masonry units and the net area for 6 solid (grouted) masonry units.

The compressive strength of masonry used in these calculations is the weighted average of the ungrouted compressive strength and the grouted compressive strength.

The load factor used for axial load is taken as 1.2.

The yield strength fy was determined from tensile tests. See Table 3-3.

As the spacing of horizontal shear reinforcement wasn't uniform for the experimental wall, thus an average spacing was calculated as the height divided by the number of bars (6).

The strength reduction factor "shall be taken as 0.80 for masonry subject to shear".

$A_{hollow} := 13.15in^2$

$A_{solid} := 25.83in^2$

$A_{nv} := (10 \cdot A_{hollow}) + (6 \cdot A_{solid}) = 286.48in^2$

$f_{mungrouted} := 3500$

$f_{mgrouted} := 2139$

$f_m := \frac{10 \cdot f_{mungrouted} + 6 f_{mgrouted}}{16} = 2989.6$

$h_w := 14.73ft$

$d_v := 12.66ft$

$P_u := 1.2 \cdot 11.43kip$

$A_{bars} := 0.11in^2$

$A_v := 6 \cdot A_{bars} = 0.66in^2$

$f_y := 77.69ksi$

$s := \frac{h_w}{6} = 29.5in$

$\gamma_g := 0.75$

$\phi := 0.80$

Nominal Masonry Shear Strength

$$V_{nm} := \left(4.0 - 1.75 \min\left(\frac{h_w}{d_v}, 1.0\right)\right) \cdot A_{nv} \cdot \sqrt{f_m psi} + 0.25 P_u = 38.673kip$$

Nominal Shear Strength Provided by Reinforcement

$$V_{ns} := 0.5 \cdot \left(\frac{A_v}{s}\right) \cdot f_y \cdot d_v = 132.03kip$$

Nominal Shear Strength - The sum of the nominal masonry shear strength and the shear strength provided by reinforcement.

$$\phi V_n := \phi \cdot (V_{nm} + V_{ns}) \cdot \gamma_g = 102.422kip$$

Maximum Limited Nominal Shear Strength

$$\phi V_{nmax} := \phi \cdot \left(4 \cdot A_{nv} \cdot \sqrt{f_m psi}\right) \cdot \gamma_g = 37.594kip$$

#2 Horizontal Reinforcement - Nominal Shear Strength (MSJC 2013)

Given & Assumptions

The ratio Mu/(Vu*dv) can be simplified for a cantilever wall to hw/dv, where hw is the height of the wall and dv is the width of the wall. Additionally, the code states this value "need not be taken greater than 1.0".

The net shear area Anv was determined as a cross section through the opening and summing the net area for 10 hollow masonry units and the net area for 6 solid (grouted) masonry units.

The compressive strength of masonry used in these calculations is the weighted average of the ungrouted compressive strength and the grouted compressive strength.

The load factor used for axial load is taken as 1.2.

The yield strength fy was determined from tensile tests. See Table 3-3.

As the spacing of horizontal shear reinforcement wasn't uniform for the experimental wall, thus an average spacing was calculated as the height divided by the number of bars (6).

The strength reduction factor "shall be taken as 0.80 for masonry subject to shear".

$A_{hollow} := 13.15in^2$

$A_{solid} := 25.83in^2$

$A_{nv} = (10 \cdot A_{hollow}) + (6 \cdot A_{solid}) = 286.48in^2$

$f_{mungrouted} := 1805.7$

$f_{mgrouted} := 2139$

$f_m = \frac{10 \cdot f_{mungrouted} + 6 f_{mgrouted}}{16} = 1930.7$

$h_w := 14.75ft$

$d_v := 12.66ft$

$P_u := 1.2 \cdot 11.43kip$

$A_{bars} := 0.05in^2$

$A_v := 6 \cdot A_{bars} = 0.3in^2$

$f_y := 77.69ksi$

$s := \frac{h_w}{6} = 29.5in$

$\gamma_g := 0.75$

$\phi := 0.80$

Nominal Masonry Shear Strength

$$V_{nm} = \left(4.0 - 1.75 \cdot \min\left(\frac{h_w}{d_v}, 1.0\right)\right) \cdot A_{nv} \cdot \sqrt{f_m psi} + 0.25 P_u = 31.752kip$$

Nominal Shear Strength Provided by Reinforcement

$$V_{ns} := 0.5 \left(\frac{A_v}{s}\right) f_y \, d_v = 60.014kip$$

Nominal Shear Strength - The sum of the nominal masonry shear strength and the shear strength provided by reinforcement.

$$\phi V_n := \phi \cdot (V_{nm} + V_{ns}) \cdot \gamma_g = 55.059kip$$

Maximum Limited Nominal Shear Strength

$$\phi V_{nmax} := \phi \cdot \left(4 \cdot A_{nv} \cdot \sqrt{f_m psi}\right) \gamma_g = 30.211kip$$

#4 Horizontal Reinforcement - Nominal Shear Strength (MSJC 2013)

Given & Assumptions

The ratio Mu/(Vu*dv) can be simplified for a cantilever wall to hw/dv, where hw is the height of the wall and dv is the width of the wall. Additionally, the code states this value "need not be taken greater than 1.0".

The net shear area Anv was determined as a cross section through the opening and summing the net area for 10 hollow masonry units and the net area for 6 solid (grouted) masonry units.

The compressive strength of masonry used in these calculations is the weighted average of the ungrouted compressive strength and the grouted compressive strength.

The load factor used for axial load is taken as 1.2.

The yield strength fy was determined from tensile tests. See Table 3-3.

As the spacing of horizontal shear reinforcement wasn't uniform for the experimental wall, thus an average spacing was calculated as the height divided by the number of bars (6).

The strength reduction factor "shall be taken as 0.80 for masonry subject to shear".

$A_{hollow} := 13.15in^2$

$A_{solid} := 25.83in^2$

$A_{nv} = (10 \cdot A_{hollow}) + (6 \cdot A_{solid}) = 286.48in^2$

$f_{mungrouted} := 1805.7$

$f_{mgrouted} := 2139$

$f_m := \frac{10 \cdot f_{mungrouted} + 6 f_{mgrouted}}{16} = 1930.7$

$h_w := 14.75ft$

$d_v = 12.66ft$

$P_u = 1.2 \cdot 11.43kip$

$A_{bars} := 0.20in^2$

$A_v := 6 \cdot A_{bars} = 1.2in^2$

$f_y := 77.69ksi$

$s := \frac{h_w}{6} = 29.5in$

$\gamma_g := 0.75$

$\phi := 0.80$

Nominal Masonry Shear Strength

$$V_{nm} := \left(4.0 - 1.75 \min\left(\frac{h_w}{d_v}, 1.0\right)\right) \cdot A_{nv} \cdot \sqrt{f_m}psi + 0.25 P_u = 31.752kip$$

Nominal Shear Strength Provided by Reinforcement

$$V_{ns} := 0.5\left(\frac{A_v}{s}\right) f_y \cdot d_v = 240.054kip$$

Nominal Shear Strength - The sum of the nominal masonry shear strength and the shear strength provided by reinforcement.

$$\phi V_n = \phi \cdot (V_{nm} + V_{ns}) \cdot \gamma_g = 163.083kip$$

Maximum Limited Nominal Shear Strength

$$\phi V_{nmax} := \phi \cdot \left(4 \cdot A_{nv} \cdot \sqrt{f_m}psi\right) \gamma_g = 30.211kip$$

20 in. Vertical Spacing of Horizontal Reinforcement - Nominal Shear Strength (MSJC 2013)

Given & Assumptions

The ratio Mu/(Vu*dv) can be simplified for a cantilever wall to hw/dv, where hw is the height of the wall and dv is the width of the wall. Additionally, the code states this value "need not be taken greater than 1.0".

The net shear area Anv was determined as a cross section through the opening and summing the net area for 10 hollow masonry units and the net area for 6 solid (grouted) masonry units.

The compressive strength of masonry used in these calculations is the weighted average of the ungrouted compressive strength and the grouted compressive strength.

The load factor used for axial load is taken as 1.2.

The yield strength fy was determined from tensile tests. See Table 3-3.

As the spacing of horizontal shear reinforcement wasn't uniform for the experimental wall, thus an average spacing was calculated as the height divided by the number of bars (6).

The strength reduction factor "shall be taken as 0.80 for masonry subject to shear".

$A_{hollow} := 13.15in^2$

$A_{solid} := 25.83in^2$

$A_{nv} := (10 \cdot A_{hollow}) + (6 \cdot A_{solid}) = 286.48in^2$

$f_{mungrouted} := 1805.7$

$f_{mgrouted} := 2139$

$f_m := \frac{10 \cdot f_{mungrouted} + 6 f_{mgrouted}}{16} = 1930.7$

$h_w := 14.75ft$

$d_v := 12.66ft$

$P_u := 1.2 \cdot 11.43kip$

$A_{bars} := 0.20in^2$

$A_v := 6 \cdot A_{bars} = 1.2in^2$

$f_y := 77.69ksi$

$s_{Ave} := 30in$

$\gamma_g := 0.75$

$\phi := 0.80$

Nominal Masonry Shear Strength

$$V_{nm} := \left(4.0 - 1.75 \min\left(\frac{h_w}{d_v}, 1.0\right)\right) \cdot A_{nv} \cdot \sqrt{f_m}psi + 0.25 P_u = 31.752kip$$

Nominal Shear Strength Provided by Reinforcement

$$V_{ns} := 0.5\left(\frac{A_v}{s}\right) \cdot f_y \cdot d_v = 354.08kip$$

Nominal Shear Strength - The sum of the nominal masonry shear strength and the shear strength provided by reinforcement.

$$\phi V_n := \phi \cdot (V_{nm} + V_{ns}) \cdot \gamma_g = 231.499kip$$

Maximum Limited Nominal Shear Strength

$$\phi V_{nmax} := \phi \cdot \left(4 A_{nv} \cdot \sqrt{f_m}psi\right) \cdot \gamma_g = 30.211kip$$

24 in. Vertical Spacing of Horizontal Reinforcement - Nominal Shear Strength (MSJC 2013)

Given & Assumptions

The ratio Mu/(Vu*dv) can be simplified for a cantilever wall to hw/dv, where hw is the height of the wall and dv is the width of the wall. Additionally, the code states this value "need not be taken greater than 1.0".

The net shear area Anv was determined as a cross section through the opening and summing the net area for 10 hollow masonry units and the net area for 6 solid (grouted) masonry units.

The compressive strength of masonry used in these calculations is the weighted average of the ungrouted compressive strength and the grouted compressive strength.

The load factor used for axial load is taken as 1.2.

The yield strength fy was determined from tensile tests. See Table 3-3.

As the spacing of horizontal shear reinforcement wasn't uniform for the experimental wall, thus an average spacing was calculated as the height divided by the number of bars (6).

The strength reduction factor "shall be taken as 0.80 for masonry subject to shear".

$A_{hollow} := 13.15in^2$

$A_{solid} := 25.83in^2$

$A_{nv} := (10 \cdot A_{hollow}) + (6 \cdot A_{solid}) = 286.48in^2$

$f_{mungrouted} := 1805.7$

$f_{mgrouted} := 2139$

$f_m := \frac{10 \cdot f_{mungrouted} + 6 f_{mgrouted}}{16} = 1930.7$

$h_w := 14.73ft$

$d_v := 12.66ft$

$P_u := 1.2 \cdot 11.43kip$

$A_{bars} := 0.20in^2$

$A_v := 6 \cdot A_{bars} = 1.2in^2$

$f_y := 77.69ksi$

$s := 24in$

$\gamma_g := 0.75$

$\phi := 0.80$

Nominal Masonry Shear Strength

$$V_{nm} := \left(4.0 - 1.75 \min\left(\frac{h_w}{d_v}, 1.0\right)\right) \cdot A_{nv} \cdot \sqrt{f_m psi} + 0.25 P_u = 31.752kip$$

Nominal Shear Strength Provided by Reinforcement

$$V_{ns} := 0.5 \left(\frac{A_v}{s}\right) \cdot f_y \cdot d_v = 295.067kip$$

Nominal Shear Strength - The sum of the nominal masonry shear strength and the shear strength provided by reinforcement.

$$\phi V_n := \phi \cdot (V_{nm} + V_{ns}) \cdot \gamma_g = 196.091kip$$

Maximum Limited Nominal Shear Strength

$$\phi V_{nmax} := \phi \cdot \left(4 A_{nv} \cdot \sqrt{f_m psi}\right) \gamma_g = 30.211kip$$

44 in. Vertical Spacing of Horizontal Reinforcement - Nominal Shear Strength (MSJC 2013)

Given & Assumptions

The ratio Mu/(Vu*dv) can be simplified for a cantilever wall to hw/dv, where hw is the height of the wall and dv is the width of the wall. Additionally, the code states this value "need not be taken greater than 1.0".

The net shear area Anv was determined as a cross section through the opening and summing the net area for 10 hollow masonry units and the net area for 6 solid (grouted) masonry units.

The compressive strength of masonry used in these calculations is the weighted average of the ungrouted compressive strength and the grouted compressive strength.

The load factor used for axial load is taken as 1.2.

The yield strength fy was determined from tensile tests. See Table 3-3.

As the spacing of horizontal shear reinforcement wasn't uniform for the experimental wall, thus an average spacing was calculated as the height divided by the number of bars (6).

The strength reduction factor "shall be taken as 0.80 for masonry subject to shear".

$A_{hollow} := 13.15in^2$

$A_{solid} := 25.83in^2$

$A_{nv} := (10 \cdot A_{hollow}) + (6 \cdot A_{solid}) = 286.48in^2$

$f'_{mungrouted} := 1805.7$

$f'_{mgrouted} := 2139$

$f'_m := \frac{10 \cdot f'_{mungrouted} + 6 f'_{mgrouted}}{16} = 1930.7$

$h_w := 14.75ft$

$d_v := 12.66ft$

$P_u := 1.2 \cdot 11.43kip$

$A_{bars} := 0.20in^2$

$A_v := 6 \cdot A_{bars} = 1.2in^2$

$f_y := 77.69ksi$

$s := 44in$

$\gamma_g := 0.75$

$\phi := 0.80$

Nominal Masonry Shear Strength

$$V_{nm} := \left(4.0 - 1.75 \min\left(\frac{h_w}{d_v}, 1.0\right)\right) \cdot A_{nv} \cdot \sqrt{f'_m psi} + 0.25 P_u = 31.752kip$$

Nominal Shear Strength Provided by Reinforcement

$$V_{ns} := 0.5\left(\frac{A_v}{s}\right) \cdot f_y \cdot d_v = 160.945kip$$

Nominal Shear Strength - The sum of the nominal masonry shear strength and the shear strength provided by reinforcement.

$$\phi V_n = \phi \cdot (V_{nm} + V_{ns}) \cdot \gamma_g = 115.618kip$$

Maximum Limited Nominal Shear Strength

$$\phi V_{nmax} := \phi \cdot \left(4 \cdot A_{nv} \cdot \sqrt{f'_m psi}\right) \cdot \gamma_g = 30.211kip$$

Axial Load 0.00 Kips - Nominal Shear Strength (MSJC 2013)

Given & Assumptions

The ratio Mu/(Vu*dv) can be simplified for a cantilever wall to hw/dv, where hw is the height of the wall and dv is the width of the wall. Additionally, the code states this value "need not be taken greater than 1.0".

The net shear area Anv was determined as a cross section through the opening and summing the net area for 10 hollow masonry units and the net area for 6 solid (grouted) masonry units.

The compressive strength of masonry used in these calculations is the weighted average of the ungrouted compressive strength and the grouted compressive strength.

The load factor used for axial load is taken as 1.2.

The yield strength fy was determined from tensile tests. See Table 3-3.

As the spacing of horizontal shear reinforcement wasn't uniform for the experimental wall, thus an average spacing was calculated as the height divided by the number of bars (6).

The strength reduction factor "shall be taken as 0.80 for masonry subject to shear".

$A_{hollow} := 13.15in^2$

$A_{solid} := 25.83in^2$

$A_{nv} := (10 \cdot A_{hollow}) + (6 \cdot A_{solid}) = 286.48in^2$

$f_{mungrouted} := 1805.7$

$f_{mgrouted} := 2139$

$f_m := \frac{10 f_{mungrouted} + 6 f_{mgrouted}}{16} = 1930.7$

$h_w := 14.75ft$

$d_v := 12.66ft$

$P_u := 1.2 \cdot 0.00kip$

$A_{bars} := 0.1in^2$

$A_v := 6 \cdot A_{bars} = 0.66in^2$

$f_y := 77.69ksi$

$s := \frac{h_w}{6} = 29.5in$

$\gamma_g := 0.75$

$\phi := 0.80$

Nominal Masonry Shear Strength

$$V_{nm} := \left(4.0 - 1.75 \min\left(\frac{h_w}{d_v}, 1.0\right)\right) \cdot A_{nv} \cdot \sqrt{f_m psi} + 0.25 P_u = 28.323kip$$

Nominal Shear Strength Provided by Reinforcement

$$V_{ns} := 0.5 \left(\frac{A_v}{s}\right) f_y \cdot d_v = 132.03kip$$

Nominal Shear Strength - The sum of the nominal masonry shear strength and the shear strength provided by reinforcement.

$$\phi V_n := \phi \cdot (V_{nm} + V_{ns}) \cdot \gamma_g = 96.211kip$$

Maximum Limited Nominal Shear Strength

$$\phi V_{nmax} := \phi \cdot (4 \cdot A_{nv} \cdot \sqrt{f_m psi}) \cdot \gamma_g = 30.211kip$$

Axial Load 5.00 Kips - Nominal Shear Strength (MSJC 2013)

Given & Assumptions

The ratio Mu/(Vu*dv) can be simplified for a cantilever wall to hw/dv, where hw is the height of the wall and dv is the width of the wall. Additionally, the code states this value "need not be taken greater than 1.0".

The net shear area Anv was determined as a cross section through the opening and summing the net area for 10 hollow masonry units and the net area for 6 solid (grouted) masonry units.

The compressive strength of masonry used in these calculations is the weighted average of the ungrouted compressive strength and the grouted compressive strength.

The load factor used for axial load is taken as 1.2.

The yield strength fy was determined from tensile tests. See Table 3-3.

As the spacing of horizontal shear reinforcement wasn't uniform for the experimental wall, thus an average spacing was calculated as the height divided by the number of bars (6).

The strength reduction factor "shall be taken as 0.80 for masonry subject to shear".

$A_{hollow} := 13.15in^2$

$A_{solid} := 25.83in^2$

$A_{nv} := (10 \cdot A_{hollow}) + (6 \cdot A_{solid}) = 286.48in^2$

$f'_{mungrouted} := 1805.7$

$f'_{mgrouted} := 2139$

$f'_m := \frac{10 \cdot f'_{mungrouted} + 6 f'_{mgrouted}}{16} = 1930.7$

$h_w := 14.75ft$

$d_v := 12.66ft$

$P_u := 1.2 \cdot 5.00kip$

$A_{bars} := 0.11in^2$

$A_v := 6 \cdot A_{bars} = 0.66in^2$

$f_y := 77.69ksi$

$s := \frac{h_w}{6} = 29.5in$

$\gamma_g := 0.75$

$\phi := 0.80$

Nominal Masonry Shear Strength

$$V_{nm} := \left(4.0 - 1.75 \min\left(\frac{h_w}{d_v}, 1.0\right)\right) \cdot A_{nv} \cdot \sqrt{f'_m psi} + 0.25 P_u = 29.823kip$$

Nominal Shear Strength Provided by Reinforcement

$$V_{ns} := 0.5 \left(\frac{A_v}{s}\right) \cdot f_y \cdot d_v = 132.03kip$$

Nominal Shear Strength - The sum of the nominal masonry shear strength and the shear strength provided by reinforcement.

$$\phi V_n := \phi \cdot (V_{nm} + V_{ns}) \cdot \gamma_g = 97.111kip$$

Maximum Limited Nominal Shear Strength

$$\phi V_{nmax} := \phi \cdot \left(4 \cdot A_{nv} \cdot \sqrt{f'_m psi}\right) \cdot \gamma_g = 30.211kip$$

Axial Load 15.00 Kips - Nominal Shear Strength (MSJC 2013)

Given & Assumptions

The ratio Mu/(Vu*dv) can be simplified for a cantilever wall to hw/dv, where hw is the height of the wall and dv is the width of the wall. Additionally, the code states this value "need not be taken greater than 1.0".

The net shear area Anv was determined as a cross section through the opening and summing the net area for 10 hollow masonry units and the net area for 6 solid (grouted) masonry units.

The compressive strength of masonry used in these calculations is the weighted average of the ungrouted compressive strength and the grouted compressive strength.

The load factor used for axial load is taken as 1.2.

The yield strength fy was determined from tensile tests. See Table 3-3.

As the spacing of horizontal shear reinforcement wasn't uniform for the experimental wall, thus an average spacing was calculated as the height divided by the number of bars (6).

The strength reduction factor "shall be taken as 0.80 for masonry subject to shear".

$A_{hollow} := 13.15\,in^2$

$A_{solid} := 25.83\,in^2$

$A_{nv} := (10\,A_{hollow}) + (6\,A_{solid}) = 286.48\,in^2$

$f'_{mungrouted} := 1805.7$

$f'_{mgrouted} := 2139$

$f'_m := \frac{10\,f'_{mungrouted} + 6\,f'_{mgrouted}}{16} = 1930.7$

$h_w := 14.75\,ft$

$d_v := 12.66\,ft$

$P_u := 1.2 \cdot 15.00\,kip$

$A_{bars} := 0.1\,in^2$

$A_v := 6\,A_{bars} = 0.66\,in^2$

$f_y := 77.69\,ksi$

$s := \frac{h_w}{6} = 29.5\,in$

$\gamma_g := 0.75$

$\phi := 0.80$

Nominal Masonry Shear Strength

$$V_{nm} := \left(4.0 - 1.75 \cdot \min\left(\frac{h_w}{d_v}, 1.0\right)\right) A_{nv} \sqrt{f'_m\,psi} + 0.25\,P_u = 32.823\,kip$$

Nominal Shear Strength Provided by Reinforcement

$$V_{ns} := 0.5\left(\frac{A_v}{s}\right) f_y\,d_v = 132.03\,kip$$

Nominal Shear Strength - The sum of the nominal masonry shear strength and the shear strength provided by reinforcement.

$$\phi V_n := \phi \cdot (V_{nm} + V_{ns}) \cdot \gamma_g = 98.911\,kip$$

Maximum Limited Nominal Shear Strength

$$\phi V_{nmax} := \phi \left(4\,A_{nv} \sqrt{f'_m\,psi}\right) \gamma_g = 30.211\,kip$$

Axial Load 20.00 Kips - Nominal Shear Strength (MSJC 2013)

Given & Assumptions

The ratio Mu/(Vu*dv) can be simplified for a cantilever wall to hw/dv, where hw is the height of the wall and dv is the width of the wall. Additionally, the code states this value "need not be taken greater than 1.0".

The net shear area Anv was determined as a cross section through the opening and summing the net area for 10 hollow masonry units and the net area for 6 solid (grouted) masonry units.

The compressive strength of masonry used in these calculations is the weighted average of the ungrouted compressive strength and the grouted compressive strength.

The load factor used for axial load is taken as 1.2.

The yield strength fy was determined from tensile tests. See Table 3-3.

As the spacing of horizontal shear reinforcement wasn't uniform for the experimental wall, thus an average spacing was calculated as the height divided by the number of bars (6).

The strength reduction factor "shall be taken as 0.80 for masonry subject to shear".

$A_{hollow} := 13.15\,in^2$

$A_{solid} := 25.83\,in^2$

$A_{nv} := (10\,A_{hollow}) + (6\,A_{solid}) = 286.48\,in^2$

$f_{mungrouted} := 1805.7$

$f_{mgrouted} := 2139$

$f_m := \frac{10\,f_{mungrouted} + 6 f_{mgrouted}}{16} = 1930.7$

$h_w := 14.7\,ft$

$d_v := 12.6\,ft$

$P_u := 1.2\,20.0\,kip$

$A_{bars} := 0.1\,in^2$

$A_v := 6\,A_{bars} = 0.6\,in^2$

$f_y := 77.6\,ksi$

$s := \frac{h_w}{6} = 29.5\,in$

$\gamma_g := 0.75$

$\phi := 0.80$

Nominal Masonry Shear Strength

$$V_{nm} := \left(4.0 - 1.75 \min\left(\frac{h_w}{d_v}, 1.0\right)\right) A_{nv} \sqrt{f'_m\,psi} + 0.25 P_u = 34.323\,kip$$

Nominal Shear Strength Provided by Reinforcement

$$V_{ns} := 0.5\left(\frac{A_v}{s}\right) f_y\, d_v = 132.03\,kip$$

Nominal Shear Strength - The sum of the nominal masonry shear strength and the shear strength provided by reinforcement.

$$\phi V_n := \phi\,(V_{nm} + V_{ns})\,\gamma_g = 99.811\,kip$$

Maximum Limited Nominal Shear Strength

$$\phi V_{nmax} := \phi\left(4\,A_{nv}\sqrt{f'_m\,psi}\right)\gamma_g = 30.211\,kip$$

Axial Load 25.00 Kips - Nominal Shear Strength (MSJC 2013)

Given & Assumptions

The ratio Mu/(Vu*dv) can be simplified for a cantilever wall to hw/dv, where hw is the height of the wall and dv is the width of the wall. Additionally, the code states this value "need not be taken greater than 1.0".

The net shear area Anv was determined as a cross section through the opening and summing the net area for 10 hollow masonry units and the net area for 6 solid (grouted) masonry units.

The compressive strength of masonry used in these calculations is the weighted average of the ungrouted compressive strength and the grouted compressive strength.

The load factor used for axial load is taken as 1.2.

The yield strength fy was determined from tensile tests. See Table 3-3.

As the spacing of horizontal shear reinforcement wasn't uniform for the experimental wall, thus an average spacing was calculated as the height divided by the number of bars (6).

The strength reduction factor "shall be taken as 0.80 for masonry subject to shear".

$A_{hollow} := 13.15in^2$

$A_{solid} := 25.83in^2$

$A_{nv} := (10 \cdot A_{hollow}) + (6 \cdot A_{solid}) = 286.48in^2$

$f_{mungrouted} := 1805.7$

$f_{mgrouted} := 2139$

$f_m := \frac{10 \cdot f_{mungrouted} + 6 f_{mgrouted}}{16} = 1930.7$

$h_w := 14.75ft$

$d_v := 12.66ft$

$P_u := 1.2 \cdot 25.00kip$

$A_{bars} := 0.11in^2$

$A_v := 6 \cdot A_{bars} = 0.66in^2$

$f_y := 77.69ksi$

$s := \frac{h_w}{6} = 29.5in$

$\gamma_g := 0.75$

$\phi := 0.80$

Nominal Masonry Shear Strength

$$V_{nm} := \left(4.0 - 1.75 \min\left(\frac{h_w}{d_v}, 1.0\right)\right) \cdot A_{nv} \cdot \sqrt{f_m psi} + 0.25 P_u = 35.823kip$$

Nominal Shear Strength Provided by Reinforcement

$$V_{ns} := 0.5 \cdot \left(\frac{A_v}{s}\right) \cdot f_y \cdot d_v = 132.03kip$$

Nominal Shear Strength - The sum of the nominal masonry shear strength and the shear strength provided by reinforcement.

$$\phi V_n := \phi \cdot (V_{nm} + V_{ns}) \cdot \gamma_g = 100.711kip$$

Maximum Limited Nominal Shear Strength

$$\phi V_{nmax} := \phi \cdot \left(4 \cdot A_{nv} \cdot \sqrt{f_m psi}\right) \gamma_g = 30.211kip$$

Aspect Ratio 0.45 - Nominal Shear Strength (MSJC 2013)

Given & Assumptions

The ratio Mu/(Vu*dv) can be simplified for a cantilever wall to hw/dv, where hw is the height of the wall and dv is the width of the wall.

The net shear area Anv was determined as a cross section through the opening and summing the net area for 10 hollow masonry units and the net area for 6 solid (grouted) masonry units.

The compressive strength of masonry used in these calculations is the weighted average of the ungrouted compressive strength and the grouted compressive strength.

The load factor used for axial load is taken as 1.2.

The yield strength fy was determined from tensile tests. See Table 3-3.

As the spacing of horizontal shear reinforcement wasn't uniform for the experimental wall, thus an average spacing was calculated as the height divided by the number of bars (8).

The strength reduction factor "shall be taken as 0.80 for masonry subject to shear".

$A_{hollow} := 13.15in^2$ $h_w := 5ft$ $s := \frac{h_w}{2} = 30in$

$A_{solid} := 25.83in^2$ $d_v := 12.66ft$

$A_{nv} := (10 \cdot A_{hollow}) + (6 \cdot A_{solid}) = 286.48in^2$ $P_u := 1.2 \cdot 11.43kip$ $\gamma_g := 0.75$

$f_{munggrouted} := 1805.7$ $A_{bars} := 0.11in^2$ $\phi := 0.80$

$f_{mgrouted} := 2139$ $A_v := 2 \cdot A_{bars} = 0.22in^2$

$f_m := \frac{10 \cdot f_{munggrouted} + 6 f_{mgrouted}}{16} = 1930.7$ $f_y := 77.69ksi$

Nominal Masonry Shear Strength

$$V_{nm} := \left(4.0 - 1.75 \min\left(\frac{h_w}{d_v}, 1.0\right)\right) \cdot A_{nv} \cdot \sqrt{f_m}psi + 0.25 P_u = 45.08kip$$

Nominal Shear Strength Provided by Reinforcement

$$V_{ns} := 0.5\left(\frac{A_v}{s}\right) \cdot f_y \cdot d_v = 43.276kip$$

Nominal Shear Strength - The sum of the nominal masonry shear strength and the shear strength provided by reinforcement.

$$\phi V_n := \phi \cdot (V_{nm} + V_{ns}) \cdot \gamma_g = 53.014kip$$

Maximum Limited Nominal Shear Strength (hw/dv $\leq$ 0.25)

$$\phi V_{nmax1} := \phi \cdot \left(6 \cdot A_{nv} \cdot \sqrt{f_m}psi\right) \cdot \gamma_g = 45.316kip$$

Maximum Limited Nominal Shear Strength (hw/dv $\geq$ 1.0)

$$\phi V_{nmax2} := \phi \cdot \left(4 \cdot A_{nv} \cdot \sqrt{f_m}psi\right) \cdot \gamma_g = 30.211kip$$

Maximum Limited Nominal Shear Strength (hw/dv = 0.45)

$$\phi V_{nmax3} := \frac{(30.211kip - 45.316kip)}{(1.0 - 0.25)} \cdot (0.45 - 0.25) + 51.29kip = 47.264kip$$

Aspect Ratio 0.84 - Nominal Shear Strength (MSJC 2013)

Given & Assumptions

The ratio Mu/(Vu*dv) can be simplified for a cantilever wall to hw/dv, where hw is the height of the wall and dv is the width of the wall.

The net shear area Anv was determined as a cross section through the opening and summing the net area for 10 hollow masonry units and the net area for 6 solid (grouted) masonry units.

The compressive strength of masonry used in these calculations is the weighted average of the ungrouted compressive strength and the grouted compressive strength.

The load factor used for axial load is taken as 1.2.

The yield strength fy was determined from tensile tests. See Table 3-3.

As the spacing of horizontal shear reinforcement wasn't uniform for the experimental wall, thus an average spacing was calculated as the height divided by the number of bars (8).

The strength reduction factor "shall be taken as 0.80 for masonry subject to shear".

$A_{hollow} := 13.15in^2$ $h_w := 10ft$ $s := \frac{h_w}{4} = 30in$

$A_{solid} := 25.83in^2$ $d_v := 12.66ft$ $\gamma_g := 0.75$

$A_{nv} := (10 \cdot A_{hollow}) + (6 \cdot A_{solid}) = 286.48in^2$ $P_u := 1.2 \cdot 11.43kip$ $\phi := 0.80$

$f_{mungrouted} := 1805.7$ $A_{bars} := 0.11in^2$

$f_{mgrouted} := 2139$ $A_v := 4 \cdot A_{bars} = 0.44in^2$

$f_m := \frac{10 \cdot f_{mungrouted} + 6 f_{mgrouted}}{16} = 1930.7$ $f_y := 77.69ksi$

Nominal Masonry Shear Strength

$$V_{nm} := \left(4.0 - 1.75 \cdot \min\left(\frac{h_w}{d_v}, 1.0\right)\right) \cdot A_{nv} \cdot \sqrt{f_m psi} + 0.25 P_u = 36.38kip$$

Nominal Shear Strength Provided by Reinforcement

$$V_{ns} := 0.5 \cdot \left(\frac{A_v}{s}\right) \cdot f_y \cdot d_v = 86.553kip$$

Nominal Shear Strength - The sum of the nominal masonry shear strength and the shear strength provided by reinforcement.

$$\phi V_n := \phi \cdot (V_{nm} + V_{ns}) \cdot \gamma_g = 73.76kip$$

Maximum Limited Nominal Shear Strength (hw/dv $\leq$ 0.25)

$$\phi V_{nmax1} := \phi \cdot \left(6 \cdot A_{nv} \cdot \sqrt{f_m psi}\right) \gamma_g = 45.316kip$$

Maximum Limited Nominal Shear Strength (hw/dv $\geq$ 1.0)

$$\phi V_{nmax2} := \phi \cdot \left(4 \cdot A_{nv} \cdot \sqrt{f_m psi}\right) \gamma_g = 30.211kip$$

Maximum Limited Nominal Shear Strength (hw/dv = 0.84)

$$\phi V_{nmax3} := \frac{(30.211kip - 45.316kip)}{(1.0 - 0.25)} \cdot (0.84 - 0.25) + 51.291kip = 39.409kip$$

Aspect Ratio 1.63 - Nominal Shear Strength (MSJC 2013)

Given & Assumptions

The ratio Mu/(Vu*dv) can be simplified for a cantilever wall to hw/dv, where hw is the height of the wall and dv is the width of the wall. Additionally, the code states this value "need not be taken greater than 1.0".

The net shear area Anv was determined as a cross section through the opening and summing the net area for 10 hollow masonry units and the net area for 6 solid (grouted) masonry units.

The compressive strength of masonry used in these calculations is the weighted average of the ungrouted compressive strength and the grouted compressive strength.

The load factor used for axial load is taken as 1.2.

The yield strength fy was determined from tensile tests. See Table 3-3.

As the spacing of horizontal shear reinforcement wasn't uniform for the experimental wall, thus an average spacing was calculated as the height divided by the number of bars (8).

The strength reduction factor "shall be taken as 0.80 for masonry subject to shear".

$A_{hollow} := 13.15in^2$

$A_{solid} := 25.83in^2$

$A_{nv} := (10 A_{hollow}) + (6 A_{solid}) = 286.48in^2$

$f_{mungrouted} := 1805.7$

$f_{mgrouted} := 2139$

$f_m := \frac{10 f_{mungrouted} + 6 f_{mgrouted}}{16} = 1930.7$

$h_w := 20ft$

$d_v := 12.66ft$

$P_u := 1.2 \cdot 11.43kip$

$A_{bars} := 0.11in^2$

$A_v := 8 A_{bars} = 0.88in^2$

$f_y := 77.69ksi$

$s := \frac{h_w}{8} = 30in$

$\gamma_g := 0.75$

$\phi := 0.80$

Nominal Masonry Shear Strength

$$V_{nm} := \left(4.0 - 1.75 \min\left(\frac{h_w}{d_v}, 1.0\right)\right) A_{nv} \sqrt{f_m psi} + 0.25 P_u = 31.752kip$$

Nominal Shear Strength Provided by Reinforcement

$$V_{ns} := 0.5 \left(\frac{A_v}{s}\right) f_y d_v = 173.106kip$$

Nominal Shear Strength - The sum of the nominal masonry shear strength and the shear strength provided by reinforcement.

$$\phi V_n := \phi (V_{nm} + V_{ns}) \gamma_g = 122.914kip$$

Maximum Limited Nominal Shear Strength

$$\phi V_{nmax} := \phi \left(4 A_{nv} \sqrt{f_m psi}\right) \gamma_g = 30.211kip$$

Opening Width 30 in. - Nominal Shear Strength (MSJC 2013)

Given & Assumptions

The ratio Mu/(Vu*dv) can be simplified for a cantilever wall to hw/dv, where hw is the height of the wall and dv is the width of the wall. Additionally, the code states this value "need not be taken greater than 1.0".

The net shear area Anv was determined as a cross section through the opening and summing the net area for 9 hollow masonry units and the net area for 6 solid (grouted) masonry units.

The compressive strength of masonry used in these calculations is the weighted average of the ungrouted compressive strength and the grouted compressive strength.

The load factor used for axial load is taken as 1.2.

The yield strength fy was determined from tensile tests. See Table 3-3.

As the spacing of horizontal shear reinforcement wasn't uniform for the experimental wall, thus an average spacing was calculated as the height divided by the number of bars (6).

The strength reduction factor "shall be taken as 0.80 for masonry subject to shear".

$A_{hollow} := 13.15in^2$

$A_{solid} := 25.83in^2$

$A_{nv} := (9 \cdot A_{hollow}) + (6 \cdot A_{solid}) = 273.33in^2$

$f_{mungrouted} := 1805.7$

$f_{mgrouted} := 2139.3$

$f_m := \frac{9 \cdot f_{mungrouted} + 6 f_{mgrouted}}{15} = 1939.1$

$h_w := 14.73ft$

$d_v := 12.66ft$

$P_u := 1.2 \cdot 11.43kip$

$A_{bars} := 0.11in^2$

$A_v := 6 \cdot A_{bars} = 0.66in^2$

$f_y := 77.69ksi$

$s := \frac{h_w}{6} = 29.5in$

$\gamma_g := 0.75$

$\phi := 0.80$

Nominal Masonry Shear Strength

$$V_{nm} := \left(4.0 - 1.75 \min\left(\frac{h_w}{d_v}, 1.0\right)\right) \cdot A_{nv} \cdot \sqrt{f_m psi} + 0.25 P_u = 30.511kip$$

Nominal Shear Strength Provided by Reinforcement

$$V_{ns} := 0.5 \left(\frac{A_v}{s}\right) \cdot f_y \cdot d_v = 132.03kip$$

Nominal Shear Strength - The sum of the nominal masonry shear strength and the shear strength provided by reinforcement.

$$\phi V_n := \phi \cdot (V_{nm} + V_{ns}) \cdot \gamma_g = 97.524kip$$

Maximum Limited Nominal Shear Strength (hw/dv $\geq$ 1.0)

$$\phi V_{nmax} := \phi \cdot \left(4 \cdot A_{nv} \cdot \sqrt{f_m psi}\right) \gamma_g = 28.887kip$$

Opening Width 38 in. - Nominal Shear Strength (MSJC 2013)

Given & Assumptions

The ratio Mu/(Vu*dv) can be simplified for a cantilever wall to hw/dv, where hw is the height of the wall and dv is the width of the wall. Additionally, the code states this value "need not be taken greater than 1.0".

The net shear area Anv was determined as a cross section through the opening and summing the net area for 8 hollow masonry units and the net area for 6 solid (grouted) masonry units.

The compressive strength of masonry used in these calculations is the weighted average of the ungrouted compressive strength and the grouted compressive strength.

The load factor used for axial load is taken as 1.2.

The yield strength fy was determined from tensile tests. See Table 3-3.

As the spacing of horizontal shear reinforcement wasn't uniform for the experimental wall, thus an average spacing was calculated as the height divided by the number of bars (6).

The strength reduction factor "shall be taken as 0.80 for masonry subject to shear".

$A_{hollow} := 13.15in^2$

$A_{solid} := 25.83in^2$

$A_{nv} := (8 \cdot A_{hollow}) + (6 \cdot A_{solid}) = 260.18in^2$

$f_{mungrouted} := 1805.7$

$f_{mgrouted} := 2139.3$

$f_m := \frac{8 \cdot f_{mungrouted} + 6 f_{mgrouted}}{14} = 1948.7$

$h_w := 14.75ft$

$d_v := 12.66ft$

$P_u := 1.2 \cdot 11.43kip$

$A_{bars} := 0.11in^2$

$A_v := 6 \cdot A_{bars} = 0.66in^2$

$f_y := 77.69ksi$

$s := \frac{h_w}{6} = 29.5in$

$\gamma_g := 0.75$

$\phi := 0.80$

Nominal Masonry Shear Strength

$$V_{nm} := \left(4.0 - 1.75 \min\left(\frac{h_w}{d_v}, 1.0\right)\right) \cdot A_{nv} \cdot \sqrt{f'_m psi} + 0.25 P_u = 29.271kip$$

Nominal Shear Strength Provided by Reinforcement

$$V_{ns} := 0.5 \left(\frac{A_v}{s}\right) \cdot f_y \cdot d_v = 132.03kip$$

Nominal Shear Strength - The sum of the nominal masonry shear strength and the shear strength provided by reinforcement.

$$\phi V_n := \phi \cdot (V_{nm} + V_{ns}) \cdot \gamma_g = 96.78kip$$

Maximum Limited Nominal Shear Strength (hw/dv $\geq$ 1.0)

$$\phi V_{nmax} := \phi \cdot \left(4 A_{nv} \cdot \sqrt{f'_m psi}\right) \cdot \gamma_g = 27.565kip$$

APPENDIX B. HYSTERESIS CURVES

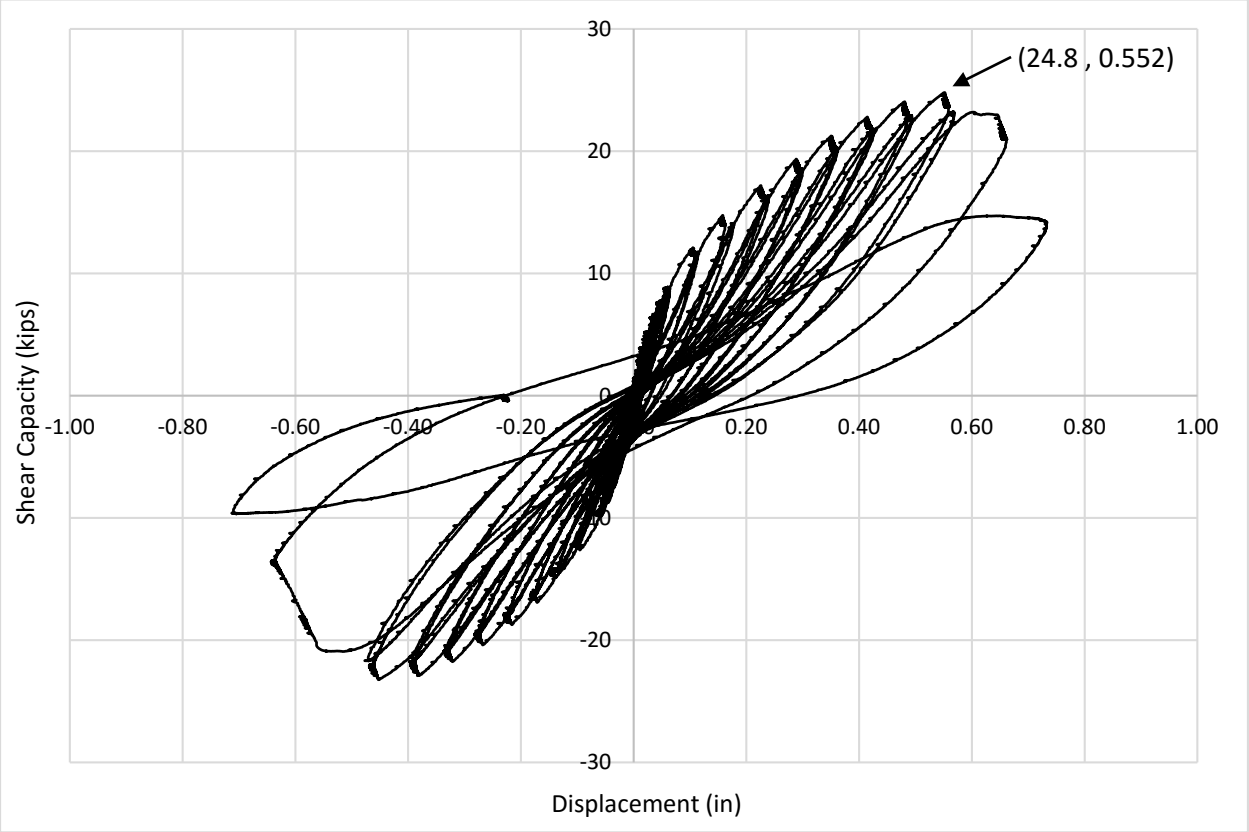

Figure B-1: Hysteresis curve for experimental wall 1

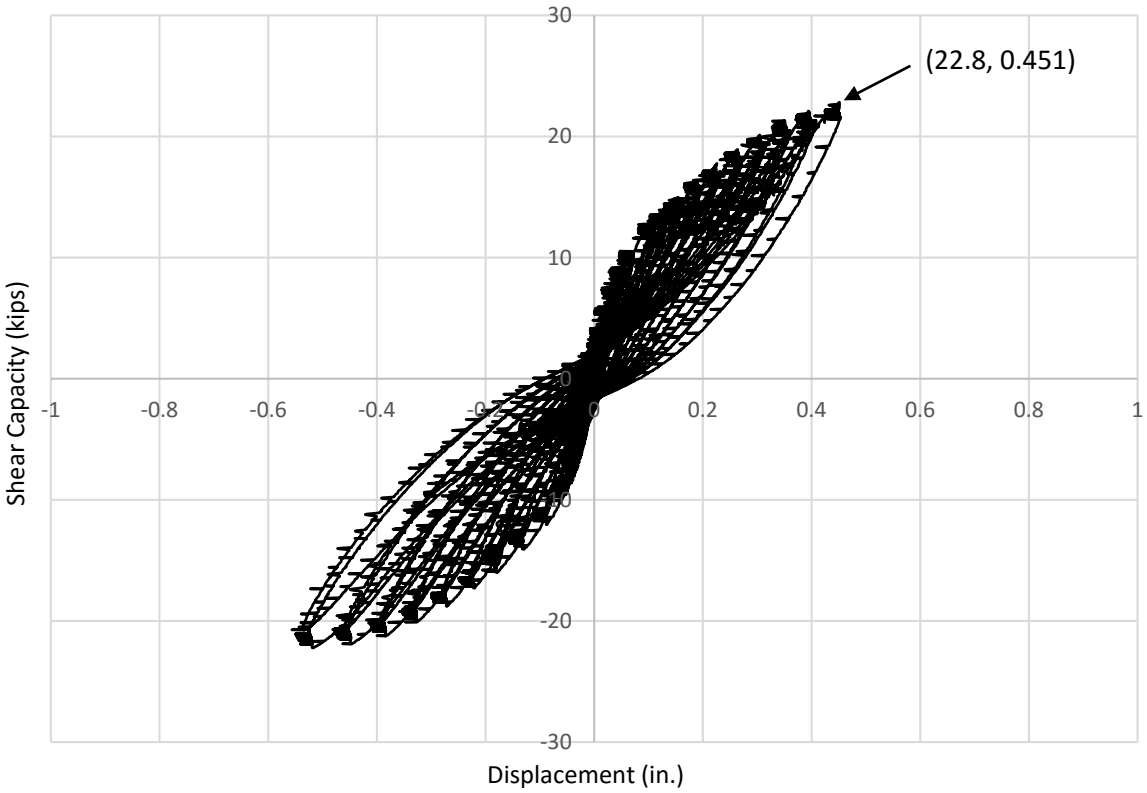

Figure B-2: Hysteresis curve for experimental wall 2

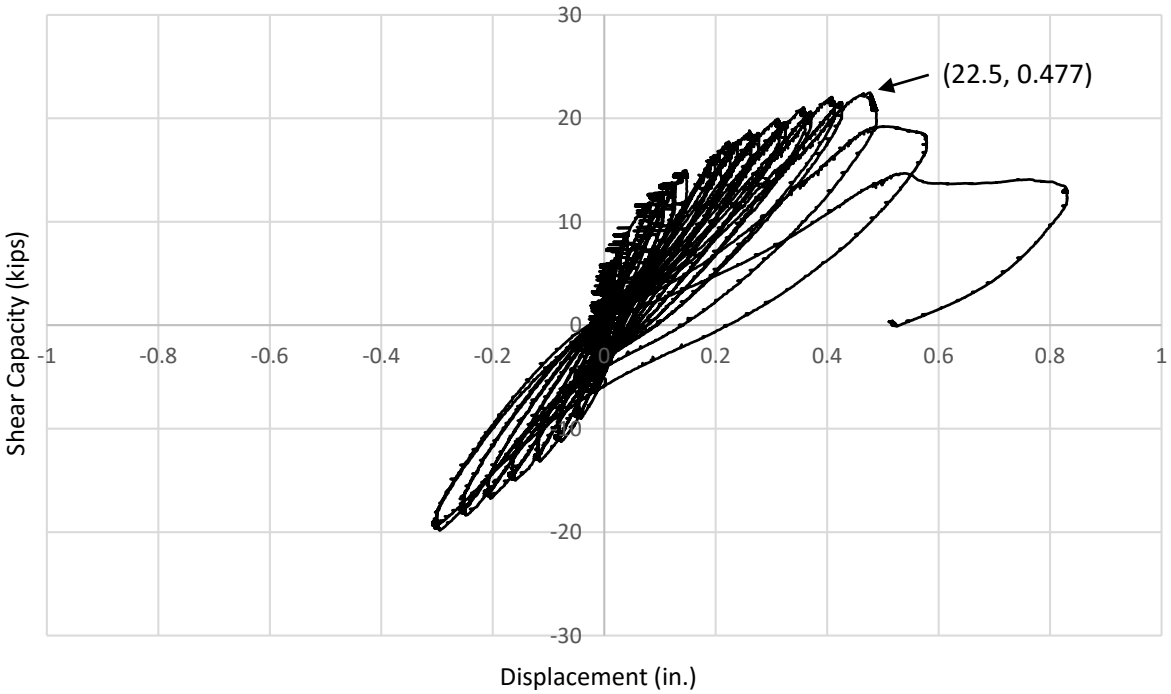

Figure B-3: Hysteresis curve for experimental wall 3

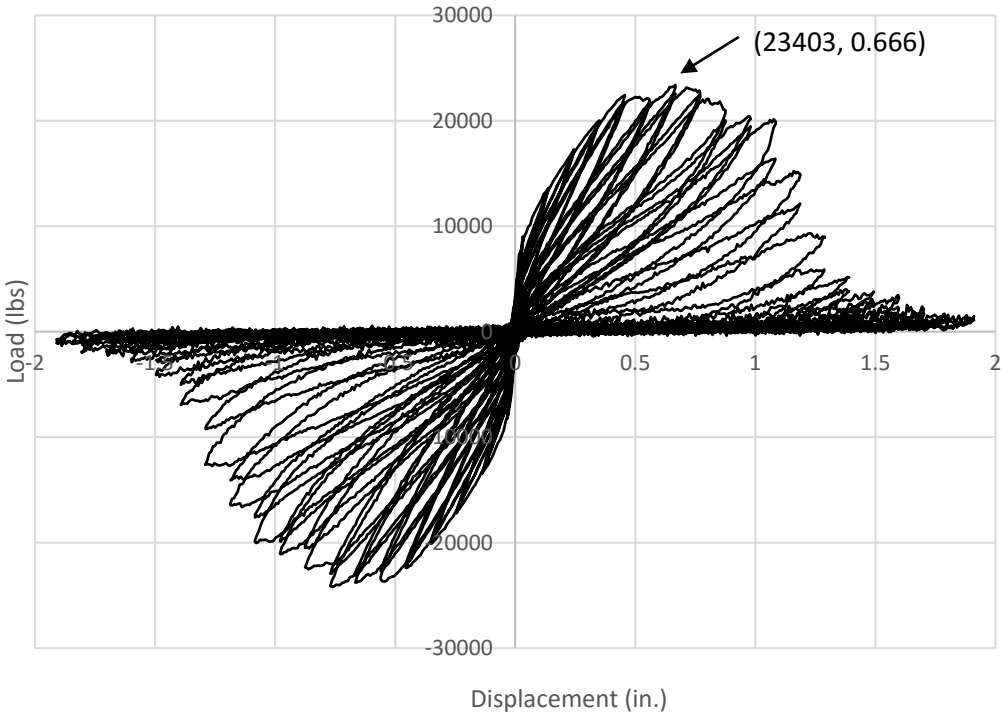

Figure B-4: Hysteresis curve for Base Model with full length trimming reinforcement

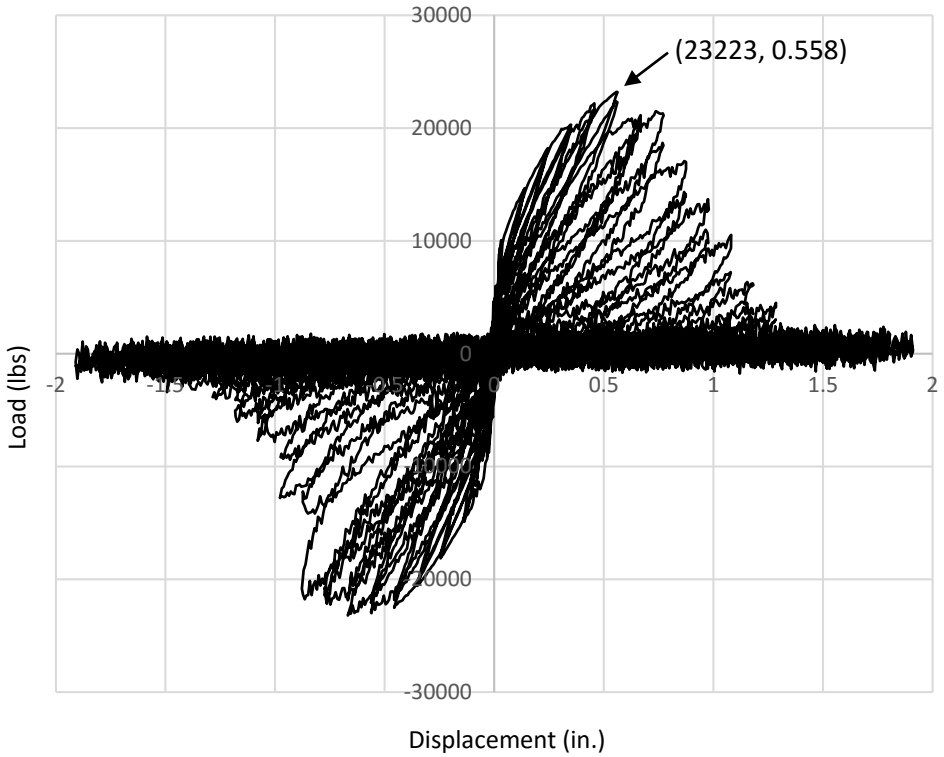

Figure B-5: Hysteresis curve for Base Model with trimming reinforcement under opening

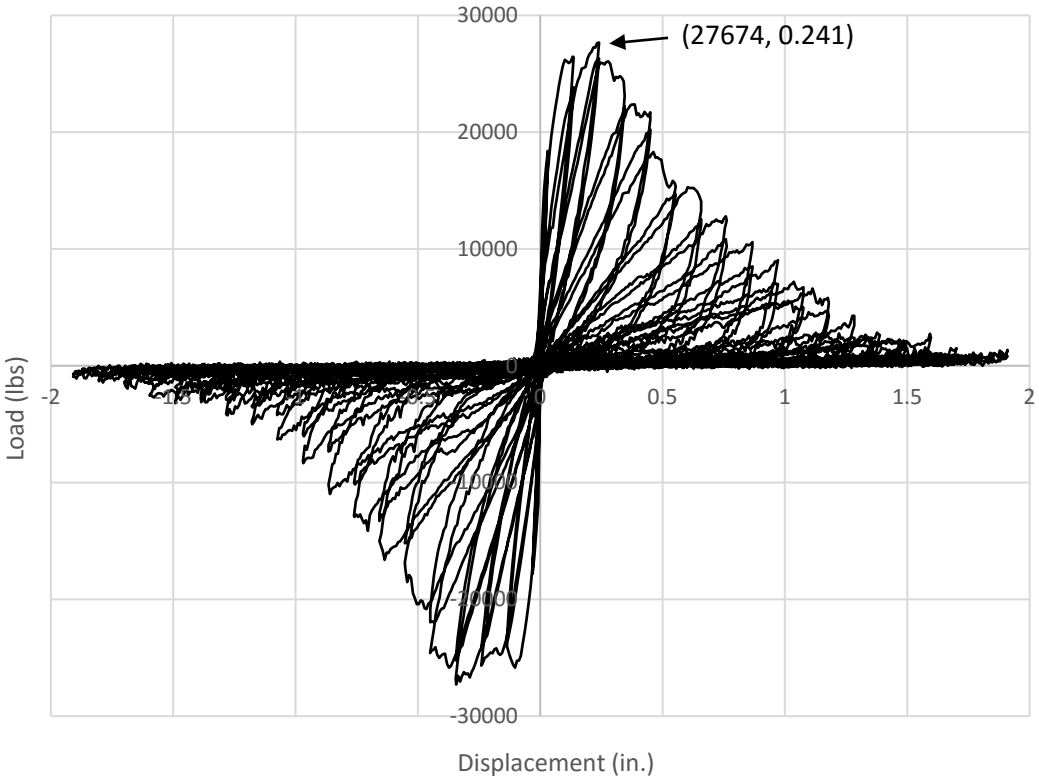

Figure B-6: Hysteresis curve for aspect ratio 0.45 (1 story)

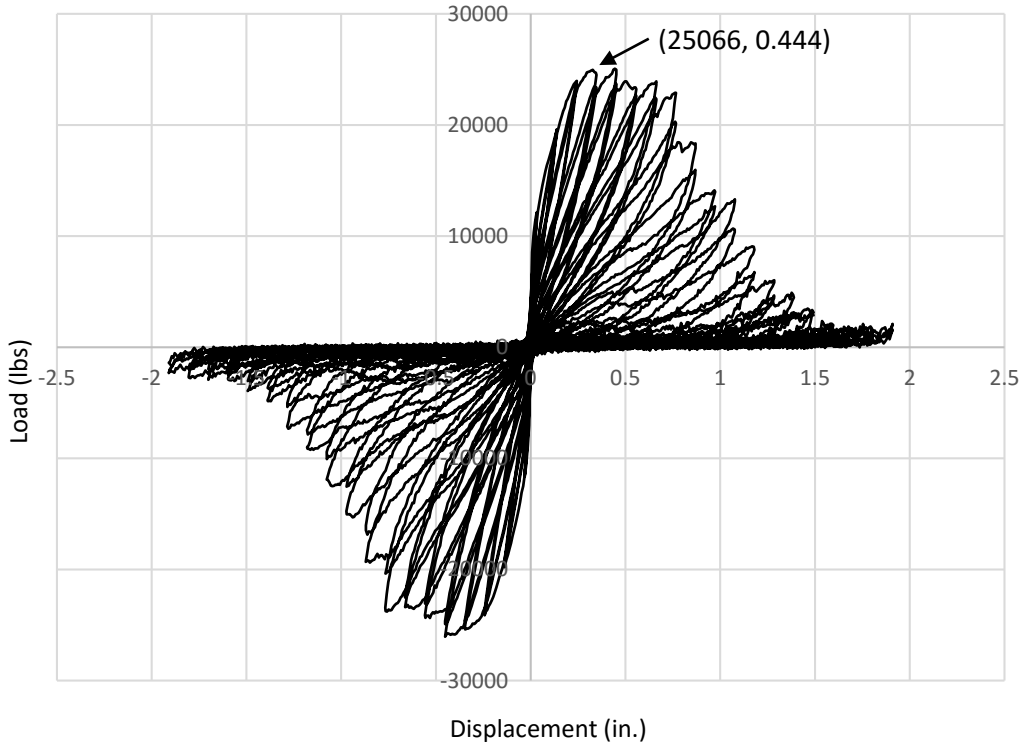

Figure B-7: Hysteresis curve for aspect ratio 0.84 (2 story)

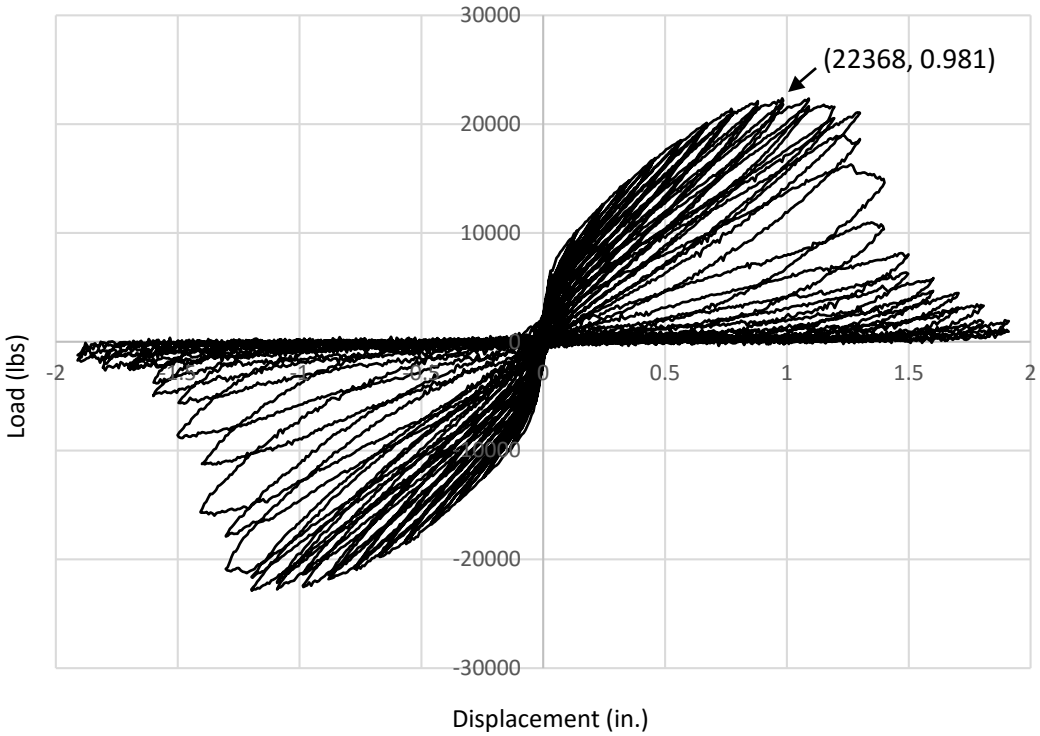

Figure B-8: Hysteresis curve for aspect ratio 1.63 (4 story)

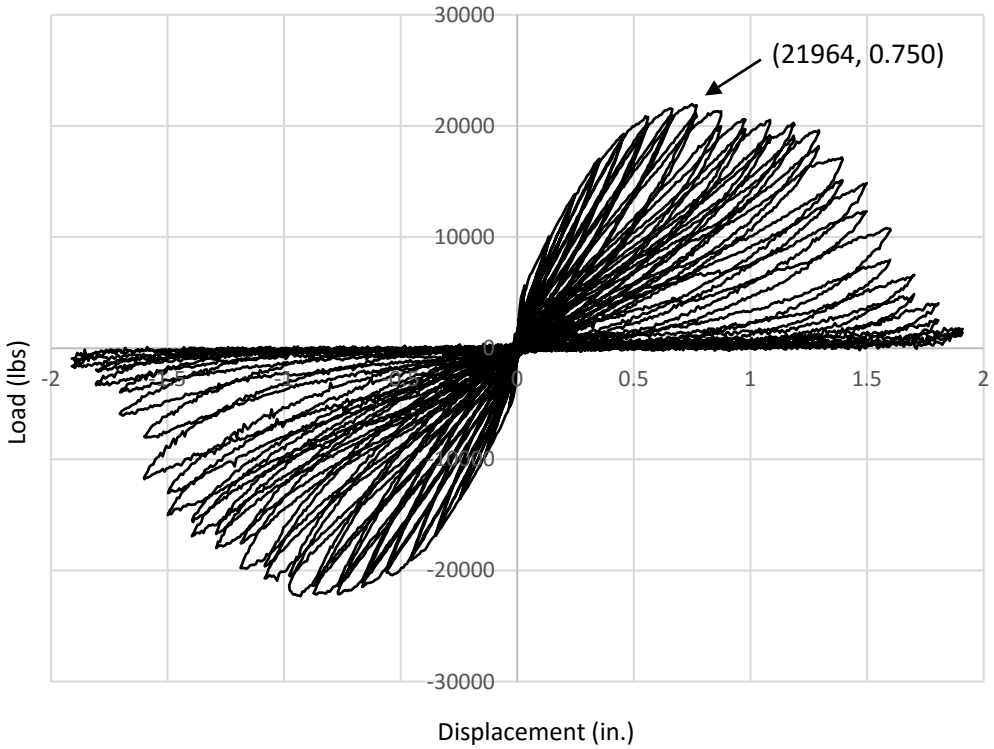

Figure B-9: Hysteresis curve for axial load 0.0 kips (0.00 psi)

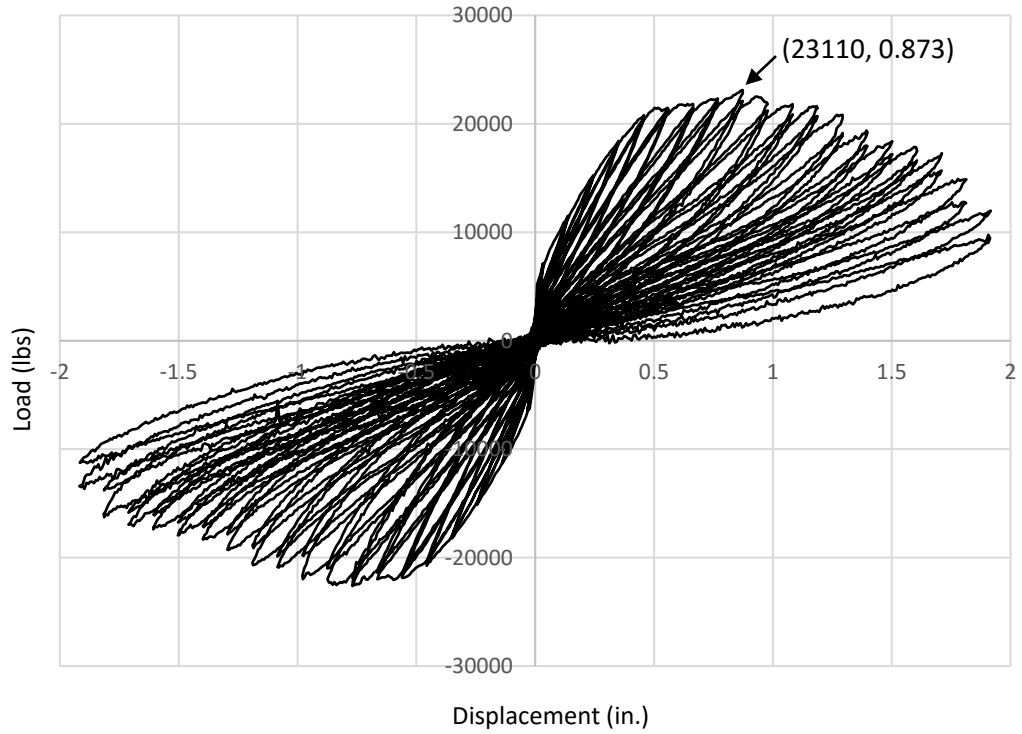

Figure B-10: Hysteresis curve for axial load 5.0 kips (9.40 psi)

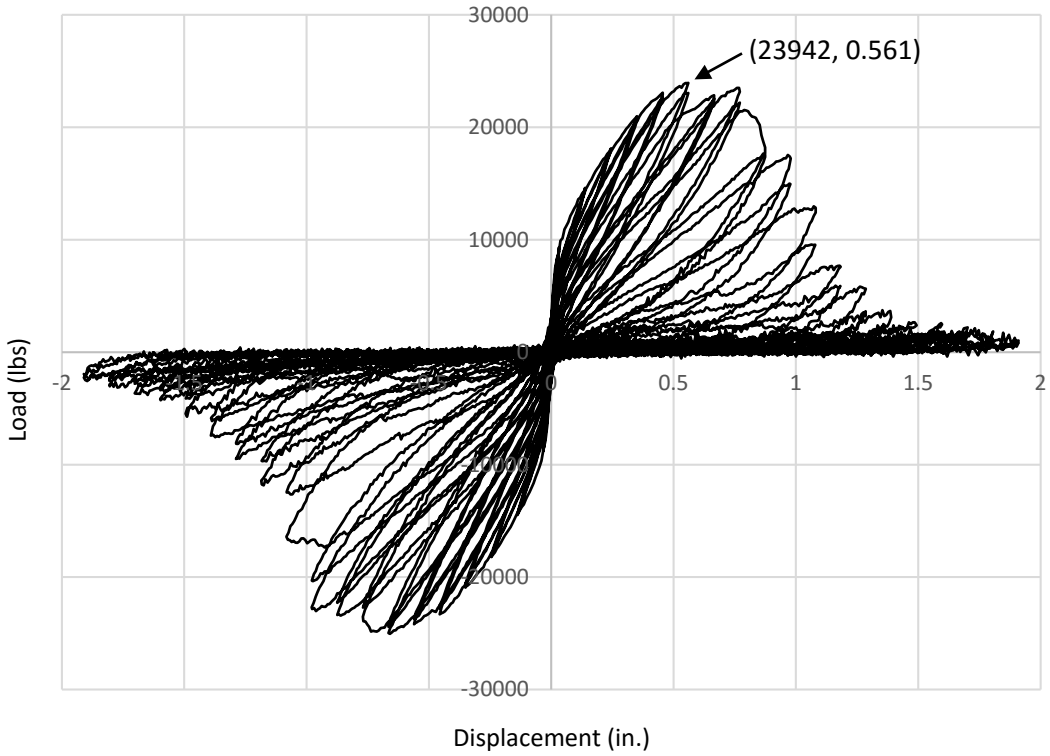

Figure B-11: Hysteresis curve for axial load 15.0 kips (28.19 psi)

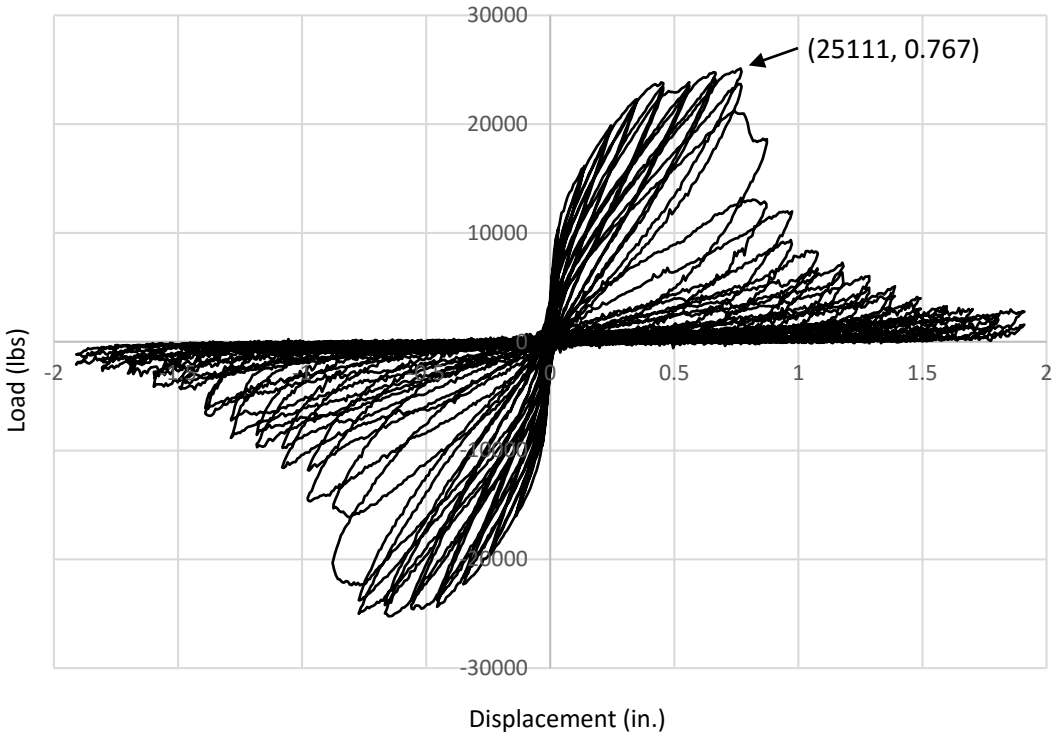

Figure B-12: Hysteresis curve for axial load 20.0 kips (37.59 psi)

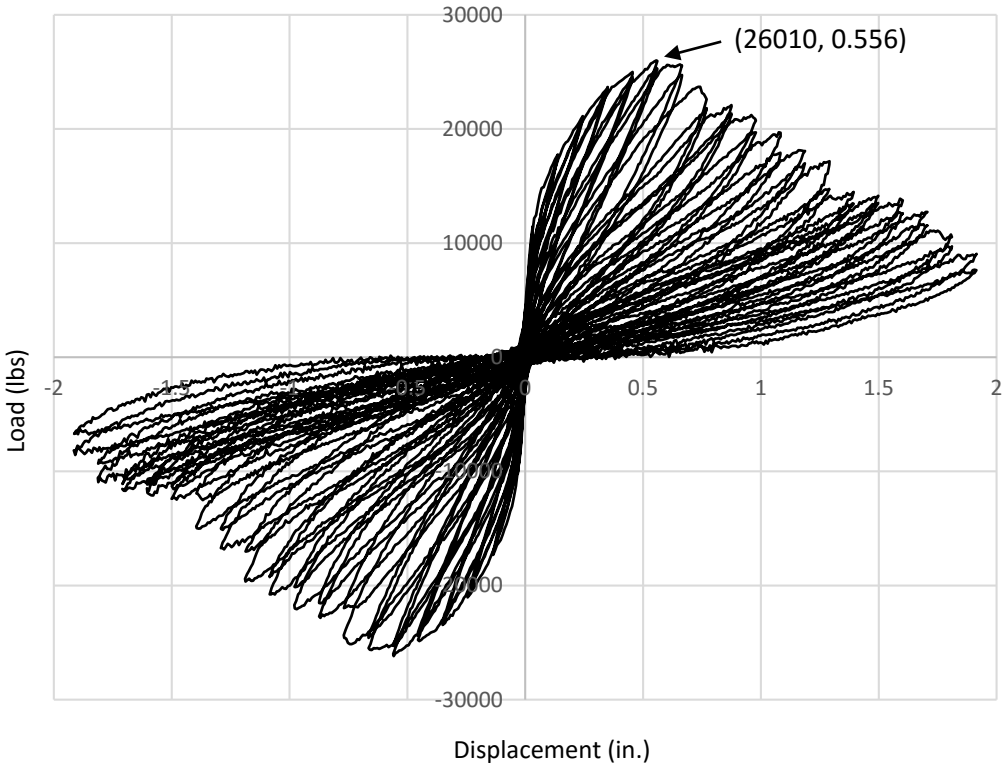

Figure B-13: Hysteresis curve for axial load 25.0 kips (46.98 psi)

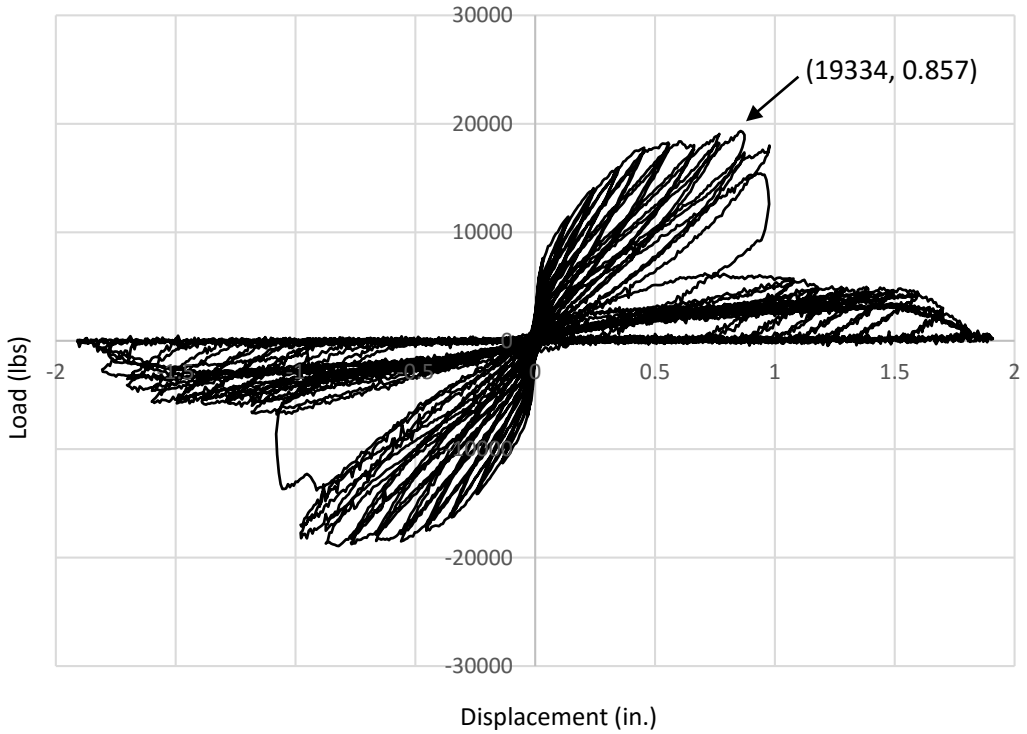

Figure B-14: Hysteresis curve for joint strength ratio of 0.010

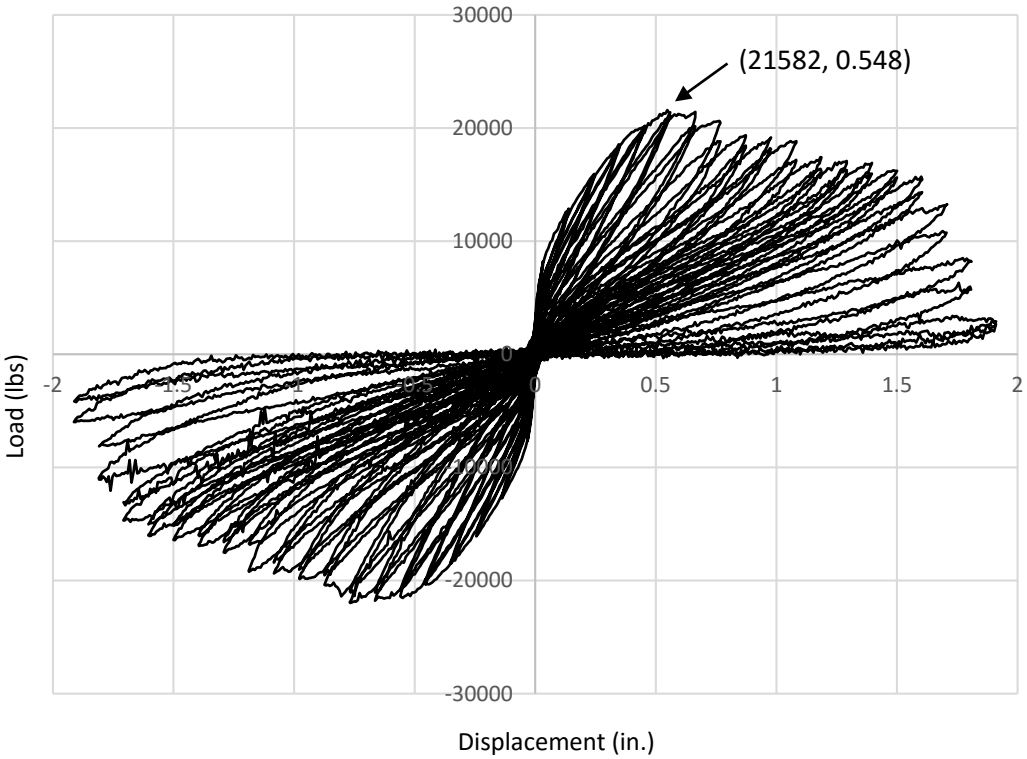

Figure B-15: Hysteresis curve for joint strength ratio of 0.015

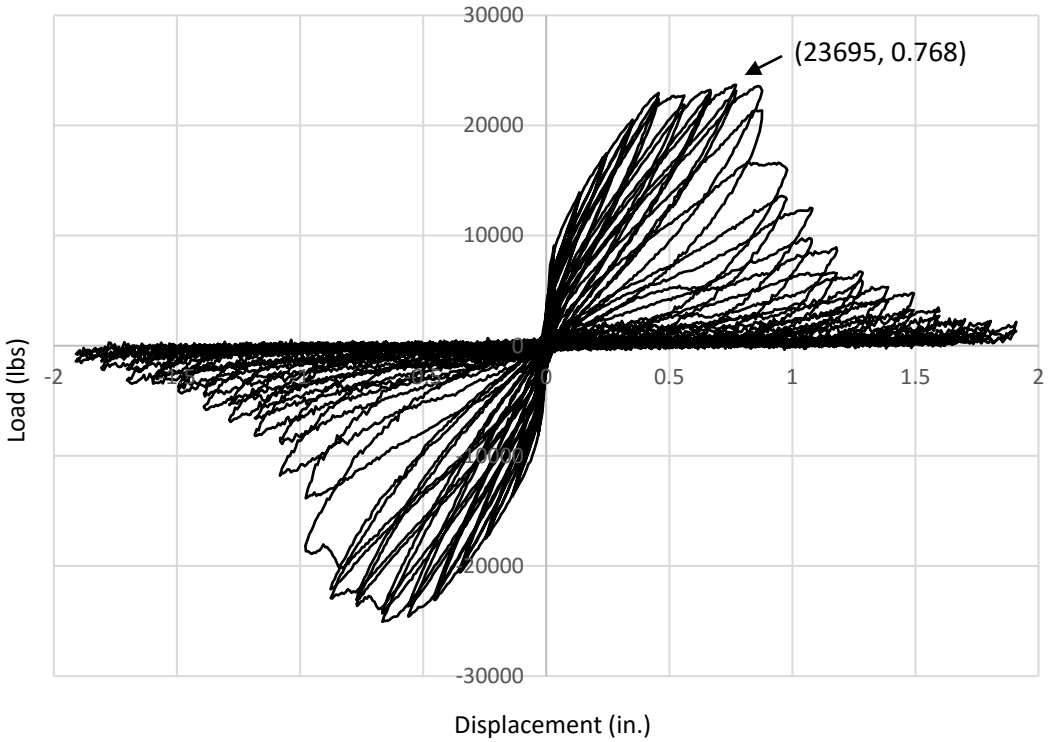

Figure B-16: Hysteresis curve for joint strength ratio of 0.020

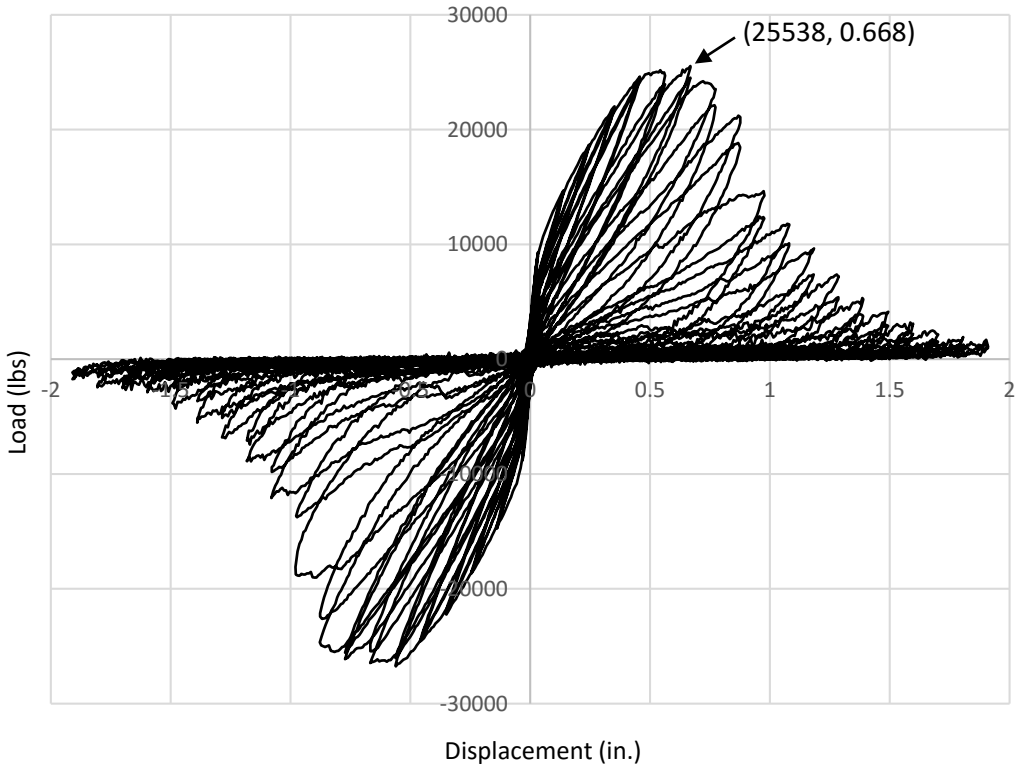

Figure B-17: Hysteresis curve for joint strength ratio of 0.025

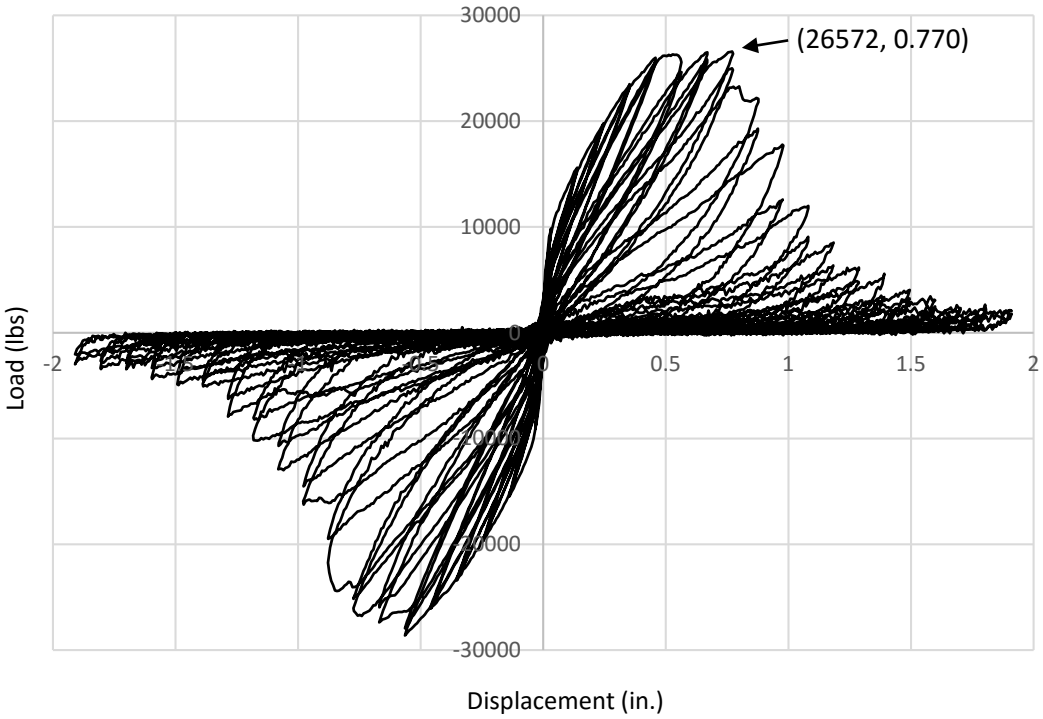

Figure B-18: Hysteresis curve for joint strength ratio of 0.030

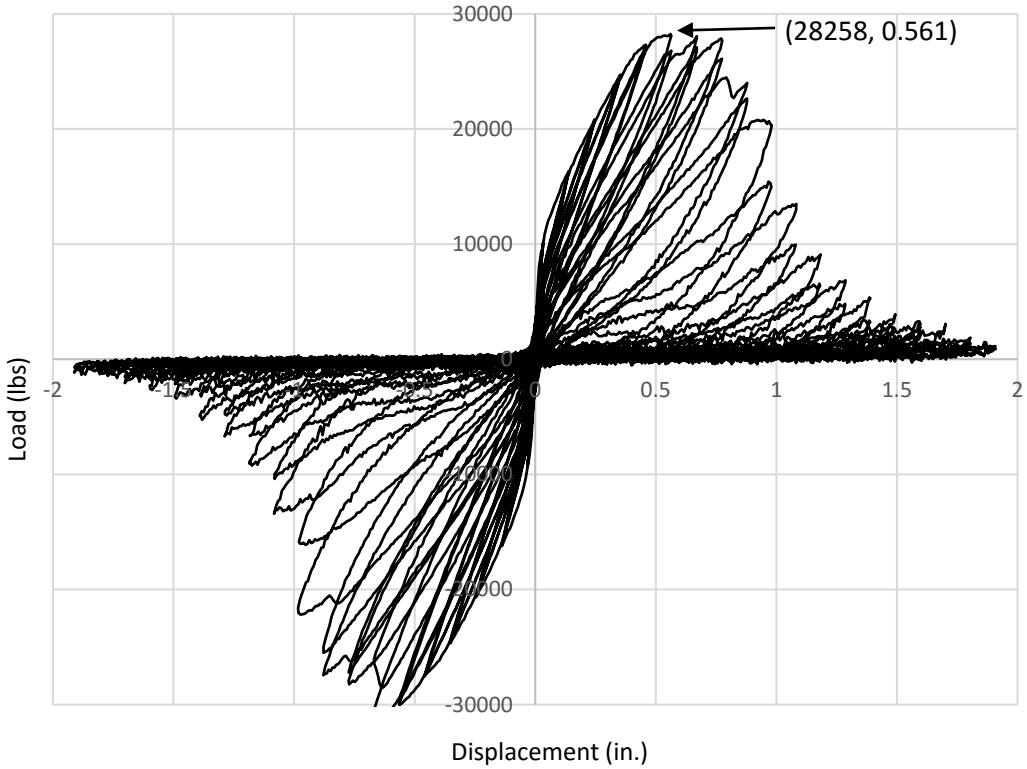

Figure B-19: Hysteresis curve for joint strength ratio of 0.035

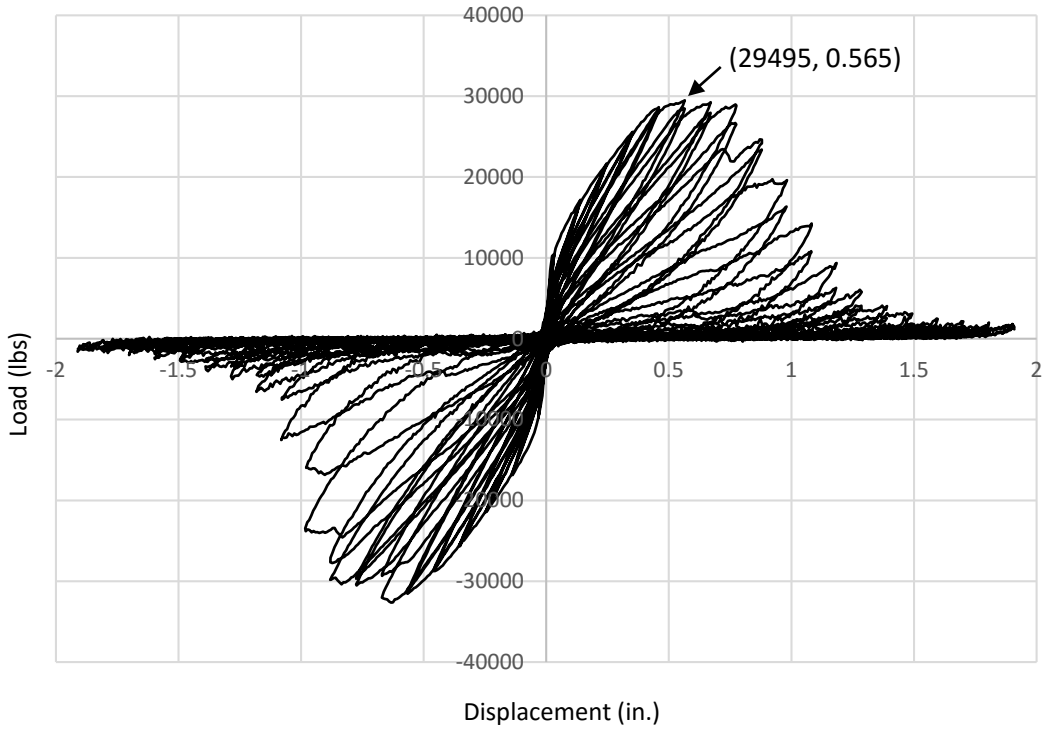

Figure B-20: Hysteresis curve for joint strength ratio of 0.040

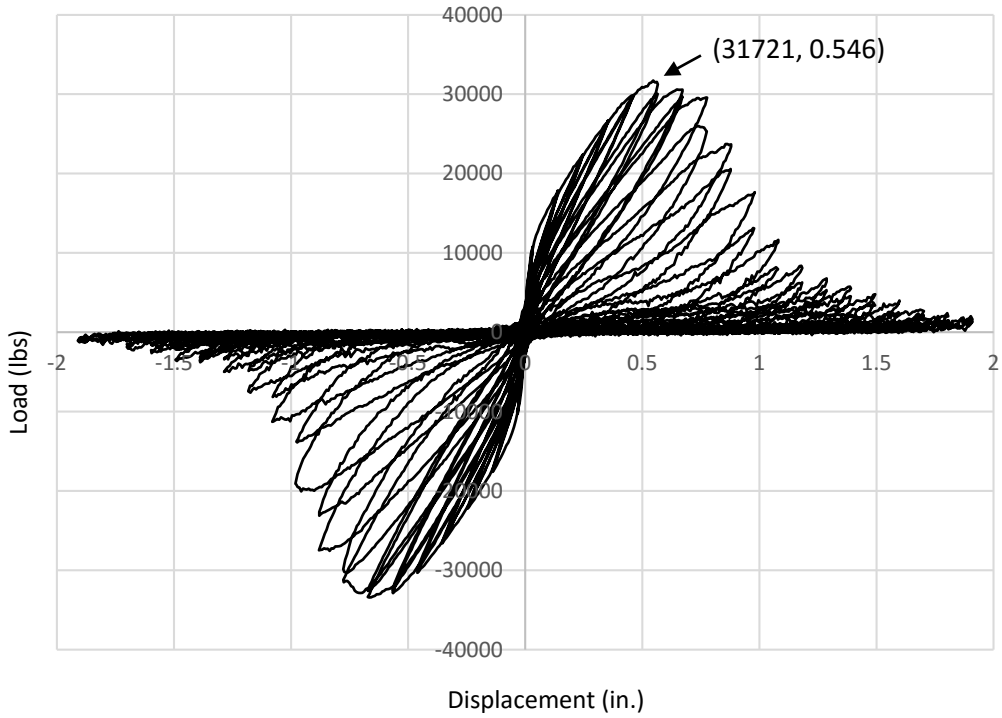

Figure B-21: Hysteresis curve for joint strength ratio of 0.045

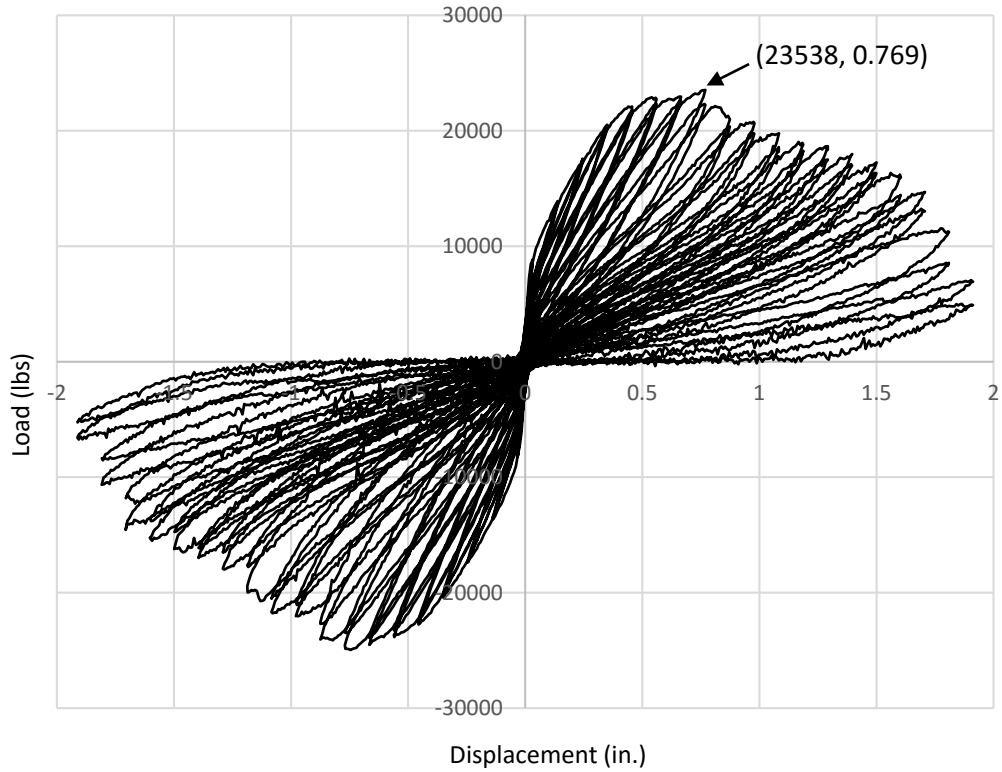

Figure B-22: Hysteresis curve for 19 in. vertical opening

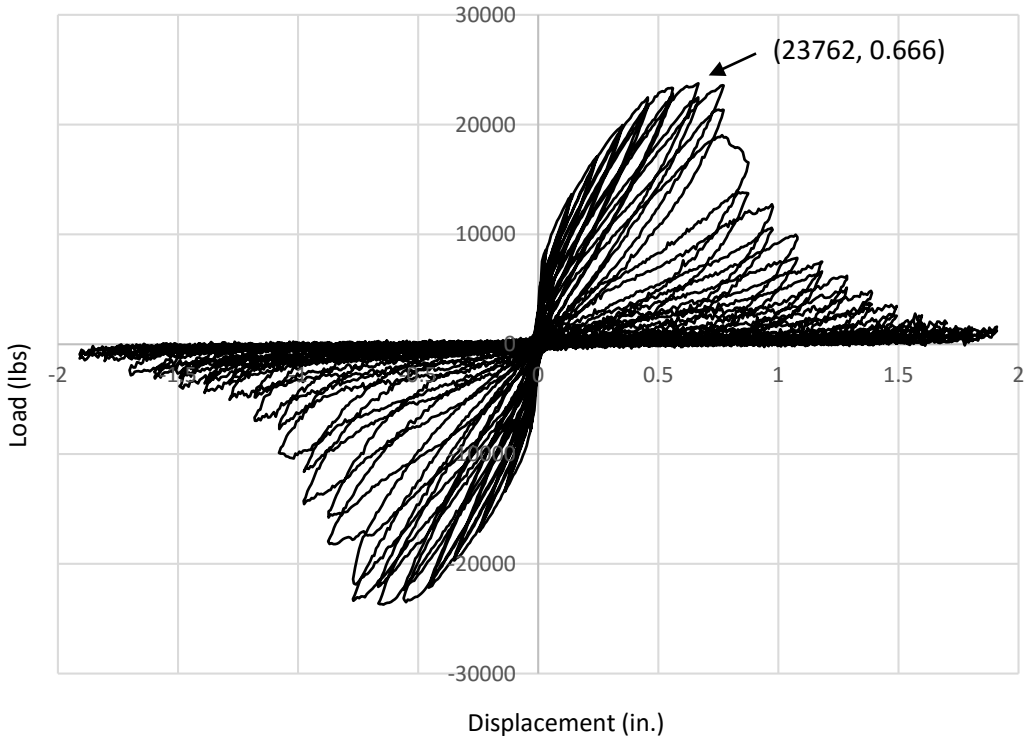

Figure B-23: Hysteresis curve for 27 in. vertical opening

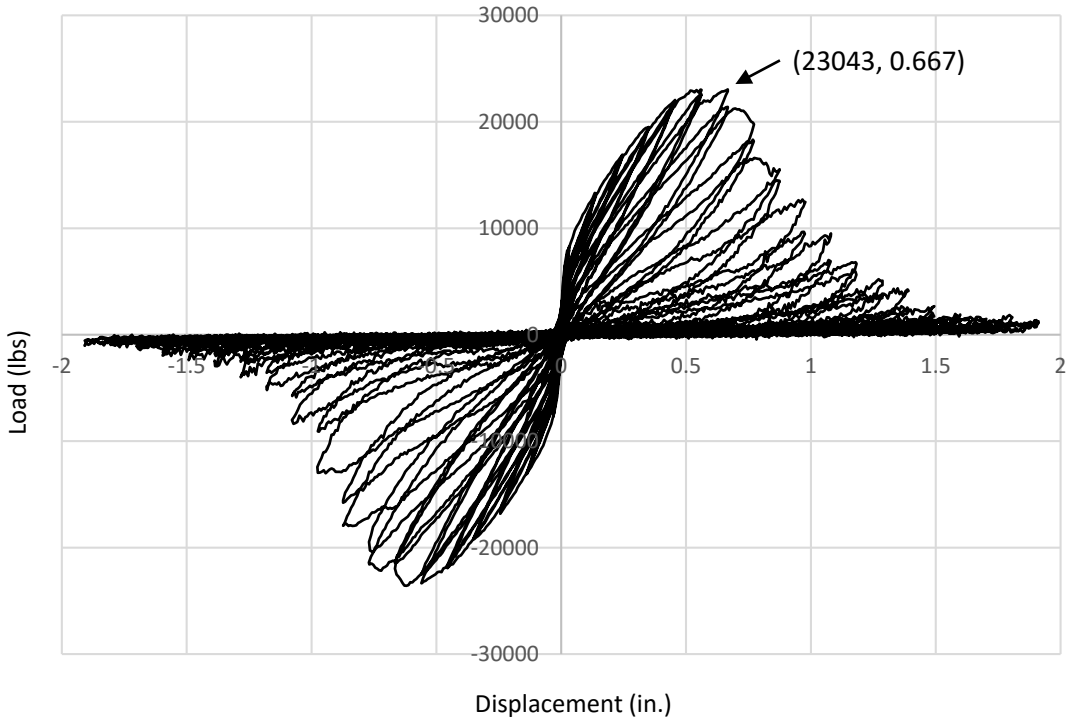

Figure B-24: Hysteresis curve for 31 in. vertical opening

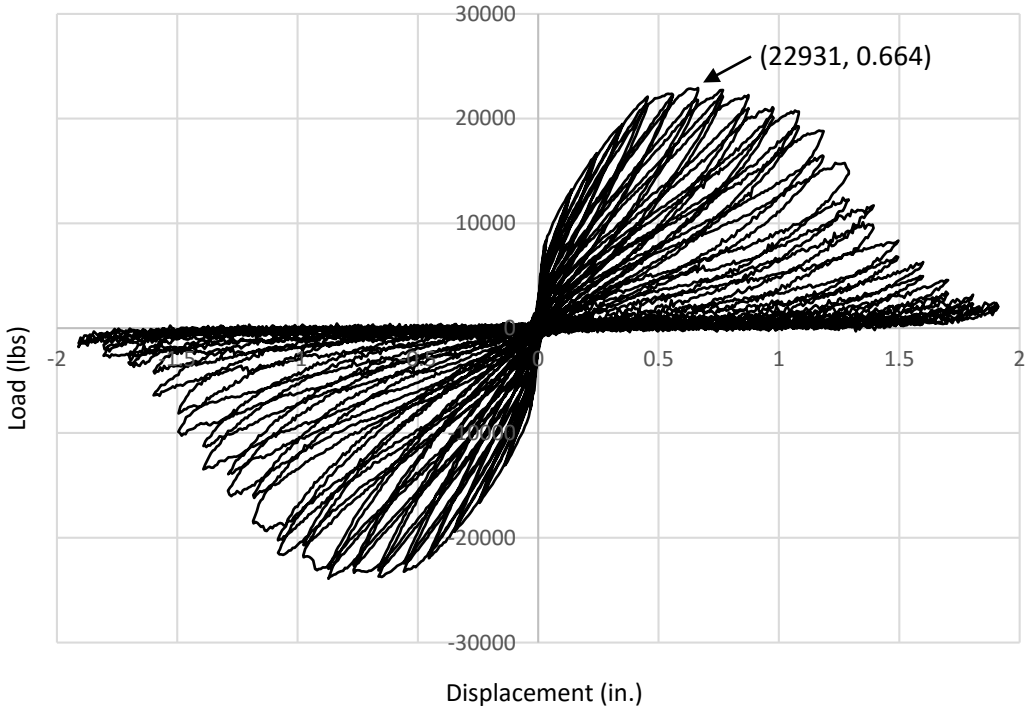

Figure B-25: Hysteresis curve for 30 in. wide opening

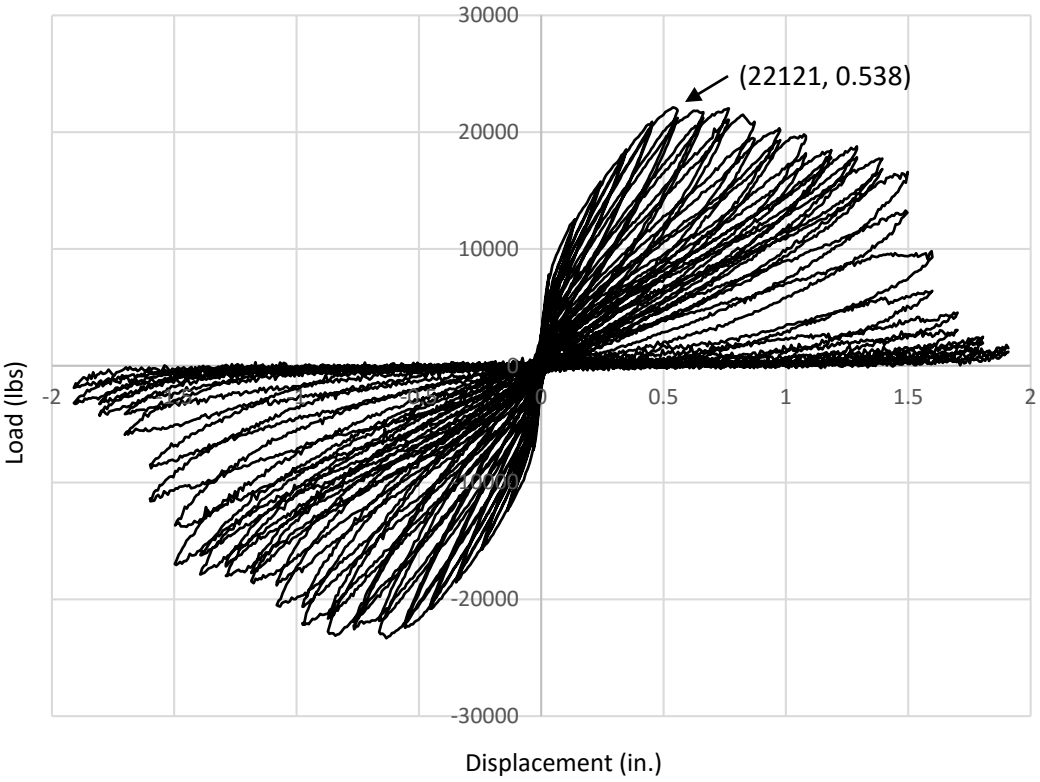

Figure B-26: Hysteresis curve for 38 in. wide opening

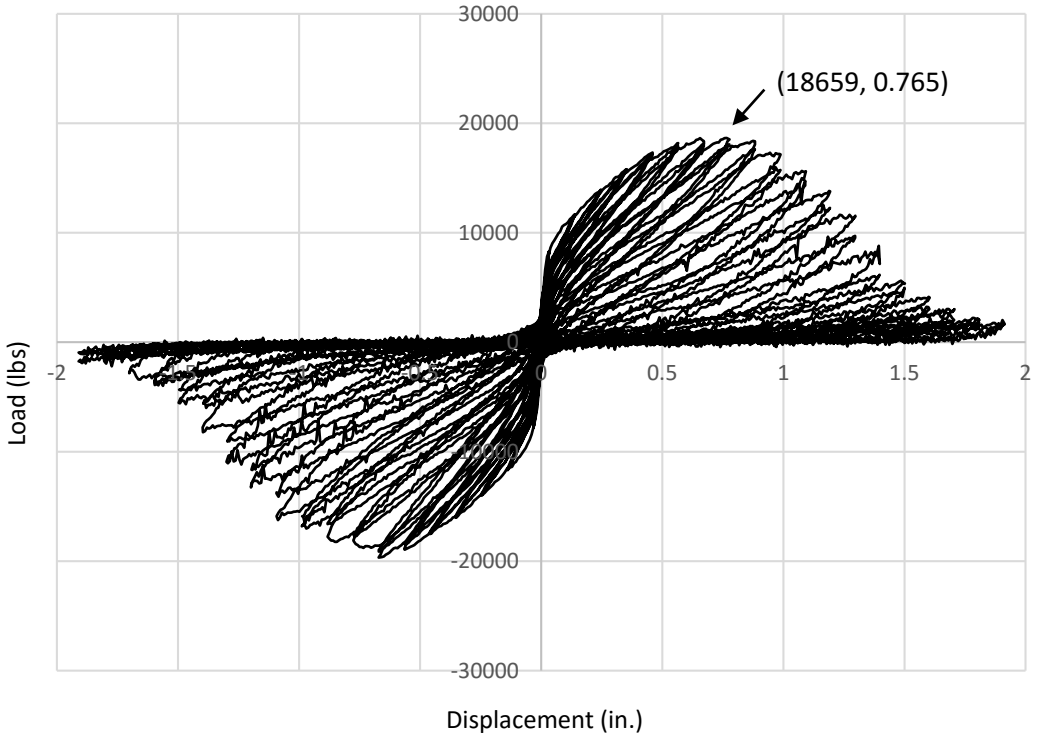

Figure B-27: Hysteresis curve for #2 vertical reinforcement

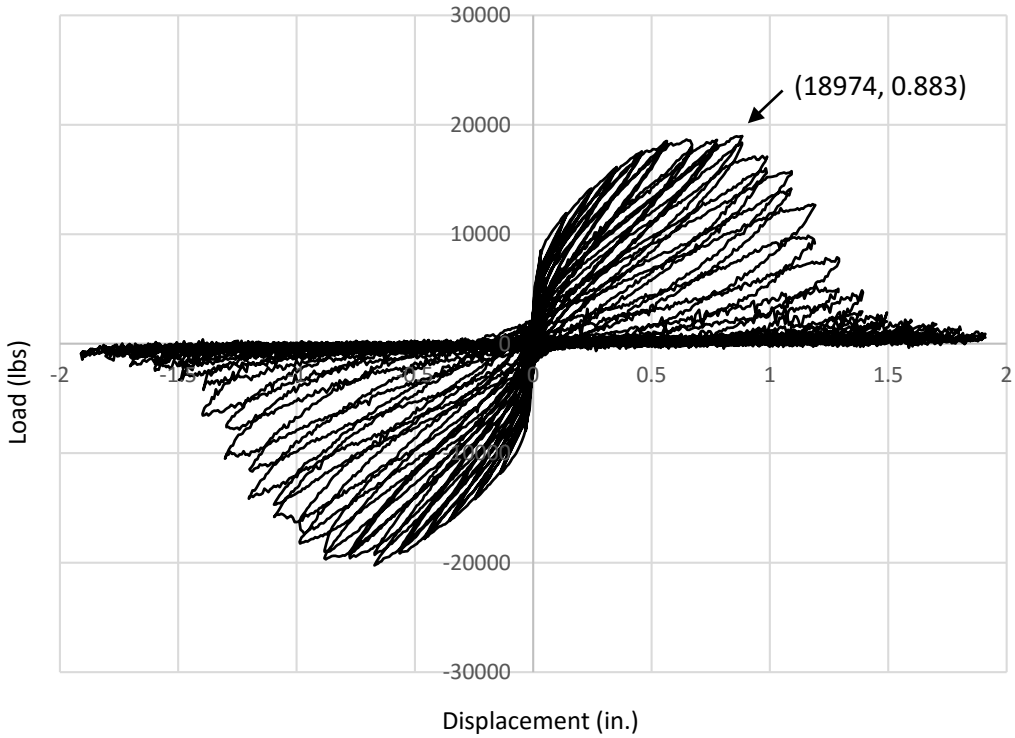

Figure B-28: Hysteresis curve for #2 vertical and horizontal reinforcement

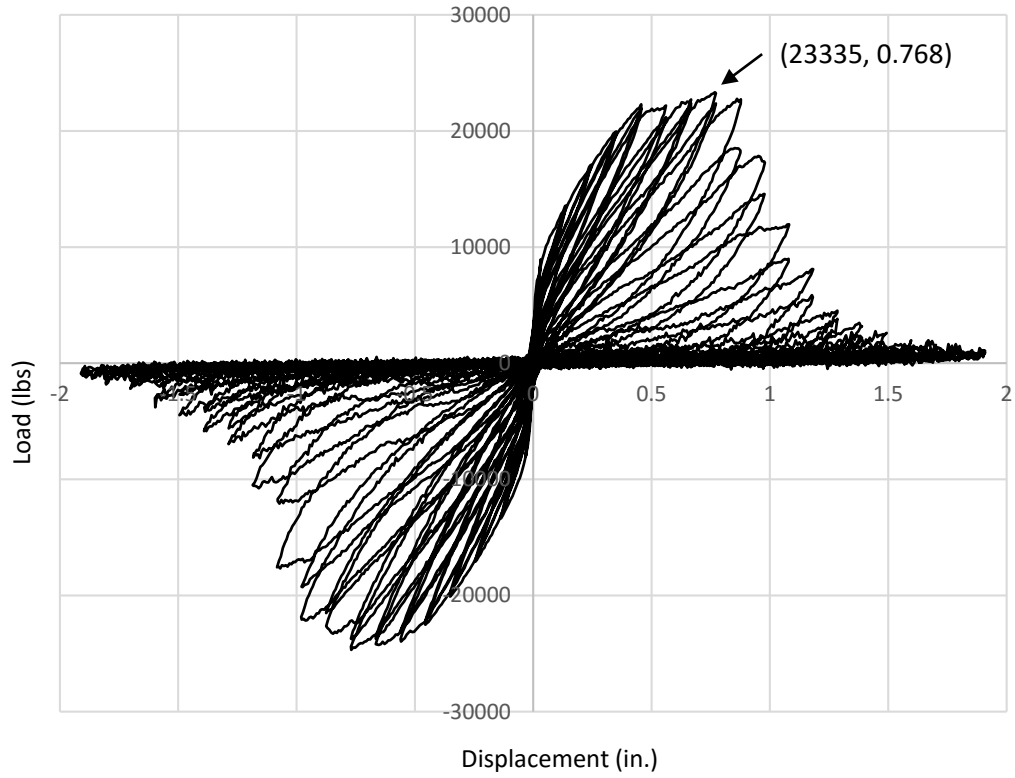

Figure B-29: Hysteresis curve for #2 horizontal reinforcement

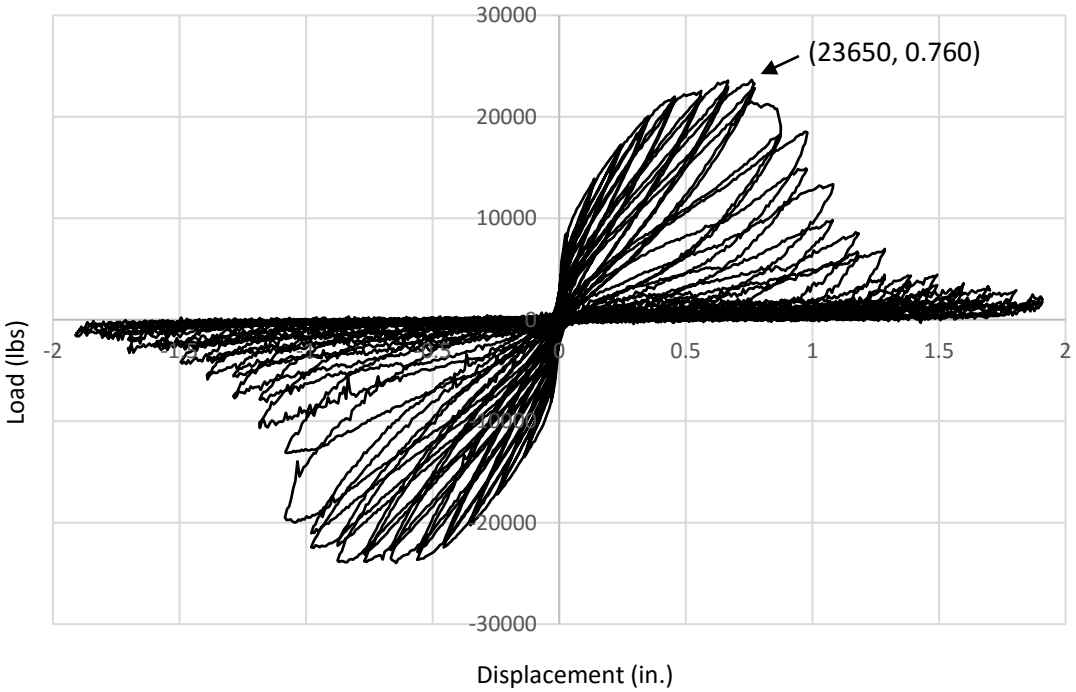

Figure B-30: Hysteresis curve for #4 horizontal reinforcement

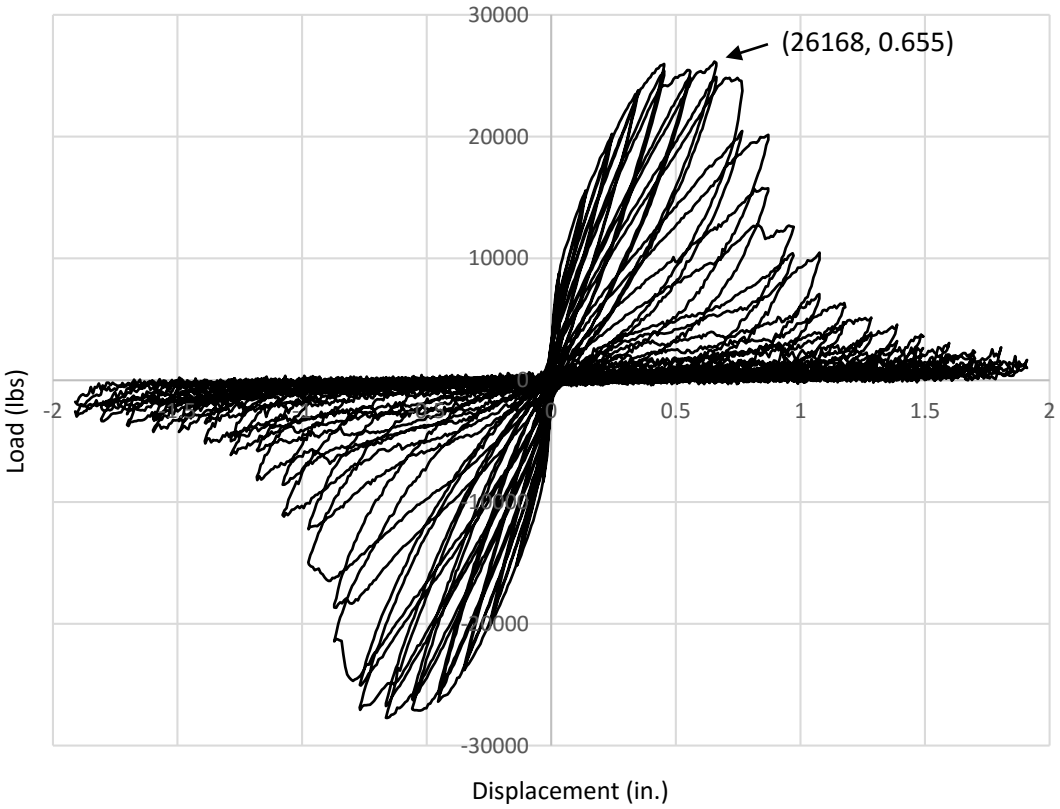

Figure B-31: Hysteresis curve for #4 vertical and horizontal reinforcement

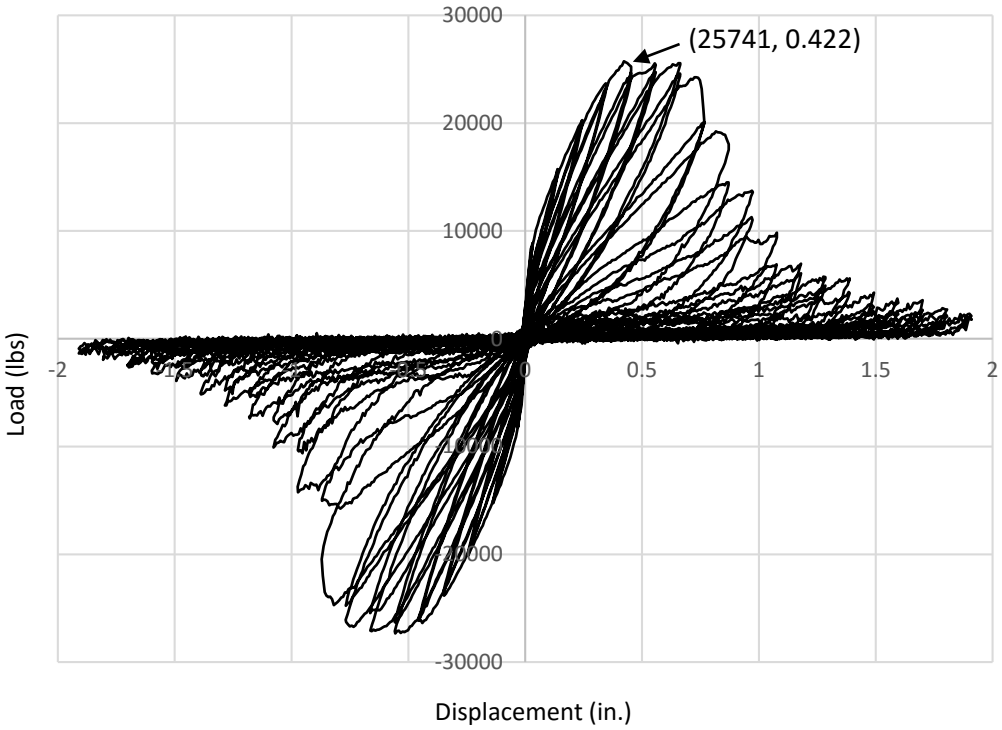

Figure B-32: Hysteresis curve for #4 vertical reinforcement

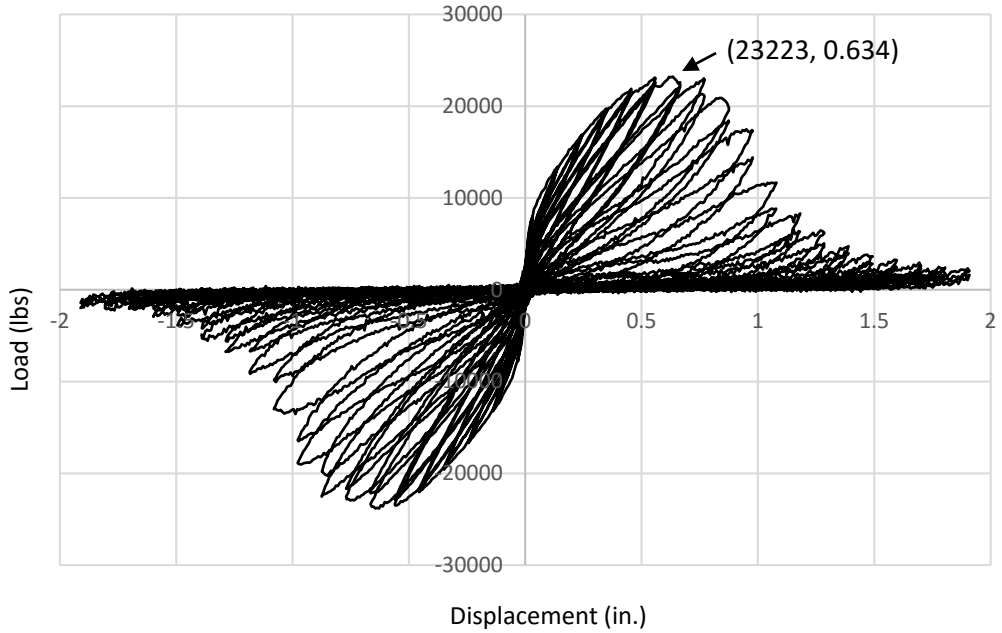

Figure B-33: Hysteresis curve for 24 in. horizontal spacing of vertical reinforcement

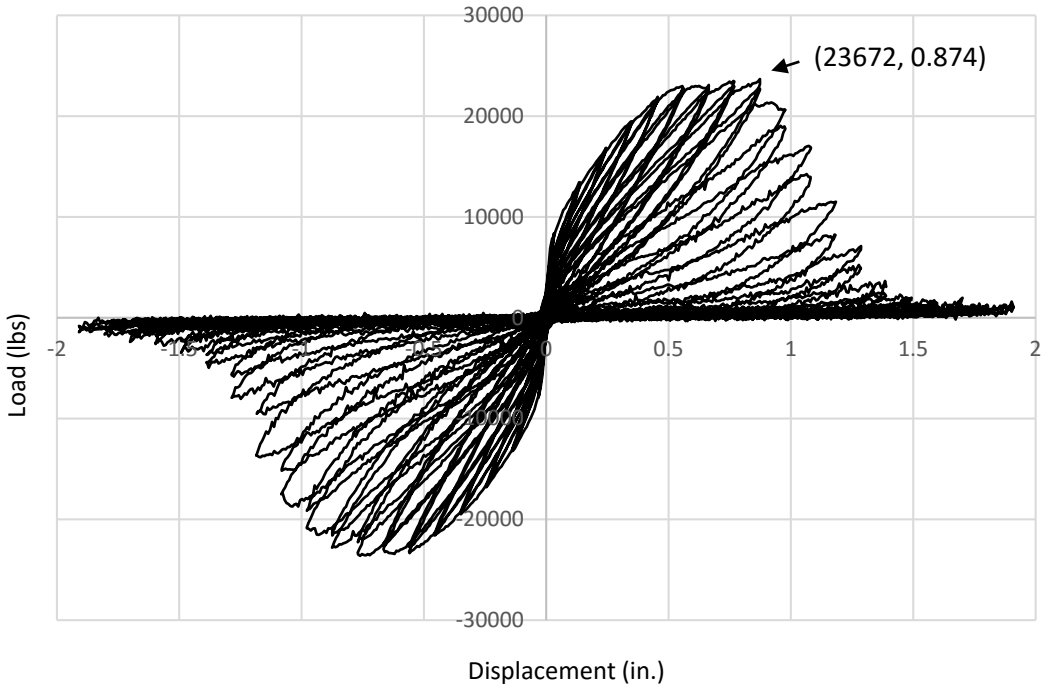

Figure B-34: Hysteresis curve for 16 in. horizontal spacing of vertical reinforcement

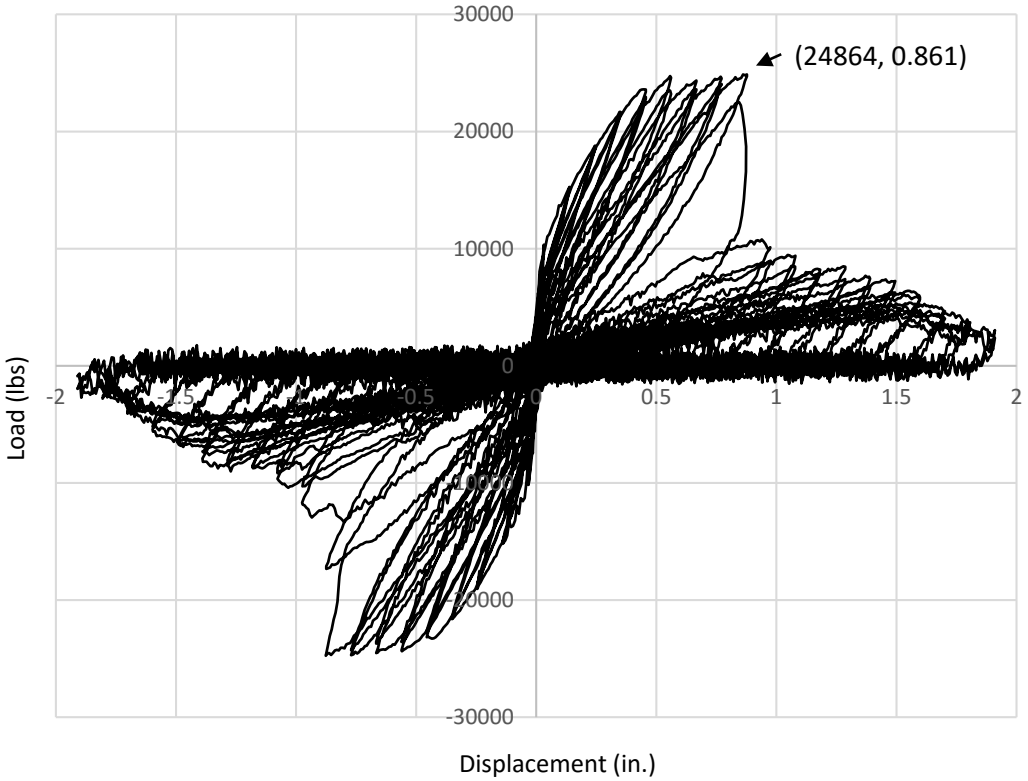

Figure B-35: Hysteresis curve for 20 in. vertical spacing of horizontal reinforcement

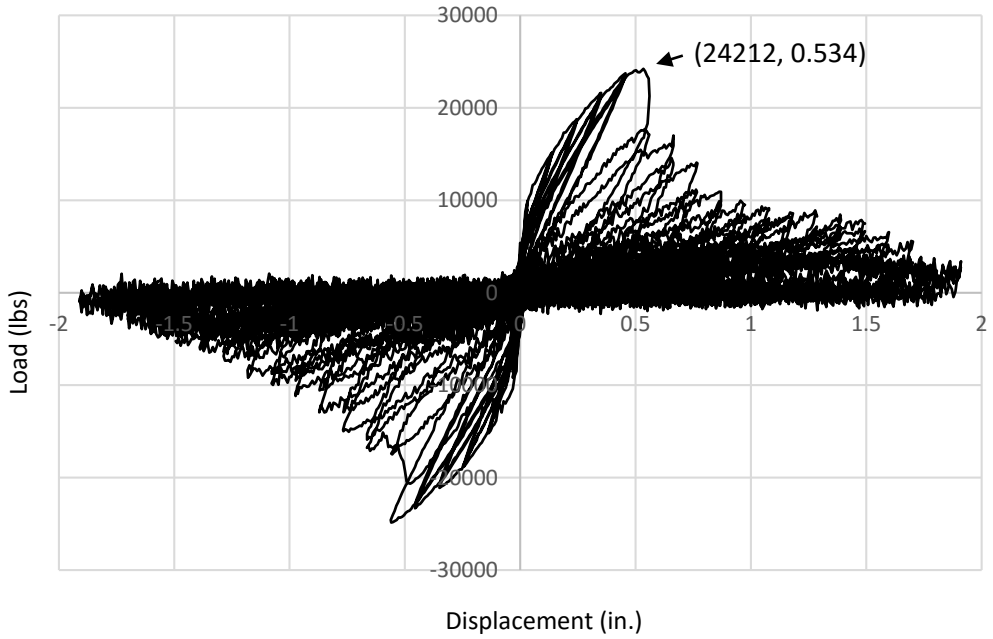

Figure B-36: Hysteresis curve for 24 in. vertical spacing of horizontal reinforcement

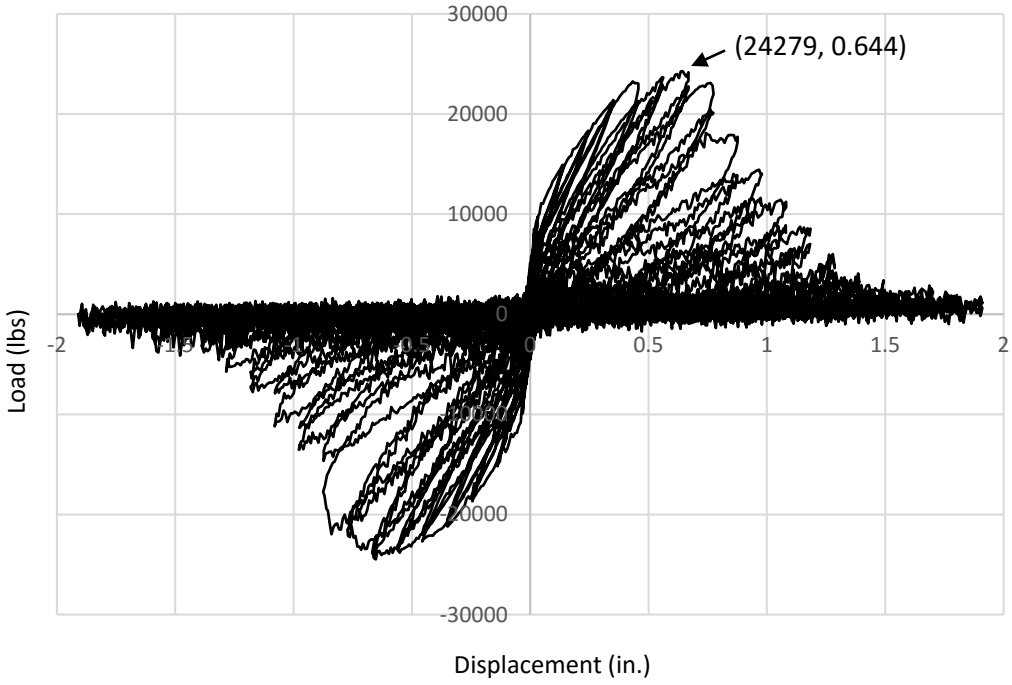

Figure B-37: Hysteresis curve for 44 in. vertical spacing of horizontal reinforcement

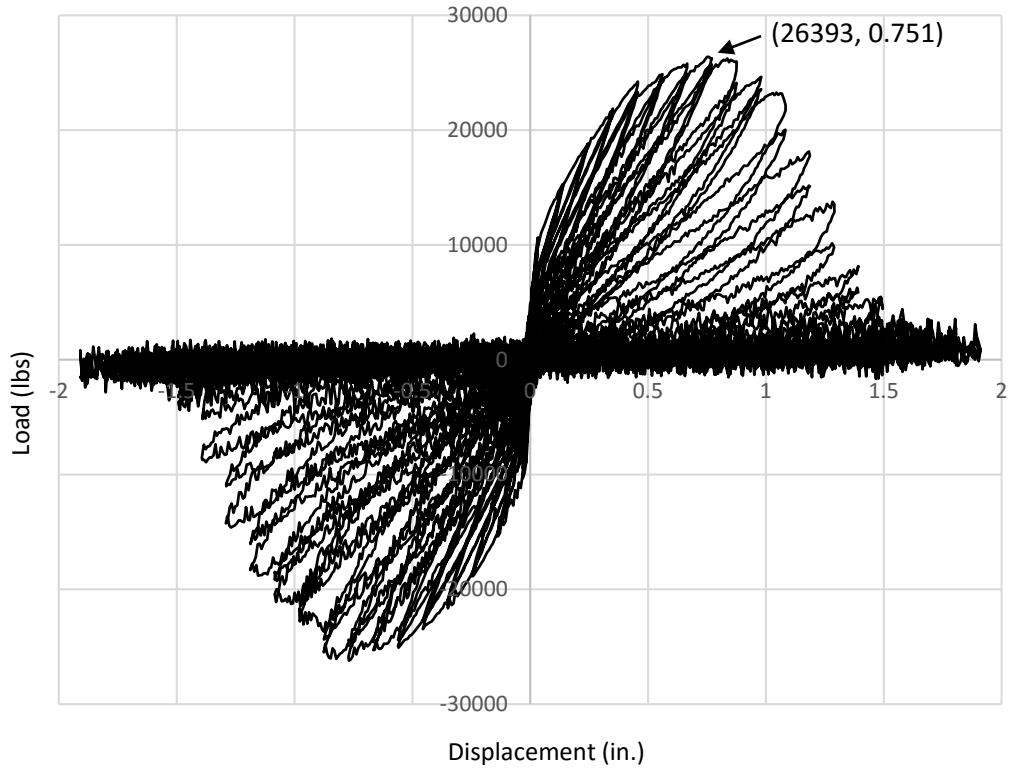

Figure B-38: Hysteresis curve for 2500 psi strength of grouted masonry

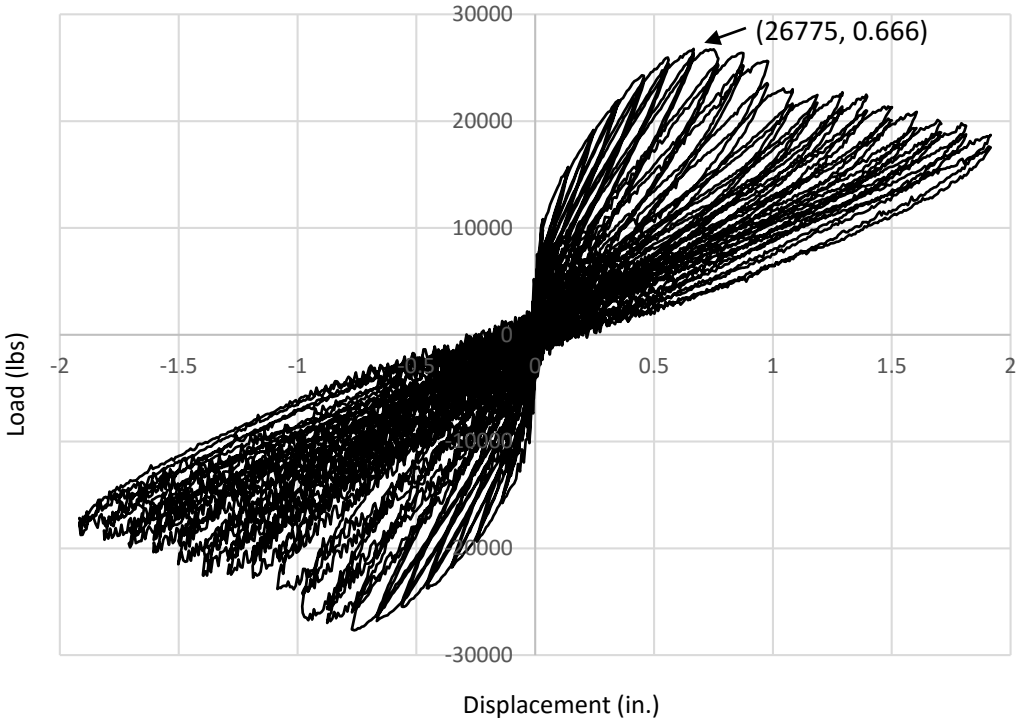

Figure B-39: Hysteresis curve for 3000 psi strength of grouted masonry

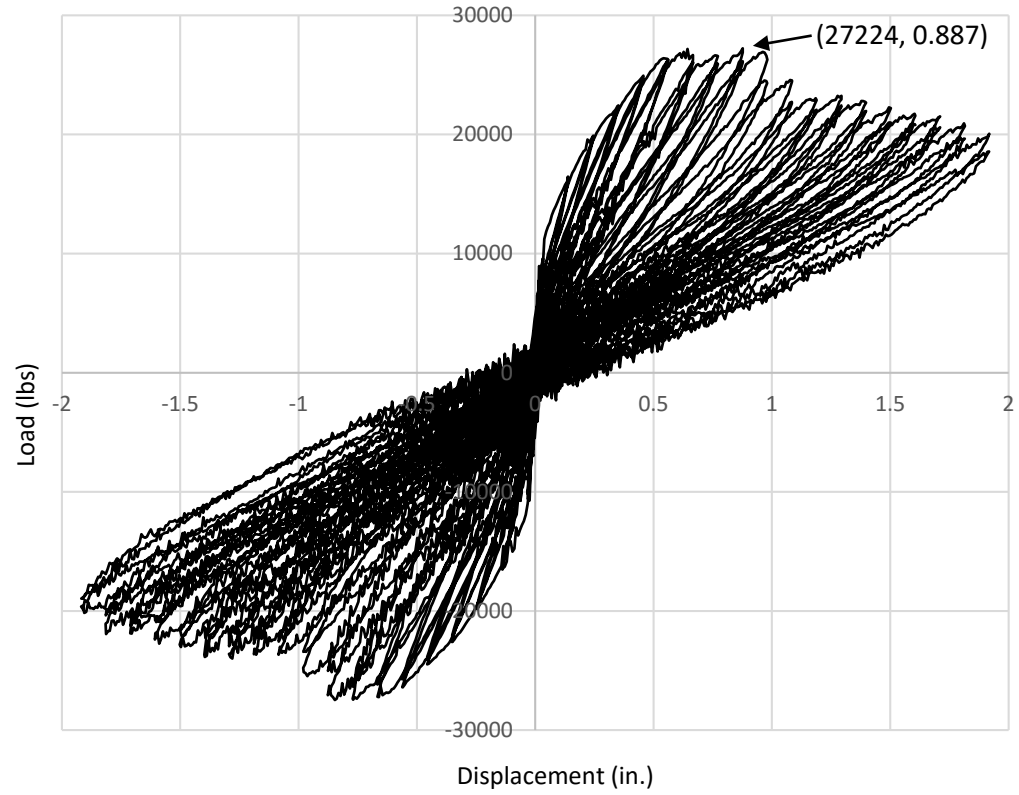

Figure B-40: Hysteresis curve for 3500 psi strength of grouted masonry

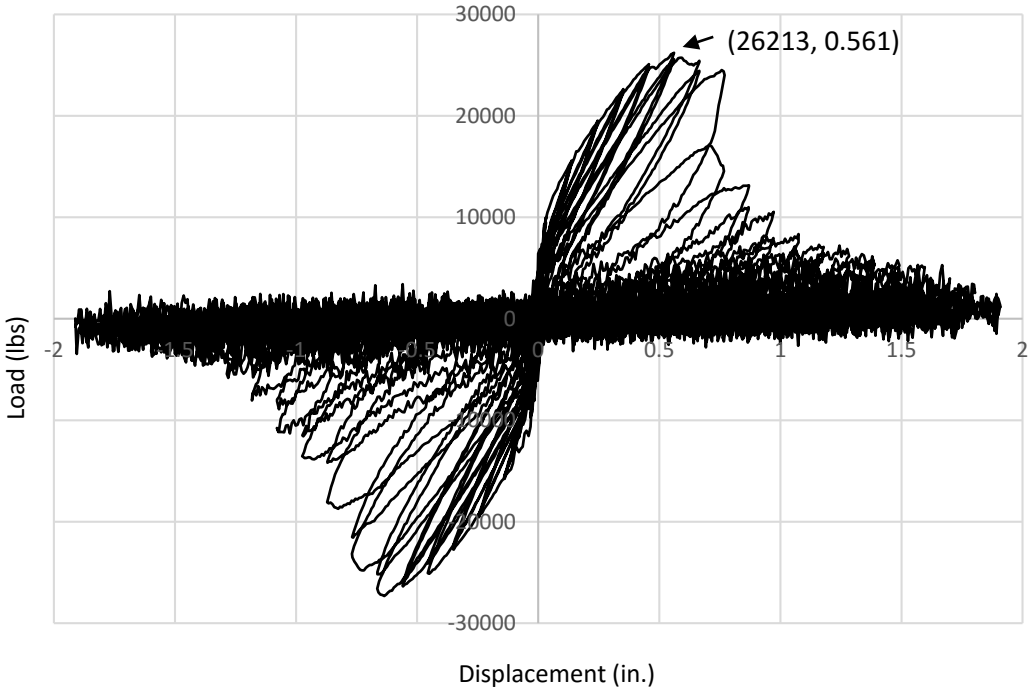

Figure B-41: Hysteresis curve for 2500 psi strength of un-grouted masonry

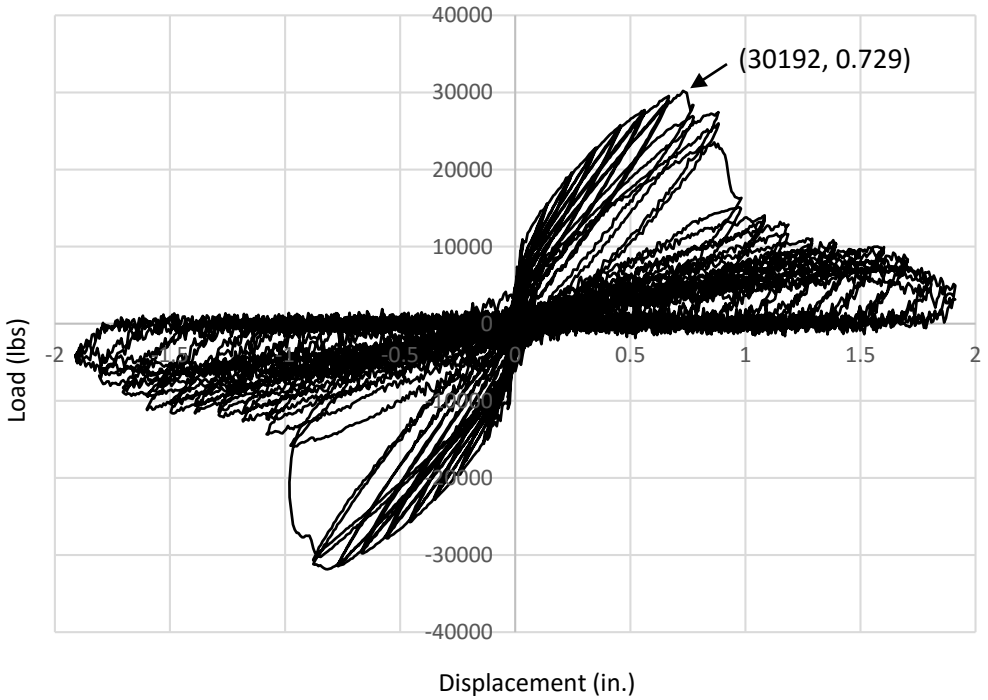

Figure B-42: Hysteresis curve for 3000 psi strength of un-grouted masonry

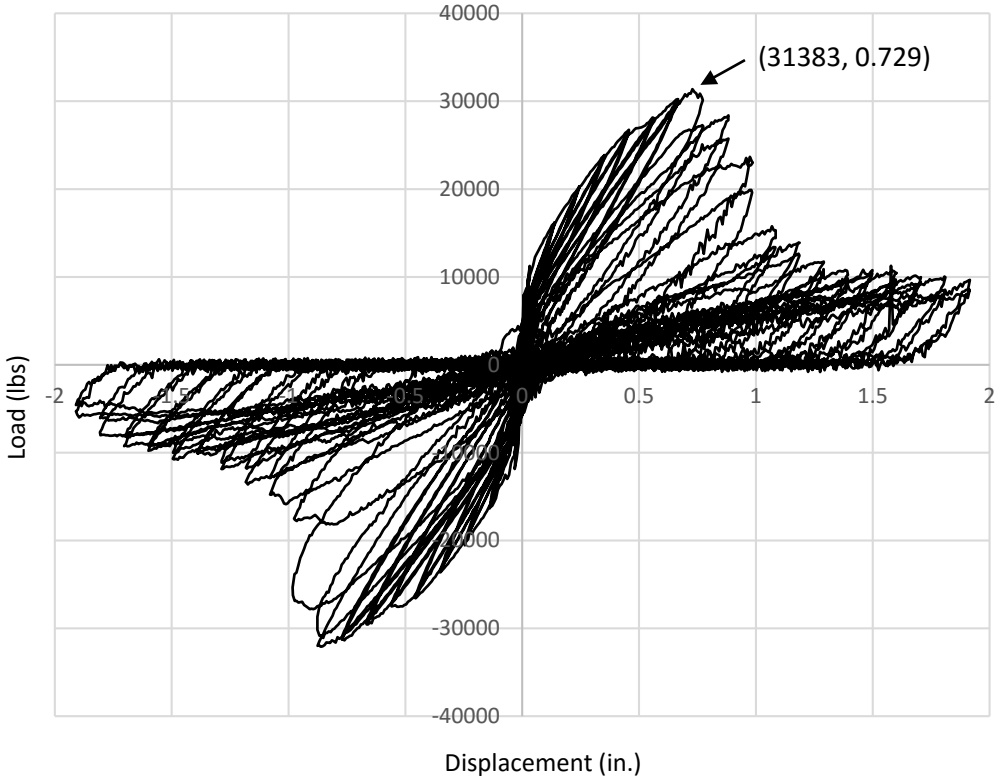

Figure B-43: Hysteresis curve for 3500 psi strength of un-grouted masonry

APPENDIX C. ADDITIONAL

Figure C-1: Enlarged view of 1st story cracks in push regime

Figure C-2: Enlarged view of 1st story cracks in pull regime

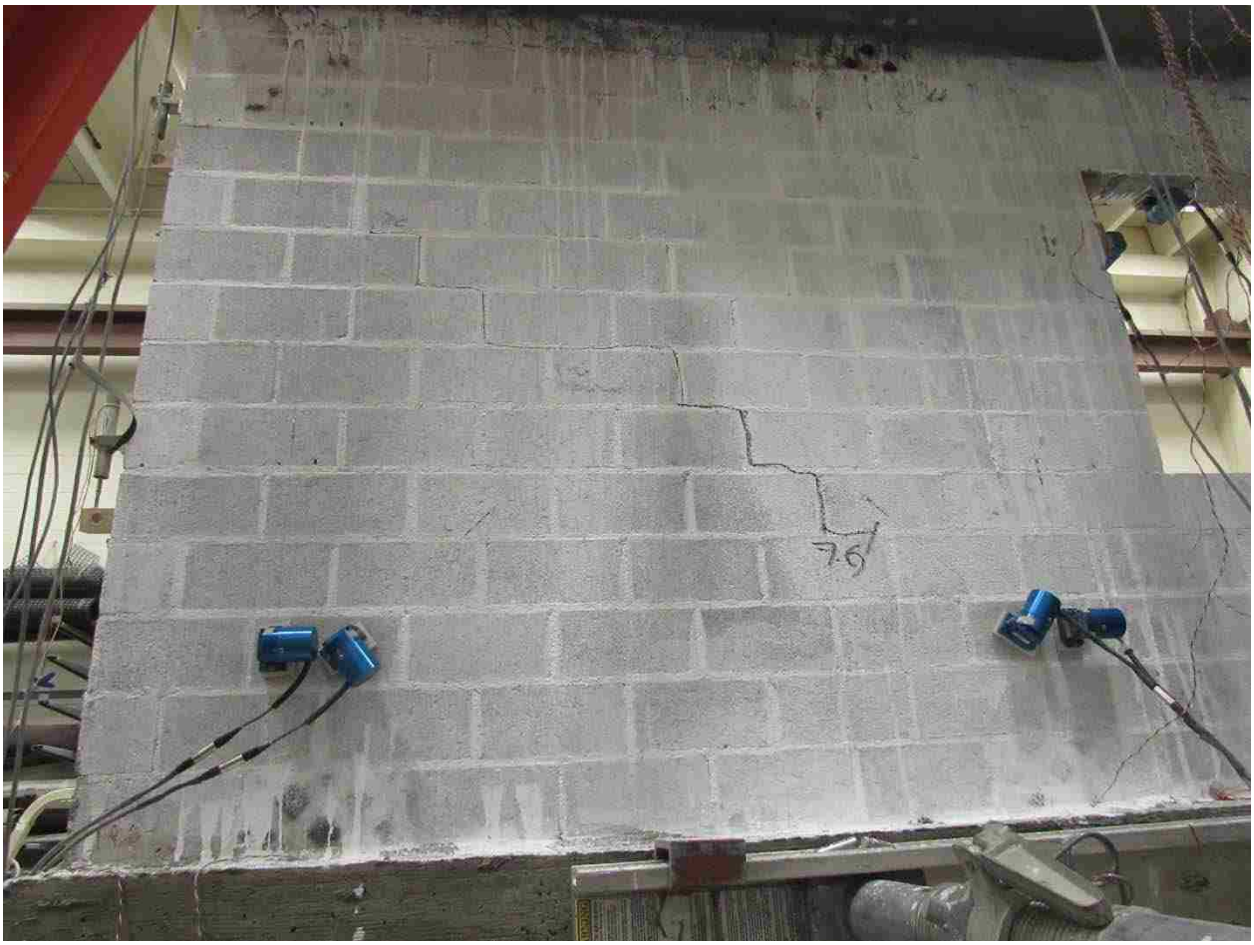

Figure C-3: Enlarged view of 2nd story cracks in push regime

Figure C-4: Enlarged view of 2nd story cracks in pull regime

Figure C-5: Enlarged view of 3rd story cracks in push regime

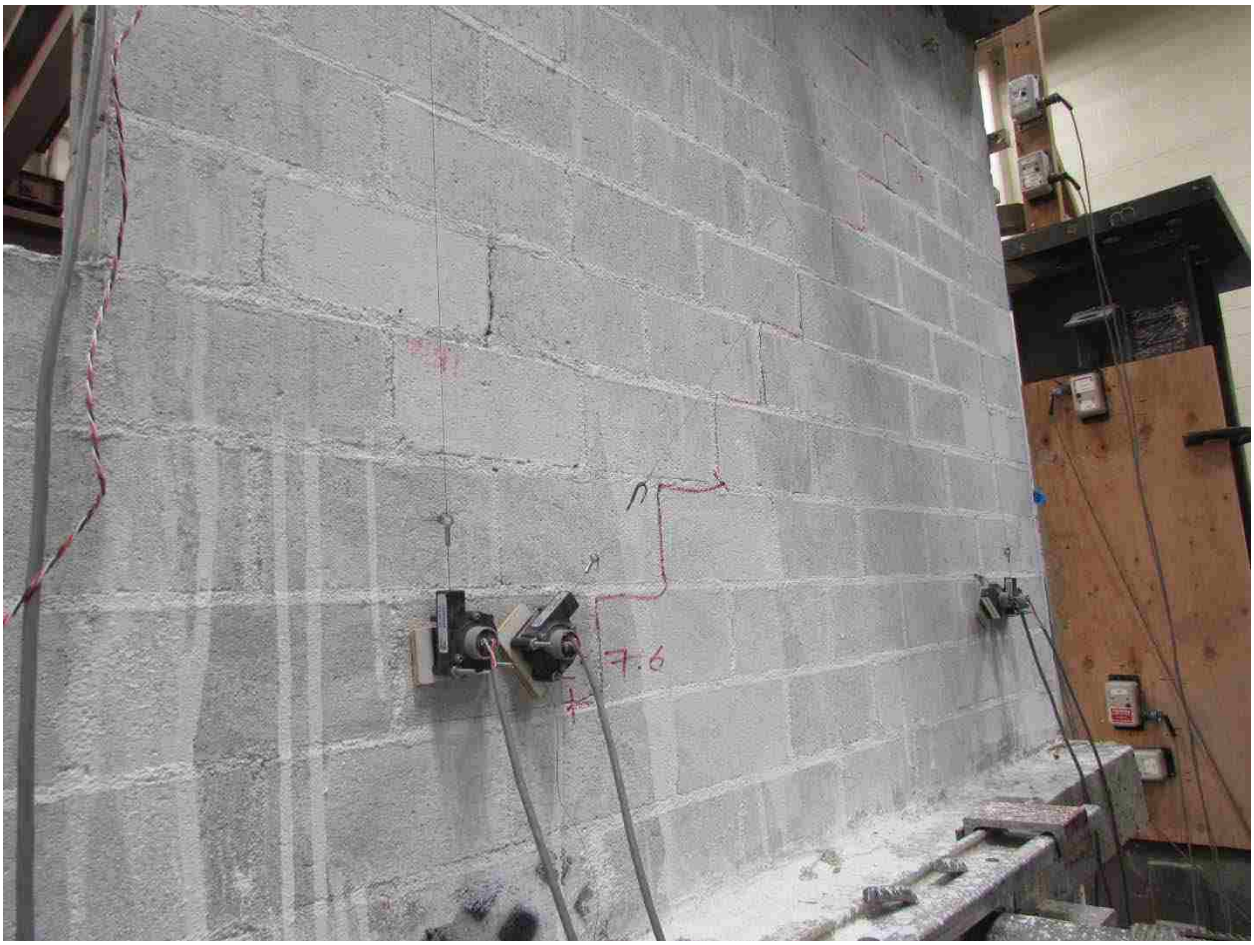

Figure C-6: Enlarged view of 3rd story cracks in pull regime

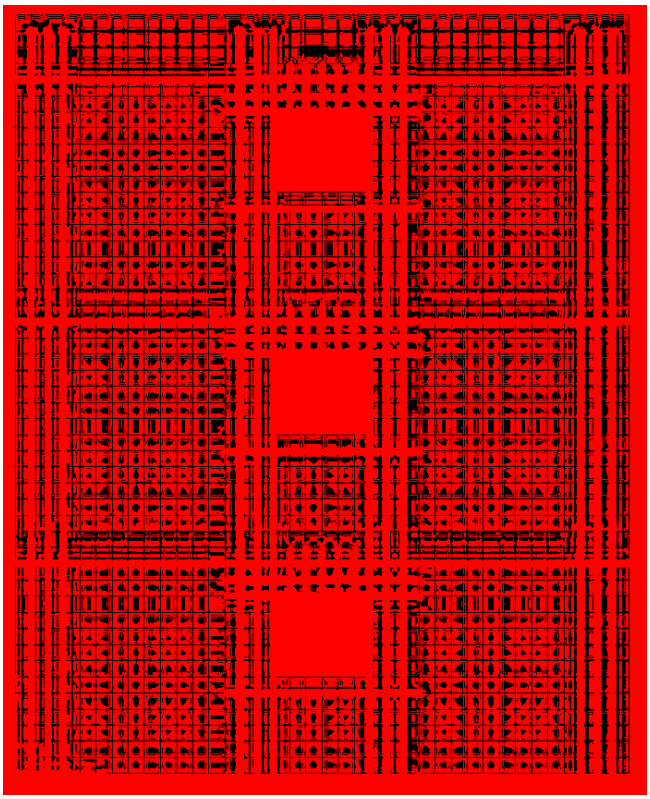

Figure C-7: Opening height reduced 1 course from walls 2 and 3 base model

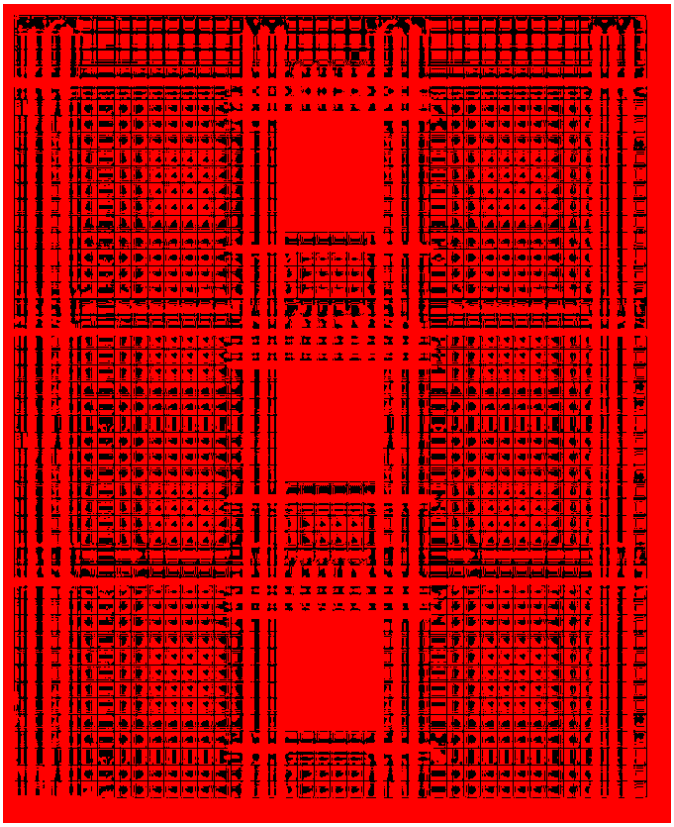

Figure C-8: Opening height increased 1 course from walls 2 and 3 base model

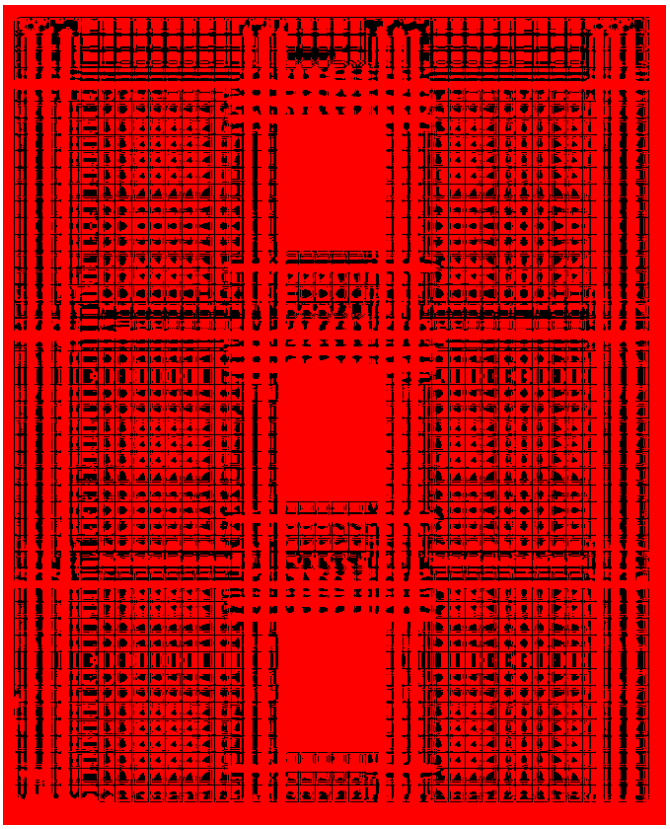

Figure C-9: Opening height increased 2 courses from walls 2 and 3 base model